THE UNIVERSITY OF HULL

Human Factors in the Operation and Maintenance of Offshore Wind Farms

being a Thesis submitted for the Degree of

Doctor of Philosophy

in the University of Hull

by

Tobenna Duval Uzuegbunam

MSc (Hons)

November 2022

Acknowledgements

I would first like to thank the Aura Innovation Centre and the University of Hull for supporting and funding my research with a PhD.

I am grateful for the support and guidance of my two supervisors. Dr Rodney Forster for his patience, guidance, and support during this research, and Professor Terry Williams who spent a good amount of time and effort supporting me throughout this project. I also would like to thank Professor Jack Hardisty who was taken from us all too soon.

Finally, I would like to thank my friends and family for their belief and encouragement to date.

Declaration

I declare that the material presented in this thesis consists of original work undertaken by the author which has not previously been submitted by me or any other person for a degree in this or any other university. Additionally, material from the work of others has been acknowledged where necessary.

Tobenna D Uzuegbunam

Nomenclature

a	Amplitude (m) / acceleration (ms^{-1})
a_w	Weighted acceleration (ms^{-1})
A	Cross-sectional area of moving fluid / Turbine swept area (m2)/ amplitude
Cp	Power coefficient (%)
E	Energy (kW)
F	Frequency (Hz)
ω	Angular velocity (radians per second)
g	Gravitational acceleration (ms^{-2})
h	Water depth (m)
H	Wave height (m)
Hs	Significant wave height (m)
$\overline{H}$	Mean wave height
K_E	Kinetic energy (J)
m	Mass (kg)
P	Potential power in a fluid (kW)
Po	Turbine power output (kW)
t	Time (s)
T	Wave period (s)
T_p	Peak wave period (s)
T_0	Zero-crossing period (s)
u, v, w	Streamwise, transverse and vertical flow directions
U	Velocity (ms^{-1})

$\bar{U}$	Mean velocity (ms^{-1})
H	Surface elevation (m)
λ	Wavelength (m)
ρ	Fluid density (kg/m^3)
$V_{cut\text{-}in}$	Cut-in speed of a turbine (ms^{-1})
$V_{cut\text{-}out}$	Cut-out speed of a turbine (ms^{-1})
V_{rated}	Rated speed of a turbine (ms^{-1})

Acronyms

IRENA	International Renewable Energy Agency
IEA	International Energy Agency
O&M	Operations and Maintenance
Co	Operational Costs
Cm	Maintenance Costs
$C_{o\&m}$	Operations and Maintenance Costs
VDV	Vibration Dose Value
MSDV	Motion Sickness Dose Value
MSI	Motion Sickness Incidence
GPS	Global Positioning System
RMS	Root Mean Square
VMMS	Vessel Motion Monitoring System
ISO	International Organization for Standardization

Abstract

Current maintenance planning strategies and decision support tools used in the operations and maintenance of offshore wind farms rarely account for the welfare of technicians and their ability to do work upon arrival. This creates uncertainties especially since current operational limits might make a wind farm accessible but vibrations from transits might be unacceptable to technicians.

The welfare of technicians is expressed by levels of discomfort and the likelihood of seasickness occurring from the vibrations felt on Crew Transfer Vessels (CTVs) in transit.

To explore technician exposure to vibration in transit, acceleration data from vessel motion monitoring systems deployed on CTVs operating in the North Sea was synchronised with sea-state data from an operational oceanographic data service (Copernicus Marine Service). Processes of dimensionality reduction and machine learning were used to model the welfare of technicians from operational limits applied to modelled proxy variables including Composite Weighted RMS Acceleration (aRMS) and Motion Sickness Incidence (MSI).

Model results revealed both satisfactory and moderate performance in predicting aRMS and MSI based on model evaluation criteria of R^2 (0.69 and 0.49) and root mean square error ($0.06ms^{-2}$ and 4%). The results of the models raise the possibility of more relevant variables needed to capture all of the information needed to achieve high predictive accuracy.

The proposed model will have applications in maintenance planning for offshore wind farms, able to account for the well-being and the ability to work in technicians in sailing decisions.

Table of Contents

Table of Figures

List of Tables

1 Introduction

1.1 Overview

The most recent report by the Intergovernmental Panel on Climate Change (IPCC), states that human-induced climate change is affecting every inhabited region across the globe, by contributing to weather and climate extremes (IPCC, 2021). This report further highlighted the need to achieve the targets set at the 2015 United Nations Climate Change Conference which aims to limit global warming below two degrees Celsius (2°C) above pre-industrial temperature levels (IPCC, 2021). More recently, the COP26 Glasgow summit set more ambitious targets towards accelerating actions towards the goals of the 2015 agreement by limiting temperature increases to 1.5°C (Arora and Mishra, 2021). To deliver on this goal, countries will need to encourage investments in renewables, accelerate the switch to electric vehicles, reduce deforestation, and accelerate the phase-out of coal, to reduce global emissions by 45% in 2030 (Masood and Tollefson, 2021). In the last two decades, wind energy has been one of the fastest-growing renewable energy solutions, with electricity generation growing by 17% (273 TWh) in 2021 (IEA and Bojek, 2022). According to the International Energy Agency, this growth was possible due to increases in wind capacity additions, however, to maintain this level of growth, one of the most important areas for improvement is cost reductions for offshore wind energy.

The UK is one of the world leaders in offshore wind energy by capacity (IEA, 2021) due to its large area of shallow seas with a high wind energy potential, the potential for expansion, and the greater potential for energy generation offshore (Díaz and Guedes Soares, 2020). The UK has invested about £19 billion between 2016 and 2021 alone to support the growth of the offshore wind sector and this trend is expected to continue as generation from wind energy in the UK is central to the transition to a carbon-neutral economy (RenewableUK, 2022). However, research has shown that about a third of the entire life-cycle cost of an offshore wind farm is attributed to the operation and maintenance phase (Seyr and Muskulus, 2019). This presents a major barrier for the industry as the current trend in offshore wind energy

shows that bigger offshore wind turbines are being built and these turbines are being built further offshore (Soares-Ramos et al., 2020). This has the potential to increase the costs and risks associated with operating in harsher weather conditions and as stated by Newman, (2015), the associated costs and risks involved need to reduce if offshore wind energy is to compete with other means of energy generation. The next section presents the thesis rationale which highlights gaps in available research.

1.2 Thesis Rationale

Current research shows that the costs and risks associated with the maintenance of offshore wind farms need to reduce for the industry to compete with other energy sources. In most cases, offshore wind farms are maintained by technicians travelling out on crew transfer vessels (CTVs) to perform maintenance activities. For the technicians on board crew transfer vessels, the main concern is their comfort, safety, and their ability to do work upon arrival at offshore wind turbines (Phillips et al., 2015). However, literature on current maintenance strategies as well as literature on available operations and maintenance decision support tools shows that the *sail and not-sail* decisions associated with maintenance planning are mostly dependent on factors such as weather, sea-state, and the availability of maintenance resources (Stock-Williams and Swamy, 2019). This exposes some uncertainties in maintenance scheduling as research shows the welfare of technicians in transit is rarely considered and where accounted for in maintenance strategies, it is usually with regard to the number of technicians (Scheu et al., 2012; Besnard et al., 2013; Endrerud and Liyanage, 2015; Dalgic, Lazakis, Dinwoodie, et al., 2015), the length of shifts (Scheu et al., 2012; Besnard et al., 2013; Dalgic, Lazakis, Dinwoodie, et al., 2015), the number of technicians per service order (Tan et al., 2016), number of service orders per technician (Dawid et al., 2016), the technician types (Irawan et al., 2017), and technician availability (Tan et al., 2016; Dawid et al., 2016; Irawan et al., 2017). This raises additional concerns as research shows that vessel motions during transits to offshore wind farms can cause discomfort (Mansfield, 2005; Scheu et al., 2018) and seasickness (Matsangas et al., 2014) to the technicians on board which can affect the ability of technicians to perform complex tasks. Additionally, the current guidance on seasickness-related issues states that individuals feeling the effects of seasickness are to

stay on board the vessel until the effects subside (G+, 2020), and the available guidance on the exposure of workers to accelerations applies thresholds to the magnitude of acceleration experienced in a workday. This creates further uncertainties such as increased waiting times from exposure to seasickness, and uncertainties where offshore wind farms are assessable based on typical crew transfer vessel limits of operation of 1.5 m of significant wave height, but exposure to vessel motion is unacceptable (Scheu et al., 2018). Therefore, there is a need to account for the comfort and health of technicians in maintenance planning in order to optimise the *sail and not-sail* decision-making process associated with maintenance scheduling in offshore wind farms. . The next section outlines the thesis aim, the thesis objectives, and the benefits of this research.

1.3 Aims, Objectives, and Benefits

This research aims to improve the decision-making process of operation and maintenance in offshore wind farms by accounting for the welfare of technicians in maintenance procedures in terms of their comfort, health, and their ability to do work upon arrival at offshore wind farms for maintenance. Simply put, this thesis aims to develop a risk-based decision support tool that predicts *sail or not sail* decisions based on the comfort level and the percentage of technicians likely to be seasick during a transit. To achieve the thesis aim, this thesis achieves some major objectives.

1.3.1 Objectives

The research objectives are:

- **Objective 1:** Model the comfort of technicians during transits on Crew Transfer Vessels using whole-body accelerations.
- **Objective 2:** Model the health of technicians during transits on Crew Transfer Vessels using the estimated incidence of motion sickness.
- **Objective 3:** Develop a criterion-based decision-making model for maintenance scheduling based on technician welfare in order to aid the *sail or not-sail* decision-making process of maintenance scheduling.

- **Objective 4:** To explore the potential of near-real-time metocean data for decision-making in the management of offshore wind-farm maintenance.

1.3.2 Benefits

In research, the application of human exposure to vibrations in operation and maintenance planning for offshore wind farms is rare, as most models are largely dependent on weather and sea state. However, research shows that vessel motions can have negative effects on technicians (Mansfield, 2005) which in turn can affect the performance, the ability to do work, and the health of technicians. As such, this research can improve planning practices and add knowledge to the existing literature by exploring risk-based decision-making in maintenance planning using the comfort and the likelihood of seasickness in transit as deciding factors. This is particularly relevant as traditional operating limits can make access to an offshore wind turbine possible but exposure to vibration might make transits uncomfortable and increase the possibility of technicians getting seasick. As such this research not only takes the well-being of technicians into consideration but also their safety and effectiveness as the symptoms of discomfort and seasickness caused by vessel motions can lead to work being done incorrectly or inefficiently or lead to workplace incidents. In addition to the effect on the well-being of technicians, symptoms of discomfort and seasickness can lead to the inability of affected technicians to do work or result in increased waiting times (Scheu et al., 2018). Therefore, by implementing comfort and motion sickness-based limitations in the *sail or not sail* decision-making, the model developed in this thesis can allow wind farm operators to apply more holistic decision-making to cater to human welfare and by so doing create a positive environment for technicians which can have an effect on employee job satisfaction and a multiplying effect on productivity (Natasha Fogaça and Francisco Antônio Coelho Junior, 2016; Salas-Vallina et al., 2020). In terms of cost, the developed model can reduce the risk of long waiting times in cases where Crew Transfer Vessel operational limits make a wind farm assessable but the experienced motions cause seasickness or discomfort-related incidents and result in missed work objectives. Additionally, in exploring human response to vessel motions, this research adds to the existing literature by exploring the use of near-real-time metocean data for decision-making. As such, this research provides a framework for assessing

technician comfort and health using near-real-time metocean data which can have further applications in other operations and maintenance activities. The next section presents an outline of the chapters contained in the thesis with a brief description of the chapter contents.

1.4 ~~Background~~ Overview of Methods

To explore human response to vessel motions at sea, this research uses data from vessel motion monitoring systems (VMMS) that have been deployed on twelve (12) participating crew transfer vessels of different sizes, operating across four (4) different wind farms in the North Sea. The vessel motion monitoring systems were each fitted with six-directional motion sensors that recorded translational and angular accelerations, Global Positioning Systems (GPS) that recorded the vessel's longitude and latitude positions during transits, an automatic identification system that recorded the vessel's information, and a 4G antenna. The data from the vessel motion monitoring systems were made available to this research from the SPOWTT project which was aimed at improving the safety and productivity of offshore turbine technicians (Earle et al., 2021). To describe the sea state during transits, this research explores the use of open-source oceanographic data synchronised with GPS data from the vessel motion monitoring systems to describe the sea state following the transit routes of the participating crew transfer vessels. The environmental data used in this study included significant wave height, peak wave period, wave direction, current velocities, sea surface height, and wind velocities. Following guidelines from the ISO 2631-1 (ISO 2631-1, 1997), mathematical signal processing was used to estimate variables of composite weighted vertical acceleration and Motion Sickness Incidence used to define the comfort and health of technicians in transit. An exploratory analysis process is used to determine the input variables from the vessel motion monitoring system data and the environmental data most relevant to the prediction of estimated composite weighted acceleration and Motion Sickness Incidence. The relevant variables are then used to model the comfort and health of technicians during transits. Operational limits were applied to the model outputs from the comfort and heath-based models which were then used as input variables for a welfare model which delivers *sail or not sail* decisions based on the comfort level and the percentage of technicians likely to be seasick during transits to offshore wind farms. The welfare model is shown to have the

potential of improving the decision-making process in maintenance planning by providing estimations of the welfare of offshore wind farm technicians.

The image in Figure 1.1 presents an overview of the methodology used in this research to achieve the thesis aim and objectives.

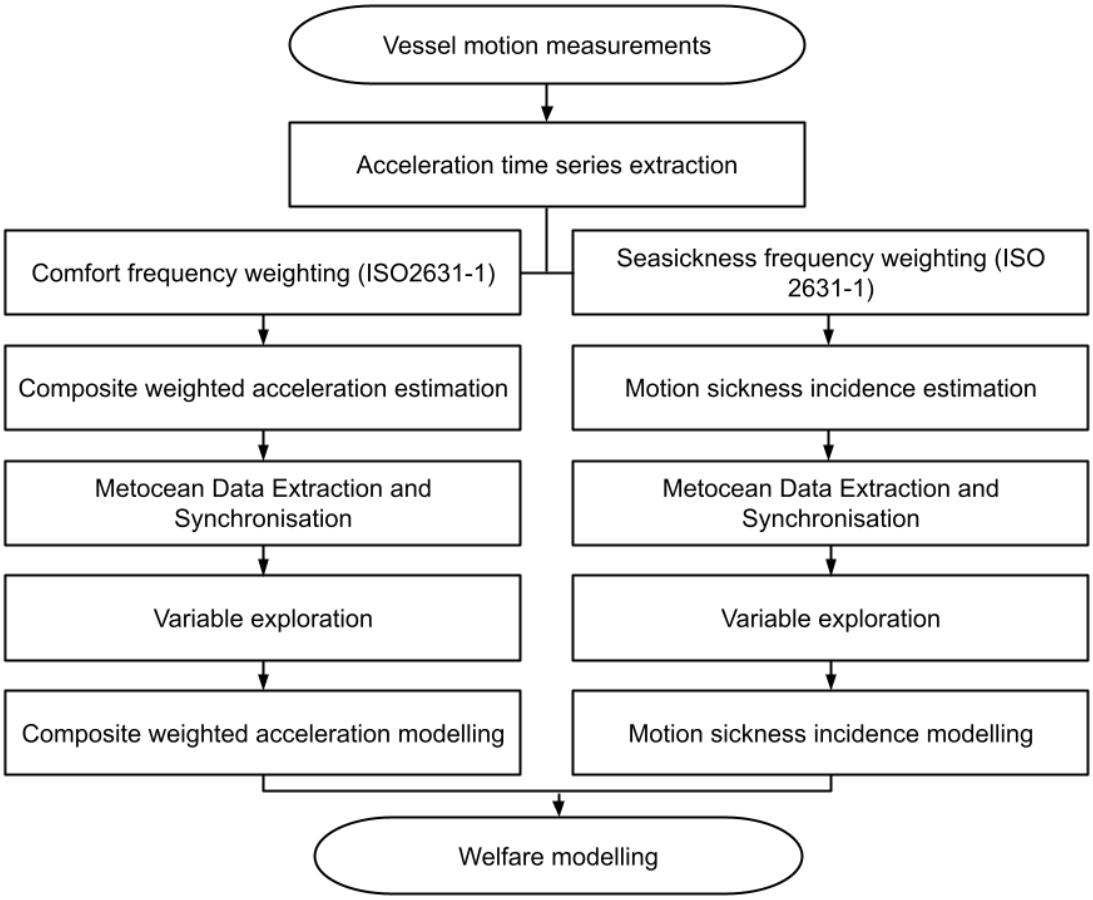

Figure 1. 1 Thesis workflow for assessing the welfare of technicians

Figure 1.1 shows the research workflow for assessing the welfare of technicians on crew transfer vessels. The initial phases of the workflow involve the measurement of vessel motions from vessel motion monitoring systems deployed on crew transfer vessels from which acceleration data can be extracted and analysed. The acceleration data is used to define health and comfort variables from Motion Sickness Incidence and Composite Weighted Acceleration parameters, respectively, with appropriate frequency weightings, applied following the guidelines of the ISO 2631-1, (1997). Following this, sea-state variables are defined using open-source oceanographic data products able to be used for hindcast analysis and forecast predictions. The defined sea-state variables are extracted and synchronised with

vessel operational variables which create a dataset for analysis and modelling. Significant relationships between variables are explored to identify the variables most relevant to the prediction of Composite Weighted Acceleration and Motion Sickness Incidence and Composite Weighted Acceleration and Motion Sickness Incidence are both modelled from the relevant input variables explored. Operational limits were applied to the outputs from the comfort-based model, which predicted Composite Weighted Acceleration, and the health-based model which predicted Motion Sickness Incidence and used as model inputs for the welfare model which predicts *sail or not sail* decisions based on the magnitude of Composite Weighted Acceleration and the percentage of Motion Sickness Incidence from the predictions of the comfort and health-based model, respectively. The next section presents an outline of the chapters contained in the thesis with a brief description of the chapter contents.

1.5 Thesis Structure

This thesis is divided into six chapters which have been arranged logically to promote understanding. This first chapter provides an overview of the research, the research rationale, the aims and objectives of the project, the benefits of this research in operation and maintenance, and a thesis structure. The second chapter provides a critical review of relevant literature relating to the thesis aims and objectives. This chapter describes the operation and maintenance of offshore wind farms, outlines uncertainties in operation and maintenance, provides an introduction to offshore wind energy as a way of introducing vessel response to sea-state, and presents a review of human response to vessel motions brought about by sea-state. The third chapter describes the methodology applied in this research in achieving the thesis aims and objectives. This chapter describes the limitations encountered during the course of the project, describes the instruments used for data collection and data used analysis, describes the project sites and timescales, and presents the data processing, data analysis, data visualization, and modelling processes used. Chapter four presents the results of the project analysis. This chapter includes a presentation of the results from meteorological data, a presentation of the results from the *in-situ* data, a presentation of the results from the instantaneous descriptive analysis, a presentation of the results from the daily descriptive analysis, and the results from the best-fit modelling of comfort using Composite Weighted

Acceleration, health using Motion Sickness Incidence, and welfare using Composite Weighted Acceleration and Motion Sickness Incidence. Chapter five provides the analysis and discussion of the results from the fourth chapter. This includes an analysis and discussion of objective one of this thesis, an analysis and discussion of objective two, an analysis and discussion of objective three, and an analysis and discussion of objective four. Finally, the sixth chapter includes a summary of the thesis findings and concluding remarks on the thesis. Following this, a reference list is provided with all the references used in this thesis. The next chapter presents a review of relevant literature relating to offshore wind farms, their maintenance, an introduction to wave theory, and literature on the vessel and human response to the sea state.

2 Background and Literature Review

2.1 Introduction

This chapter provides an overview of the available literature in the areas concerning the operation and maintenance of offshore wind farms as they relate to the human response to accelerations caused by sea state. A critical analysis of the most relevant studies and publications in this research area is presented with an exploration of available methodologies and their results in order to highlight the relevant gaps in research and establish a framework to achieve the thesis research aims and objectives.

This chapter is separated into sections. This first section of this chapter presents a brief introduction and outlines the sections contained within this chapter. The second section presents an introduction to offshore wind energy by discussing its role as a viable source of renewable energy that could mitigate the effects of climate change and presents a description of the mechanism for generating energy from the wind. The third section of this chapter describes operation and maintenance in offshore wind energy, describes the different types of maintenance operations, the resources required, and the main influential factors affecting offshore wind operations. This section also explores available research in maintenance strategies for offshore wind farms and highlights some uncertainties that exist in maintenance operations, thereby, expressing the need to improve maintenance scheduling as a way of optimising operations and maintenance in offshore wind farms. The fourth section presents an introduction to wave theory to lay the foundation for exploring the response of vessels to sea states during maintenance transits. The fifth section of this chapter explores the literature on vessel responses to accelerations caused by sea-state while section six explores the literature on the human response to accelerations including the effect on the comfort of humans and the effect on the health of humans. This section also explores relevant methodologies for assessing the comfort and health of humans exposed to accelerations during transits. Here relevant gaps are addressed, and section seven provides a summary of the key findings from the literature review. The image in Figure 2.1 below presents the described sections above for this chapter

Section 2.1	• Introduction
Section 2.2	• Introduction to offshore wind energy
Section 2.3	• Operations and maintenance of offshore wind
Section 2.4	• An introduction to wave theory
Section 2.5	• Vessel response to sea-state cause accelerations
Section 2.6	• Human response to sea-state caused accelerations
Section 2.7	• Summary

Figure 2. 1 Chapter structure by sections

2.2 Introduction to Offshore Wind Energy

This section introduces offshore wind energy as a viable renewable energy source capable of meeting global energy demands. It describes wind turbines, the main components of wind turbines, and how power can be generated from the wind using wind turbines.

In recent years, the need to reduce the impact of climate change has become more apparent with current targets for emissions reduction set at limiting the increase in average global temperature to below 2˚C above the pre-industrial levels (IPCC, 2020). The International Renewable Energy Agency (IRENA, 2019) states that coupled with energy efficiency, renewable energy is a key contributor to mitigating the effects of climate change and can provide 90% of the carbon dioxide emission reductions needed by 2050. According to the International Energy Agency (IEA), however, renewable energy only accounted for 23.2% of global power generation in 2019 (IEA, 2020). There is, therefore, a need for more research and development into renewable energy sources and into improving energy generation from these sources.

The most promising renewable energy sources in recent years have been wind and solar photovoltaic technologies which in 2019 accounted for 64% of the 6% increase in renewable energy generation (IEA, 2020). This trend is projected to continue as cost reductions and advances in technologies in wind and solar PV make both technologies viable replacements for traditional means of energy generation (IEA, 2020). Wind energy is one of the most cost-

efficient renewable technologies (Hevia-Koch and Klinge Jacobsen, 2019; IEA, 2020), with the technically accessible amount of energy reaching up to 300 million GWh per year, according to Ehrlich, (2013). Modern wind energy is generated either onshore, where wind energy is generated on land, or offshore, where wind energy is generated at sea. As one of the cheapest sources of energy, onshore wind energy can compete with conventional forms of energy generation, however, some disadvantages this form of energy generation has over offshore wind energy generation include land use, visual impacts, and noise pollution as highlighted by Hevia-Koch and Klinge Jacobsen, (2019). On the other hand, offshore wind energy is considerably more expensive with high capital costs, however, according to Díaz and Guedes Soares, (2020) in their review of the status of offshore wind farms, the major reasons for the interest in offshore wind energy over onshore wind energy are higher wind speeds, reduced noise pollution, and reduced visual impacts. Due to the United Kingdom's large wind resource, investments into wind energy have continued to grow with more investments going into offshore wind recently, recording a sustainable growth of 10,383 MW in 2020 - a 4.1% increase from the previous year (IRENA, 2021). Similarly, the global offshore wind industry is projected to grow from 14 GW, recorded in 2016, to 41 GW in 2022 with no signs of slowing down (IRENA, 2021).

2.2.1 Power from Wind

Electricity from wind energy is usually generated using wind turbines. Wind turbines extract energy from the wind by converting the kinetic energy in the wind to electrical energy as air flows around the blades of a wind turbine and lift and drag forces from the wind act upon the blades turning the rotor which generates electricity through a generator. Current turbines are usually classified by the orientation of their rotors to the ground including vertical axis wind turbines (VAWTs) with rotors parallel to the ground, and horizontal axis wind turbines (HAWTs), which have rotors perpendicular to the ground (Andrews and Jelley, 2007).

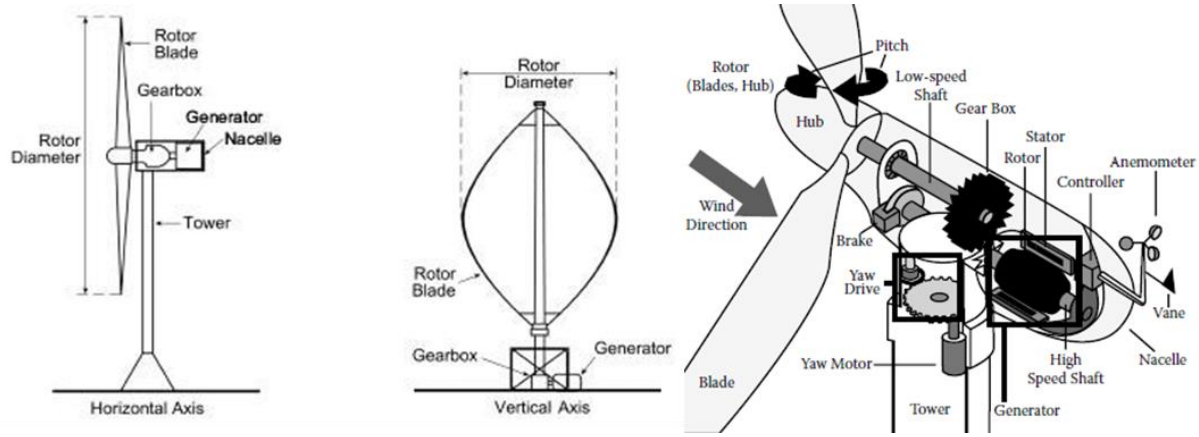

Figure 2. 2 From left to right: i. Horizontal and vertical axis wind turbine; ii. The main components of a wind turbine (Salem, 2016).

Figure 2.2 presents an illustration of a horizontal-axis wind turbine and a vertical-axis wind turbine on the left, and an illustration of the main components of a typical wind turbine on the right.

The mechanism of operation for both classifications of wind turbines is such that the **blades** of the wind turbine capture the power from the wind in form of lift or drag forces to turn the **rotor** which transfers rotational energy to the turbine shafts. Connected to the rotor, the **low-speed shaft** transfers the rotational energy from the rotor to the gearbox which increases the speed of rotation from the low-speed shaft and transfers the rotational energy to the **high-speed shaft.** The energy from the gearbox to then transferred to the **generator** from the high-speed shaft which converts the rotational energy to electrical energy. The components of the turbine are housed in the **nacelle** and the **yaw mechanism** turns the nacelle in the direction of the wind using electrical motors and information from an **anemometer** or wind vane which measures wind speed and direction. The nacelle, rotor and blades of the turbine are carried at height by the **tower**, and the electricity generated from the generator is transported through cables to a local substation for use in the electricity grid. Therefore, the kinetic energy, K_E, of a mass of air, m, and moving through the blades of a wind turbine with a velocity U can be expressed by:

$$K_E = \frac{1}{2} \times m \times U^2 \qquad 2.1$$

The mass of air passing through the blades of the turbine, m, is determined by the density of air, ρ, the cross-sectional area of the rotor, A, and the velocity of air, U, expressed as:

$$m = \rho \times A \times U \qquad 2.2$$

Substituting equation 2.2 into equation 2.1 results in an expression for the potential power from the wind, P, expressed as:

$$P = \frac{1}{2} \times \rho \times A \times U^3 \qquad 2.3$$

However, not all wind power incident on a wind turbine is converted to energy. The fraction of power extracted by the turbine is determined by the type, size, and efficiency of the turbine. As such a power coefficient or a turbine's coefficient of performance, *Cp* is introduced to consider power output depending on a turbine's average efficiency. (Andrews and Jelley, 2007). The expression for the coefficient of power is the ratio between the power output, P_O, and the available power, *P, shown as:*

$$C_P = \frac{P_O}{P} \qquad 2.4$$

Therefore, power P, extracted from a wind turbine can be written as:

$$P_O = \frac{1}{2} \times C_P \times \rho \times A \times U^3 \qquad 2.5$$

The German scientist Albert Betz provides an estimate for the amount of energy a wind turbine can convert from the kinetic energy of the wind was given by 59.3%. This is a theoretical upper limit known today as the Betz Limit. In practice, a wind turbine is only able to extract between 35% to 45% of energy from the wind, and this percentage varies between wind velocities and the specific type and size of wind turbine (Salem, 2016). To express the output power from a wind turbine, wind turbine manufacturers use a power curve to show a turbine's performance. The power curve shows the output power of a specific wind turbine at various wind speeds. Figure 2.3 below is an image of a wind turbine's power curve.

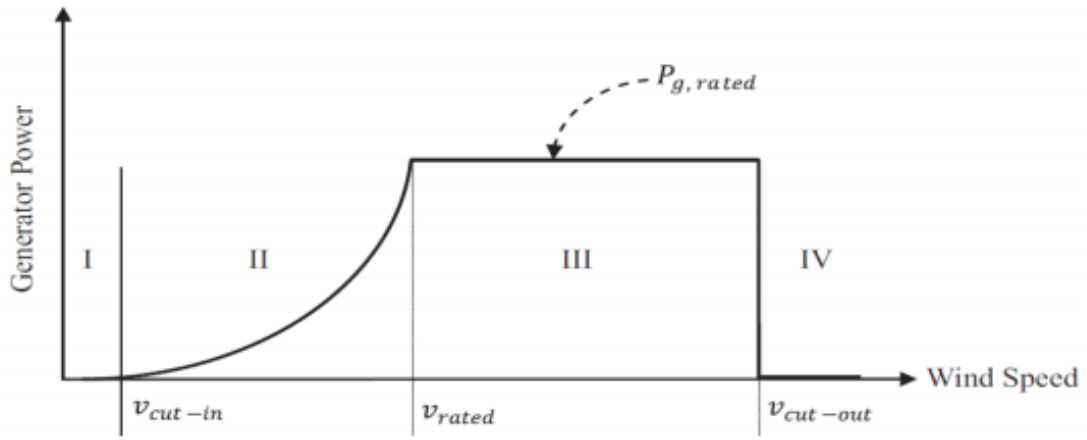

Figure 2. 3 Power curve with regions of operation (Salem, 2016)

The image shows a plot of the generator power from a modern wind turbine against the wind speed incident on the wind turbine. The power curve is divided into four sections, each representing a phase in a wind turbine's power generation. The cut-in speed, $V_{cut\text{-}in}$, is the minimum velocity at which a wind turbine will generate power. The rated speed, V_{rated}, is the speed at which a wind turbine reaches its designed rated power. The cut-out speed, $V_{cut\text{-}out}$, is the speed at which a wind turbine exceeds safe operations and is shut down. In Figure 2.3 above, the operating regions of a modern wind turbine are given. In section (I), no power is produced before the cut-in speed. The second section of Figure 2.3 (II) shows the region where the cut-in speed is reached, and power is generated but not at the wind turbine's designed rated power. In section (III), full power production is achieved when the wind speed reaches the rated speed of the wind turbine, and the desired power is generated labelled $P_{g\text{-}rated}$ in the figure above. In section (IV), no power is produced due to dangerously high wind speeds called cut-out speeds, and the turbine is shut down (Salem, 2016). While a wind turbine's power curve is an estimate of the performance of that wind turbine, the inevitable nature of machines means that wind turbines are prone to breakdowns which as a result, affect the overall performance of a wind turbine. The frequency of breakdowns as well as the downtime of wind turbines define the operational period of a wind turbine – referred to as the availability of a wind farm. This is exacerbated in the case of offshore wind farms where access to offshore wind farms in harsh marine conditions could also extend the downtimes of offshore wind turbines, which in turn increases the cost associated with maintaining offshore wind turbines and farms. This is highlighted by Díaz and Guedes Soares, (2020) who state that the challenge the offshore wind industry faces is in improving efficiency and reducing costs,

and Feng et al., (2010) in their publication on the early experiences with UK offshore wind farms, who state that the limitations of offshore wind energy generation were in the lack of operating experience on large-scale offshore wind farms and more importantly, the possible risks of energy capture owing to low reliability and availability. Further publications have examined the operation and maintenance phase of wind farms (e.g., Röckmann et al., (2017)), pointing to the greater logistical and health & safety challenges related to the harsh marine environments of offshore wind farms and the need for better and more informed operational strategies for offshore wind energy generation. Therefore, it is important to explore the operation and maintenance of offshore wind farms to understand the costs and risks associated. The next section of this chapter explores the operation and maintenance of offshore wind farms.

2.3 Operation and Maintenance of Offshore Wind Farms

This section provides a description of operation and maintenance in offshore wind farms, the types of maintenance, resources used in maintenance activities, the uncertainties involved in operation and maintenance, and the influential factors affecting maintenance activities to highlight the areas that can be improved through the objectives of this thesis.

2.3.1 Introduction

The offshore wind industry is relatively new compared to other conventional forms of energy generation and is one of the more promising renewable energy sources. However, due to the risks of performing maintenance in rougher weather conditions offshore and the current trend of building new offshore wind farms further offshore (Soares-Ramos et al., 2020), the operations and maintenance (O&M) costs of offshore wind farms are higher than most other renewable energy sources (Xia and Zou, 2023). Apart from an increase in operational expenditure, the challenges resulting from the current trend in the offshore wind industry could include the availability of wind farms as well as the safety of O&M personnel (Xia and Zou, 2023). The next section describes operation and maintenance in the context of offshore wind farms.

2.3.2 Operation and Maintenance

Wind turbines require regular maintenance for component deterioration due to fatigue, wear and tear, failed or failing components, corrosion, and erosion. (Asgarpour and van de Pieterman, 2014). This process is often referred to as operation and maintenance (O&M) - a combined term that refers to activities that support the continuous operation of a wind turbine or wind farm and its assets. It can then be concluded that the main purpose of maintenance operations is to maintain the physical integrity of a wind farm and its assets, minimize turbine downtimes, optimise electricity generation, and increase the overall availability of the wind farm. These processes usually begin after the commissioning of a wind farm project and continue until its decommissioning at the end of its lifecycle (BVG Associates, 2019). The aspects referred to as operations in a wind farm usually refer to high-level asset management activities such as planning, administration, and environmental and remote monitoring (Hassan et al., 2013), while the aspects of O&M referred to as maintenance, involve the repair and upkeep of wind turbines within a wind farm as well as wind farm assets. These activities could include continuous monitoring of the wind turbines, inspections, servicing, and repair of critical components over the wind farm's lifetime (Sørensen, 2009). The operations and maintenance phase of an offshore wind farm life cycle in itself consists of phases which define the way maintenance is carried out. Medina-Lopez et al., (2021) describe these phases to include in-warranty operation, post-warranty operation and late-life operation. The definition of these phases is related to the entity in control of the site's running. For instance, depending on contract agreements, the in-warranty operation phase or the first 3–5 years of energy production sees the wind farm owner with limited control, the post-warranty phase allows the wind farm owner to either bring operations in-house or sign new contracts and as such, the wind farm owner needs to understand the risk associated with operations, reliability, and access. (Medina-Lopez et al., 2021). Therefore, this is a crucial phase in the life cycle of an offshore wind farm often accounting for up to a third of the cost of an offshore wind farm (Scheu et al., 2012), and according to Hassan et al., (2013), this aspect of O&M by far accounts for the largest cost, risk, and effort.

2.3.2.1 Types of Maintenance

The various activities that are described as maintenance activities for offshore wind farms are usually grouped across publications into preventive/proactive maintenance and corrective maintenance (Hassan et al., 2013; Asgarpour and van de Pieterman, 2014).

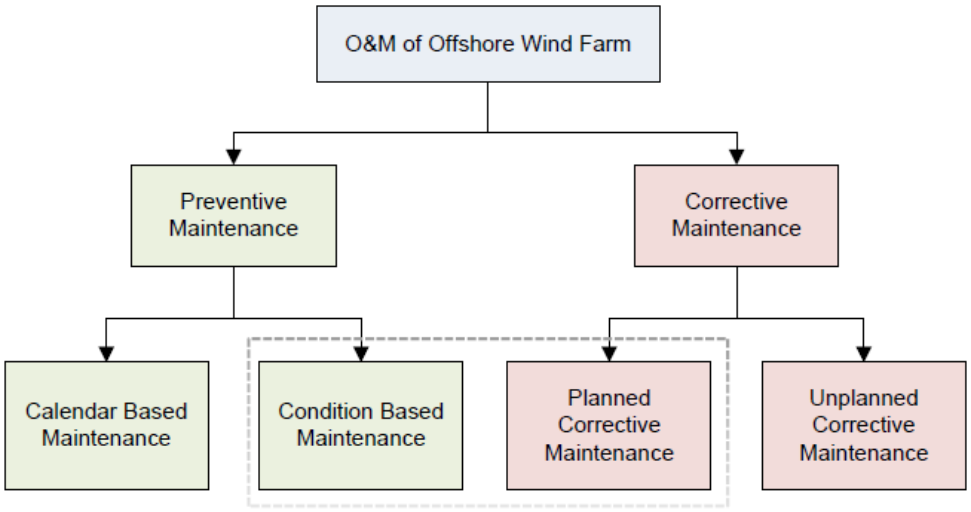

Figure 2. 4 Types of maintenance (Asgarpour and van de Pieterman, 2014).

Preventive/Proactive maintenance

Wind farm operators usually take steps to prevent and/or postpone foreseeable failures or breakdowns by either monitoring deterioration and/or performing activities that prevent these breakdowns such as minor repairs (Shafiee et al., 2016). The measures taken are referred to as proactive maintenance measures and these maintenance activities are aimed at reducing the chances of sudden system failures. Preventive maintenance can further be categorized into calendar-based maintenance and condition-based maintenance.

Calendar-based maintenance often requires scheduled maintenance activities, undertaken after a specified period to reduce the probability of system breakdowns and extend over the life of a turbine or wind farm. These activities could include inspections, planned adjustments and planned replacement of parts, and lubrication. An example of a preventive maintenance procedure is the regular inspection of the lifts within turbines to ensure that they remain functional for maintenance purposes.

Predictive maintenance or condition-based maintenance activities involve the use of sensors and advanced analytical methods to measure the degradation of a system or component. As such the component failure is not known but is expected (Asgarpour and van de Pieterman, 2014).

Corrective maintenance

Corrective maintenance on the other hand occurs after breakdowns and faults occur. These maintenance activities are carried out in order to return the wind turbine or wind farm to normal working operation. Such activities are generally more expensive than proactive maintenance activities as they require short-term planning for vessels, spare parts, and available technicians needed at short notice (Asgarpour and van de Pieterman, 2014). Additionally, faults or breakdowns that require the shutdown of a wind turbine usually lead to a loss of revenue as a decrease in turbine availability causes an increase in loss of revenue (Carroll et al., 2017). The processes involved in corrective maintenance can be further categorized into two – planned corrective maintenance and unplanned corrective maintenance.

Planned corrective maintenance occurs following the observed degradation of a component/system that results in or might result in a breakdown. Plans to address observed degradation are then put in place and maintenance is carried out on a scheduled date.

Unplanned corrective maintenance occurs after a component fails unexpectedly resulting in the shutdown of the wind turbine.

It is then clear that the type of maintenance carried out can greatly affect the cost of overall operation and maintenance for an offshore wind farm.

2.3.2.2 The cost of Operations and Maintenance

The costs of operation and maintenance in offshore wind energy can be up to a third of the overall life-cycle cost of an offshore wind farm (Scheu et al., 2012). Musial and Ram, (2010) describe the high cost of offshore wind farm projects as a major barrier to the offshore wind industry. They state that the cost of offshore wind nearly doubles that of its onshore counterpart and highlight O&M as one of the reasons for the associated high costs of offshore wind farms. An estimate of this cost is given by BVG Associates, (2019) in their guide to

offshore wind farms. They estimate that for a 1 GW offshore wind farm, O&M could amount to about £75,000 per megawatt year. Their estimates include the cost of insurance, environmental studies, compensation payments, and other internal asset costs. The chart in Figure 2.6 below represents a breakdown of the elements that contribute to the Levelized cost of energy (LCOE) for a typical offshore wind farm project where the combined cost of operations and maintenance costs amounted to 28.2% (ORE Catapult, 2022).

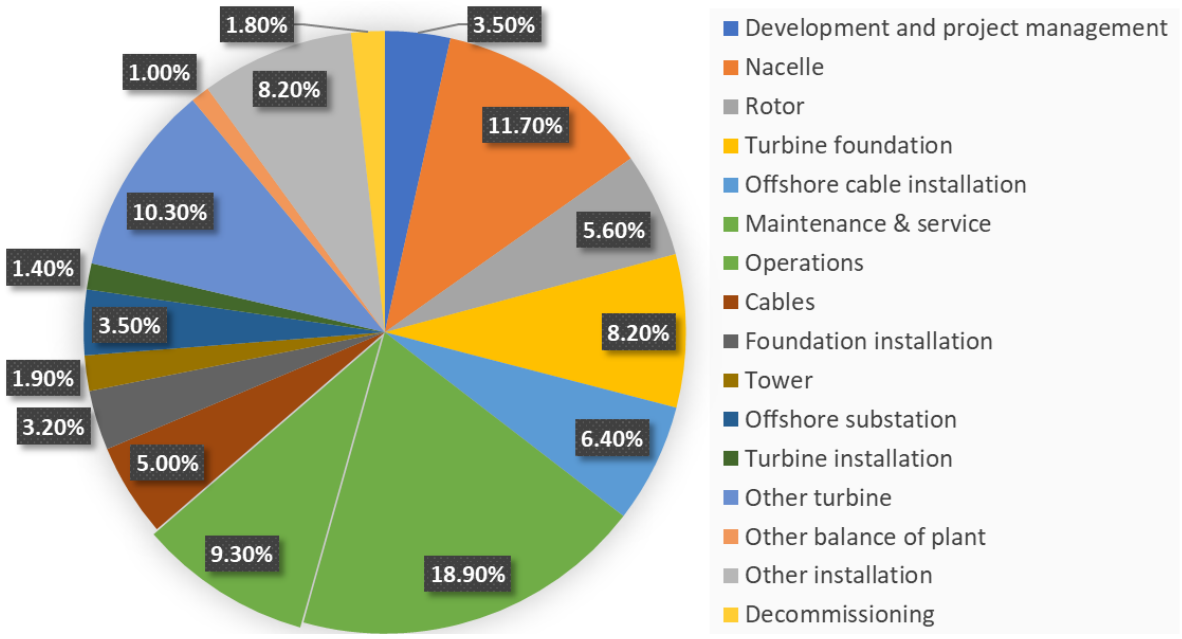

Figure 2. 5 Life-cycle cost breakdown of a typical offshore wind farm project. Adapted from (ORE Catapult, 2022).

Shafiee et al., (2016) give a good breakdown of the costs of operation and maintenance activities in their publication. They separate the cost of O&M into two parts - the operational expenses, C_O, and the maintenance expenses, C_M, expressed as:

$$C_{O\&M} = C_O + C_M \qquad 2.6$$

According to Shafiee et al., (2016), the cost of operation could relate to rental and lease payments, insurance costs, and transmission charges. This is in line with the description of operational activities by Hassan et al., (2013) where operational costs were described as high-level management activities. On the other hand, and also in line with Hassan et al., (2013), Shafiee et al., (2016) describe the costs associated with maintenance to include costs incurred by activities that maintain the availability of an offshore wind farm such as transport to repair failed turbines, cost of spare parts, and maintenance technicians who carry out maintenance

activities, etc. A vital highlight from the publication by Shafiee et al., (2016) is that due to the nature of operations activities, it is far easier to estimate the cost of operations on an annual basis. In contrast, maintenance costs vary across the type of maintenance operation needed and as such, can be difficult to estimate on an annual basis, especially with unscheduled maintenance activities, which incur higher costs than scheduled maintenance. This is worth noting as it points to the previously mentioned case study by Newman, (2015) published by ORE Catapult which found that unscheduled maintenance activities or reactive maintenance activities such as in the cases of breakdowns, and proactive maintenance activities, constituted 65% of O&M costs. It should be noted that while the case study by Newman, (2015) gives insight into the cost of O&M, different variables could also affect the associated costs such as the amount of downtime during failures which add to the cost of O&M as stated by Scheu et al., (2012) and Ravindranath, (2016). An estimation of potential cost savings due to higher availability is given by Scheu et al., (2012) where downtime losses were quantified and a strong linear correlation between availability and production losses was discovered. This shows that a small increase in availability can lead to high-cost savings. This, therefore, exposes some uncertainties in the offshore wind industry. Today, the immature nature of the offshore wind industry is one of the main reasons for the operational risks associated with reliability and energy production. However, this risk and uncertainty could reduce as the industry matures and as operations and maintenance practices improve which is a current focus in both industry and academia (Gilbert et al., 2021). This means that with the continued adoption of offshore wind energy and improvements in technology and maintenance procedures, the cost and risk involved with O&M can be reduced using improved technology as well as more efficient O&M procedures that increase turbine availability and accessibility. Nevertheless, the many moving parts of a wind turbine will still make 100% availability unattainable. As such, major improvements in the resources need to access offshore wind farms, as well as more cost-effective methods for maintenance, are vital. The next section in this chapter explores the main resources used for O&M activities.

2.3.3 Resources for Operation and Maintenance Activities

This section discusses the major resources used in the operation and maintenance of offshore wind farms. The challenges associated with each major resource are given and the available methodologies used to mitigate these challenges are discussed. The common influential

factors surrounding the use of these resources and the operation and maintenance of offshore wind farms, as discovered in the literature, are also highlighted.

2.3.3.1 Introduction

Uit het Broek et al., (2019) stated that the diverse nature of resources used in the O&M of offshore wind farms, as well as the availability of these resources, challenge the design of a cost-effective program for maintaining offshore wind farms. As the type of resources needed for maintenance activities of offshore installations differ from those used onshore, the experience from the maintenance of onshore wind farms is not entirely transferable (Michiel et al., 2019). Specialized vessels and personnel are needed in the offshore environment, which varies concerning the cost, location, and weather. The major resources currently used in the operation and maintenance phase of offshore wind are described below.

2.3.3.2 Spare parts

Often, maintenance activities require various spare parts, the supply of which offers a high potential for cost savings (Tracht et al., 2013). Usually, the sourcing of spare parts is left to the turbine supplier during warranty periods, and up to the project owner once out of warranty (Hassan et al., 2013). The transportation of these spare parts of different sizes through the harsh conditions of the marine environment often requires specialized access vessels and support equipment such as nacelle cranes, each with its limits. In order not to suffer a significant loss of revenue due to turbine downtimes from shortages, efficient maintenance strategies that consider the complexities of spare parts, their transport, and support equipment are needed (Tracht et al., 2013). A subdivision of spare parts is given by the British Standards Institution, (2010) [BS EN 13306:2010], where spare parts are separated into repairable and consumables. Consumables here refer to spare parts that do not require repair and as such tend to be lower-cost items with a relatively fixed mean time between failures; while repairable are usually expensive, plagued with low inventory levels, and variable mean time between failures (Tracht et al., 2013). An effective spare parts management system would, therefore, ensure the provision of spare parts when needed for maintenance processes and at the same time, maintain a low-cost inventory. There have been some approaches to effectively managing spare parts in available publications such as Wang and Syntetos, (2011) who used a maintenance-driven model to improve the prediction

accuracy of spare parts by estimating useful lifecycles. Another approach was taken by Tracht et al., (2013) to plan spare parts maintenance by accounting for restrictive factors, such as meteorological conditions and the availability of maintenance resources. These are a few steps taken that are necessary to mitigate turbine downtime and reduce inventory costs. The main challenges in these models appear in the uncertainties related to failure rates, availability of other resources such as access vessels to transport spare parts, available technicians to perform maintenance operations and most of all, the reliance on meteorological conditions i.e., sea state and wind speed for available weather windows to perform maintenance activities. In any case, the type of spare parts needed for a maintenance activity also determines the type of vessel needed for a maintenance operation. For instance, the carrying capacity for helicopters can only accommodate smaller spare parts and therefore, would not be suitable for maintenance operations requiring bigger spare parts. In cases like these, more specialized vessels are needed to perform maintenance operations that may have access limitations such as the influence of wave height.

2.3.3.3 Access Vessels

The deployment of vessels is crucial in guaranteeing access to offshore wind farms for maintenance activities. As Stålhane et al., (2017) state, access vessels are one of the dominant resources in the operation and maintenance of offshore wind farms with as much as 45% of the total O&M costs being vessel-related costs. The sub-sections below describe the most used access vessel in the offshore wind farm industry.

2.3.3.3.1 Crew transfer vessels (CTV).

Crew transfer vessels (CTVs) are high-speed small-sized vessels of about 12 to 30 metres able to transport between 12 to 16 technicians from onshore operations bases to wind turbines and offshore substations for O&M activities at speed up to 20 to 25 knots (BVG Associates, 2019). These vessels typically operate up to a limit of a 1.5 m significant wave height and are the most used form of transport in O&M operations due to their cost-effectiveness and speed (Phillips et al., 2015). These vessels are typically used for wind farms close to shore and in operation, crew transfer vessels press up against the turbine boat landing which allows personnel to step across to a ladder (BVG Associates, 2019; Gilbert et al., 2021).

The challenges associated with crew transfer vessels are listed in the Crown Estates 2013 publication of "A guide to UK offshore wind operations and maintenance" to include sea-state access limits of up to 1.5m significant wave height, and the risk to passengers during maintenance operations (BVG Associates, 2019). The use case of crew transfer vessels varies between wind farm operators, but a cost estimate for chartering a crew transfer vessel was given by BVG Associates, (2019) to be about £2,500 per day depending on vessel type and availability.

Figure 2. 6 Image of a crew transfer vessel (Hassan et al., 2013)

2.3.3.3.2 Service operation vessels (SOV).

Service operation vessels (SOVs) differ from CTVs in size, function, and carrying capacity. Service operation vessels are equipped with liveable quarters, a mess, welfare facilities, workshops, and storage facilities for spare parts as well as all necessary maintenance materials (BVG Associates, 2019). As such, they perform the dual function of offshore accommodations services and transport vessels. They accommodate between 50 and 100 passengers, have an operational speed of 15 knots and are equipped with a hydraulic walk-to-walk gangway. The use of the hydraulic gangway enables technicians to walk safely onto a wind turbine's platform which allows access to wind farms between 3 m and 4 m significant wave heights (BVG Associates, 2019). Typically, service operating vessels are used to maintain wind farms further offshore and will usually stay for up to three weeks at sea, thereby, eliminating the daily transits associated with crew transfer vessels. This means that technicians are almost always on-site depending on shift patterns (Orsted, 2019). BVG

Associates, (2019) estimate the cost of Service Operating Vessels to be about £25,000 per day depending on the type, size, and region.

Figure 2. 7 Image of a service operation vessel (Orsted, 2019)

2.3.3.3.3 Helicopters

While not as well established as using workboats to access offshore wind farms, helicopters have been used as access vessels for both O&M and search and rescue activities for a few years. Hassan et al., (2013) highlight the use case for helicopters for O&M in the offshore wind industry, stating that crew transfer vessels and service operating vessels are relatively inexpensive and carry significantly more technicians than helicopters, however, helicopters improve response times and accessibility to wind farms. This is because helicopters are not limited by sea conditions although wind speed and visibility can impact their use case. Hassan et al., (2013) go further to explain that the major reasons for low adoption in operations are cost and carrying capacity. As such, there is some uncertainty as to how widespread helicopter use might be in the future. BVG Associates, (2019) estimates the cost to charter a helicopter to be about £1.5 million per year depending on a lot of factors including type, availability, and contracts.

Figure 2. 8 Airbus helicopter accessing a wind turbine (Durakovic, 2020)

There are more specialized vessels used in O&M activities such as jack-up vessels which are self-elevating platforms used for transporting and lifting large components of wind turbines, however, these are used in both the construction and operational phase of offshore wind farms.

2.3.3.3.4 Daughter craft

Daughter crafts are hybrid vessels that transport technicians between SOVs, where they live offshore, to turbines to perform maintenance activities. In addition to this, daughter crafts can perform emergency safety and recuse operations as well as support trips to ports. These vessels can support about 12 personnel (24 persons in emergencies), are about 12 m in length and can travel at speeds reaching up to 25 knots (Snyder, 2020; Reid, 2021).

Figure 2. 9 Image showing a daughter craft (Buljan, 2021)

2.3.3.4 Technicians

Wind farm technicians perform maintenance activities on turbines. In the offshore wind industry, technicians are usually trained in both technical and health and safety skills with several certifications to ensure they are qualified to fulfil the roles needed by offshore wind farms while ensuring their safety as well as others. According to BVG Associates, (2019), about £500 per MW per year could be spent on training technicians. An interview conducted by Mette et al., (2018) on "healthy offshore workforce" describes the regular shift hours for offshore technicians to be twelve hours a day with a work schedule that consists of two weeks of work and an accompanying two weeks off work or free time.

Figure 2. 10 Image of a technician on the nacelle of an offshore wind turbine (Hassan et al., 2013)

The maintenance resources described above work together to improve the availability of offshore wind farms. In Hassan et al (2013) 'Guide to UK offshore wind operations and maintenance', the availability of a wind farm is a measure of its performance and access to offshore wind farms is one of the major hurdles in maintaining or increasing availability. The publication states that getting technicians on and off turbines and substations is vital to O&M, especially in cases of unscheduled maintenance. It goes on to highlight factors affecting access such as transit time and weather constraints and states that maximising access and availability will ultimately result in reducing the cost of energy. The next section discusses the relevant influential factors affecting the operations and maintenance of offshore wind farms.

2.3.4 Influential Factors in the Operation and Maintenance of Offshore Wind Farms

This section discusses the major influential factors in the operation and maintenance phase of offshore wind energy. Special attention is given to the role of wave height, which is largely considered the most influential factor in an offshore environment, in the accessibility of wind farms and the use of its resources. Gaps in the literature are explored regarding the effect of wave motions on wind farm technicians in transit and their ability to do work.

2.3.4.1 Introduction

The general conclusion from most publications is that the major factors influencing the scheduling and cost of maintenance in offshore wind farms are the rate of turbine failures, weather, and the availability of maintenance resources including spare parts, access vessels, and maintenance crews (Hassan et al., 2013; Seyr and Muskulus, 2019). Other factors such as regulations and health and safety organisational procedures designed to reduce risks can also affect maintenance procedures in offshore wind farms (Seyr and Muskulus, 2019).

2.3.4.2 Failure rates

Both offshore and onshore wind farm projects are designed to last between 25 to 30 years of operation. It is therefore important to maintain the reliability of wind farms throughout their operation. The complex nature of the components working in wind turbines means that turbines are prone to failure. One of the more cited definitions of a failure in wind turbines is given by Kaidis et al., (2015), in which a wind turbine failure is said to be the inability of a subassembly to perform its designed function. They state that for a wind turbine to be considered to have a failure, the duration of the event must be greater than an hour and must require human intervention to return the turbine to its original state. In the assessment by (Kaidis et al., 2015), pitch systems, frequency converters, and control systems were identified to have the greatest failure rates and verification of the bathtub curve as a broad representation of failures in wind turbines was given. The bathtub curve has long been used to represent the general change in the frequency of failure throughout a machine's operation.

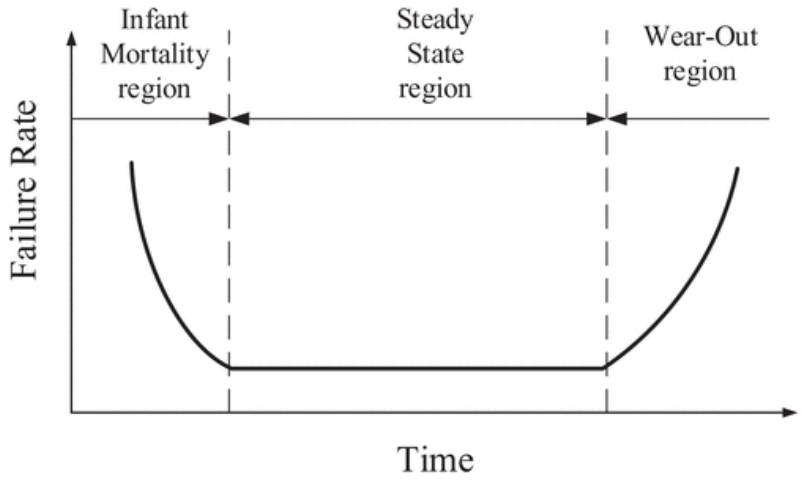

Figure 2. 11 Image of a bathtub curve (Zheng et al., 2020)

Figure 2.11 below represents the bathtub curve in the context of wind turbines. The bathtub curve shows a change in the rate of failure over the life cycle of a typical wind turbine and is separated into regions. The infant mortality region shows a high rate of failures usually at the warranty phase of the life cycle of a wind farm. This high rate gradually reduces coming to a period of low and stable failures called the steady-state region. The rate of failures then increases following this to a point of deterioration called the wear-out region, which often is at the end of a turbine's life cycle (Zheng et al., 2020). Turbine failures are usually recorded by the SCADA system.

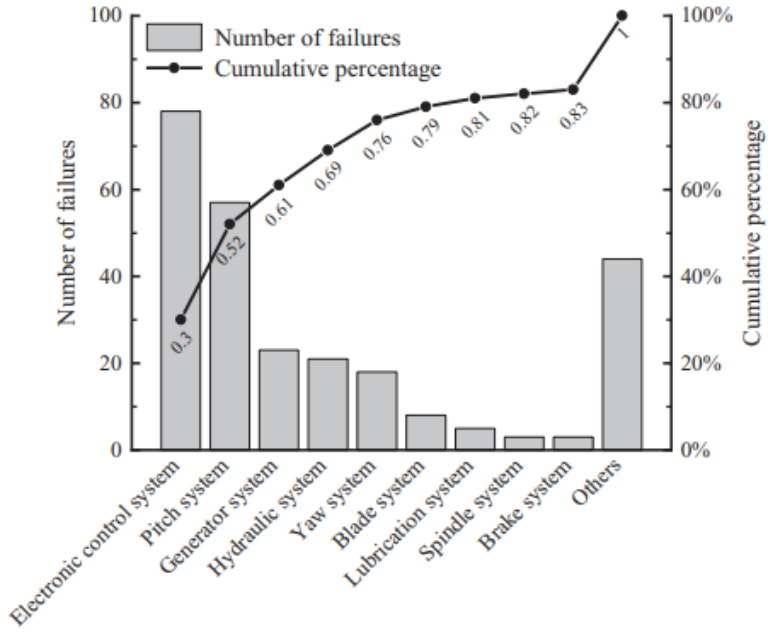

Figure 2. 12 Number of system failures in a wind turbine (Zheng et al., 2020).

Figure 2.12 shows the number of system failures recorded by a SCADA system for a wind turbine. The figure gives an expression for the frequency of failures for various components in a wind turbine. The various failures can either require scheduled maintenance or corrective maintenance as the result of a wind turbine failure – the state where the wind turbine is no longer operational. This in turn results in additional costs to O&M as highlighted by Scheu et al., (2012) and Ravindranath, (2016). There have been further breakdowns of the relationship between failure rate and the cost of O&M including a more recent publication by (Zheng et al., 2020) who used the mean time between failures in a wind turbine to evaluate the intensity of failure, thereby, representing the conditional probability of a failure to occur. Their final comprehensive evaluation was used to calculate the proposed availability of wind turbines –

the number of hours a wind turbine is operational. Overall, the frequency of failures in wind turbines is still a topic of vital import, with more research and funding being put into evaluating its relationship to cost and modelling this relationship to aid maintenance strategies. Hassan et al., (2013) express the need for cost reduction associated with failures in discussing the key concepts of O&M in offshore wind farms. This report also highlights access to offshore wind farms as a major concept with a focus on overcoming the operational limitations of weather and sea conditions. The next subsection of this thesis discusses the weather and sea conditions as major influential factors in the O&M of offshore wind farms.

2.3.4.3 Weather and Sea Conditions

In most relevant studies, one of the most important factors in accessing offshore installations is the sea state. Sea-state is a term that usually combines meteorological conditions such as wave height, wave direction, and wave period (Seyr and Muskulus, 2019). These meteorological factors play an important role in the costs and risks involved in O&M procedures and in the case of wave height, often determine whether a maintenance operation will take place. Currently, significant wave height (Hs) is used as a metric in the offshore wind industry to express wave conditions and in most cases where Crew Transfer Vessels are used, O&M activities are usually carried out at a threshold of 1.5 m (Röckmann et al., 2017). However, each access vessel has its own significant wave height threshold of operability, such as 4 m for Service Operation Vessels (SOVs) (Scheu et al., 2018). This is particularly important as stated by Röckmann et al., (2017), the accessibility of a wind farm by a vessel is correlated with the occurrence of significant wave heights. As such if the cumulative occurrence of significant wave heights equal to or less than 1.5 m is 80% in the case of Crew Transfer Vessel use, this would mean that for 20% of the time, the wind farm would be inaccessible. Subsequently, for an access vessel with a 4.0 m threshold, if the cumulative occurrence of 4.0 m significant wave height increases to 90%, this could mean a possible 90% decrease in access days. Similar statements are made by Röckmann et al., (2017) and Stavenuiter, (2009) who state that an increase in safe working heights from 1.5 m to 2 m could increase accessibility by 15% for certain vessels and an increase to 3 m could increase the number of access days to 310 days a year. This could therefore cumulate in a significant cost reduction in offshore wind energy due to the relationship between accessibility and cost. Current solutions to the possibility of larger wave heights are specialized vessels with

specialized systems for the safe transfer of O&M personnel such as walk-to-work hydraulic systems in service operating vessels that compensate for the vessel's motions. This, therefore, highlights the need for forecasting both the accessibility of wind farms and also in decision-making during scheduling as research has shown that the accessibility of offshore wind farms is greatly constrained by the sea-state (Miedema, 2012; Röckmann et al., 2017). Domain knowledge of specific offshore sites, as well as personalised interviews, inform that other meteorological factors can also influence O&M activities such as ocean tides and currents. The decision of whether an operation is going to be performed, therefore, depends on the threshold created by weather windows, the application of which is determined by weather forecasts. The uncertainties in weather forecasts, therefore, can be a cost-driving factor, as wind farms and costs of activities are primarily driven by the expected offshore operational hours and waiting times for weather windows, suitable for offshore operations (Gintautas and Sørensen, 2017). Generally, short-term meteorological forecasts are used to inform the decision-making process in maintenance planning, but meteorological forecasts can be imperfect and as stated by Browell et al., (2017), such imperfections could affect this decision-making process. The study by Scheu et al., (2012) on maintenance strategies for offshore wind farms showed a strong dependence between the number of operations and the reliability of the short-term weather forecasts. Similar results expressing the limitations of weather imposed on the number of operations were also found in an earlier study by Lange, (2005) while analysing the uncertainty in power predictions from wind energy. He found that deviations in predicted forecasts and measured forecasts lead to financial uncertainties in wind farms. There is, therefore, a need for continued improvements to optimize the different aspects of O&M such as reducing cost, improving decision-making, and reducing risks (Feng et al., 2010; Musial and Ram, 2010; Newman, 2015). Further reference to the importance of better forecasting in O&M was in a publication by Gintautas and Sørensen, (2017), who stated that more reliable weather forecasts and as such weather windows, would result in better accessibility. In addition, Seyr and Muskulus, (2019) stated that there is a need to improve the decision-making processes in operation and maintenance by regarding more influential factors, including uncertainties, and by acquiring and analysing more accurate data.

2.3.4.4 Availability of maintenance resources

The maintenance resources used in the offshore wind industry are described in section 2.3.3 of this thesis including spare parts, access vessels, and maintenance technicians. Currently, there are no standard practices or procedures for the procurement of maintenance resources as such, practices differ between wind farm operators and between wind farms. The relationship between the maintenance resources is, however, explained by Seyr and Muskulus, (2019) who state that to repair failures in offshore wind farms, trained technicians capable of performing desired maintenance are crucial and as some maintenance procedures not only need technicians but tools and spare parts, and so the availability of needed tools and spare parts is also important for the completion of maintenance activities. Additionally, to transport technicians as well as tools and spare parts from onshore bases or ports to offshore wind turbines transport vessels are required. The type of occurring failure determines the number of technicians needed, the equipment needed, and the access vessel used. As such, all three resources need to be considered in maintenance planning. The next section describes typical maintenance strategies used in maintaining offshore wind farms.

2.3.5 Maintenance Strategies

Section 2.3.4 describes the various factors of importance in the operation and maintenance of offshore wind farms and highlights the need for the consideration of these factors in maintenance planning. This section gives a generalized view of maintenance strategies in offshore wind farms and evaluates relevant O&M methodologies.

In daily O&M planning and activities, choices of maintenance resources, as well as relevant influential factors that might affect operations, need to be taken into consideration to successfully complete a maintenance activity. A publication by Stock-Williams and Swamy, (2019) gives a good description of this typical maintenance planning process in stages using the image in Figure 2.13 below.

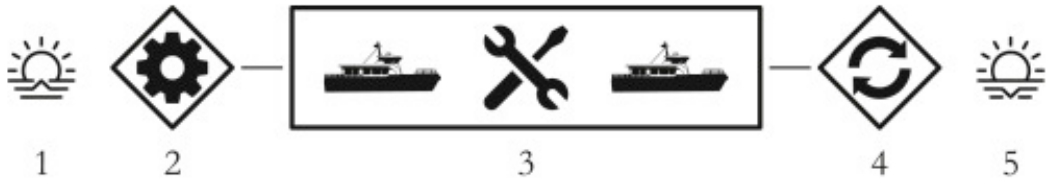

Figure 2. 13 A schematic overview of the daily maintenance process of an offshore wind farm (Stock-Williams and Swamy, 2019).

In the first stage, an offshore wind farm manager reviews a list of pending maintenance activities in the morning. A transfer plan is then created from this in stage two which assigns maintenance service orders to technicians and in turn, assigns the technicians to vessels based on the nature of the maintenance required and the available weather forecast. Stage three sees the implementation of the transfer plan and at stage four, upon the return of the vessel to port, service orders are updated. In the fifth stage, a preliminary transfer plan is made for the next day using updated service orders and current pending maintenance. An important challenge highlighted by Stock-Williams and Swamy, (2019) is the presence of complications that could arise in the implementation of a transfer plan. They state that these complications can include differences in expected maintenance durations and inaccuracies in weather forecasts which can make some offshore turbines inaccessible or make some technicians too seasick to perform work. Uncertainties like these promote the need for better-informed decision-making in maintenance strategies as well as improved technologies that can not only reduce the cost of operations, but also the risks involved.

The following subsections provide a summary of the maintenance strategies and tools applied for different factors associated with operation and maintenance in the available literature. These include strategies specific to the frequency of failures, strategies specific to the optimization of maintenance resources, strategies specific to the optimization of access vessel use, and strategies for optimizing sea state.

2.3.5.1 Summary of Relevant Operations and Maintenance Models

The earliest publications on wind farm strategies concern onshore wind farms, however, these methods are not entirely transferable due to the differences in means of transport and the influence of external environmental factors. More recent publications into maintenance

strategies in offshore wind farms have observable differences in the aspect of O&M being optimized.

Various researchers have attempted to optimize maintenance strategies in wind farms to reduce the cost of operation and maintenance by modelling the frequency of failures. In optimizing failure rate, the observable difference between methods lies in the presentation of failure, either in using historical data to predict failure or using assumed mean time between failures calculated from observed failures (Seyr and Muskulus, 2019). Rademakers et al., (2008) made a compelling assessment for estimating the cost of O&M in offshore wind farms by modelling costs through failure rates. Using an O&M Cost Estimator (OMCE), they processed information from SCADA systems, load measurements, O&M data, and condition monitoring collected over 5 years to estimate one to 5 years' future cost. They denote that the failure frequencies of the different wind turbine components have a significant influence on the O&M costs of an offshore wind farm. The type of maintenance required, and the strategies taken for maintenance activities then determine the overall availability of offshore wind farms. Modelling the failure of wind turbine components has for this reason been of particular focus in reducing costs. In recent research, the modelling of failure across publications using wind turbine components has been explored from as few as three components (Hofmann and Sperstad, 2013; Sperstad et al., 2014), to as many as nineteen components (Endrerud et al., 2015). A comprehensive summary of relevant failure models is given by Seyr and Muskulus, (2019) in a review of decision support models for O&M in offshore wind farms. It should, however, be noted that O&M models a representation of the input data that make up the model including the components involved in the model. Variations in effectiveness could then occur between models and between wind farms. As such a good model should incorporate all the factors that influence O&M in offshore wind farms. It should also be noted that at the time of writing, there are no widely used O&M models.

A few researchers have implemented the maintenance resources into optimizing operation and maintenance in offshore wind farms. Across publications, researchers include maintenance resources relevant to individual case studies which can describe some resources, but often do not include all resources. An interesting application where maintenance resources are applied in O&M models is the model by Besnard et al., (2013).

Their model was used in a case study when the output of the model includes the number of maintenance technicians required for an O&M activity, the estimated length of shifts, the location of accommodation, and the choice of transfer vessels and/or helicopters. Similarly, Endrerud et al., (2015) consider the availability of technicians but further separate the type of technicians required by the used case into electricians and technicians. Their model also accounts for access vessels needed with the amount of waiting time determined by the type of failure. On the other hand, publications such as Halvorsen-Weare et al., (2013) and Dinwoodie et al., (2013), focus more on optimizing vessel size by creating decision-support models that account for uncertainties in fleet optimizations across a few scenarios.

The choice of access vessel used for a maintenance activity is usually chosen based on cost, carrying capacity, response time, sea-state conditions, and safety regulations (Ravindranath, 2016). In their study on optimizing vessel fleets in O&M, Halvorsen-Weare et al., (2013) proposed an optimisation model that indicates which vessel types should be either purchased or chartered and which infrastructure is needed such as onshore ports and helicopter bases. In relating access vessel use cases to cost, Dalgic et al., (2015) developed a simulation tool to improve resource allocation costs. Their tool includes a range of access vessels that not only includes helicopters and CTVs but also jack-up vessels to support day-to-day O&M activities. In testing the robustness of O&M models, Sperstad et al., (2014) tested six decision-support tools for determining the size and composition of the CTV fleet, with the aim of reducing uncertainties in both modelling assumptions and input data. The commonality between the various models implementing vessel section as output is the use of sea-state or weather-based criteria within models. This is due to individual sea-state restrictions from the different types of access vessels such as the 1.5 m threshold for crew transfer vessels.

As one of the more important factors in O&M activities, sea-state criteria are mostly present in O&M strategies and decision-making models (Seyr and Muskulus, 2019). Improvements in modern technology have improved forecasting over the years (Seyr and Muskulus, 2019), however, inaccuracies in weather forecasts still cause complications during maintenance activities. These complications can include maintenance delays, the inability of technicians to transfer safely onto turbine platforms and reported seasickness in technicians (Stock-Williams and Swamy, 2019). A case study by the Offshore Renewable Energy Catapult concluded that new effective weather-based O&M decision-making tools and efficient O&M strategies could

potentially decrease unscheduled maintenance activities and even shift some previously unscheduled activities to scheduled maintenance activities. The report states that this shift would, therefore, go a long way toward reducing the risks and costs associated with offshore wind energy as well as signal a more mature and stable offshore wind industry (Newman, 2015). The statement by Newman, (2015) has also been emphasized by earlier reports including the assessment of barriers and opportunities in large-scale offshore wind farms by Musial and Ram, (2010) and a report on early experiences with offshore wind farms in the UK by Feng et al., (2010). A more popular model which implements sea-state in optimizing O&M called NOWIcob was developed by Hofmann and Sperstad, (2013) to reduce maintenance costs. The model assumes accurate weather forecasts for creating weather windows in modelling operations and maintenance costs. A different application was made by Dinwoodie et al., (2013) where a multivariate autoregressive time-series is used to model correlated wind speeds and wave heights in order to simulate the costs of operation and lost revenue, based on wind farm specifications, weather conditions and maintenance strategies. This study emphasises that wave height is the major factor in the accessibility of offshore wind farms and expresses the effect on the availability due to extended downtime with cost implications. Similarly, Endrerud et al., (2015) simulated the operation and maintenance phase of offshore wind operations using wave height and wind speed as integral components of logistics. The novelty in their model is that the model enables vessel fleet configuration, supply base locations, wind turbine technology, staffing and work processes. Dinwoodie et al., (2013), and Hagen et al., (2013) modelled sea state but included more than just wave height and wind speed, adding more parameters e.g., wind direction, wave direction, and wave period. They also included seasonal variations to improve their model. While estimating waiting times Douard et al., (2012) improved upon the already existing ECUME tool using meteorological site characteristics and seasonality. In so doing, their model included uncertainties in the variability in the meteorological site conditions.

The various models and methodologies apply different levels of importance to maintenance resources and influential factors in optimizing O&M activities. A notable commonality between these strategies is that most models estimate cost savings in optimizing O&M. However, Newman, (2015) and Musial and Ram, (2010) express optimizing O&M as the need to also reduce the risks involved in O&M to make the offshore wind industry more

competitive and more attractive to employees, reducing turnover of staff. Additionally, Hassan et al., (2013) in their guide to UK offshore wind operations and maintenance, describe not only cost but risk as the key areas of concern in O&M. In doing so, key uncertainties in optimizing O&M in offshore wind farms were exposed.

2.3.6 Uncertainties in the Operation and Maintenance of Offshore Wind Farms

The section discusses the uncertainties existing with available research into the operation and maintenance of offshore wind farms.

2.3.6.1 Uncertainty in decision-making

It has been established from the available literature that access is a major concern in the maintenance of offshore wind farms (Hassan et al., 2013). Halvorsen-Weare et al., (2013) discuss the cost implications of the specialised vessels used in the transportation of personnel, spare parts, and tools, to offshore wind farms such as crew transfer vessels, service operating vessels, helicopters, and even specialised vessels for tasks such as cable-laying. Laura and Vicente, (2014) also point to the use-case of these transport systems and their dependence on the type of maintenance required and the distance from the ports of exit. The frequency of failures implies the need for a maintenance activity which drives the costs associated with the operation time of vessels and technician labour costs. This is especially costly in corrective maintenance procedures. Van Bussel and Schöntag, (1997) state that unplanned maintenance events for repairs/replacement of failed offshore wind turbine components account for a high percentage of procedures between 50-70%. Further research has gone into cost-saving measures that take weather delays into account. This is because, O&M costs are not limited to the cost of repair alone, but also, the cost of downtime (Scheu et al., 2012; Ravindranath, 2016). However, downtime is also dependent on the accessibility of offshore wind farms. Li et al., (2016) express revenue loss by calculating the required time of a planned or unplanned service and the productivity level. Therefore, efficient maintenance strategies aimed at reducing costs and maintaining or improving the availability of offshore wind farms are a necessity (Ding and Tian, 2012). Nielsen and Sørensen, (2011) state that to reduce the overall lifetime costs of an offshore wind farm, an efficient plan for O&M needs to be developed to handle failure risks. The offshore wind industry is relatively

new and there are numerous uncertainties in the current operational O&M procedures such as when and how to schedule maintenance operations (Stock-Williams and Swamy, 2019).

A study (Pahlke, 2007) on offshore wind farm companies exposed the need for decision-support tools. The study states while a few companies already had decision-support tools for O&M, up to 70% of respondents expressed a need for decision-support models. In addition, most of the decision-support tools reported in the literature are mainly based on simulations without real case study applications (Li et al., 2016). The importance of decision-support tools is further emphasised by Li et al., (2016) who state that through the use of statistical data, the development of better maintenance schedules could potentially minimise maintenance expedition costs. Section 2.3.5 of this thesis discusses decision-support tools used in O&M activities. The common objective between these support tools is to estimate optimum maintenance strategies for test offshore wind farms, rather than an optimum maintenance strategy for all offshore wind farms. As such, these models usually have a use case specific to individual case study wind farms (Li et al., 2016). The variations between support tools, however, can be seen in the overall aim of each model - in most cases, cost-effective maintenance – and the relevant factors used to generate the model. While cost-effective maintenance is vital to the offshore wind industry, studies have shown that reducing the risks involved in maintenance practices will reduce uncertainties associated with the industry (Musial and Ram, 2010; Newman, 2015). There seems to be an absence of risk reduction measures in the available decision-support models, especially with regard to the harsh marine conditions and the effects on wind farm technicians. The next sub-section discusses the uncertainties arising from accounting for technicians in decision-making.

2.3.6.2 Uncertainties in Accounting for Technicians

In recent years, decision-support tools have been created by a few researchers with different model outputs in offshore wind farms. The aims of these support tools have included the estimation of wind energy potential (Schillings et al., 2012), the forecasting of operations in wind farms (Scheu et al., 2012), to O&M estimation of costs and revenue losses in wind farms (Dinwoodie et al., 2013), and even to provide simulations of the entire operational phase of offshore wind farms including all activities and costs (Hofmann and Sperstad, 2013). Decision-support tools in offshore wind farms usually aim to estimate the optimal cost-effective

maintenance strategy or plan. Most tools evaluate the maintenance cost as an output based on the levelised cost of energy (LCOE) (Myhr et al., 2014; Li et al., 2016). This gap in methodology exposes risk-related uncertainties especially as little consideration is made to the health of technicians and their ability to do work on offshore turbines.

In an interview conducted by Mette et al., (2018), the work carried out by wind farm technicians was considered demanding and required high concentration with access and transfer to offshore installations considered particularly demanding. Their study goes further to highlight several problems facing offshore wind technicians including the high risks of accidents, lengthy and inconsistent work times brought about by bad weather, and finally, the problem of seasickness, which as interviewees reported, could further complicate tasks such as transfer to offshore installations. The well-being of wind farm personnel is considered an important component of operating and maintaining an offshore wind farm (Crown Estate, 2021). This is addressed in the offshore wind report by the Crown Estate to include the ability of technicians to access offshore installations, the transit time in terms of shift patterns, transit durations, maintenance durations, and the accessibility of wind farms in harsh weather conditions. Several publications have addressed the uncertainties in technicians accessing offshore installations such as Scheu et al., (2012) who created a decision support model that accounted for crew size in specific weather restrictions and varying turbine components. Their model assumed transit times for two types of vessels (ordinary and cranes) and includes adjustable carrying capacity for the vessels, and variable wave height and wind speeds to study the effect on the availability of the wind farm. In accounting for technicians, limitations of working hours were set at a maximum of 7.5 days, and if exceeded, ongoing operations are aborted, and the affected vessel returns to shore. A little variation to accounting for technicians was made by Besnard et al., (2013) who presented a model that optimized maintenance support organisation using the number of maintenance technicians, location of accommodation and the choice of transfer vessels (and helicopters) and used an alternative to maximum working-hours in the form of a length of daily shifts (12-hours). An obvious finding in this paper was that offshore accommodation with technicians available at any time was preferred. However, this is not always the case in reality. Similarly, Dalgic, Lazakis, Dinwoodie, et al., (2015) also used the length of daily shifts at 12 hours per day in logistics planning for offshore wind farms. Their paper considered the type of vessel (including a CTV,

helicopter, offshore access vessel, and jack-up vessel) with its personnel carrying capacity and access restrictions, its travel duration, and its costs. A different approach was taken by Endrerud and Liyanage, (2015) who, depending on the type of failure, also determined the number of technicians and vessels needed, including a deterministic waiting time for spare parts. Other offshore wind farm schedule optimization models available in the literature account for the number of technicians per service order (Tan et al., 2016), the number of service orders per technician (Dawid et al., 2016), technician types (Irawan et al., 2017), and technician availability (Tan et al., 2016; Dawid et al., 2016; Irawan et al., 2017).

From the available literature, it can be seen that in accounting for technicians in optimizing O&M, terms used include the number of technicians (Scheu et al., 2012; Besnard et al., 2013; Endrerud and Liyanage, 2015; Dalgic, Lazakis, Dinwoodie, et al., 2015), the length of shifts (Scheu et al., 2012; Besnard et al., 2013; Dalgic, Lazakis, Dinwoodie, et al., 2015), the number of technicians per service order (Tan et al., 2016), number of service orders per technicians (Dawid et al., 2016), technician types (Irawan et al., 2017), and technician availability (Tan et al., 2016; Dawid et al., 2016; Irawan et al., 2017). Therefore, it could be noted that these models focus more on optimizing costs and have little consideration for the health of technicians as they travel to offshore wind farms as well as their ability to do work upon arrival. It could be argued that some available models include wave height thresholds such as Scheu et al., (2012), and as such, accounts for the health and safety of personnel. Based on policy standards, the wave height thresholds are usually set at 1.5 m for smaller vessels, and about 4 m for larger vessels (Phillips et al., 2015), however, as Mette et al., (2018) highlighted, some safety factors such as seasickness, which according to their research, can affect experienced technicians, have been overlooked in models and research. Furthermore, the current guideline set by G+ in the “Offshore Wind Good Practice Guidelines Wind Farm Transfer” states that “individuals feeling the effects of seasickness are to stay on board vessel until effects subside”. This means that in cases where seasickness occurs, the mean time to repair and overall maintenance duration would be extended, and in extreme cases result in a return to port and a reschedule of maintenance. This not only exposes the need for accounting for technicians in reducing risk but also the need to account for technicians in reducing operational costs. Therefore, it could be said that the full scope of accounting for personnel safety has not been fully explored.

To fully understand the effect of the sea state on the health of technicians and their ability to do work during O&M activities, section 2.6 of this thesis will explore human exposure to vessel accelerations brought about by the sea-state. In order to lay the foundation for that section, the next section of this thesis, section 2.4, introduces necessary ideas about wave theory.

2.4 An Introduction to Wave Theory

2.4.1 Introduction

Section 2.3.2 describes the importance of operation and maintenance in maintaining an offshore wind farm's integrity and section 2.3.3 describes the access vessels used to transport technicians for maintenance activities. During transits to wind farms, however, technicians on vessels experience accelerations brought about by the movement of the surface of the sea which can have various effects on technicians during operation and maintenance activities. Therefore, it is important to understand the propagation of ocean waves, the response of vessels to the waves, the effect of vessel accelerations on technicians and how they can affect operations and maintenance. This section provides an introduction to the fundamentals of wave theory, describes vessel response to sea-state, and describes the human response to accelerations from the available literature.

2.4.2 Wave Theory

Vessel accelerations are oscillatory mechanical movements of marine vessels brought about by ocean surface waves. These waves are a combination of different wave types which can be identified by their period and wavelength. Holthuijsen, (2007) provides a good description of these wave types in order of the longest to shortest including trans-tidal waves, tides, storm surges, tsunamis, seiches, infra-gravity waves, wind-generated waves or wind waves, and capillary waves.

2.4.2.1 Simple Waves

A simple definition for surface waves can be in the way they are visually perceived - as vertical motions of the ocean’s surface. Young, (1999) states that provided the water depth changes by less than 20% to 30% within one wavelength, linear wave theory provides reasonable

approximations for describing ocean waves. Therefore, the simplest way to define a wave mathematically is:

$$a(t) = A\sin(2\pi f t) \qquad 2.\ 7$$

Here, a(t) is the acceleration in ms^{-2} at time t. A is the wave's amplitude and f is the wave's frequency measured in hertz Hz. In some cases, the frequency can also be expressed in radians per second (w) as:

$$\omega = 2\pi f \qquad 2.\ 8$$

To describe waves in this manner, some assumptions must be made. The Coriolis force must be ignored, the water depth is uniform, the waves assume a two-dimensional flow, and surface tension and viscosity are ignored (Miles, 1957), however, in reality, the sea state we observe is usually a combination of multiple waves of varying frequencies moving in different directions which combine to form random waves (Mansfield, 2005).

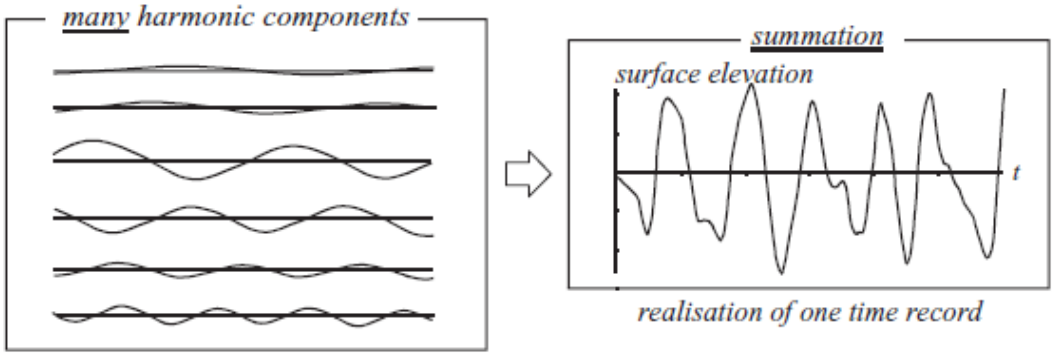

Figure 2. 14 Image showing the combination of many harmonic waves to form a random sea-state (Holthuijsen, 2007).

A few factors influence the formation of random surface waves which transform waves including interactions with offshore structures, and interactions with the seabed (Young, 1999). The list of transformations below only includes transformations relevant to the thesis aim:

- Refraction: In some cases, waves change direction towards shallower waters due to interactions with the seabed or interactions with ocean currents in a phenomenon called refraction (Holthuijsen, 2007).

- Breaking: Wave breaking occurs when the base of a wave can no longer support its top which causes it to collapse. This phenomenon usually occurs when waves run into shallower waters, or when two opposing waves combine (Young, 1999).
- Tides: The tides are periodic oscillations of large bodies of water caused by the earth's rotation and the gravitational forces of the moon and the sun (Hardisty, 1990). The gravitational forces of the Moon and Sun cause bulges on large bodies of water following coherent amplitude and phase relationships which cause both semi-diurnal tides (twelve-hour tidal periods i.e., experiencing two high tides and two low tides each day) and diurnal tides (twenty-four-hour tidal periods i.e., one high tide and one low tide) (Toffoli and Bitner-Gregersen, 2017).
- Wave-tide Interaction: When wind-generated waves propagate towards coastal regions, they usually interact with ocean currents or tides which cause transformations that modify the size and shape of propagating waves in a phenomenon called wave-tide interactions (Longuet-Higgins and Stewart, 1964). The effects of wave-current interactions on sea-state vary from changes to wave propagation in terms of growth and decay (Yu, 1952), to increases or decreases in wave height and wave steepness in cases of strong opposing currents and flowing currents respectively (Ris, 1997; Davidson et al., 2008; Rusu et al., 2011).
- Reflection: A wave reflects when it strikes a surface such as coastal headlands. When this happens, it changes direction, at an angle equal to the angle made by the incident wave on the surface it is reflecting off. An example of this phenomenon occurring in the open ocean is when standing waves are created as harmonic waves reflect off an offshore structure or obstacle (Holthuijsen, 2007).

The individual and combined occurrence of each of the wave transformations can and are computed in wave forecasting models which are applied in various disciplines. All of the above are relevant to the discussion of vessel motion, particularly in the shallow shelf seas where all present-day wind farms are located.

2.4.2.2 Wave Measurement

In-situ Observations

In-situ, observational methods refer to on-site or in-position measurements taken by instruments placed on the ocean's surface or below the ocean's surface. These include:

- **Wave buoys**: Wave buoys are one of the most well-known methods of measuring waves. They are surface floating instruments equipped with accelerometers (and in some cases GPS sensors) that measure the vertical displacement of the ocean's surface as a function of time using accelerometers. Though well suited for deep water sites, wave buoys are expensive, require regular removal of marine growth to avoid a change in weight and drag, and might accurately follow the water surface in the presence of currents and steep waves (Medina-Lopez et al., 2021).
- **Wave Poles, Pressure Transducers, Current Meters, and Echo-sounder:** Wave poles are wires submerged from platforms into the water surface that measure the electrical resistance of the dry areas of the wire. On the other hand, echo-sounders, current meters, and pressure inducers are placed at the seabed rather than being submerged, and echo-sounders measure the position of the water surface using sonic beams, while pressure transducers use linear wave theory along with measured wave-induced pressure fluctuations to estimate wave characteristics. Current meters, on the other hand, measure wave-induced orbital motions to estimate wave characteristics (Holthuijsen, 2007).
- **Wave Radar:** Positioned looking downwards, from a high platform or tower, the return time of a pencil-thin radar beam can be used to estimate wave shape.

In-situ measurements provide a relatively accurate way of measuring sea state, however, as these instruments are expensive, their placement in offshore wind farm sites is sparse. Wind and sea-state measurements are usually measured on-site for a period of two years before construction. Whilst wind measurements are critical for monitoring the electrical yield of the farm and are measured continuously during the operational phase, wave measurements are not always continued. As *in-situ* instruments are only able to provide measurements in areas where instruments can be moored, spatial coverage is limited. As such, to describe the sea state in operation and maintenance planning, numerical models are typically used.

Numerical Modelling

The numerical modelling of wave energy resources is typically achieved using third-generation spectral models such as SWAN, ROM, WaveWatch or Meteo France WAve Model MFWAM (Holthuijsen, 2007; Warner et al., 2008; Uchiyama et al., 2010; Olabarrieta et al., 2011). These models solve the wave action balance equation by Hasselmann et al. (1988) on a grid which discretises the ocean domain of interest (Medina-Lopez et al., 2021). Modern forecast models account for most wave transformations including the non-linear transfer of energy between wave frequencies, bottom friction, and wave breaking, where the fetch is the main energy source. These models are typically used for various applications including forecasting (M.J. Lewis et al., 2019), ocean modelling, and salt and sediment transport modelling (Warner et al., 2008; Cho et al., 2012), and extend to various industries like the oil and gas industry, coastal protection, ecological studies, and the offshore wind industry (Wolf and Prandle, 1999). Within these industries, the information from wave models can be used to plan marine-based activities mostly affected by surface waves such as loads on ships, offshore installations, mooring systems, major port activities, and scheduling purposes (Toffoli and Bitner-Gregersen, 2017). However, in modelling wave characteristics, models require calibration and validation with *in-situ* measurements (Medina-Lopez et al., 2021).

Remote-Sensing Methods

Remote sensing is a more modern way of measuring waves and is the process of monitoring physical properties and characteristics using reflections of electromagnetic radiation from aerial platforms and devices. For instance, remote sensing imaging techniques such as stereo photography involve taking images of the earth's surface from cameras on aeroplanes at quick intervals, while non-imaging radar on ships can be used to detect obstacles around the ship. On the other hand, altimetry techniques can include laser altimetry where a downward-facing laser is used to measure the distance between the laser and the earth or sea surface, usually from satellites. (USBR, 2001; Holthuijsen, 2007). The limitations of remote-sensing methods include cost and the early-stage nature of some remote-sensing techniques (Holthuijsen, 2007).

The results of the measuring techniques are often presented in form of statistical terminologies described in the section below.

2.4.2.2 Statistical Description of Ocean waves

There are a few statistical descriptors used in journals and used by oceanographers to describe ocean waves. The most common of these descriptors include:

- Wave Height: Wave height (H) is one of the most important wave parameters. It is the vertical distance between the wave crest and wave trough (Holthuijsen, 2007). Where, $\overline{H}$ is the mean wave height, i is the sequence of waves on record, and N is the number of waves, the statistical representation of the mean wave height is:

$$\overline{H} = \frac{1}{N}\sum_{i=1}^{N} H_i \qquad 2.\ 9$$

- Significant Wave Height: Significant wave height (Hs) is a term more commonly used in forecasts and in research to describe sea-state and it is the average of the highest one-third of waves in a record. Where j is the rank number of the highest waves based on the height (Holthuijsen, 2007), significant wave height can be expressed statistically as:

$$H_{1/3} = \frac{1}{N/3}\sum_{j=1}^{N/3} H_j \qquad 2.\ 10$$

- Wave period: The wave period is the time it takes to complete a single wave cycle in seconds and is inversely proportional to the frequency of the wave. In most cases, the wave period will be defined as dominant or peak wave period T_p, which is the wave period with the highest energy and is the reciprocal of peak frequency, f_p (Holthuijsen, 2007) expressed as:

$$T_P = {}^{1}/_{f_p} \qquad 2.\ 11$$

  Where The peak frequency, fp is commonly estimated from spectra obtained from sampled data (Young, 1999). Another common term for wave period is the zero-crossing period (T_0). The mean of the zero-crossing wave period can be statistically represented as:

$$\overline{T_0} = \frac{1}{N}\sum_{i=1}^{N} T_{0,i} \qquad 2.\ 12$$

- Wave Direction: This is the dominant direction of wave propagation with time. It is usually represented as the mean wave direction Θ_m which is the average of individual wave directions in a time series.

Section 2.3 of this thesis emphasised the importance of weather and sea-state on operations where the accessibility of an offshore wind farm can be determined by numerous parameters, with sea-state conditions being the most important factor to consider, able to significantly affect the deployment of technicians, equipment to wind turbines and able to affect the costs of both planned and unplanned maintenance activities. However, section 2.3.6 also exposed uncertainties where the welfare of technicians is not accounted for in planning maintenance activities. As such, it is important to explore the effects of transits to offshore wind farms on technicians' health, comfort, and ability to do work upon arrival at turbines. Section 2.5 below, therefore, explores the impact of the sea state on marine vessels as a way to explore the impact of vessel accelerations on human passengers.

2.5 Vessel Response to Sea-State

2.5.1 Introduction

Most offshore wind maintenance activities use marine vessels such as crew transfer vessels and Service Operating Vessels, as discussed previously, with crew transfer vessels (CTV) being the most used class of vessels (Gilbert et al., 2021) with sizes ranging between 12 to 30 meters (Phillips et al., 2015). As marine vessels transit between the port and offshore wind farms to transfer technicians, the physical forces of the sea act on the vessels which generate varying oscillatory motions or accelerations in such a way that the motion of a vessel at sea, therefore, depends on the sea-state (Shaw, 1954). The technicians on these vessels are, therefore, affected by the movement of the vessels, which can have negative effects on their health, comfort, and ability to do work.

Therefore, in order to understand human responses to accelerations, understanding a vessel's response to sea state is important.

In general, a floating rigid structure is assumed to undergo six independent translational and rotational degrees of freedom (Figure 2.15), though in some cases floating structures could be restrained to have fewer degrees of freedom such as when fastened to the seafloor or anchored to a platform (Shaw, 1954).

2.5.2 Translational/Linear Motion

For floating structures, translational motions refer to vertical, lateral, and fore-and-aft motions. One of these motions is the heave motion, which is the linear vertical motion, or the up-and-down motion of a floating structure usually described using the coordinate system as the z-axis motion from the centre of gravity (Kluijven, 2016). The surge motion is the front-to-back (bow to stern in boats) longitudinal motion of a floating structure usually described using the x-axis, and the sway motion is the lateral side-to-side (bow to stern in boats) transverse motion of a floating structure described using the y-axis (Shaw, 1954).

2.5.3 Rotational Motion

Floating bodies are also capable of rotational motions including the yaw motion, which is the motion about the z-axis, the side-to-side tilting roll motion about the x-axis, and the front-to-back tilting pitch motion about the y-axis (Kluijven, 2016).

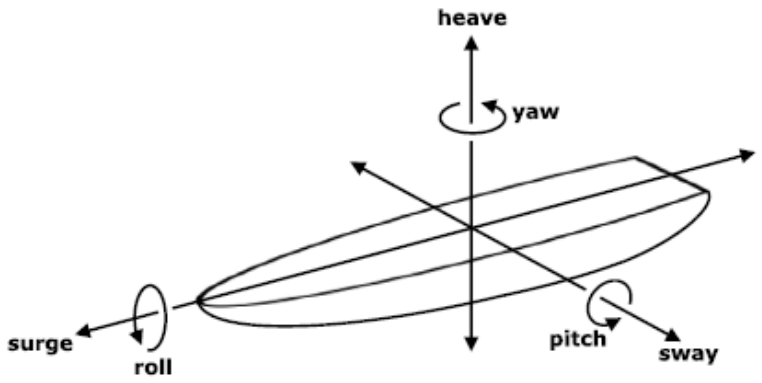

Figure 2. 15 The general six degrees of freedom for a floating structure (Scheu et al., 2018).

The next section of this chapter describes the mechanisms and human response to accelerations caused by the sea state.

2.6 Human Response to Acceleration

The effect of accelerations on humans has been explored as early as the 1950s, yet due to the complex nature of accelerations on humans, it is difficult to obtain a simple analytical expression for this effect (Shaw, 1954). However, studies suggest that humans perceive accelerations in two ways – localized and whole-body accelerations (Mansfield, 2005). Whole-body accelerations are relevant to this thesis as accelerations caused by vessels are usually transmitted through the base of the vessels, backrests, and seat surfaces, which can affect comfort, performance, and health (Mansfield, 2005). The effects of these motions are described by Griffin, (1990) in the "Handbook of Human Vibration" and are documented in the code of practice for controlling risks due to whole-body accelerations including causing discomfort and motion sickness, the effects on performance, health and safety, and the aggravation of pre-existing injuries (Maritime and Coastguard Agency - Great Britain, 2009). The classification of these motions with respect to their frequency and magnitude of acceleration in causing some of the above effects has been explored in literature by Mansfield, (2005), and is represented in Figure 2.16 below.

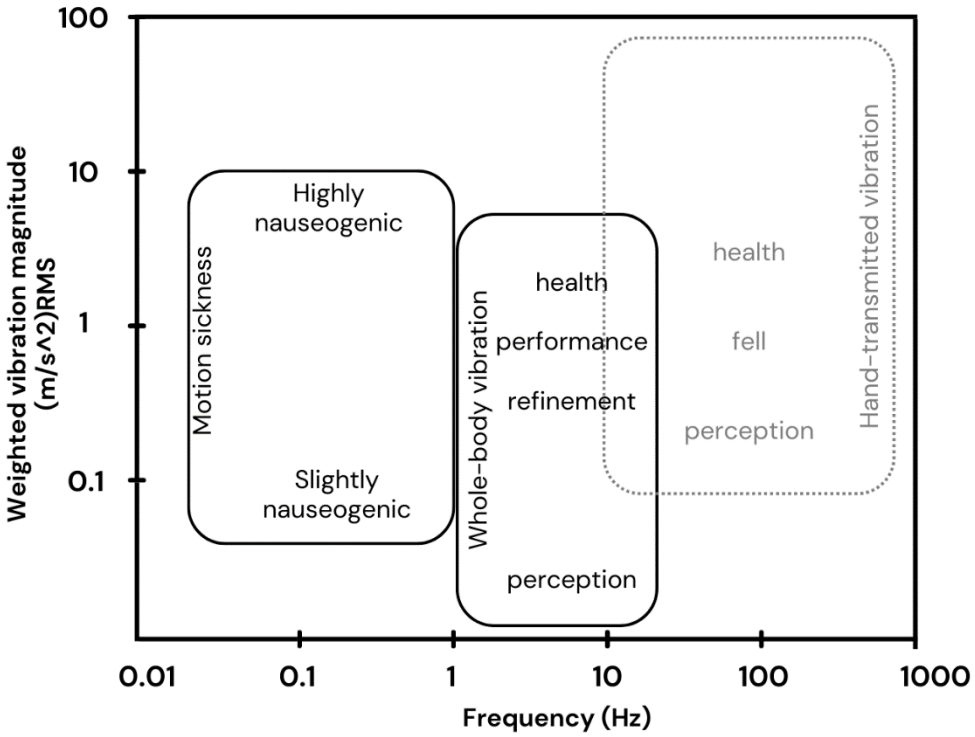

Figure 2. 16 Classification of human perceived acceleration by frequency and magnitude adapted from Mansfield, (2005).

Figure 2.16 presents a classification of human perceived acceleration by frequency and magnitude of acceleration adapted from Mansfield, (2005) to show the magnitudes of acceleration and frequencies relevant to this thesis including frequency and weighted vibration magnitudes concerning whole-body vibrations and motion sickness.

2.6.1 The Discomfort-based Effects of Accelerations

Mansfield, (2005) describes the term discomfort as an absence of comfort. This is because apart from pain receptors, physiologically there is no comfort receptor in the human body. Though not able to cause pain, however, there exists a range of accelerations known to cause discomfort in humans. This acceleration-caused discomfort can lead to distraction, annoyance (Marjanen and Mansfield, 2011), reduction of human reaction time (Newell and Mansfield, 2008), impairment of balance (McPhee et al., 2009) and mental fatigue in high-speed vessels as expressed by Olausson, (2015) and Leung et al., (2006), though it can be hard to differentiate between physical and mental fatigue and Stevens and Parsons, (2002) suggest

that mental fatigue is a manifestation of physical fatigue. In addition to fatigue, studies also show that in high-speed vessels, transits can cause a reduction in physical capacity (Myers et al., 2012). Myers et al., (2012) investigated the physiological consequences of three-hour transits stating the performance of participants was reduced after transits. The performance of the participants was tested for handgrip, vertical jump and push, and shuttle run, some of which are relatable in offshore wind maintenance.

2.6.1.1 Evaluating the Effect of Acceleration on Passengers

Evaluating acceleration exposure is fundamental in ensuring the comfort and safety of passengers, however, factors like the speed of the vessel, as well as the sea state, and the heading of the vessel can make the prediction of acceleration complicated (Olausson, 2015). Typically, when analysing the motion of a floating structure for human exposure to acceleration, the response amplitude operator (RAO) is used along with wave energy spectra to produce response spectra for the floating structure (Jenkins et al., 2021). The Root Mean Square (RMS) value is then calculated from the response spectra over a range of significant wave heights and wave periods from which limiting conditions can be added. Simulated applications involve the use of numerical models to describe various sea-state conditions from significant wave heights and wave periods which are then combined with numerical seat models such as from the findings of Griffin, (1990). This is because experimental measurements would require time-consuming methods of measuring sea state, and accelerations measured on vessels will be restricted to the vessel measured (Olausson, 2015). As such operating conditions can be expressed for a range of sea states and vessel parameters such as vessel speed such as the operational profile represented by Olausson, (2015) in Figure 2.17. For instance, Olausson, (2015) presents an illustration for a generalized operational profile using vessel speed and sea states in Figure 2.17.

		Sea state			
		Calm	Mod.	Severe	
Speed	High	12%	6%	2%	**20%**
	Med	30%	15%	5%	**50%**
	Low	18%	9%	3%	**30%**
		60%	**30%**	**10%**	

Figure 2. 17 An operational profile illustrated by Olausson, (2015)

As illustrated, the exposure is defined as a percentage of time in each condition ranging between high and low, and sea-state, which ranged between severe and calm from which working conditions can be evaluated. This method of defining operational profiles is used in most studies along with design decisions such as vessel speed as with Derakhshanjazari et al., (2018), (Hostens and Ramon, 2003) and (Eger et al., 2011) where speed had a significantly increasing effect on the magnitude of acceleration, as well as vessel shape, and displacement (Garme et al., 2014). However, it should be noted in most of these publications, these parameters are chosen regarding ship design with little consideration for human comfort. It also should be noted that mathematical models exist that model ship response to sea-states (Zarnick, 1978; Keuning, 1994; Akers, 1999), however, these models are usually not in relation to human exposure to accelerations.

For most whole-body accelerations, it is assumed that participants are in a seated position and that accelerations are transferred from the seats to the passengers (Mansfield, 2005). For these positions, international standards provide guidance on the thresholds of perceptions and optimal operating conditions, most commonly the ISO 2631-1 and the BS 6841. Both standards provide guidance for the assessment of whole-body accelerations using RMS of frequency-weighted acceleration, with the ISO 2631-1 being the most recent standard and as such the most relevant. The standards define frequency weightings for application to acceleration from the floor to the seat, and backrest in both translational and rotational axes of motion (Mansfield, 2005). The standards also present methods of assessing accelerations in multi-axis directions using root-mean-square (RMS) of the frequency-weighted

acceleration and acceleration dose value (VDV), further suggesting criteria by which the quantities can be evaluated. The root-mean-square (RMS) of acceleration is expressed using the magnitude of acceleration over a number of time steps (ISO 2631-1, 1997):

$$RMS = \sqrt{\frac{1}{n}\sum_{i=1}^{n} a_i^2} \qquad 2.\ 13$$

Here, a_i is the magnitude of acceleration, and n is the time steps.

The RMS of acceleration used is then weighted acceleration which means that more relevant accelerations are amplified and nonrelevant frequencies are filtered out using band-limiting low and high-pass filters (Scheu et al., 2018). It should, however, be noted that the weightings expressed in this thesis are specific to the ISO 2631-1, (1997), and the BS 6481 applies different frequency weightings and filtering techniques (Scheu et al., 2018). The weighted RMS of acceleration, expressed in metres per second squared (m/s^2) or radians per second squared (rad/s^2) for rotational acceleration, is expressed as:

$$a_w = \left[\frac{1}{T}\int_0^T a_w^2(t)dt\right]^{\frac{1}{2}} \qquad 2.\ 14$$

Here, $a_w(t)$ is the weighted acceleration as a function of time in metres per second squared (m/s^2) or radians per second squared (rad/s^2) for rotational acceleration, while T is the measurement duration in seconds ISO 2631-1, (1997). Additionally, the ISO 2631-1, (1997) suggests a combination of RMS weighted acceleration in form of a vector sum when accounting for multiple axes of acceleration expressed as:

$$a_{xyz} = \sqrt{k_x a_{wx}^2 + k_y a_{wy}^2 + k_z a_{wz}^2} \qquad 2.\ 15$$

Here, a_{xyz} is the weighted frequency RMS vector sum of accelerations, a_{wx}, a_{wy}, and a_{wz} are the weighted frequency acceleration in the x, y, and z-axis, respectively, and K_x, K_y, and K_z are multiplying factors of 1.4, 1.4, and 1.0, respectively, which are used when fore and aft measurements at the backrest or area of principal support can not be made (Mansfield, 2005).

Regarding the weighted frequencies highlighted above, the ISO 2631-1, (1997) provides frequency weighting curves dependent on the posture of exposed persons, the direction of acceleration and the nature of the acceleration measurement and the method of evaluation for health, comfort, and perception. The frequency weightings are designed to model, using mathematical digital signal processing, the response of the human body to wave phenomena or model the human response to accelerations as a whole (Mansfield, 2005). In applying frequency weightings to amplify relevant frequencies in estimating the health, and comfort of passengers, ISO 2631-1, (1997) suggests two principal frequency weightings and three additional frequency weightings. The frequency weightings provided by the ISO 2631-1, (1997) are presented in Table 2.1 below, in relation to the barycentric axes of the human body, as seen in Figure 2.19 below.

Frequency Weighting	Application Area	Direction	Frequency Range
W_k	Whole-body	z-seat surface	0.5 – 80 (Hz)
W_d	Whole-body	x-seat surface; y-seat surface	0.5 – 80 (Hz)
W_f	Motion sickness	z-vertical	0.1 – 0.5 (Hz)
W_c	Whole-body	x-seat back	0.5 – 80 (Hz)
W_e	Whole-body	Rotational rx, ry, rz-seat surface	0.5 – 80 (Hz)
W_j	Head	Vertical- recumbent (head)	0.5 – 80 (Hz)

Table 2. 1 ISO 2631-1 Guide for the application of frequency weighting. Adapted from ISO 2631-1, (1997).

The defined axis of rx, ry, and rz are described in Figure 2.18 below.

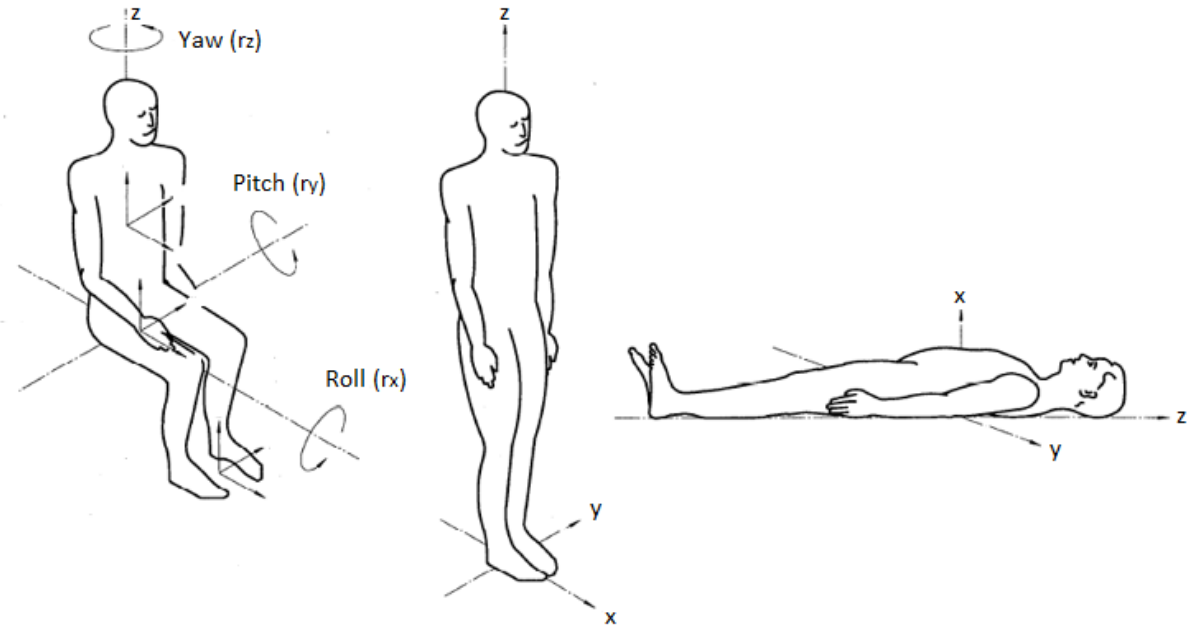

Figure 2. 18 The barycentric axes of the human body. Image adapted from ISO 2631-1, (1997)

The two principal frequency weightings suggested for the health and comfort of passengers include W_k for the vertical direction, W_d for the x and y directions and persons in recumbent positions (ISO 2631-1, 1997). The additional frequency weightings include W_c for seated measurements, W_e for rotational acceleration measurements, and W_j for accelerations under the head of persons in recumbent positions (ISO 2631-1, 1997). Using a high-pass and low-pass filter, lower and upper-frequency band limitations can be applied with Butterworth characteristics, and the tolerance of the combined frequency weighting and band-limiting of ±1 dB is suggested by ISO 2631-1, (1997). As stated by Mansfield, (2005) W_k, W_b, and W_d are the most used frequency weightings, especially for whole-body accelerations. In comparison with the British standard, W_k provides slightly higher perception accelerations than W_b used in the British standard for seated whole-body z-axis accelerations, generating higher values for weighted acceleration (Mansfield, 2005). An obvious limitation to the use of frequency weightings is that they are modelled from observed and experimental studies, as such they are a representation of sample size and not an individual representation of human response. However, this thesis applies the use of frequency weighting and the metric for measuring human response to vibration under the guidance of international standards because, at the time of writing, there is little evidence to show that an alternative means of assessing complex accelerations exists (Mansfield, 2005).

Acceleration dose value (VDV) or the integral of accelerations to the fourth power dose, on the other hand, is mostly used in relation to shocks where using RMS of acceleration underestimates the effects of peak values of accelerations (Mansfield, 2005). The fourth power acceleration dose value (VDV) in metres per second to the power 1.75 ($m/s^{1.75}$) for linear accelerations, or in radians per second to the power 1.75 ($rad/s^{1.75}$) for rotational accelerations, can be expressed as:

$$VDV = \left\{ \int_0^T [a_w(t)]^4 dt \right\}^{\frac{1}{4}} \qquad 2.16$$

Here, $a_w(t)$ is the instantaneous frequency-weighted acceleration, and T is the measurement of duration in seconds (ISO 2631-1, 1997).

Other measures for assessing accelerations exist such as using root-mean-quad as suggested by Kjellberg & Wikström, (1985b) who state that using weighted root-mean-square of acceleration may overestimate results.

The guidelines of the ISO 2631-1 are based on experience and research results which outline suggested criteria where these quantities can be evaluated including the magnitude of RMS accelerations with discomfort. This is presented in Table 2.2 below shows approximate thresholds of human comfort for passengers exposed to accelerations for up to eight hours (ISO 2631-1, 1997).

The magnitude of Acceleration in ms^{-2}	Comfort Reaction
Less than 0.315	Not uncomfortable
0.315 – 0.630	A little uncomfortable
0.500 – 1.000	Fairly uncomfortable
0.800 – 1.600	Uncomfortable
1.250 -2.500	Very uncomfortable
Greater than 2.000	Extremely uncomfortable

Table 2. 2 Estimations for comfort response to periodic accelerations ISO 2631-1, (1997).

This subjective scaling mechanism is generated from relevant studies cited in the ISO 2631-1 and has been used in various studies such as Huston et al., (2000) and Shoenberger, (1982), where subjects were asked to rate stimuli based on acceleration using the same scales. Variations may exist in the terms used to describe discomfort between these studies, but corroborations exist in the magnitude thresholds used in these studies including studies such as Mansfield et al., (2000), and Wikström et al., (1991) where discomfort was rated with magnitude estimations for industrial trucks, and more relevant to this study, Nielsen, (1987) which presented the most used criteria for limiting motion exposure on different kinds of works on vessels using the magnitude of accelerations during transits and depending on activities performed or expected to be performed by passengers. It should however be noted that these thresholds depend on various internal and external factors such as individual susceptibility, passenger activities, and the duration of exposure (ISO 2631-1, 1997). For this reason, these thresholds should not be considered limits but rather indicators of likely reactions to the stated levels of acceleration magnitudes. The relationship between travel duration and discomfort has also been explored by researchers such as Clevenson et al., (1978), Griffin & Whitham, (1998), Kjellberg & Wikström, (1985a) and Kjellberg & Wikström, (1985b), who all suggest that low acceleration magnitude levels are acceptable over longer periods than higher levels stating that the effect of the acceleration on the human body is reduced with increasing exposure time. The image below in Figure 2.19 presents a relationship between duration and weighted RMS of acceleration in moving trucks by Maeda and Morioka, (1998).

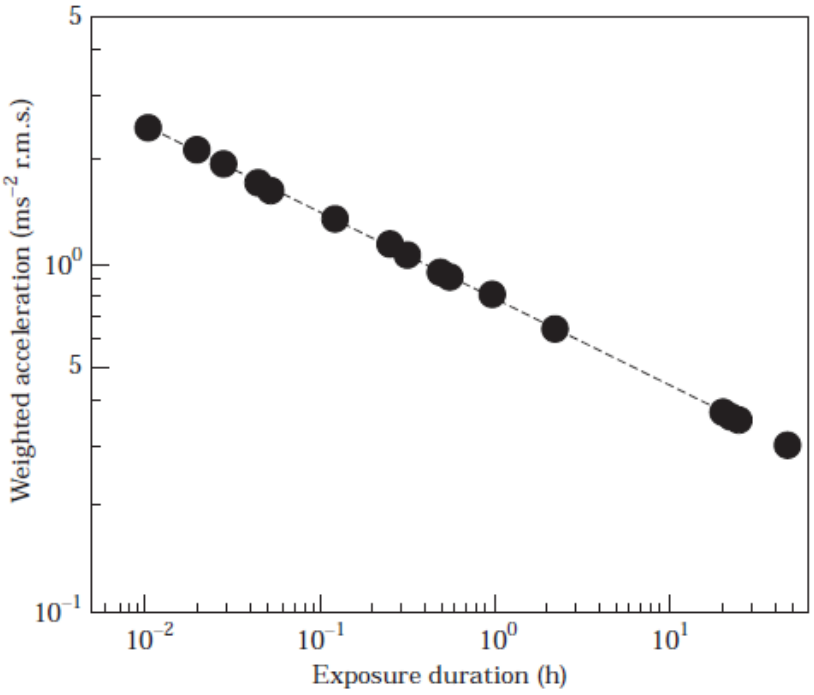

Figure 2. 19 Comparison of frequency-weighted acceleration to health risks (Maeda and Morioka, 1998).

Conversely, experimental studies including Miwa et al., (1973) and Griffin & Whitham, (1980) state the opposite, demonstrating an increase in discomfort with exposure time, however, the difference between these sets of studies is that Griffin & Whitham, (1980) performed their analysis on much shorter time-scales with a maximum duration of two minutes while other studies used either a daily dose or performed analysis on durations up to eight hours. The subjective scaling mechanisms based on RMS acceleration have not been limited to the levels of discomfort, and some researchers have also applied limits to the type of work being performed. Nielsen, (1987) introduced limiting motion criteria for different kinds of work that have been cited in a lot of publications. This publication presented criteria for limiting motion exposure for different kinds of works on naval vessels between light manual work, heavy manual work, and intellectual work, with some of the criteria used in this paper originating from the criteria introduced by Payne, (1976) for quantifying ride comfort. The table below presents limiting motion criteria by work description according to Nielsen, (1987).

RMS Vertical Acceleration (g)	RMS Lateral Acceleration (g)	Roll (˚)	Work Description
0.2	0.1	6.0	Light manual work

0.15	0.07	4.0	Heavy manual work
0.10	0.05	3.0	Intellectual work
0.05	0.04	2.5	Transit for passenger
0.02	0.03	2.0	Cruise liner

Table 2. 3 Limiting motion criteria by work description according to Nielsen, (1987).

2.6.2 The Health-based Effects of Accelerations

The most common health-based effect of whole-body accelerations is lower back pain (Griffin, 1990; Cardinale and Pope, 2003; Mansfield, 2005), however, in a survey of reported injuries by Ensign et al., (2000) these could also include sprains, chronic pain, fractures, dislocations, headaches, and tiredness. Other researchers have identified health-related effects of whole-body accelerations in connection with low-frequency noise such as digestive disorders (Griffin, 1990) However, these are long-term effects of acceleration on human health and though accelerations could increase the probability of injuries, research suggests that there is limited statistical data to support the influence of accelerations on injuries Olausson, (2015). On the other hand, the most common short-term health-based effect of vessel accelerations on passengers is motion sickness (Coyte et al., 2016).

2.6.2.1 Motion Sickness

This section describes motion sickness in relation to marine travel called seasickness. It discusses the known causes and symptoms of motion sickness, human susceptibility to motion sickness, available prevention methods and cures, and finally, this section discusses the effect of motion sickness on human performance using available literature.

Motion sickness (MS) is a common feeling of unwellness usually associated with discomfort and vomiting and brought about by provocative motions (Stevens and Parsons, 2002). Motion sickness can be induced on land, sea, air, and in virtual environments (Koohestani et al., 2019). The most widely accepted theory of motion sickness was proposed by Reason and Brand, (1975) who stated that motion sickness can develop when there is a sensory mismatch between the visual, vestibular, and somatosensory inputs. However, other susceptibility factors such as gender, drugs, environment, and internal factors like psychology, though do not on their cause motion sickness but can increase the susceptibility to motion sickness in

the human body in the presence of sensory conflict (Kluijven, 2016). It is important to note that the theory surrounding motion sickness is still very ambiguous (Zhang et al., 2016) and new findings concerning motion sickness are still being reported. For instance, Stoffregen and Smart, (1998) suggest that postural stability should be considered a precursor to motion sickness, while Kluijven, (2016) states that excessive amounts of alcohol can simulate motion sickness in that it can cause dehydration and feelings of nausea, and that upon the application of external acceleration, the feelings of nausea can be amplified which can trigger vomiting in passengers. This can also be said for coffee intake in passengers which can trigger nausea in the body and can also be amplified upon the application of external acceleration (Kluijven, 2016). Additionally, the environment can also play a role in inducing motion sickness. For instance, the duration of travel is a major contributing factor in motion sickness susceptibility as small encounters with accelerations might not be enough to cause motion sickness, however, prolonged exposure to accelerations can induce motion sickness even in the most experienced sailors (Kluijven, 2016). However, research also suggests that there can be adaptation where the sensory conflict can experience inhibitory innervations cancelling reafference which means excessive exposure to sensory conflict can be cancelled (Zhang et al., 2016). This theory is also supported by ISO 2631-1, (1997) which suggests that long periods of exposure to motions increase the occurrence of motion sickness even over several hours, however, after extended exposure, adaptation occurs, and the occurrence of motion sickness reduces. As such the individual experiencing motion sickness can overcome the sensation after a period. Other environmental factors that can induce motion sickness can be a lack of visual reference to the motion being experienced especially in ships (Kluijven, 2016), as well as temperature and fumes from ship engines which can cause nausea (Kluijven, 2016).

2.6.2.2 The Effect of Motion Sickness on Health and Human Performance

The main symptom of motion sickness is nausea which can result in vomiting, sweating, and pallor (Dobie, 2019). Other short-term effects can be hyper-salivation, stomach awareness, feelings of drowsiness, fatigue, and lethargy (Lackner, 2014; Zhang et al., 2016), and though the symptoms of motion sickness are still being investigated (Zhang et al., 2016), these symptoms can affect the human performance over various tasks. Motion sickness has also been known to affect human performance in relation to comfort, well-being, and cognitive performance (Smyth et al., 2019). Similarly, Kluijven, (2016) states that the incidence of the

symptoms of seasickness can not only decrease work ethic but also, the probability of an accident occurring can increase significantly resulting in serious work injuries. In this report, 49% of the crew members on a large vessel admitted that work activities suffer from symptoms of seasickness. These findings are corroborated in various studies on the subject, including the study of the effects of seasickness on cognitive functions by Bos, (2004) where 60% of test subjects did not complete a task when subjected to motions causing seasickness, a variation from the baseline of 5% when subjects were not subjected to seasickness-causing accelerations. Additionally, Matsangas et al., (2014) showed that after extended exposure to motion sickness, there were significant decreases in memory, arithmetic functions, and time to complete tasks. Relating to passengers on marine vessels, Calvert, (2005) studied the effect of motion sickness on crew performance along with Cheung and Nakashima, (2006) and Malek et al., (2009), all of which concluded that motion sickness negatively affected crew performance in terms of adaptation and cognitive performance. In more recent years, Pisula et al., (2012) used data collected from three vessels to determine that problems most associated with vessel motion were more related to difficulties with physical tasks. They state that there were fewer correlations between cognitive tasks and vertical accelerations. Their findings do not diminish the work of other authors but instead suggest that physical tasks might be more affected by motion sickness than cognitive tasks and as such might be an area of greater concern. Therefore, the overall conclusion from available literature is that motion sickness can affect human performance (Bos, 2004) and that the rate of illness is affected by the magnitude of vessel oscillations and the duration of journeys (Matsangas et al., 2014), though after prolonged passive motion, the sensory conflict may receive inhibitory interventions that cancel the effects of the sensory conflict (Zhang et al., 2016). Though these correlations exist across publications, some variations can be found in the rate of illness among passengers. As already addressed earlier in this section, motion sickness is a complex phenomenon, and it can be hard to obtain a simple analytical expression for its effects, especially since some symptoms of motion sickness have gone unrecognised until recent years such as drowsiness as suggested by Lackner, (2014). In modern research, more expansive symptoms of motion sickness have been grouped into four categories including cognitive symptoms such as dizziness, temperature-related symptoms such as sweating, sopite symptoms such as fatigue, and gastrointestinal symptoms such as nausea and vomiting (Earle et al., 2021). In addition to this, publications have reviewed motion sickness in different

modes of transport, and for different durations of travel. Not only this, but the susceptibility factors also mentioned earlier in this section could affect the rate of illness in passengers as well as the differences in survey methodologies used across publications. These differences were highlighted by Matsangas et al., (2014) who used incentives during surveys which could influence the outcome of the dexterity tests taken. Furthermore, the greater portion of publications survey and model motion sickness on much larger vessels such as naval vessels and as such are not suitable for operation and maintenance in offshore wind farms where primary transport vessels are Crew Transfer Vessels.

It should be noted that methods and medications exist that can prevent and suppress motion sickness. These include anticholinergics, antihistamines, monoamine antagonists, and some stimulants and sedatives (Spinks and Wasiak, 2011; Zhang et al., 2016; West Essex Medicines, 2022). However, these medications are not without side effects, including drowsiness, dry mouth, blurred vision, nausea, diarrhoea, skin reactions in cases of patch use and headaches (Rubio et al., 2011; NHS, 2020). Other than pharmacological methods, there are also behavioural and habituation methods that can either help prevent or suppress the incidence or the effects of motion sickness such as using ginger, forward-looking, using horizon glasses and eating energy-dense and high-sodium diets low in vitamin A and C (Zhang et al., 2016). However, clinical trials for some of these recommendations have had conflicting outcomes (Zhang et al., 2016).

2.6.2.3 Modelling the Effect of Motion Sickness

The various symptoms and the effects on human performance caused by motion sickness make predicting the exposure to motion sickness fundamental to both ensuring the comfort and safety of passengers, and also fundamental to ensuring the efficient completion of tasks. Concerning the maintenance of offshore wind farms, Phillips et al., (2015), state that while the ability of technicians to perform tasks is important, motion sickness is an issue for the well-being of technicians.

The first established method for evaluating the incidence of motion sickness was developed by O'Hanlon and McCauley, (1974). Their algorithm for evaluating the incidence of motion used a laboratory-controlled manner, where the real-life scenario of vessels experiencing the six-axis of acceleration can be replicated by correlating the vertical axis of acceleration to

motion sickness. This metric for evaluating sickness was based solely on the incidence of vomiting which at the time was regarded as the sole symptom of motion sickness. As stated, further research into motion sickness in recent years has identified other symptoms (Lackner, 2014), however, the model by O'Hanlon and McCauley, (1974) is still widely used for various applications relating to the evaluation of motion sickness ranging from evaluations in fishing vessels by Bao-Ji and Song-Nan, (2019), to ship design (Cepowski, 2012). Variations to the original model have been also implemented for various use cases. Typically, numerical modelling has generally been used to apply vessel and sea-state parameters where time-consuming experimental measures would have been used such as Piscopo & Scamardella, (2015), where linear and parabolic relationships were found between estimated motion sickness and significant wave height, wave period, and wave direction respectively for catamarans. However, motion sickness in this study was expressed in a value called overall motion sickness (OMSI), which expresses Motion Sickness Incidence for a particular area on the vessel. Guidelines for assessing Motion Sickness Incidence can be found in international standards including ISO 2631-1, (1997). The ISO2631-1, as well as various studies, highlights motions at frequencies below 0.5 Hz (between 0.1 Hz and 0. 5 Hz) as able to induce motion sickness and assesses motion sickness from weighted acceleration determined for the z-axis of acceleration. ISO 2631-1 quantifies whole-body acceleration concerning human health using the incidence of motion sickness and provides a frequency range based on frequency weightings of the root mean square acceleration (RMS), extended below 1 Hz. The standard as well as relevant studies suggest that vertical accelerations of about 0.15g root mean square values (RMS) and horizontal accelerations of about 0.12g RMS are the limits of acceptable operational conditions. In using weighted RMS of acceleration, the z-axis is usually considered when estimating the incidence of motion sickness in humans and a frequency weighting of W_f, defined in Table 2.2, is appropriate for passengers in a seated position. Using this, ISO 2631-1 outlines two metrics for assessing the incidence of motion sickness including Motion Sickness Dose Values (MSDV) and Motion Sickness Incidence (MSI). According to Mansfield, (2005) the only validated measure for sickness related to sea state is MSDV, though it is only recommended for use with vertical acceleration and with a W_f frequency weighting. The MSDV is determined from measurements of acceleration throughout the observation. It is the squared root of the integral of the weighted z-axis acceleration, measured in metres per second to the power of 1.5 ($m/s^{1.5}$):

$$MSDV_z = \left\{ \int_0^T [a_w(t)]^2 dt \right\}^{\frac{1}{2}} \qquad 2.17$$

Here, $a_w(t)$ is the instantaneous frequency-weighted acceleration in the z-axis direction, and T is the measurement of duration in seconds for durations up to 6 hours (ISO 2631-1, 1997). Higher values of motion sickness dose value, therefore, indicate higher occurrences of motion sickness in passengers ISO 2631-1, (1997).

On the other hand, because available literature suggests that individual susceptibility to motion sickness can vary based on a number of factors including gender and age, the Motion Sickness Incidence gives a generalized method of estimating the probability of accelerations to induce vomiting as a percentage. The Motion Sickness Incidence can be described as:

$$MSI_{vz} = K_m \cdot \left\{ \int_0^T [a_w(t)]^2 dt \right\}^{\frac{1}{2}} \qquad 2.18$$

Here, Km is a constant equal to 1/3 in a mixed population of men and women but varies based on the population exposed to motions between 0.333 hours to 6 hours. Also, $a_w(t)$ is the instantaneous frequency-weighted acceleration in the z-axis direction, and T is the measurement of duration in seconds (ISO 2631-1, 1997).

Practical experience, as well as experimental studies, shows that values of Motion Sickness Incidence of between 20% to 25% are associated with the limits of acceptable conditions (Phillips et al., 2015). It should, however, be noted that various factors can influence the prediction of motion sickness including the duration of exposure. Literature suggests that increases in exposure duration increase the incidence of motion sickness (ISO 2631-1, 1997; Stevens and Parsons, 2002; Kluijven, 2016). A review by (Stevens and Parsons, (2002) illustrate this relationship shown in Figure 2.20 below where Motion Sickness Incidence is plotted against time in days.

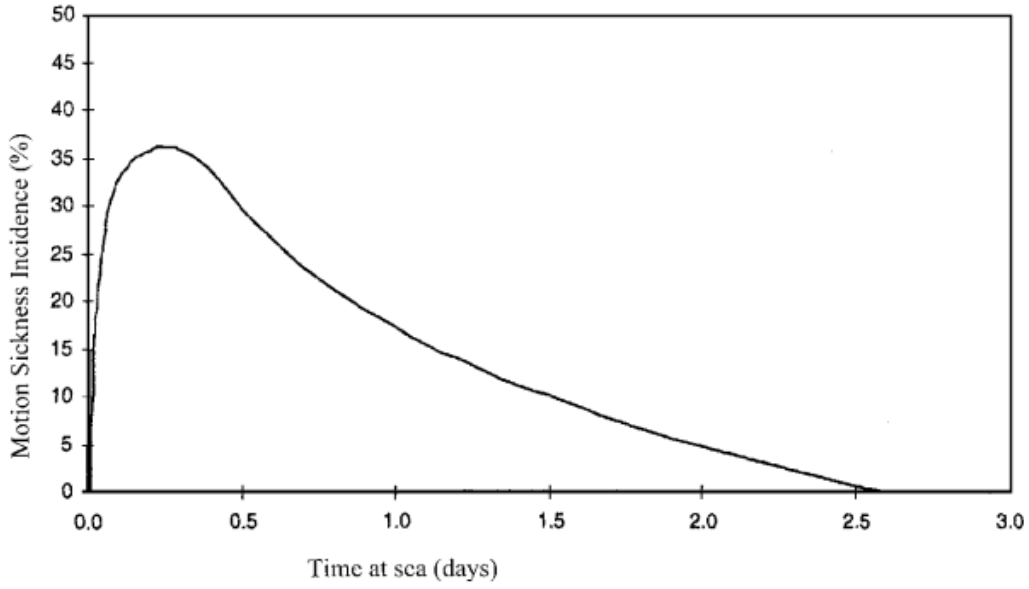

Figure 2. 20 Motion Sickness Incidence over time (Stevens and Parsons, 2002).

Other relationships with the incidence of motion sickness are found in the study by Cheung and Nakashima, (2006) who reviewed the effects of oscillatory frequencies on motion sickness with dominant frequencies causing nausea in humans between 0.1 Hz to 1 Hz. Their study lists both the design of the vessel and the nature of the wave as important factors in the characteristic frequency of oscillation of a floating vessel. The application of vessel parameters and sea state in predicting the incidence of motion sickness is more common in studies optimizing ship design such as Youn and Park, (2020), Cepowski, (2009), Cepowski, (2012), and Rumawas et al., (2018). These studies explored predicting Motion Sickness Incidence at the design stage, using vertical accelerations as well as ship parameters such as hull shape, areas in contact with water, design speed, and much more (Polymeropoulos et al., 2020). The study by Rumawas et al., (2019) goes further to include habitability indexes that account for noise levels. Their study is relevant because this accounts for susceptibility factors not usually included even in international standards. The reasoning behind the addition was stated by the authors as accounting for noised-caused sleep interruptions in passengers which can probably influence fatigue, thereby, making passengers more susceptible to motion sickness.

A common observation in most studies on motion sickness is the use of vertical accelerations in predicting Motion Sickness Incidence (Cepowski, 2009; Rumawas et al., 2018) and while vertical accelerations are of interest in limiting performance, recent publications have stated

that angular motions are also of interest with regards to their influence on ship axis accelerations (Phillips et al., 2015). The application of vessel roll in estimating motion sickness was explored by Joseph and Griffin, (2008) who found that motion sickness increased with an increase in the magnitude of rotational oscillations and pitch oscillations. These findings are correlated with earlier findings by Wertheim et al., (1999) though the authors also state that the alternative motions in themselves are not sickness-provoking but combined with vertical motions produce more motion sickness than the classic model. Similar correlations have been made in research concerning lateral oscillations such as Donohew and Griffin, (2004) whose study supports motion sickness causing frequencies in the lateral direction between 0.0315 Hz to 0.25 Hz depending on the weighting used. Using just vertical accelerations to assess the incidence of motion sickness, Dallinga et al., (2002) found that the singular use of vertical accelerations was insufficient as input for estimating Motion Sickness Incidence in their study on the human factors in the operation and maintenance of ferries. They propose the use of the roll and transverse motions as secondary inputs to be used alongside vertical motions. Similarly, Khalid et al., (2011) perform a combination of both theories to create a model combining horizontal motions with vertical motions to predict the incidence of motion sickness for 10 different vessels. The study found that the new model was marginally more accurate than traditional models using only vertical motions. However, these conclusions are not shared across studies. An early study by Morton et al., (1947), found that various frequencies from as low as 0.125 Hz, for vertical motion combined with pitch oscillations, produced similar illness rates with and without roll motions, and concluded that roll motions did not contribute to sickness and the incidence of sickness with the roll and vertical motion combined was not significantly different from that with the vertical motion alone. More recently, Cepowski, (2009) stated that alternative motions only had a slight influence on the prediction of motion sickness and based his model solely on vertical accelerations using a mathematical interrelation to describe the effect of waves, in terms of wave height, and ship design parameters on the incidence of motion sickness. The differences in opinion across studies can be attributed to various factors including new knowledge of motion sickness symptoms in research, differences in sample sizes, differences in transit durations, differences in survey and assessment methodologies, and susceptibility factors such as personal health and lifestyle. Furthermore, the assessment of motion sickness is performed across various

vessel types ranging from high-speed crafts to large naval vessels, ranging between different transport types, and ranging between simulations and experimental studies.

Another finding from the available literature is that most publications relate to vessel design with limiting criteria and the implementation of human factors in boats concerning comfort and safety-related issues are limited Rumawas et al., (2019). As such, the evaluation of the Motion Sickness Incidence of the vessels evaluated would be within the limits of the standards of human effectiveness (Alkan, 2011). In addition, shocks induced by slamming are not readily accounted for though most crew members will try to avoid slamming as much as possible using economically acceptable changes in heading and speed as a principle of good seamanship (Phillips et al., 2015). The ISO 2631-1, (1997), however, suggests that the levels of slamming between 5 to 10 per hour are unacceptable for passenger comfort depending on the severity of the slamming (Phillips et al., 2015). In addition to international standards, UK regulations also provide guidance on protecting workers from risks due to whole-body accelerations. The next section describes available legislation on whole-body accelerations.

2.6.3 Available UK Legislation on Whole-body Acceleration

The Control of Vibration at Work Regulations 2005 follows proposals submitted by the Health and Safety Commission and is based on a European Union Directive requiring similar laws on protecting workers from risks caused by vibration (The Control of Vibration at Work Regulations, 2005). These regulations were introduced to reduce instances of back pain from whole-body vibration and are also represented in the code of practice for reducing the risks from whole-body vibration on ships by the Maritime and Coastguard Agency (Maritime and Coastguard Agency - Great Britain, 2009). These regulations introduce an action value limit of 0.5 m/s^2 for 8-hour durations (assumed to be a typical shift length) where employers should introduce technical and organisational measures to reduce exposure and an exposure limit value of 1.15 m/s^2 for 8-hour durations which should not be exceeded. The suggested actions that should be taken by an employer where exposure limits are exceeded include:

- A reduction of a worker's exposure to vibration to below the limit;
- Identifying why limits were exceeded;
- Adopting measures to prevent limits from being exceeded in future.

Though there are no specific regulations concerning motion sickness, employers have a duty of care to their employees. Under Health and Safety at Work etc Act 1974 (Health and Safety at Work Etc Act, 1974) and the Management of Health and Safety at Work Regulations 1999 (Management of Health and Safety at Work Regulations, 1999), employers should identify causes of injury or illness, assess the likelihood and seriousness of the risk, and take action to eliminate and control the risk.

2.6.4 Limiting Criteria for O&M

As helicopters can operate independently from sea-state conditions – only limited by visibility and wind speed (Scheu et al., 2018) – Crew Transfer Vessels (CTVs) and service operational vessels (SOVs) are the major O&M vessels with sea-state limitations. Literature suggests limits of operation in CTVs to be up to 1.5 m of significant wave heights while SOVs have much larger limitations at about 4.0 m due to available walk-to-work assisted transfers (Scheu et al., 2018). Industry practices have also identified other operational limits such as limits to wind speed, and in some cases wave peak periods (Gintautas and Sørensen, 2017).

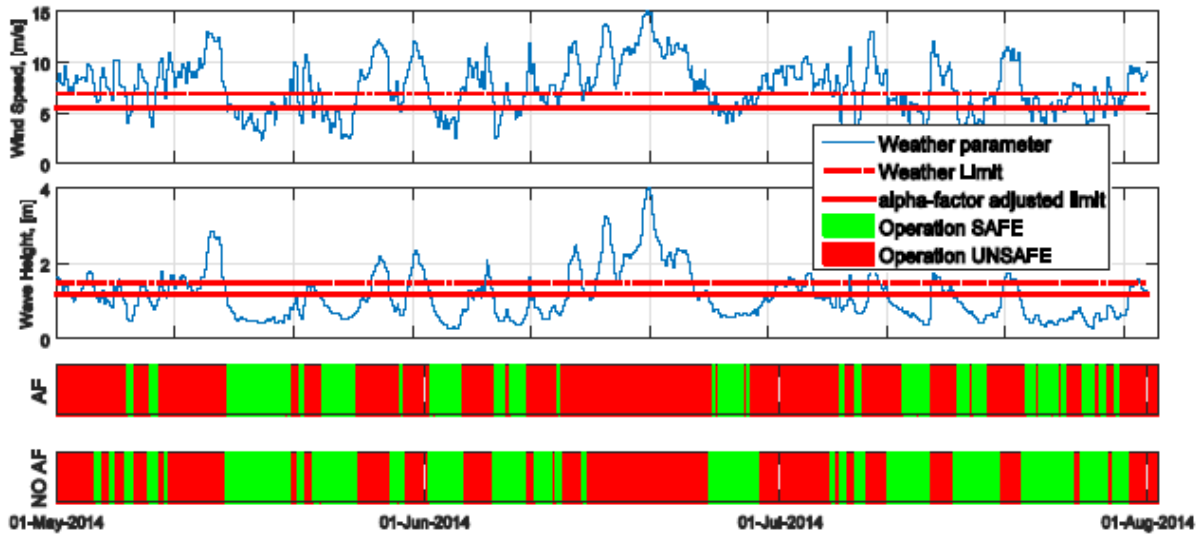

Figure 2. 21 Image showing operational weather limits for O&M (Gintautas and Sørensen, 2017).

The plots in Figure 2.21 present limits of operation specific to crew transfer vessels, illustrated by Gintautas and Sørensen, (2017). However, literature has shown that operational limits for O&M vessels in sufficient as research into human exposure to accelerations show that human comfort, health, and performance are affected by vertical and horizontal accelerations Scheu

et al., (2018). According to Scheu et al., (2018), there may be times when access to a wind farm is possible but exposure to motion is unacceptable leading to increased waiting time. It should be noted that current industry guidelines suggest the implementation of suspension seating, ventilation, and window positioning as mitigating measures to undertake where seasickness may make a person unfit at the point of transfer (RenewableUK, 2015). In terms of the duration of working hours, studies give evidence of increased risk of health associated with long-term exposure to whole-body acceleration (ISO 2631-1, 1997). However, literature has also exposed the need to optimize operation and maintenance decision-making to reduce the risks associated with maintenance activities. Additionally, Phillips et al., (2015) also state that there is little consensus and experience with respect to the limits of vessel motion at the point of transfer, and even less considering the human response to acceleration. As such more methods that account for the comfort, safety, and performance of technicians in decision-making are vital in optimising operations and maintenance and identified motion criteria should be treated the same way as weather windows (Scheu et al., 2018).

2.7 Summary

The current growth and potential of offshore wind energy show that as a renewable energy source, offshore wind energy can achieve the UK's energy targets in mitigating the effects of human-caused climate change. However, experience shows that the operation and maintenance phase of the offshore wind farm life cycle contributes about a third of the cost, and as such, there is a need to optimize the costs and risks associated with this phase of offshore wind energy to compete with traditional energy generation means. The literature review presented here highlights the need to optimise maintenance scheduling and generally, the planning of maintenance activities in offshore wind farms has involved accounting for weather and sea-state, and the availability of maintenance resources to determine whether a wind turbine is accessible. More recently, decision-support tools have been developed to aid this decision-making process by modelling daily maintenance planning based on the key factors described in this chapter. However, literature on operation and maintenance strategies and models also shows that day-to-day scheduling does not typically account for the welfare of technicians and their ability to do work upon arrival at offshore wind farms.

Where technicians were accounted for in research, it was typically related to the number of technicians available, the length of shifts, the number of technicians per service order or the number of service orders per technician, the type of technician available, and the availability of technicians for work orders. This exposes some uncertainties in maintenance scheduling and a gap in the literature as research has shown that accelerations caused by vessels in transit to offshore wind farms affect the comfort and health of the technicians on board which can affect the technicians in a number of symptoms including discomfort, seasickness, and inability to do work. Additionally, the available guidance on the discomfort caused by accelerations in the offshore wind industry is limited, but there is some guidance (though also limited) on the occurrence of seasickness-related issues which states that individuals feeling the effects of seasickness are to stay onboard the vessel until the effects subside. This creates further uncertainties such as increased waiting times, especially in cases where wind turbines are assessable but exposure to accelerations is unacceptable. Therefore, there exists a need to account for the comfort and health of technicians in maintenance planning.

This thesis explored the development of a technician welfare model in order to close the identified gap in research by applying comfort and health operational limits to *sail or no sail* decisions to ensure the comfort, health, and safety of technicians during transits to offshore wind farms for maintenance activities. The next chapter describes the chosen methodology used to model the technician welfare during transits for offshore wind farm operations.

3 Methodology

3.1 Introduction

The literature review exposed a relevant gap in research. Current operations and maintenance strategies rarely account for the welfare of technicians during transits to offshore wind farms, only accounting for weather windows and the availability of maintenance resources when planning maintenance operations. However, studies show that vessel motions during transits to offshore wind farms can affect the comfort, health, and ability to do work of technicians on board vessels and as such, can impact the successful completion of maintenance activities. This thesis presents a decision support tool that can aid wind farm operators in the *sail or not sail* decision-making process in maintenance planning by modelling the health and comfort of technicians as a way of accounting for technician welfare during transits to offshore wind farms.

The following sections outline the methodologies used in achieving the thesis aim and objectives. This section provides a brief introduction and outlines the subsequent sections within this chapter. The second section presents the observed limitations to the data used in this research, and the limitations to data collection encountered in this research. The third section describes the type of data used within the research, the instrumentation used in data collection, their principles of operation, and the typical data output of each instrument. The fourth section presents a general description of the project sites while the timescale for data collection is provided in section five. Section six describes the processes of data processing, data visualization, and data analysis used to achieve the thesis aim and objectives. Section seven describes the data analysis, feature engineering, and data visualisations used on the dataset within this study. Section eight presents a description for modelling the comfort, health, and welfare of technicians. Finally, section nine presents a summary of the key details from this chapter.

3.2 Limitations to Data and Project Scope in Meeting Thesis Objectives

This section describes the limitations of the data collected and the data collection methods within the scope of this thesis.

3.2.1 Forecast and Remote sensing data

In-situ observations from moored buoys, met masts, and tide gauges provide the most assessable data for scheduling purposes, however, *in-situ* data only describes data collected adjacent to the measuring instrument. This means that relevant meteorological data such as wind speed and significant wave height were limited to coastal regions and a few on-site wave riders located at wind farms. As such, the data available was insufficient to cover the project sites and did not cover areas of transits between ports or onshore platforms and wind farms that are travelled by crew transfer vessels during maintenance activities. To mitigate this, this research uses metocean products to increase the spatial coverage of the data collected and cover the transits between wind farms and ports. The use of numerical models has been used to describe sea-state for various uses including human response to motions (Olausson, 2015), and in recent years, satellite remote sensing has become an efficient tool for global surveying (Dubovik et al., 2021). Satellite data is able to provide an optimum source of reliable data for a wide range of purposes including monitoring the dynamics of coastlines dynamics, topographic surveys, monitoring ocean surfaces, changes in sea level, sea surface temperature, ocean turbidity, ocean salinity, mapping of water current, ocean ecosystems, fisheries, and so much more. (Fu et al., 2019). For this reason, hindcast metocean data were chosen to give accurate spatial coverage of the project sites, with forecast-mode metocean data used to provide prediction data in line with the thesis's aim to aid decision-making with forecast information. Metocean data, produced using a blend of *in-situ*, satellite, and model output data assimilation techniques, also mitigated the limitations of using satellite data alone, including filling existing gaps in temporal and spatial coverage made from instrument trajectory, especially in lower timeframes, and the escape of data from capture which can occur due to backscatter in higher temporal and spatial variability (Dubovik et al., 2021). In this thesis, data has been processed and validated in order to avoid large gaps in datasets and where gaps were present, the data cleaning process employed in section 3.6 of this chapter

involved interpolating between missing data points in both lower and higher time frames except where missing data points were defined as relevant to the study such as major storm events.

3.2.2 In-situ data

This project required vessel motion measurements and employed the use of secondary data from the 'Safety and Productivity of Offshore Wind Technician Transit' (SPOWTT) project which was aimed at improving the safety and productivity of offshore turbine technicians (Earle et al., 2021). The vessel motion measurements were acquired using vessel motion monitoring systems (VMMS) that were deployed on crew transfer vessels to measure on-site data. The difference in project aims and objectives meant that some assumptions had to be made regarding the calibration of the accelerometers on the vessel motion monitoring systems (VMMS), and the placement of the VMMS on the participating vessels which can create errors from the physical constraints of the device, and errors concerning the location of the device in relation to the technicians on board the vessel as this project translates vessel vibrations to human vibrations. Additionally, as the vessel measurements were collected for a different project, there was some sampling variability between datasets as meteorological datasets, even at instantaneous levels, were recorded at much lower frequencies than the data from the accelerometers. In addition, there also existed spatial variability between the accelerometer data – collected in motion during transit - and the meteorological data acquired from metocean data products. The variabilities between datasets were reduced by matching the frequencies of both datasets and synchronising GPS data and time stamp data between both datasets. This could, however, create a loss of contributions to the variance from the smaller and larger motions whose time scales are smaller and longer than the record length, respectively.

3.2.3 Scope

The objectives of this thesis centre on the operation and maintenance of offshore wind farms and as such, only operation and maintenance transits were considered. Due to distinct reasons including weather restrictions, vessel repairs, and non-maintenance-based activities, the number of consecutive maintenance transits was affected within the data collection timeframe. This, therefore, reduced the size of the dataset used in the project analysis and

variable modelling. This was important because the performance of the resulting models created in this project could benefit from a larger dataset which can also reduce errors that can arise from a reduced dataset, especially when performing machine learning processes. In addition to this, further adjustments had to be made to the thesis objectives to adapt the scope of the research to available datasets including processes such as model validation with subjective measurements for comfort and seasickness which can be implemented through adapted questionnaires and parameter definition for seasickness and comfort more specific to crew transfer vessels

3.3 Data and Instrumentation

Wind farm operators use forecasting along with relevant risk criteria, in the binary *sail or no sail* decision-making process associated with planning maintenance activities. This makes forecast data a vital aspect of maintenance planning (Scheu et al., 2012). Forecasting information is usually provided by national meteorological agencies (e.g., UK Met Office) or commercial providers (e.g., ABPmer, Oceanweather Inc.) usually in terms of wind speed (Soukissian and Papadopoulos, 2015) and wave height (Endrerud and Liyanage, 2015; Endrerud et al., 2015). This thesis utilizes metocean data, and *in-situ* data to measure meteorological and acceleration data, respectively, at transit routes for operation and maintenance transits in the research project sites. This section describes the instruments used within the project to measure vessel motions and meteorological data.

3.3.1 In-situ data

A vessel motion monitoring system (VMMS) was used to gather data on participating operation and maintenance vessels in order to describe and model the relationship between sea-state-caused vessel motions and human factors relating to comfort and seasickness. The VMMS device (Xsens, 2017) was developed and calibrated by BMO Offshore (Offshore Energy, 2016), an external partner aligned with the SPOWTT project where data permissions were acquired, and data made available after data collection had subsided. The devices were deployed on four (4) wind farms located in different areas in the North Sea to ensure spatial variability of sea-state conditions and deployed on twelve (12) participating crew transfer

vessels of different sizes ranging from 18-metre hull length to 27-metre hull length. The participating vessels were operated by four (4) distinct offshore wind farm operators which ensured variability in the modes of operation maintenance procedures and activities. Table 3.1 presents a summary of the information recorded by the VMMS including the number of sailing O&M sailing days recorded, vessel sizes, and the data collection period.

Site	No. of sailing days	Vessel sizes (m)	Data collection period
Southern site 1	440	23 - 24	03/01/2019 -31/10/2019
Northern site 1	184	23 - 27	20/07/2019 -31/10/2019
Southern site 2	121	22 - 23	03/01/2019 -28/02/2019
Western site 1	105	18	14/08/2019 -26/10/2019

Table 3. 1 Summary of VMMS transit information

The image in Figure 3.1 presents a schematic diagram of the vessel motion monitoring system.

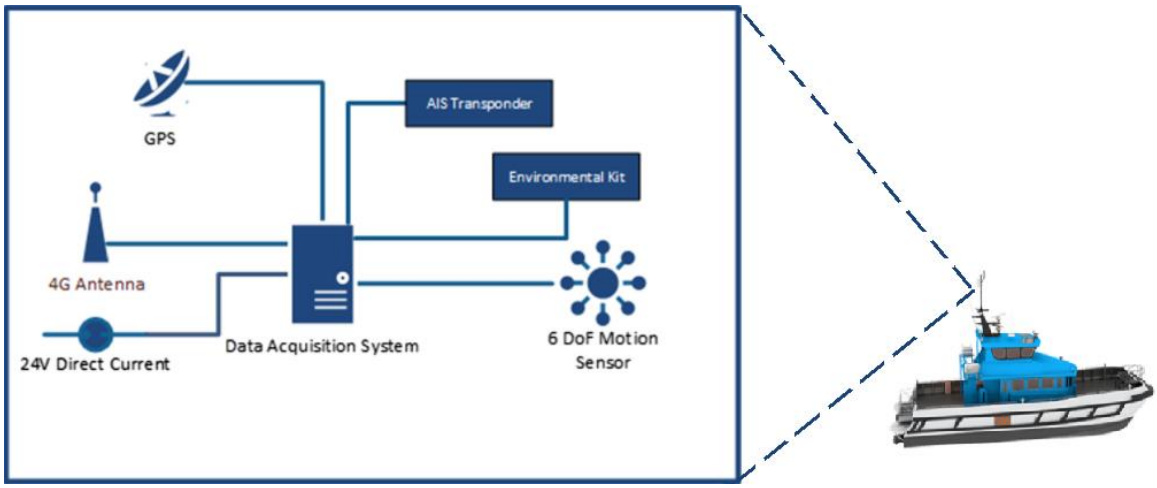

Figure 3. 1 A schematic diagram of the vessel motion monitoring system. Image adapted from Earle et al., (2021).

Figure 3.1 shows a schematic of the device used to measure vessel motions. The device is a data acquisition system coupled with a 4G antenna, an automatic identification system transponder, a GPS, and a six-directional motion sensor. The resulting output from the device includes data on vessel type, vessel speed, vessel heading, longitude and latitude GPS locations, the translational (i.e., accelerations in the x-axis, y-axis, and z-axis) and angular

accelerations (i.e., accelerations in roll, pitch, and yaw) at 40 Hz. Table 3.2. below is a summary of output parameters from the Vessel Motion Monitoring System (VMMS).

Parameter	Unit
Translational acceleration	Acceleration due to gravity (g)
Rotational acceleration	Degrees (˚)
Vessel heading	Degrees (˚)
Vessel speed	Kilometre per hour (Km/h)
Longitude and latitude	degree

Table 3. 2 Output parameters from the vessel motion monitoring system (VMMS).

Data from each of the devices deployed resulted in a total of 2500 transit trips between ports and wind farms, including the testing and measuring phases of the project.

3.3.1.1 Mode of operation

The VMMS measures and logs vessel motions with the help of coupled accelerometers. The working principle of the accelerometer is to convert mechanical energy into electrical energy. The accelerometer records the accelerations or vibrations of the vessel on a micro-scale by measuring changes in velocity caused by the movement of the vessel. The changes sensed by the accelerometer then get converted into an electric voltage which in turn is used to record vessel orientation. Six-axis accelerometers were used within this project which combined the readings of a 3-axis accelerometer with a 3-axis gyroscope. Thereby measuring the acceleration in the x-axis, the y-axis, and the z-axis as well as the angular acceleration around the x-axis, y-axis, and z-axis called the roll, pitch, and yaw.

3.3.2 Metocean and Satellite data

Meteorological data used in this thesis was acquired and licenced from:

- Copernicus Marine Service (CMEMS) for metocean and satellite products (marine.copernicus.eu)
- Cefas, licensed under the Cefas WaveNet Non-Commercial Licence v1.0 (wavenet.cefas.co.uk)

- Channel Coastal Observatory (CCO), licenced under the Open Government Licence v3.0, for *in-situ* validation data (coastalmonitoring.org).

The Copernicus program employs the use of earth-observing satellites called Sentinel satellites to provide free data for global-level monitoring and numerical ocean products for sea-state description. The various missions from the satellites provide data on physical, bio-geophysical, and biological variables used for ocean and land research activities (Malenovský et al., 2012). The satellite-based instruments used to provide data for land and sea research activities include spectroradiometers, infrared radiometers, microwave radiometers, satellite altimeters, satellite scatterometers, and synthetic-aperture radar (CMEMS, 2020).

This research used hindcast satellite data and metocean data from numerical models in areas surrounding participating wind farms and exit ports, and for periods within the scope of the project to achieve the thesis objectives. Operational data products from the Copernicus Marine Service consisted of hindcast datasets for wave, wind, current, and sea surface height characteristics. For ocean wave datasets, hindcast data from the Atlantic - European Northwest Shelf product NWSHELF_REANALYSIS_WAV_004_015 was used, provided at approximately 1.5 km resolution from the WAVEWATCH-III wave model (Lewis et al., 2019) which was forced by lateral boundary conditions from the Met Office Global wave forecast model. The product outputs included wave parameters for the significant wave height, period, and directional characteristics. The model operates using 6-hourly analysis and 3-hourly forecasted winds from the IFS-ECMWF atmospheric system and provides daily analyses for the global sea surface waves as well as 10-day forecasts. (CMEMS, 2020). For current and tidal datasets, the hindcast data from the Atlantic - European Northwest Shelf product NORTHWESTSHELF_ANALYSIS_FORECAST_PHY_004_013 was used. The product outputs were generated from the NEMO (Nucleus for European Modelling of the Ocean) ocean model (Tonani et al., 2019) at 1.5km resolution for hindcast data of currents, and sea surface heights. The model provides hourly instantaneous, quarter-hourly, and daily 24-hour temporal resolutions (CMEMS, 2020). For wind datasets, remotely sensed surfaced winds from scatterometers and radiometers were used for hindcast data of the Global Ocean Wind (Product WIND_GLO_WIND_L4_REP_OBSERVATIONS_012_006). Outputs from this product were from scatterometers (the ASCAT scatterometers on MetOp-A, MetOp-B and MetOp-C

at 0.125 and 0.25 degrees; the OSCAT scatterometer on Scatsat-1 at 0.25 and 0.5 degrees; the HSCAT scatterometer on HY-2B at 0.25 and 0.5 degrees) on the Sentinel satellites (CMEMS, 2020). The data reported included stress-equivalent wind and wind stress, wind stress curl, and divergence in the northward and eastward directions. See Appendix B for more product information.

Though not used towards the creation of the models used towards the thesis objectives, this research explored the use of satellite products to describe sea state variables used as model inputs. Satellite-based datasets included Global Ocean Spectral Parameters from near-real-time Satellite Measurements (product WAVE_GLO_PHY_SPC_L4_NRT_014_004). The dataset included measurements of significant wave height, partition peak period and partition peak or principal direction from Sentinel-1A and Sentinel-1B SAR missions. Similarly, the current dataset was acquired from Global Ocean Gridded Sea Surface Heights and Derived Variables (product SEALEVEL_GLO_PHY_L4_MY_008_047). The dataset presents satellite altimeter measurements of directional current and sea surface heights. The modes of operation for the satellite-based devices described are listed below including altimeters, satellite scatterometers, and synthetic-aperture radar SAR.

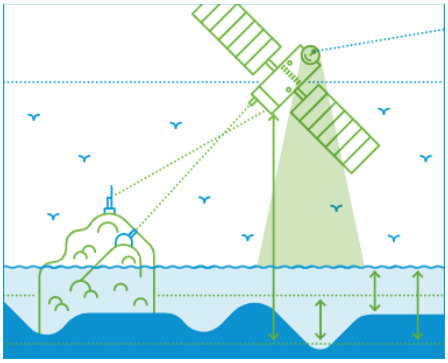

The **satellite altimeters** measure global surface topography by measuring the time taken for an electromagnetic pulse - sent from the satellite - to reach the earth's surface and back after being reflected off the surface. Ocean-based outputs include sea surface height, ocean surface wind speed, wave height and sea ice.

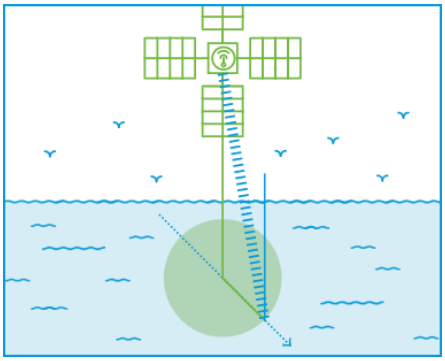

The **satellite scatterometer** is a radar sensor that scans the Earth and measures the scattering effect produced. Ocean-based outputs include ocean near-surface wind speed and direction, rainfall, and sea ice concentration.

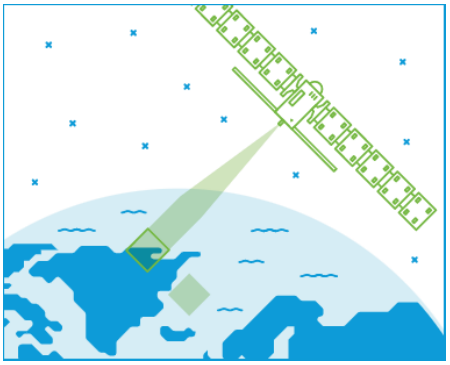

The **synthetic-aperture radar (SAR)** is a radar that creates two-dimensional or three-dimensional images of the Earth's surface with finer spatial resolution. Ocean outputs include surface waves, sea ice monitoring and wind data.

Figure 3. 2 Top to bottom: i. Image of a satellite altimeter; ii. Image of a satellite scatterometer; iii. Image of synthetic-aperture radar (SAR), adapted from CMEMS, n.d.

Satellite and model data was downloaded in netCDF-4 format for processing. The downloaded data had undergone pre-processing measures with initial cross-validation with in-situ data for the numerical model data.

Table 3.3. below presents a summary of the meteorological parameters from the instruments highlighted above in this thesis.

Measure	Parameter	Unit
Current	Northward current velocity	Meters per second (ms^{-1})
	Eastward current velocity	Meters per second (ms^{-1})
	Sea surface height above the geoid	Meters (m)
Wave height	Sea surface significant wave height	Meters (m)
	Sea surface wave direction	Degrees (˚)
	Wave period	Seconds (s)
Wind speed	Northward wind velocity	Meters per second (ms^{-1})
	Eastward wind velocity	Meters per second (ms^{-1})

Table 3. 3 Summary of meteorological parameters.

The next section describes the project site used in this research.

3.4 Site Selection

This section describes project sites for data collection and data analysis used within the scope of this project to meet the thesis objectives.

Data for the SPOWTT project was collected from 12 Crew Transfer Vessels (CTVs) operating across four 4 distinct wind farms located in the North Sea (see Table 3.1 above). The project sites include the operating wind farms, the ports of exit, and the area travelled by Crew Transfer Vessels. The project sites were located in the South of the North Sea for Southern site 1 and Southern site 2, the North of the North Sea for Northern site 1, and the West of the North Sea for Western site 1.

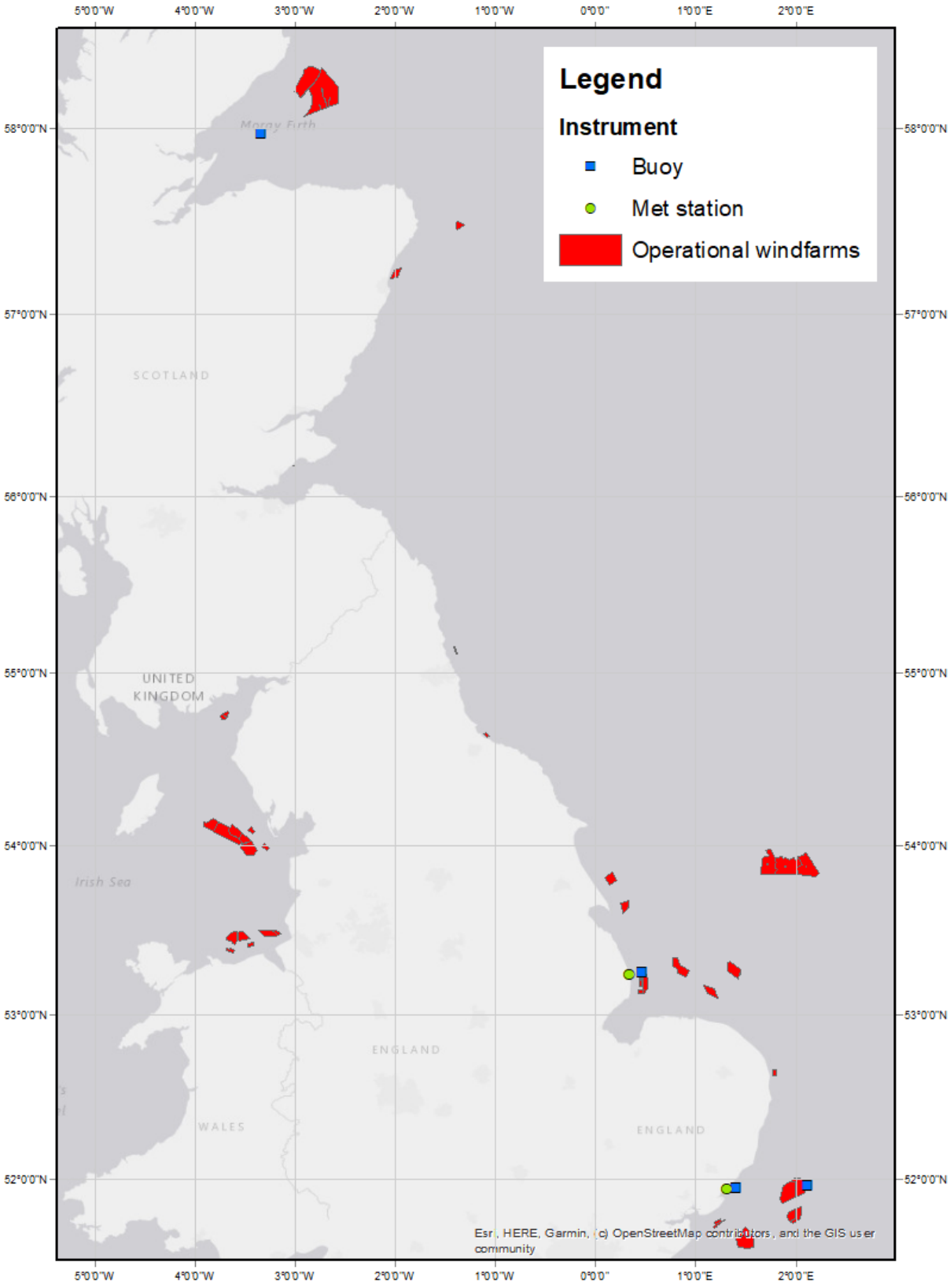

Figure 3. 3 Locations of available operational wind farms in red coloured polygons, with relevant buoys in blue, and met stations in green. The image contains data provided by The Crown Estate that is protected by copyright and database rights, Cefas, licensed under the

Cefas WaveNet Non-Commercial Licence v1.0, and the channel coastal observatory (CCO) licenced under the Open Government Licence v3.0.

Figure 3.3 presents a map of the North Sea area, showing operational offshore wind farms in the United Kingdom and the relevant available buoys and met stations considered in this thesis for metocean data validation. While the map shows operational wind farms in the region, the specific wind farms used towards the thesis aims are not highlighted following the terms to which the project data was made available. As such the wind farms are identified by their locations on the made including Southern site 1, Southern site 2, Northern site 1, and Western site 1.

3.4.1 Southern site 1

Data from southern site 1 included data from three (3) crew transfer vessels of sizes ranging between 23 and 24 metres. Data from the vessel motion monitoring systems deployed on the crew transfer vessels recorded longitude and latitude GPS locations, the speed and heading of the vessels, translational (i.e., accelerations in the x-axis, y-axis, and z-axis) and angular accelerations (i.e., accelerations in roll, pitch, and yaw) at 40 Hz. The distance between the port of exit and the wind farm for southern site 1 was about 40 km with an added 10 km for the wind farm's extension. The average transit time for participating vessels was recorded at about 1.3 hours, the average speed of the participating vessels was recorded at about 42.7 km/h (23 knots), and the average distance to turbines within the wind farms travelled by the vessels was recorded at about 54.8 km. Data collection for this site commenced on the 3rd of January 2019 and concluded on the 31st of October 2019.

3.4.2 Northern site 1

Similar to southern site 1, data from northern site 1 were collected from 3 (three) crew transfer vessels including a 27-metre vessel, a 24-metre vessel, and a 23-metre vessel. The vessel motion monitoring systems deployed on the vessels in northern site 1 recorded similar datasets to the systems deployed in southern site 1. The distance between the port of exit and the wind farm for northern site 1 is about 21 km, the average transit time for participating vessels between the exit port and wind farm was recorded at about 0.7 hours, and the average speed of the participating vessels recorded was about 29.7 km/h. Data collection commenced on the 3rd of January 2019 and concluded on the 31st of October 2019.

3.4.3 Southern site 2

Data from southern site 2 were collected from the vessel motion monitoring systems deployed on 3 (three) crew transfer vessels of sizes ranging between 23 and 22 metres. The distance between the port of exit and the wind farm for southern site 2 is about 60 km with an added 10 km for the wind farm's extension. The average transit time for participating vessels was recorded at about 1.2 hours, the average speed was 47.7 km/h, and the average distance to the turbine travelled by the participating vessels is 62 km. Data collection commenced on the 27th of November 2018 and concluded on the 28th of February 2019 with gaps in data collection within this period. Meteorological and *in-situ* data used in southern site 2 were similar to the datasets used in project sites 1 and 2, however, the data collected was adjusted to the GPS locations of the vessels participating in southern site 2.

3.4.4 Western site 1

Data from western site 1 were collected from the vessel motion monitoring systems deployed on 3 (three) 18-metre crew transfer vessels. The distance between the port of exit and the nearest turbine on the wind farm is about 50 km. The average transit time for the participating vessels was recorded at about 1.3 hours, the average speed was 47.7 km/h, and the average distance to the turbines travelled by the participating vessels is 54.8 km. Being the site for the initial test phase of the project, data collection commenced on the 4th of August 2018 and concluded on the 26th of October 2019 with gaps in data collection within this period. As with previous project sites, meteorological and *in-situ* data used were adjusted to the GPS locations of the vessels participating in western site 1.

3.5 Temporal Selection

The section describes the timescale used in this thesis and the reasoning behind the time-scale selection.

Overall, data collection from all participating wind farms began in August of 2018 and concluded in October 2019, however, the data collected in 2018 was pilot data used to refine data collection methods and initially used to create a general overview of a vessel and journey characteristics. Therefore, this thesis uses datasets from 2019 which had the largest and most

overlapping sampling timescales between participating vessels and wind farms. As such, data from 2018 were filtered using cleaning processes described in section 3.6 to allow for proper time stamping between datasets. It was important for the timestamps to coincide between vessels and wind farms and at the same time for enough data to be available for analysis. As such, the time scale for the entire study was limited between the 3rd of January and the 31st of October.

3.6 Data Processing, Analysis, and Visualisation

This thesis followed a structured approach to data analysis and modelling including a descriptive analysis performed after data cleaning and processing, a diagnostic analysis to identify and process outliers within datasets, and a predictive analysis to model thesis objective responses. This section describes the processes of data processing, data analysis and data visualization undertaken within the scope of this thesis to achieve the thesis aims.

This project utilized MATLAB software for data analysis and modelling procedures. The MATLAB software has the advantage of integrating a deep learning toolbox which allows the use of simpler codes to perform complex commands. The MATLAB software also allows the creation of scripts which was specifically beneficial as this project required the application of specific feature engineering calculations to large datasets. As a result, the application of the same feature engineering procedures, where new variables are created from existing variables in a dataset, was used on multiple datasets with little or no changes. In addition, the software also has various added toolboxes for machine learning useful to the modelling phases of the thesis.

3.6.1 Data Processing of VMMS Data

Data from the Vessel Motion Monitoring System (VMMS) was imported into the MATLAB workspace for initial processing. The data from the VMMS device was stored as MATLAB files and stored with timestamps according to the date and time of transit for each vessel in their respective wind farms of operation. The dataset included recordings for the vessel's longitude and latitude, the vessel's speed, and heading, and the translational (i.e., accelerations in the x-axis, y-axis, and z-axis) and angular accelerations (i.e., accelerations in roll, pitch, and yaw)

of the vessels at 40 Hz for daily transits by each participating Crew Transfer Vessel. The initial dataset contained numerical data and did not contain logistical or categorical data. It was discovered that parameter identifiers such as names or titles differed between vessels and wind farms. This was most likely because the VMMS used a combination of different accelerometers, and though calibrated similarly, the accelerometers included different identifying numbers between vessels and wind farms. As such, parameters within each dataset were found to have multiple entries with varying identifiers, with most containing empty cells or not-a-number (NaN) values. To mitigate this and streamline the process of analysis, a cleaning and filtering process was needed to first remove empty parameters from the datasets and then select the parameter from the list of parameters with multiple entries that contained the most data as well as the most accurate data. This was done using "if", "else if", and "else" statements to test various conditions for the availability of data under each parameter for conditional assignments that create a dataset with only the required parameters and parameters with data within them. The code containing the filtering statements was then applied to a loop function that repeated the filtration process for each transit dataset. To process the VMMS data more efficiently, daily transit datasets were stored as tables using the "table" function to provide a detailed report on all data within using the "summary" function, and for ease in manipulating the data in datasets. This code was used to streamline the analysis process so that lines of code could be added to a script which would perform similar cleaning processes for every O&M transit. While most missing data were removed from the dataset, missing data considered relevant to the thesis analysis such as missing timestamps within variables were identified using 'NaT' for date and time-related values and 'NaN' for all else.

The scope of this thesis defines an operation and maintenance (O&M) transit as a transit originating at an exit port on a CTV that travels to a wind farm and travels back to its exit port or another, within an operation and maintenance day. As such, it was necessary to explore the VMMS data to identify where the vessel was at different points during the transit. . A process of discretization was then applied to acceleration data from vessel transits to better understand transits during O&M activities and create categorical variables of CTV positioning during transits. This was done using one of two methods – using frequency changes in acceleration data and standard deviation in acceleration signals. It was, however, discovered

that the acceleration data contained significant variations at different periods during transit which when combined with domain knowledge of O&M activities, could be used to identify vessel characteristics. As such, summary statistics were calculated for the entirety of daily vessel transits, using four-sectioned windowing (dividing transit signal into equal parts) on acceleration signals, as well as the standard deviation of the acceleration signal. Through this process, classifications of transits were created. The classifications created included features to classify the vessel's activity in transit and at wind farms. To validate results, peaks in the frequency domain of the acceleration signal were matched with peaks in summary statistics of peak prominence and differences in the acceleration signal, as well as the distance between the port and wind farm of the participating wind farms and the speed of the vessel showing when the vessel is in motion in comparison with peaks in acceleration. The process of discretization highlighted relevant points during vessel transits needed to represent the welfare of technicians. The points used included outward transit to the wind farms, transit within the wind farms, and daily dose transit durations for the entire O&M day. These points were relevant as the outward transits can provide estimations of sickness and comfort at the point of transfer, the transits within the wind farms could account for service trains – where more than one wind turbine is serviced by a crew transfer vessel - and the daily dose transit can present a general estimation of comfort and seasickness that can be applied to decision making. Figure 3.4

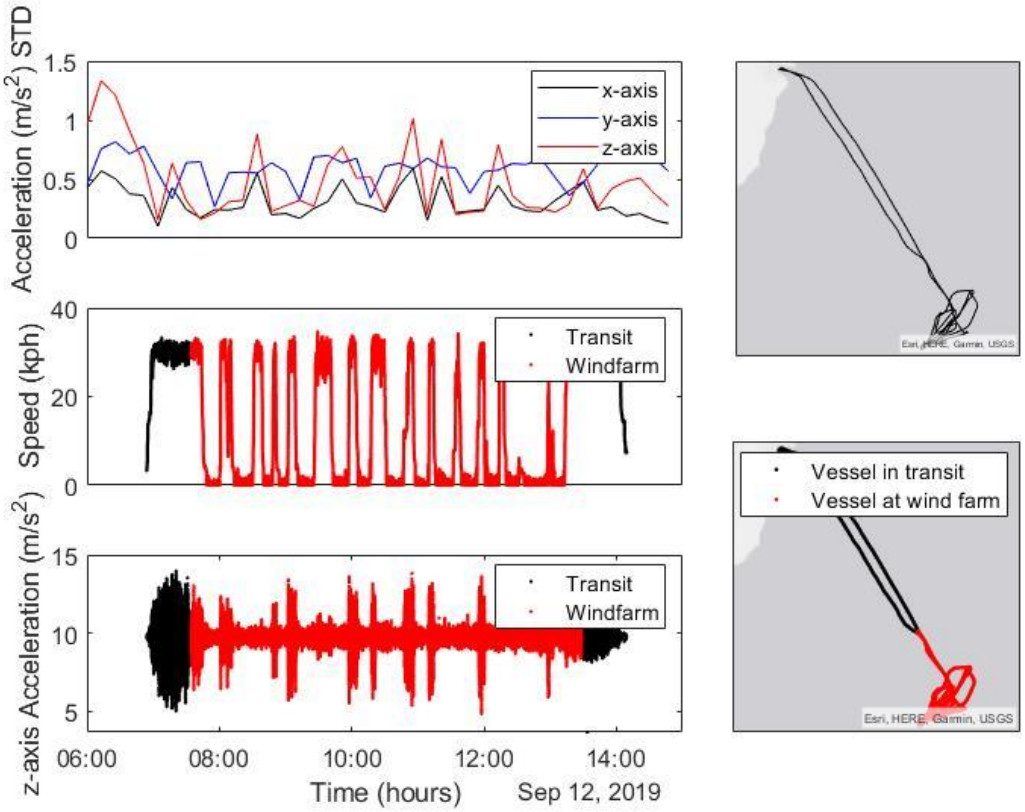

Figure 3. 4 Plot showing the discretization process including the standard deviation of x,y, and z-axis acceleration signals, a plot of the CTV transit track plotted using GPS coordinate data before the process of discretization, a plot of the speed of the vessel and the z-axis acceleration after discretization has been applied, and a plot of the CTV transit track plotted using GPS coordinate data after the process of discretization.

After the vessel transit characteristics had been explored from the discretization process, it was discovered that transit with the dataset was not O&M transits following the scope of this thesis. As such, additional filtering processes were used to separate defined O&M transits from other transits. This was done using "if", "else if", and "else" statements for conditional assignments on the created variables for CTVs in transit or at wind farms where transit data not defined as O&M transits were removed from the dataset. In addition, due to the size of the datasets which included 40 Hz data from 3 vessels each on 4 wind farms, a script was created to streamline the analysis process whereby the same data processing measures were applied for daily transits by each participating Crew Transfer Vessel using a loop function. This resulted in a total of eight hundred and fifty (850) defined O&M transits between four (4) wind farms and twelve (12) crew transfer vessels (CTVs).

To explore the VMMS data further, stacked plots of the variables in the transit datasets were created. The stacked plots included plots of acceleration data in the x, y, and z-axis, plots of roll, pitch and yaw acceleration data, and a plot of the vessel speed.

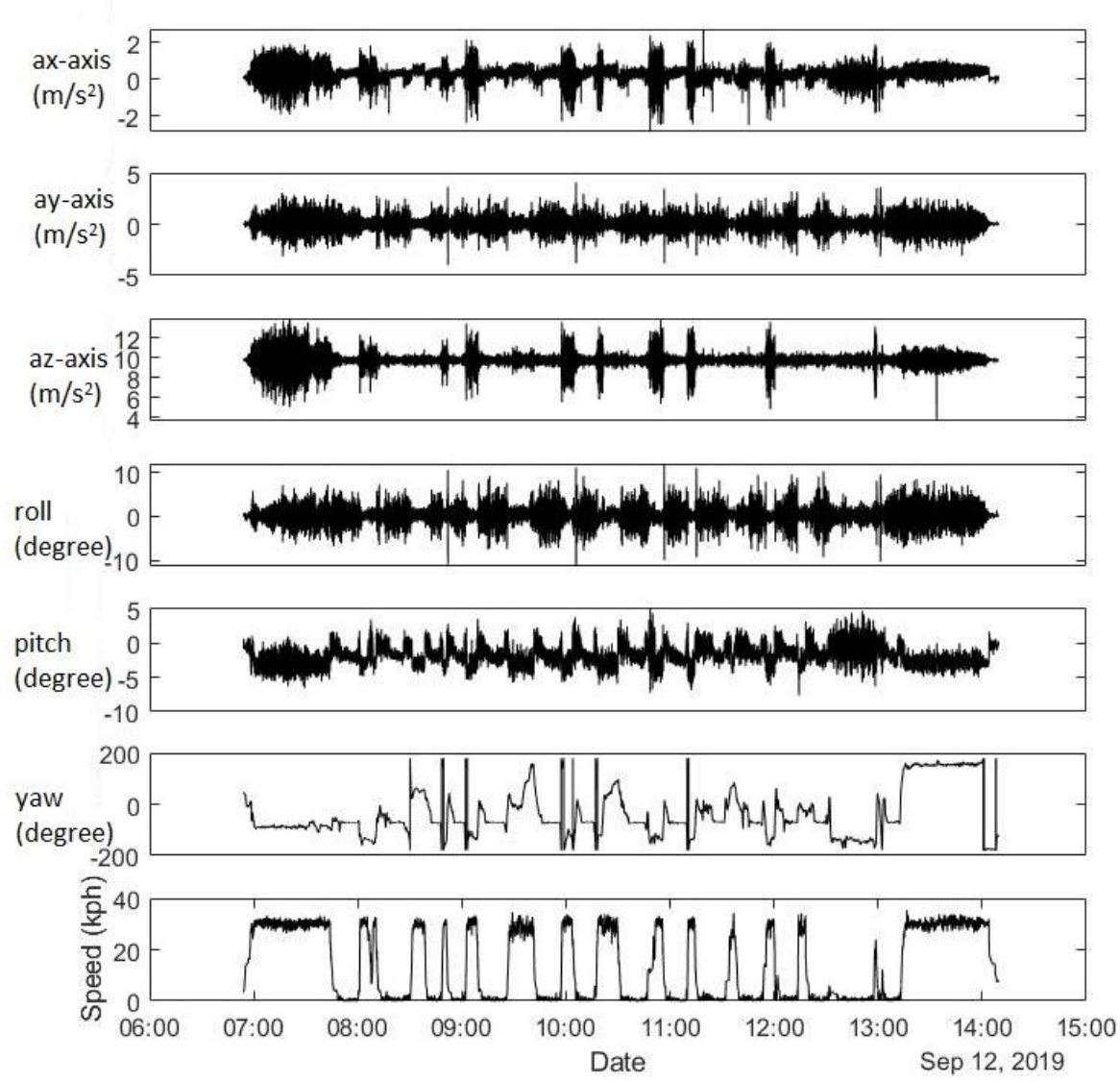

Figure 3. 5 Image showing a sample stacked plot of VMMS data from a CTV on an O&M transit day. From top to bottom: i. Vessel x-axis acceleration in m/s^2; ii. Vessel y-axis acceleration in m/s^2; iii. Vessel z-axis acceleration in m/s^2; iv. Vessel roll acceleration in degrees; v. Vessel pitch acceleration in degrees; vi. Vessel yaw acceleration in degrees; vii. Vessel speed recorded in kph

3.6.2 Data Processing of Meteorological Data

Meteorological data used in this thesis was open-sourced oceanographic data for current, wind, and wave data described in Appendix B of this thesis and licensed from Copernicus Marine Service (CMEMS). The meteorological data was collected to inform the sea-state

around the participating crew transfer vessels on transit routes to and from wind farms during O&M activities. This was done to account for the lack of spatial coverage from existing in-situ devices along transit routes. The meteorological data was downloaded in netCDF-4 format and imported into the MATLAB workspace for initial processing. To describe the sea state in transit sites, four data points from the VMMS GPS data were used to describe the area between the wind farm and the exit port. This was done by randomly segmenting transit routes between wind farms and ports plotted from VMMS data and selecting the geographical area surrounding the transit route for download. Since all transits in project sites typically followed similar routes, this was done manually four times to create geographical regions for the four sites in longitude and latitude data. Having identified the regions of interest, Copernicus Marine credentials were set to access and download data by setting the longitude and latitude parameters required to subset and download files. This also included a time range and specific ocean variables, Therefore, the code was used to download the meteorological data using the GPS data as reference points for the four sites. The individual netCDF-4 files were read using and the variables relevant to the study were extracted using file dimensions. The variables extracted from the current, wind, and wave files include:

- Northward and Eastward current velocity measured in meters per second (ms^{-1})
- Sea surface height above geoid measured in metres (m)
- Northward and Eastward wind velocity measured in meters per second (ms^{-1})
- Sea surface wave period in seconds (s)
- Significant wave height in metres (m)
- Sea surface wave direction in degree (˚)
- Longitude data measured in degrees east
- Latitude data measured in degrees north

The northward and eastward current velocity data variables and the northward and eastward wind component data variables were used to create new variables of current velocity measured in meters per second (ms^{-1}) and current direction measured in degrees (˚), and wind speed measured in meters per second (ms^{-1}) and wind direction measured in degrees (˚), respectively. This was done by calculating the magnitude of the u and v velocity components i.e., the northward and eastward components. The direction variable of both current and

wind data was then converted to the direction in degrees from the inverse trig function of tan seen in the equations below.

$$U_{wind/current} = \sqrt{(u^2 + v^2)} \qquad 3.\ 1$$

$$\theta_{wind/current} = tan^{-1}\, v/u \qquad 3.\ 2$$

Where $U_{wind/current}$ is wind speed and current speed in ms^{-1}, u is the northward velocity component of the wind or current and v is the eastward velocity component of the wind or current; $\Theta_{wind/current}$ is wind and current direction in degrees (˚).

Another process of feature engineering was applied to the current dataset to transform the sea surface height variable into a new variable called tidal range in order to better understand the relationship between current data and VMMS data. This was done by finding the difference between the maximum and minimum sea surface height within a period and expressed in metres. A final table including newly created (feature-engineered) variables were saved and exported in readable excel formats.

Missing data points in all four sets of data were identified and represented with 'Nan.' The meteorological datasets were recorded in timescales ranging from tri-hourly to daily datasets, as such, synchronisation processes were applied to change all the temporal resolutions of the datasets to $1.1574074074074 \times 10^{-5}$ Hz or a daily/24-hour resolution using the retime function which is a straight forward method of retiming a signal to match another in MATLAB. For instance, the wave dataset was downloaded in tri-hourly resolution, the dataset was aggregated to the daily mean using the mean in the retime function in MATLAB which generated a mean value. This process was repeated for transit periods measured by the VMMS data to ensure all transit days were accounted for within O&M transits over eight months. *In-situ* meteorological data was used to validate metocean sea-state data to ensure that there was sufficient spatial coverage of transit routes travelled by participating crew transfer vessels. Data from sea-surface directional waverider buoys, tide gauges, and met masts were used in the validation process for their locations either in the part of the port of exit for participating crew transfer vessels or at participating wind farms. Buoys are an

accurate means of point measurements for sea-state (Seemann et al., 2015) and met masts though limited provide useful wind datasets. The data from the *in-situ* instruments were open-sourced data provided by Cefas and funded by Environment Agency, licensed under the Cefas WaveNet Non-Commercial Licence v1.0, and from the channel coastal observatory (CCO) licenced under the Open Government Licence v3.0. More information on meteorological data can be found in Appendix B. The validation process was done by performing a simple regression analysis on metocean and in-situ data and the variables tested included significant wave height (m) and wind speed (ms^{-2}).

To explore the meteorological, stacked plots of the variables were created. The stacked plots included plots of acceleration data in the x, y, and z-axis, plots of roll, pitch and yaw acceleration data, and a plot of the vessel speed.

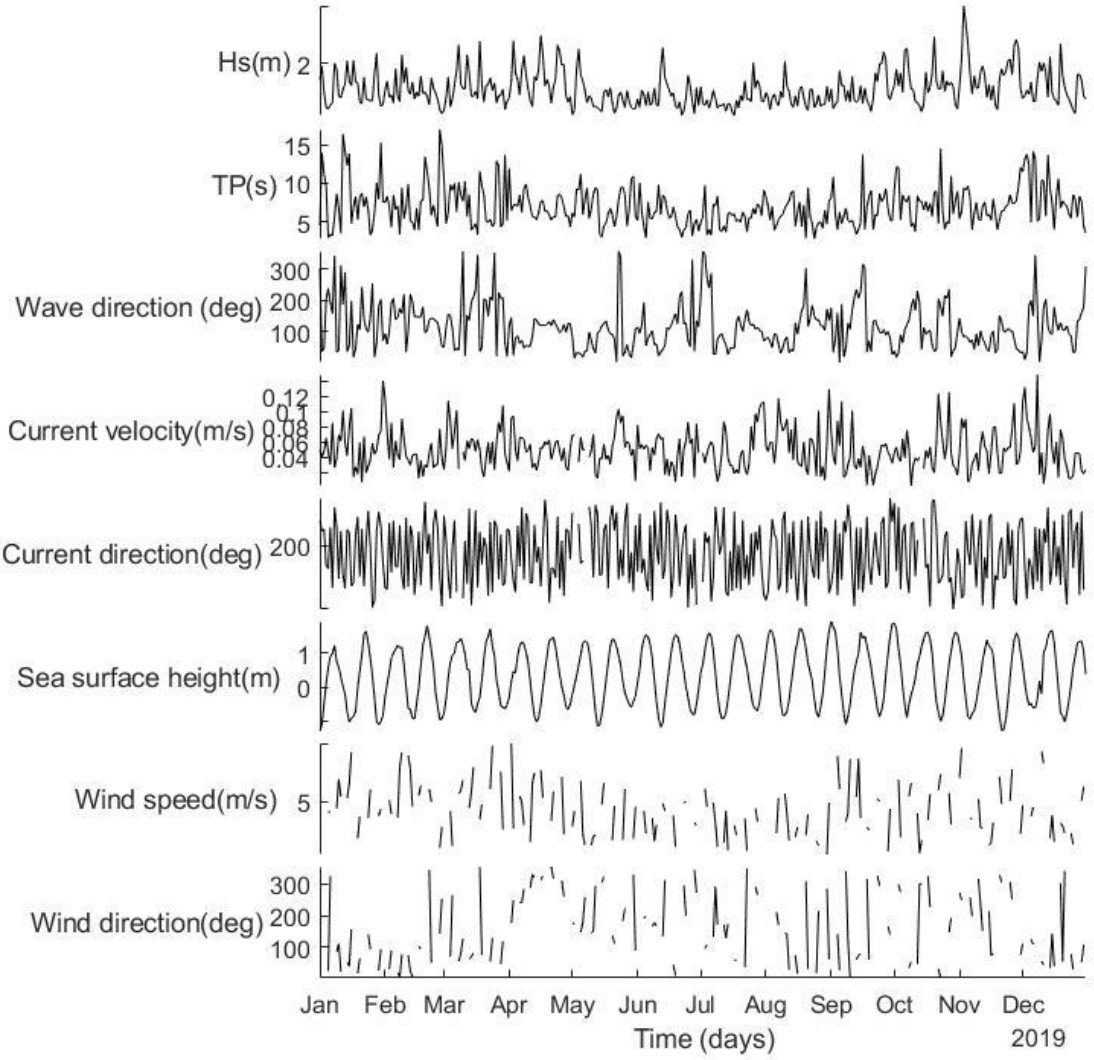

Figure 3. 6 Image showing a sample stacked plot of meteorological data. From top to bottom: i. Hs, Significant wave height (m); ii. Θwave, Wave direction (°); iii. TP, Peak wave period (s); iv. Uwind, Wind speed (m/s); v. Θwind, Wind direction (°) vi. Ucurrent, Current velocity (m/s); vii. Θcurrent, Current direction (°); viii. SSH, Sea surface height (m);

3.7 Technician Welfare Analysis

To achieve the thesis's aim of developing a welfare model, this research uses proxy metrics to estimate the level of comfort and the likelihood of seasickness in technicians including Composite Weighted Acceleration and Motion Sickness Incidence, respectively. Both metrics were chosen as measurable metrics for the short-term effects of vessel motions on

passengers able to represent subjective levels of discomfort and passenger short-term health in relation to travel at sea. These metrics were also chosen based on the availability of data within this study concerning whole-body accelerations. Motion Sickness Incidence was chosen as a measurable metric for the likelihood of a technician vomiting from exposure to accelerations during transit and its use has been documented in various studies (Cepowski, 2009, 2012; Piscopo & Scamardella, 2015; Rumawas et al., 2018), as well as international standards. In addition to this, Motion Sickness Incidence is a recognisable metric used in various marine-based industries that would be understandable to offshore wind farm operators. The discomfort of technicians is subjective, however, available studies show that there is a relationship between the magnitude of acceleration and the levels of discomfort experienced by travellers (Mansfield et al., 2000), as such, Composited Weighted Acceleration was used in this thesis to express the total experienced weighted acceleration with time following the guidance from the ISO 2631-1 for exploring human response to acceleration (ISO 2631-1, 1997). The weighted acceleration method was used in this thesis because it accounts for transient vibration and occasional shocks using an integration shorter time constant. As stated in section 2.6.1, other measures for assessing accelerations exist such as using root-mean-quad in relation to vibration dose values as suggested Kjellberg & Wikström, (1985b), However, these methods are not widely used and are used mostly in relation to shocks (Mansfield, 2005). This ISO standard was used because it is the most recent standard for estimating human response vibration. As such, the proxy metrics were created from acceleration and timestamp data and from guidelines of the ISO 2631-1 presented in equations 2.14 and 2.18 of sections 2.6.1 and 2.6.2, respectively, to explore the relevant variables for the prediction. The process described below presents the methods used to explore the human response to vessel motions at sea from instantaneous measurements.

3.7.1 Feature engineering welfare variables

both create a duration variable, in seconds, and create the proxy variables used to describe comfort and seasickness in technicians. The duration variable was created from the timestamp data recorded by the VMMS by subtracting succeeding timestamps from previous timestamps. To generate the weighted acceleration proxy variable, the Root Mean Square (RMS) of acceleration was calculated from equation 2.14 in section 2.6.1 of this thesis. This was done using the z-axis acceleration and the duration variable created as well as using the

vector sum of translational acceleration variables of the x, y, and z-axis as represented in equation 2.15. The rotational acceleration data including the roll, pitch, and yaw, were not included in the vector sum following guidance from international standards. Appropriate multiplying factors including K_x, K_y, and K_z with values of 1.4, 1.4, and 1.0, respectively, were included to account for dominant accelerations such as z-axis accelerations (Mansfield, 2005). The appropriate weightings were also applied to the acceleration signal before calculation following the ISO 2631-1 guide for the application of frequency weightings seen in Table 2.1 of the second chapter. Frequency weightings are applied to model human response to vibration phenomena from a time-series signal rather than the mechanical characteristics of the vibrating structure (Mansfield, 2005). As such, this thesis applies frequency weightings to transform the measured acceleration data from the VMMS into human response signals. While frequency weightings have limitations expressed further in section 2.6.1 of this thesis, at the time of writing there was no better alternative method for assessing human response to complex vibrations (Mansfield, 2005). Applied weightings depend on the posture of passengers, as such, weightings in this thesis are applied under the assumption that technicians on the CTVs are in seated positions. As such, whole-body vibration weighting for persons in seated positions expressed as W_k for z-axis accelerations, W_d for x and y-axis, and W_f for z-axis for Motion Sickness Incidence, were used. The weightings are defined by s-domain Laplace operator equations in one-third octaves, and band-limiting transfer functions as well as weighting transfer functions expressed in the ISO 2631-1 are used to limit the influence of the out-of-band frequencies. High-pass and low-pass filters are used to achieve high and low-frequency band limitations, respectively, while the frequency weighting is expressed in the weighting transfer functions. The weighting curves were defined by the equations below:

High-pass filter

$$H_h(p) = \left| \frac{1}{1 + \sqrt{2}\,\omega_1/p + (w_1/p)^2} \right| = \sqrt{\frac{f^4}{f^4 + f_1^4}} \qquad 3.3$$

Low-pass filter

$$H_l(p) = \frac{1}{1 + \sqrt{2}\,p/\omega_2 + (p/w_2)^2} = \sqrt{\frac{f^4}{f^4 + f_2^4}} \qquad 3.4$$

Acceleration velocity transition

$$|H_t(p)| = \left|\frac{1 + p/\omega_3}{1 + p/(Q_4\omega_4) + (p/\omega_4)}\right| = \sqrt{\frac{f^2 + f_3^2}{f_3^2}} \cdot \sqrt{\frac{f_4^4 \cdot f_4^2}{f^4 \cdot Q_4^2 + f^2 \cdot f_4^2(1 - 2Q_4^2) + f_4^4 \cdot Q_4^2}} \quad 3.5$$

Step

$$H_s(p) = \left|\frac{1 + p/(Q_5\omega_5) + (p/\omega_5)^2}{1 + p/(Q_6\omega_6) + (p/\omega_6)^2} \cdot \left(\frac{\omega_5}{\omega_6}\right)^2\right| \quad 3.6$$

Where, $H_h(p)$ and $H_l(p)$ are the band-limiting transfer functions; $H_t(p)$ and $H_s(p)$ are weighting transfer functions; $\omega_n = 2\pi f_n$ and f_n = corner frequency (ISO 2631-1, 1997; Paddan et al., 2012).

Therefore, the total frequency applied as described by the ISO 2631-1, (1997) was:

$$H_{ISO}(p) = H_h(p) \cdot H_l(p) \cdot H_t(s) \cdot H_s(p) \quad 3.7$$

Similarly, a variable of Motion Sickness Incidence is created in the MATLAB workspace by applying whole-body vibration weighting for persons in seated positions expressed as W_f for the dominant z-axis accelerations, following ISO 2631-1, (1997) guidelines. Following the weighting, additional high-pass and low-pass filter frequencies were applied from equation 3.3 to 3.7 above and band-pass filtering and re-filtering processes were applied for phase correction before calculating the Root Mean Square of acceleration (aRMS) used to evaluate the Vibration Dose Value (VDV), Motion Sickness Dose Value (MSDV), and Motion Sickness Incidence (MSI), using the expressions from ISO 2631-1, (1997) shown in equation 2.14, equation 2.15, equation 2.17, and equation 2.18 of chapter 2, respectively. However, as the new variables of Motion Sickness Dose Value (MSDV) and Motion Sickness Incidence (MSI), both represent the likelihood of seasickness occurring, the Motion Sickness Dose Value was regarded as redundant to achieving the thesis's objectives during the dimensionality reduction process described below. The feature engineering process for generating technician comfort and technician health variables was performed for several iterations over the entire VMMS datasets for all twelve vessels transiting four wind farms.

3.7.2 Daily Dose Welfare Analysis

The VMMS data were imported into MATLAB workspace using a loop function that performed the feature engineering process described in Section 3.7.1, on each transit dataset. As this research aimed to estimate technician welfare for daily transits, a daily dose value was needed to represent the welfare metric. As such, daily aggregates from 40 Hz to 1 Hz by a method of daily mean were used to present a daily dose value for the variables in the dataset which prepared the data for predictive modelling and reduced the processing time for each analysis. The workflow included the creation of a matrix of the dominant accelerations in g, the duration of the journey in seconds, the vessel speed data, vessel heading data, and the application of whole-body vibration weightings for the estimation of the root mean square of acceleration (aRMS), the Vibration Dose Value (VDV), the Motion Sickness Dose Value (MSDV), and the Motion Sickness Incidence (MSI) in each dataset Following this, the mean function was applied iteratively using a loop function to transit files, thereby, creating daily values for each variable. The daily VMMS data were tabulated for easy synchronisation and stored in the MATLAB workspace, as well as exported to readable Excel format.Similarly, the already aggregated meteorological dataset was imported to the MATLAB workspace. A join function in MATLAB code was used to synchronise the meteorological datasets to the VMMS dataset (now on a daily timescale) using timestamps and GPS data as key joining variables with the VMMS dataset as the principal dataset. As such dates with corresponding data in the meteorological dataset were merged to the same data in the VMMS dataset for GPS locations corresponding to wind farms in the VMMS data.. The identified missing values were recognised to be mostly missing at random (MAR), meaning conditional on other variables such as unknown internal decisions within operators, or missing not at random (MNAR), where missing data was due to weather conditions such as in the wind datasets. As such these missing data values were not replaced or removed from the data set but ignored so as not to introduce bias and not to reduce the size of the dataset. For VMMS data, identified missing data points were due to non-maintenance transit days. A moving mean method over 30 days was used to identify outliers within the dataset and set thresholds were used to identify transient spikes in the dataset. Outliers were investigated in diagnostic processes to avoid scaling favourable to a few large data points or biased distribution mean. Having classified the outliers present in the dataset as meaningful to the study, data exploration processes were

performed to explore relationships between the variables in the dataset and satisfy the thesis objectives.

3.8 Welfare Modelling

This section describes the processes employed to model the comfort of technicians from Composite Weighted Acceleration and the health of technicians from Motion Sickness Incidence. To identify relevant variables for the model inputs, a dimensionality reduction process is employed to explore the relationships that are most relevant to predicting Composite Weighted Acceleration for the comfort model, and the variables most relevant to the prediction of Motion Sickness Incidence for the health-based model.

3.8.1 Dimensionality Reduction

Dimensionality reduction in this thesis was used to select a subset of the most relevant variables in the combination of VMMS and meteorological datasets for the predictive modelling of technician welfare. The variables identified following the feature engineering process included the Composite Weighted Acceleration, Motion Sickness Incidence, vessel duration, vessel speed, vessel heading, vibration dose value, motion sickness dose value, significant wave height, wave direction, wave period, wind speed, wind direction, sea surface height, tidal range, current speed, and current direction. As such this process identified which input variables to include and which irrelevant variables to exclude for predictive modelling in order to train models faster, simplify the models, improve accuracy and reduce over-fitting where a model does not generalize well on unseen data based on training data. There are various known methods for feature selection and dimensionality reduction in supervised machine learning such as Principal Component Analysis (PCA), filtering, wrapper, and embedding (Chandrashekar and Sahin, 2014), however, this thesis employs a few including filtering, Principal Component Analysis (PCA), based on the type of dataset and the aim of the thesis. Having a dataset with such high dimensionality meant that before modelling the welfare of technicians, feature selection processes were needed to select relevant variables for modelling welfare. This was done in order to determine which variables will enable the

model created to make accurate predictions from the variables that will not enable the model to make accurate predictions based on their statistical properties.

The filter method was chosen above the wrapper and embedded methods of feature selection as it ranks variables based on uni-variate metrics, in this thesis correlation coefficients (Kumari and Swarnkar, 2011), and is not typically embedded in the machine learning process. As such domain knowledge can be applied to the dataset. Wrapper and embedded methods, on the other hand, are not model agnostic and can be embedded in the machine learning algorithm (Lal et al., 2006). This thesis, however, applies domain knowledge to the dataset to remove redundant variables such as the Vibration Dose Value (VDV) and the Motion Sickness Dose Value (MSDV), which are other proxy indexes for comfort and the likelihood of seasickness, and wind data which is highly correlated with significant wave height data. Motion Sickness Incidence (MSI), however, was chosen as a percentage value, because it is the most used predictor of illness induced by motion (Cepowski, 2012). As such, this made the two selected variables redundant. Following this, a pairwise Pearson correlation coefficient filter section method was performed to compare the strengths of the linear relationships between the predictor variables and the response variables and discard weakly related features. After identifying weakly related variables within the dataset. This was performed by loading the 850 observations of O&M transits for the fourteen variables into the MATLAB workspace, where the analysis was performed using the “coeff” function. The plots in Figure 3.7 shows visualisations of the Pearson correlations analysis performed. The image of the pairwise Pearson correlation coefficient was created to compare the relationships between the response variables of Motion Sickness Incidence and composite weighted RMS of acceleration, and the predictor variables of vessel duration, vessel speed, vessel heading, vibration dose value, motion sickness dose value, significant wave height, wave direction, wave period, wind speed, wind direction, sea surface height, tidal range, current speed, and current direction.

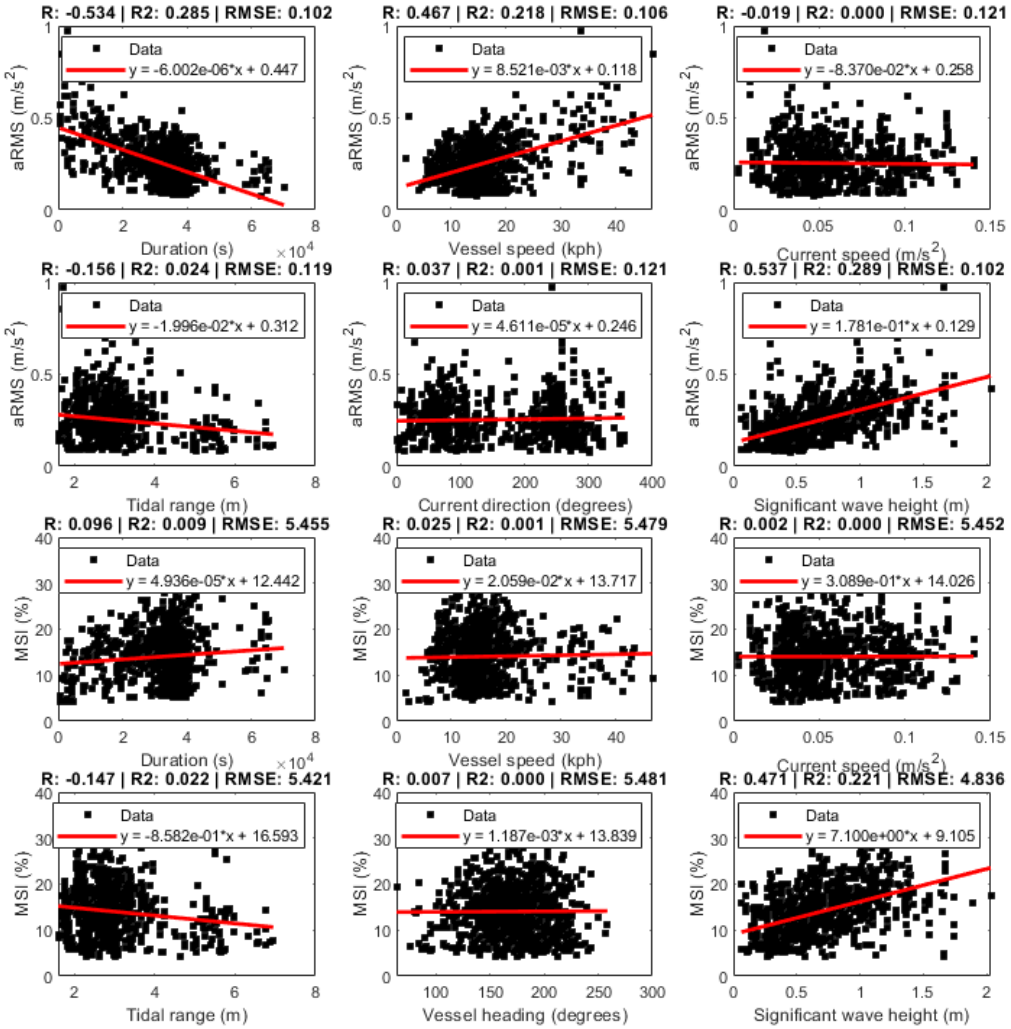

Figure 3. 7 Image showing a Pearson correlation coefficient analysis

Following the filter method, a Principal Component Analysis (PCA) was performed as the previous filter method could select variables with the most relationships with the variables being predicted, however, a variable could be an important influencer when combined with other variables but may not show strong relationships on its own. Therefore, the aim of the PCA was to select the main predictor variables from the dataset of variables. The first step taken in the PCA was applying weighting to the variables. When all variables are in the same unit, it is appropriate to compute principal components for raw data. However, when the variables are in different units or the difference in the variance of different columns is substantial, as in this case, scaling of the data or the use of weights is often preferable. Following this, the percentage variance or variance thresholding is performed which creates

a vector containing the per cent variance explained by the corresponding principal component and plotted using the “pareto” function as seen in the scree plot in Figure 3.8. The process was followed to first variables by percentage variance that explains roughly three-quarters of the total variability in the standardized ratings, so that might be a reasonable way to reduce the dimensionsFollowing this, the PCA is visualised in a single plot through orthonormal principal component coefficients for each variable and the principal component scores for each observation. In this plot, all variables are represented by a vector and the direction, and length of the vector indicates how each variable contributes to the two principal components in the plot. Thereby showing the most relevant variablesin the dataset. The variables selected were the vessel duration, vessel speed, tidal range, current speed, significant wave height, and current direction for Composite Weighted Acceleration, and vessel duration, vessel speed, tidal range, current speed, significant wave height, and vessel heading for Motion Sickness Incidence. Figure 3.8 presents a visualisation of the variance thresholding for principal component analysis.

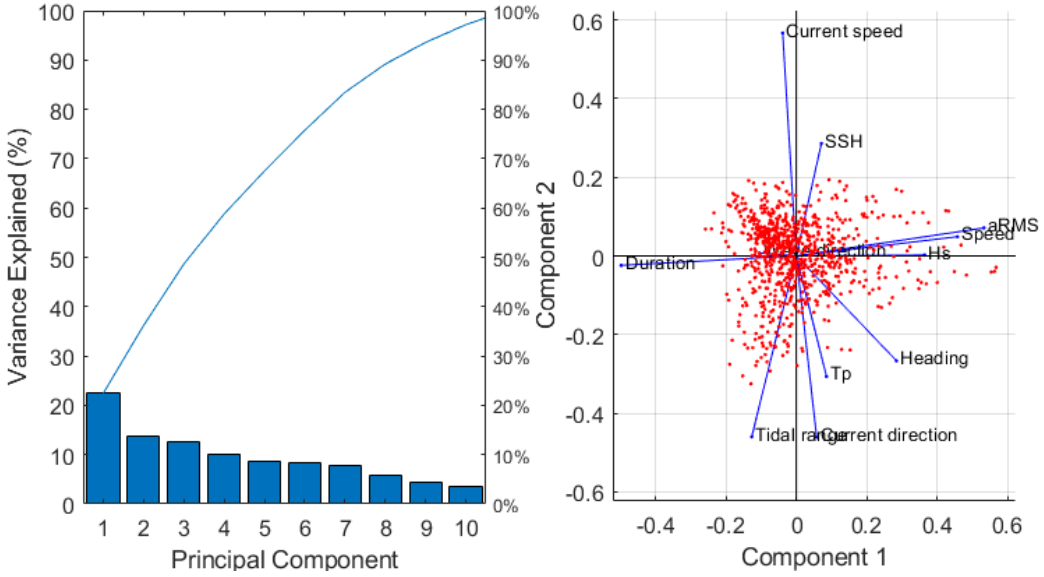

Figure 3. 8 Plot of a principal component analysis

The next sections describe the modelling of the comfort-based model, the health-based model, and the welfare model.

3.8.2 Modelling the Comfort of Technicians

This section describes the process of model selection and validation undertaken to create the health-based model to achieve the first objective of this thesis.

Having identified relevant predictor variables for the comfort model in section 3.8.1 above, the selection of a model to predict the welfare of technicians is based on the numeric output required. In the case of the comfort analysis a numeric value for Composite Weighted Acceleration. As such the required model for the thesis objective is a regression model. This thesis uses machine learning processes to train, validate, and test the model of best fit within the MATLAB workspace. A machine learning model was defined as the following general equation,

$$\hat{y}_i = \beta_0 + \sum_{i=1}^{n} \beta_i X_i + e_i \qquad 3.8$$

Where i = 1, 2,… n; $\hat{Y}_i$ is the proxy variable in the i^{th} sample, X_i composes of the input variables in the i^{th} sample (assumed to be a known constant measured without error), β_i is the coefficient for the input variables and e_i is the residual error.

The dataset was separated into a training dataset, a validation dataset, and a testing dataset using the hold-out function. This was performed following a standard machine learning approach to validate the performance of the model selected after training (Stetco et al., 2019). The original dataset (n_t = 850 transits) was split randomly into a six hundred and thirty-seven (637) training set (75% of the dataset) and a two hundred and twelve (212) testing set (25% of the dataset). The training dataset includes the set of data used to train the model with the purpose of deploying the model to accurately predict responses from new data (not within the training data) based on the training data. The training dataset was also subdivided into a validation set which is used simultaneously during model training to validate the model by adjusting for hyperparameters. This ensured the model was not overfitting to the data in the training dataset and by so doing created a more generalized model. The model's performance at predicting Composite Weighted Acceleration was assessed using fivefold cross-validation which split the data in the training set into five partitions, with each partition containing the same amount of data points. This was done within the MATLAB workspace

using cross-validation functions. The dataset was trained using the regression learner app in the MATLAB workspace, alternatively, the model can also be trained using the code presented in Appendix C of this thesis. This process is repeated iteratively for different models in the MATLAB workspace until a model of best fit was selected. The dataset was trained against multiple regression models including linear regression models such as a linear model, interaction linear, robust linear, and stepwise linear; regression tree models including fine tree, medium tree, and coarse tree; support vector machines (SVM) including linear SVM, quadratic SVM, cubic SVM, fine gaussian SVM, medium gaussian SVM, and coarse gaussian SVM; Gaussian process regression (GPR) models including rational quadratic GPR, squared potential GPR, matern GPR, and exponential GPR; and ensemble tree models including boosted trees and bagged trees. A Gaussian Process Regression (GPR) model was identified as the model with the best fit which has, in recent years, been identified as an efficient tool for estimating predictions and able to describe nonlinear relationships between predictor variables and response variables (Baiz et al., 2020). Table 3.4 presents a summary of the models trained on the training set to identify the GPR model.

Table 3. 4 Summary of trained models used to identify the model of best fit

Regression Model	R^2 (aWRMS)	RMSE (aWRMS)	R^2 (MSI)	RMSE (MSI)
Linear	0.51	0.08	0.29	4.63
Interactions linear	0.52	0.08	0.27	4.68
Robust linear	0.50	0.09	0.28	4.64
Stepwise linear	0.53	0.08	0.27	4.69
Fine tree	0.40	0.09	0.25	4.77
Medium tree	0.43	0.09	0.30	4.62
Coarse tree	0.46	0.09	0.31	4.57
Linear SVM	0.50	0.09	0.27	4.68

Quadratic SVM	0.54	0.08	0.37	4.35
Cubic SVM	0.54	0.08	0.38	4.32
Fine Gaussian SVM	0.21	0.12	0.24	4.78
Medium Gaussian SVM	0.56	0.08	0.41	4.20
Coarse Gaussian SVM	0.51	0.08	0.33	4.47
Boosted tree	0.58	0.08	0.45	4.02
Bagged trees	0.56	0.08	0.45	4.02
Squared exponential GPR	0.61	0.08	0.43	4.02
Matern 5/2 GPR	0.59	0.08	0.42	4.02
Exponential GPR	0.60	0.08	0.43	4.02
Rational quadratic GPR	**0.63**	**0.07**	**0.46**	**4.02**

Therefore, the model outputs numerical values of the proxy variables which can be modelled as:

$$\hat{y}_i = f_{GP}(x_i) + v \qquad 3.\ 9$$

Where $\hat{Y}_i$ is modelled output, the i^{th} sample; i = 1, 2,… n; X_i contains the input variables (x_1, x_2, x_3,… x_n); v is the Gaussian noise, f_{GP} is the Gaussian process model with zero mean (Rasmussen, 2004) and covariance function of the form k (x, x') for rational quadratic expressed as:

$$k(x, x') = \delta_1^2 \left(1 + \frac{\|x - x'\|^2}{2p\delta}\right)^{-p}, p \in N \qquad 3.\ 10$$

Here σ^2 is the variance; p is the length of scales for each input; $p \in N$ is a parameter that determines the degree of the polynomial (Rasmussen, 2004). Comprehensive descriptions of GPR methods are presented by Rasmussen, (2004) and Schulz et al., (2018), however, the GPR

model is created in MATLAB using the regression learner app and tested on the testing set using the fitgrp function with 'KernelFunction = rationalquadratic, BasisFunction = constant, Standardize = true, PredictMethod = Exact', as the model specification. The application of GPR has been used in various fields including medicine (Tonner et al., 2017), energy (Roberts et al., 2013), and animal nutrition (Baiz et al., 2020), however, to the best of my knowledge, its use in motion sickness analysis is not yet reported. In integrating the model outputs into the welfare model, discussed in section 3.8.4, ISO 2631-1 limits of operation are applied to define vessel transits such as how comfortable a transit will be or whether transits should be attempted based on the level of discomfort experienced.

The accuracy of predicting Composite Weighted Acceleration was tested following training and testing, using standard statistical machine learning measures including the coefficient of determination (R^2) which is best used in measuring regression model performance (Stetco et al., 2019), Mean Absolute Error (MAE), Mean Squared Error (MSE), and Root Mean Squared Error (RMSE).

The Root Mean Squared Error provided a measure of how far apart the predicted and observed values of Motion Sickness Incidence and Composite Weighted Acceleration were from the observed values.

$$RMSE = \sqrt{\sum (Y_i - X_i)^2 / n} \qquad 3.\ 11$$

Where Yi was the predicted value of Composite Weighted Acceleration and Motion Sickness Incidence, and Xi was the mean value of Composite Weighted Acceleration and Motion Sickness Incidence.

The coefficient of determination (R^2) presented the proportion of the variance in the dependent comfort and health variables of Composite Weighted Acceleration and Motion Sickness Incidence that was predictable from the independent variables of vessel duration, vessel speed, vessel heading, significant wave height, current speed, current direction, and tidal height. R^2 is expressed as:

$$R^2 = 1 - ({}^{RSS}/_{TSS}) \qquad 3.\ 12$$

Where TSS is the sum of squares and RSS is the residual sum of squares in the model.

The Mean Squared Error MSE presented the squared difference between the predicted and observed values of Motion Sickness Incidence and Composite Weighted Acceleration expressed as:

$$MSE = {}^{1}/_{n} \times \sum (Y_i - X_i)^2 \qquad 3.13$$

Where n was the sample size

The Mean Absolute Error MAE was used to show the average difference between predicted and observed values of Motion Sickness Incidence and Composite Weighted Acceleration. It is expressed as:

$$MAE = \frac{1}{n} \sum |X_i - Y_i| \qquad 3.14$$

These measures for the model's performance were included to investigate how well the models predicted proxy indexes, where 1 is perfect prediction and 0 is uncorrelated for the coefficient of determination, and all other measures present information on the model's errors. In addition, the RMSE, MSE, and MAE present measures through which improved models can be tested against with regard to predicting the proxy variables. As such, the metrics used show how well the selected input variables predicted proxy variables and measure residuals as a means of assessing technician welfare where proxy variables are assumed to have a good relationship with comfort and the likelihood of seasickness. In application, the explored input variables will be used in the model created to generate sailing decisions, therefore, there is a need to measure their accuracy in making predictions. For instance, where a minimal amount of variance resides in the residuals, the model can be seen to perform well, however, where more than half of the variance is in the residuals, then more work is needed.

3.8.3 Modelling the Health of Technicians

This section describes the process of model selection and validation undertaken to create the health-based model to achieve the second objective of this thesis.

Similar to the comfort-based model, the identified relevant predictor variables for the health-based model (section 3.8.1) were used to predict a value for Motion Sickness Incidence, a numerical output used as a proxy indicator for the percentage of technicians likely to be seasick during transits. As with the previous model, machine learning processes were used to train, validate, and test the model of best fit within the MATLAB workspace. The machine learning processes identified a Gaussian process regression (GPR) model as the model with the best fit. In integrating the model outputs into the welfare model, ISO 2631-1 limits of operations were applied to define the percentage of technicians likely to get sick. After training and testing, the efficiency of the model was tested using statistical measures including the coefficient of determination (R^2), Mean Absolute Error (MAE), Mean Squared Error (MSE), and Root Mean Squared Error (RMSE).

Visualisations of model results and model performance were shown from a response plot showing predicted and estimated values of Composite Weighted Acceleration and Motion Sickness Incidence were plotted. A predicted against observed values plot, and a predicted against observed values plot showing the number of data points in the dataset was presented to show how well the model performs on a perfect prediction line and indicates if and where the model overestimated or underestimated values. Finally, a histogram of residuals plot, and a residual plot with the number of datasets, were then used to describe the model's performance. The histograms of residuals indicate the range of variance in the data set and the response plot with data points confirms the models' performance. Similar plots were created to visualise the health-based model including a response plot showing predicted and estimated values of Motion Sickness Incidence, a predicted against observed values plot, a predicted against observed values plot showing the number of data points in the dataset, a histogram of residuals plot, and a residual plot with the number of datasets was then used to describe the model's performance. An example of the visualisations is presented in Figure 3.9 below.

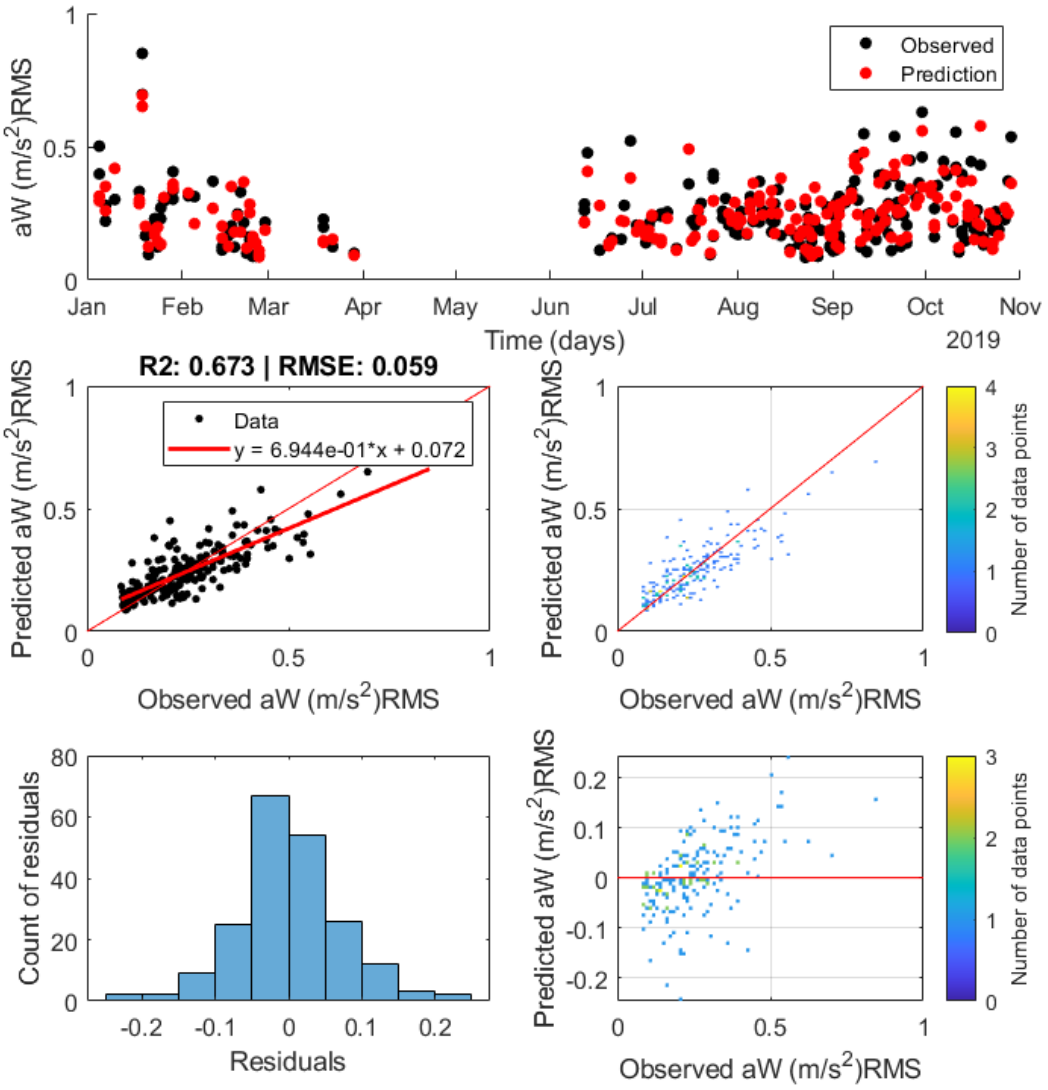

Figure 3. 9 A plot showing model results and performance including, from top row: i. A response plot of observed Composite Weighted Acceleration and predicted Composite Weighted Acceleration with time; the second row left to right: ii. Predicted against the observed plot of Composite Weighted Acceleration, iii. Predicted against the observed plot of Composite Weighted Acceleration with the number of data points; the third row left to right: iv. Histogram of residuals, v. Residual plot with the number of data points.

3.8.4 Modelling the Welfare of Technicians

This section describes the process of modelling the welfare of technicians in achieving the thesis aim.

In operation, the welfare model applies the limiting criteria defined by ISO 2631-1 to the outputs of the comfort and health-based model to make *sail or not sail* decisions. For the comfort-based model, this research uses the recommendation by the ISO 2631-1 expressed in sections 2.6.1 and 2.6.2 of this thesis, to describe technician discomfort based on the identified relationship between discomfort and the magnitude of acceleration. Table 2.2 presents the ISO 2631-1 guideline for likely human reactions to vibrations which shows a range of magnitudes of acceleration between 0 ms^{-2} to 2 ms^{-2} which have defined human reactions ranging from not uncomfortable to extremely uncomfortable. In applying the scales described, logic decisions are created in the MATLAB workspace using "if" and "else" statements, where predicted values of Composited Weighted Accelerations less than 0.315 ms^{-1} are defined as good sailing conditions and values of predicted Composite Weighted Acceleration greater than or equal to 0.315 ms-1, are defined as good sailing conditions and values of predicted Composite Weighted Acceleration greater than or equal to 0.315 ms^{-1} are defined as not good sailing conditions. Similarly, the health-based model applies operational conditions based on limits of acceptable working conditions and the duration of exposure which suggests a threshold of 20% Motion Sickness Incidence (Stevens and Parsons, 2002; Phillips et al., 2015; Saha et al., 2020). As such, logic decisions for *sail or not sail* decisions are described when predicted values of predicted Motion Sickness Incidence less than 20% are defined as good sailing conditions and predicted values of Motion Sickness Incidence greater than or equal to 20% are defined as not good sailing conditions.

To visualise the welfare model, plots of predicted Motion Sickness Incidence and predicted composited weighted acceleration were plotted showing the ISO 2631-1 threshold. This was used to indicate the levels of operability based on technician health and comfort. A resulting plot show categorised decisions of *sail and not-sail* was then presented to show simple logic decisions, where green described *sail* decisions and red described *not-sail* decisions.

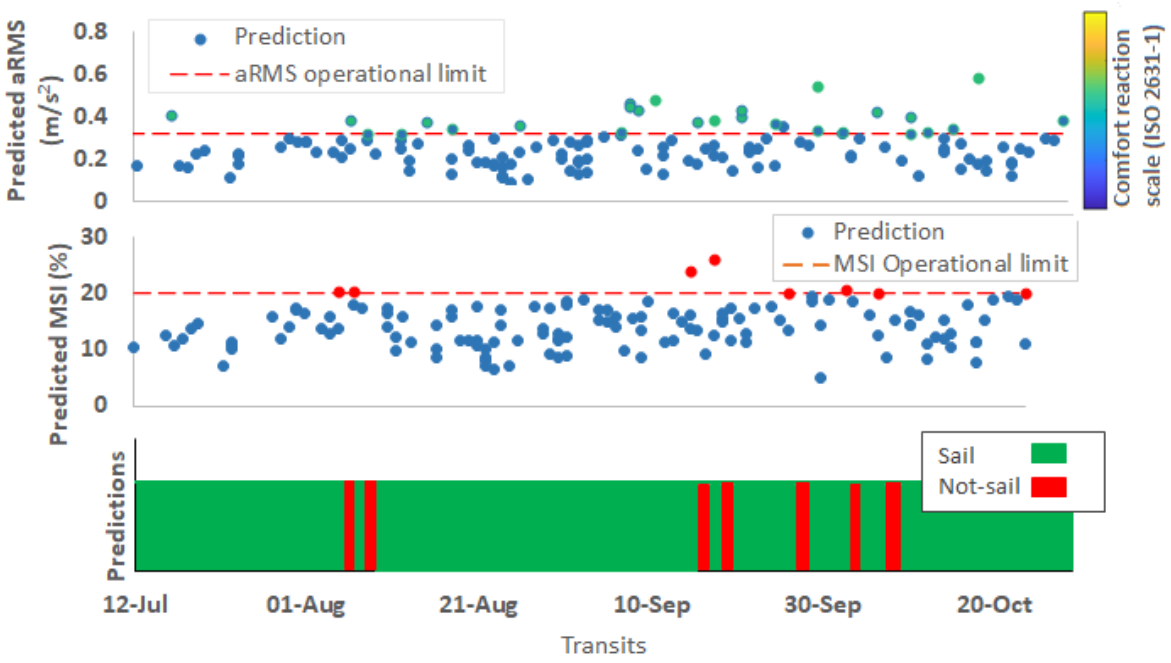

Figure 3. 10 Welfare model showing predicted sailing decisions.

3.9 Conclusion

This chapter described the methodologies used to collect data, process data collected, analyse the data collected, and model the estimated sickness and comfort of technicians on crew transfer vessels during operation and maintenance transits.

In-situ vessel data was collected using vessel motion monitoring systems (VMMS) which recorded vessel acceleration data in the six-axis of freedom as well as GPS data, vessel speed data, timestamp data, and vessel heading data. The site selection for this thesis was based solely on the availability of data and the participation of wind farm operators and vessels across four wind farms (4), four wind farm operators, and twelve (12) crew transfer vessels operating in the North Sea. The data collection for this project lasted for a year, however, data used for the analysis process covered eight months resulting in eight hundred and fifty defined operation and maintenance transit days after data processing and cleaning. Metocean data was used to represent meteorological data in the project sites and MATLAB code was used to synchronise metocean data to vessel transits between port and wind farms using the GPS coordinates of crew transfer vessels. The meteorological data included wind, wave, and current data. An analysis was performed on the vessel motion monitoring system

dataset to instantaneously describe operation and maintenance transits, and feature engineering processes were used to create Motion Sickness Incidence and Composite Weighted Acceleration variables based on equations 2.14 and 2.18 of chapter two. A daily dose value of the dataset was created and after feature engineering processes, the total number of variables in the combined dataset was brought to sixteen variables. Dimensionality reduction processes were performed to identify variables most relevant to predicting Motion Sickness Incidence and Composite Weighted Acceleration in order to improve the model performance. The processes involved included a feature section based on domain knowledge, a pairwise correlation between variables, a variance thresholding analysis, and a principal component analysis (PCA). Seven input variables were identified including vessel duration, vessel speed, vessel heading, current speed, current direction, tidal range, and significant wave height. Using machine learning processes, a Gaussian process regression (GPR) model was identified as the model with the best fit for predicting both Motion Sickness Incidence and Composite Weighted Acceleration based on the input variables. After the models had been trained, validated, and tested, statistical measures including the coefficient of determination (R^2) mean absolute error (MAE), mean Squared Error (MSE), and root-mean-squared error (RMSE), were used to show the models effectiveness. The outputs of the comfort and health-based model were used as inputs for the welfare model by applying limiting criteria defined by the ISO 2631-1 to make *sail* or *not sail* decisions in a logic model where values of Composite Weighted Acceleration below 0.315 ms^{-1} and Motion Sickness Incidence below 20% were categorised as a *sail* decision. Similarly, values of Composite Weighted Acceleration equal to or above 0.315 ms^{-1} and Motion Sickness Incidence equal to or above 20% were categorised as a *not-sail* decision. The results of the methodology described in this chapter are presented in the following chapter – Chapter Four.

4 Results

4.1 Introduction

This chapter provides representations and descriptions of the meteorological data and *in-situ* data collected by the Vessel Motion Monitoring System to meet the thesis objectives.

This project defines an operation and maintenance (O&M) transit as the transport from an O&M vessel originating from a port of exit onshore to a participating wind farm and concludes at its original port of exit (or a different exit port) within a day. As such transits outside the scope of this definition were not considered in the research analysis. The vessel motion monitoring system data collected includes data from four project sites, collected over a single year between January to October of 2019. Figure 4.1 below presents a frequency distribution of the defined O&M transits for the four project sites collected within the data collection period.

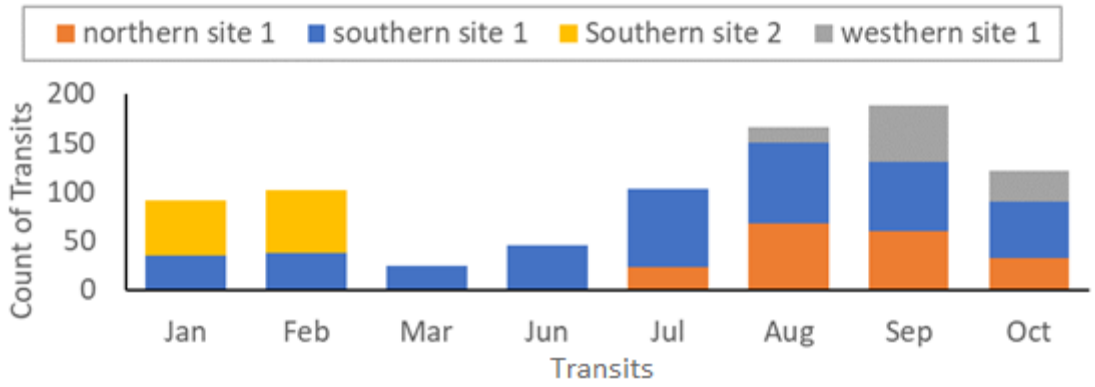

Figure 4. 1 Figure showing the distribution of operation and maintenance (O&M) transit by the four participating project sites over a year.

From Figure 4.1, Southern site 1 accounts for the majority of O&M transits with a sample size of n1 = 440 recorded transits. Similarly, project sites 2, 3, and 4 recorded O&M transits of n2 = 184, n3 = 121, and n4 = 105, respectively, bringing the total number of definable O&M

transits for the entire project to nt = 850 transits. Data from the vessel motion monitoring system also showed that on most maintenance days, daily O&M transits are undertaken by more than one maintenance vessel resulting in more than one transit in a single day. The data also shows that data from some sites including Southern site 2 and Western site 1 contain data that only cover part of the year. This coincides with rougher weather and sea state conditions during winter months where operational conditions would prevent O&M transits. Therefore, models created from this data will not cover the entire seasonal variability during the year which can affect future predictions for the uncovered months. Southern site 1 and western site 1 also appear to have noticeably higher durations than the other two sites which suggest longer daily O&M transits and longer time in completing maintenance tasks which could affect estimations for weighted accelerations and motion sickness incidences.

Chapter description

The results presented in this chapter are structured between each of the project sites and the nature of the analysis needed to achieve the exploratory thesis objectives outlined in Figure 4.2 below.

Figure 4. 2 Figure showing project data analysis flow chart.

As seen in Figure 4.2, descriptive analysis processes were performed on both the meteorological dataset and the *in-situ* dataset to better understand the dataset and pair finding with domain knowledge before further diagnostic analysis is performed to explore specific features. The predictive analysis is performed to achieve the thesis objective of modelling the welfare of technicians on crew transfer vessels.

This chapter is separated into sections. This first section (Section 4.1) provides an overview of the dataset used within the project, defines relevant project terms, and provides a description of the sections contained within this chapter. Section 4.2 presents the results from southern site 1 including the results of the remote sensing meteorological data, the results of the VMMS in-situ data, and the results of the analytical process undertaken to achieve the thesis

objectives. Section 4.3 presents the results from northern site 1 including the results of the remote sensing meteorological data, the results of the VMMS in-situ data, and the results of the analytical process undertaken. Section 4.4 presents the results from southern site 2 including the results of the remote sensing meteorological data, the results of the VMMS in-situ data, and the results of the analytical process undertaken. Section 4.5 presents the results from western site 1 including the results of the remote sensing meteorological data, the results of the VMMS in-situ data, and the results of the analytical process undertaken. Section 4.6 explores the relationships between relevant variables and presents the results of the modelling process undertaken to achieve the thesis aims and objectives including modelling the comfort of technicians, modelling the health of technicians, and modelling the welfare of technicians. Finally, section 4.7 provides a summary and conclusion of the results of sections 4.2 to 4.6. A discussion of the results provided in this chapter is given in the following chapter – chapter five.

4.2 Descriptive Analysis of Southern site 1

This section presents the results of the data collected for southern site 1.

4.2.1 Meteorological Data from Southern site 1

As discussed in section 3.3 of chapter three of this thesis, meteorological data including wind speed and wind direction, significant wave height, wave period and wave direction, sea surface height, current velocity, and current direction, were acquired and licenced from the Copernicus Marine Service (CMEMS). The meteorological data for Southern site 1 was collected from periods between 03/01/2019 and 31/10/2019. The multi-sourced data was recorded at different temporal resolutions, with the wave data which included significant wave height (Hs) measured in metres, wave period (Tp) measured in seconds, and wave direction (Θ_{wave}) measured in degrees, available as tri hourly data points. The current data was available at an hourly temporal resolution and included sea surface height (SSH) measured in metres, current velocity ($U_{current}$) and wave direction $\Theta_{current}$ in degrees, both calculated from northward and eastward current velocity v and u and measured in metres per second and degrees, respectively. This was done in MATLAB space by calculating the

magnitude and direction of the current vector. Future engineering processes were applied to the sea surface height variables of the current dataset to create a new variable containing tidal range in metres. The wind data were recorded daily and included wind speed (V_{wind}) and direction Θ_{wind} calculated from northward and eastward wind components v and u and measured in metres per second and degrees, respectively. This was done in the MATLAB workspace by calculating the magnitude and direction of the wind vector. MATLAB code was used to synchronise all three environmental datasets including the wave dataset, the current dataset, and the wind dataset using timestamps and dates as the merging variable. The synchronised environmental dataset was then synchronised with the Vessel Motion Monitoring System (VMMS) dataset to correlate with the movements of the vessels as they travel to wind farms using timestamps, dates, and vessel GPS locations.

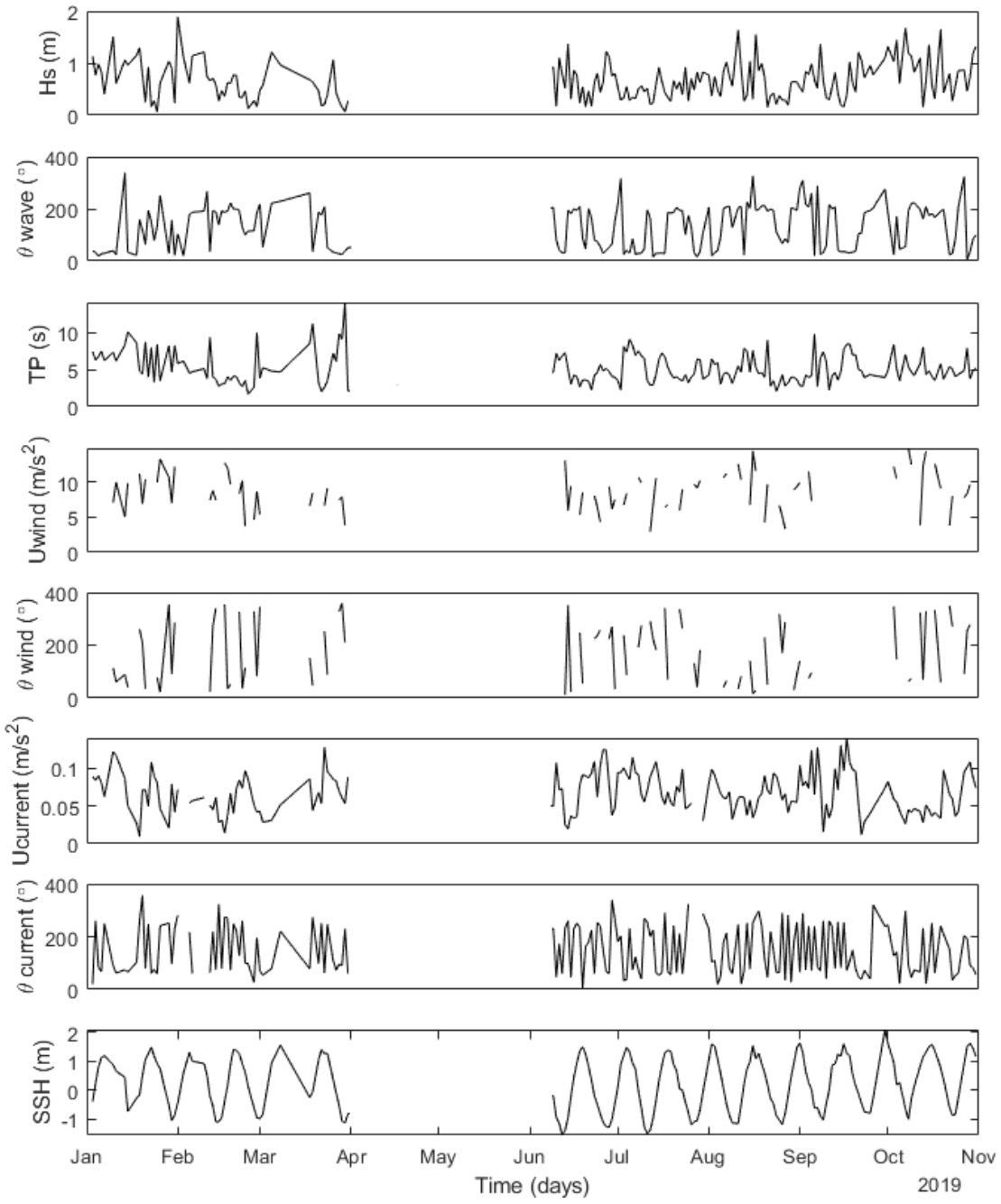

Figure 4. 3 Meteorological data for Southern site 1. From top to bottom: i. Hs, Significant wave height (m); ii. Θwave, Wave direction (°); iii. TP, Peak wave period (s); iv. Uwind, Wind speed (m/s); v. Θwind, Wind direction (°) vi. Ucurrent, Current velocity (m/s); vii. Θcurrent, Current direction (°); viii. SSH, Sea surface height (m);

Figure 4.3 above is a stacked plot arranged from top to bottom which presents the daily meteorological dataset for Southern site 1. The plot shows that the significant wave height for southern site 1 ranged between 0.06 metres and 1.89 metres with an average height of about 0.65 m during the 8-month project data collection period. There were periods of rough

weather resulting in higher than 1.5 m significant wave heights in the autumn and winter months. Wave direction ranged between 5 degrees and 339 degrees with an average direction of about 128 degrees. The peak wave period ranged between 1.71 seconds and 14.09 seconds and recorded an average peak wave period of around 5.21 seconds. Recorded current velocities ranged between 0.009 m/s and 0.14 m/s with an average current velocity of 0.07 m/s and distinct periods of higher current velocities in the autumn and winter months. The current direction ranged between 5.71 degrees and 356.82 degrees. The sea surface height and tidal range during the project period ranged from -1.55 m to 2.09 m and 1.82 m to 3.68 m, respectively. The wind speeds for the project period ranged between 2.91 m/s and 14.74 m/s with increased activity in the autumn and winter months which recorded wind speeds greater than 9.0 m/s coinciding with increased wave activity in the autumn and winter months. The average wind speed in the project time scale was 8.576 m/s. Wind direction ranged between 10 degrees and 359 degrees with an average of 176 degrees.

4.2.2 VMMS Data from Southern site 1

This section presents the results of the Vessel Motion Monitoring System collected at Southern site 1. The data collected using the VMMS includes GPS location data, vessel speed data, vessel heading, translational acceleration data (i.e., accelerations in the x-axis, y-axis, and z-axis) and angular accelerations (i.e., accelerations in roll, pitch, and yaw) at 40 Hz. For eight (8) months, beginning on 03/01/2019 to 31/10/2019, Southern site 1 recorded 440 O&M transits from 3 (three) maintenance vessels (CTVs) with Vessel 1 recording 176 transits, Vessel 2 recording 110 transits and Vessel 3 recording 154 transits. Figure 4.4 presents the total O&M transits from the three participating crew transfer vessels at Southern site 1.

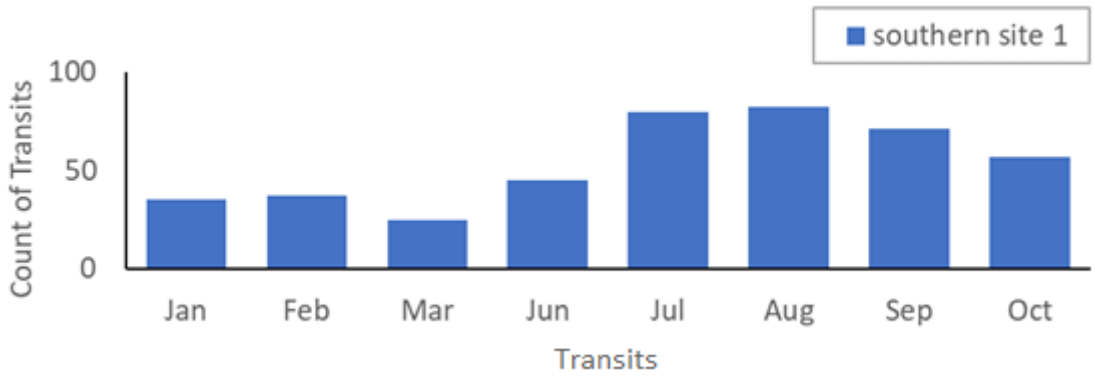

Figure 4. 4 Figure showing the distribution of operation and maintenance (O&M) transits by three CTVs at Southern site 1.

Figure 4.4 shows an increase in O&M transits in the summer months and a reduction or absence of transits in the autumn and winter months which corresponds to higher wave and wind activity in the autumn and winter months for the project period. The reduction and absence of transits correspond to periods of rougher weather where significant wave heights were recorded above 1.5 m - the threshold for crew transfer vessels (CTVs) used in the offshore wind industry (Phillips et al., 2015) - and where the wind speed was recorded above 10 m/s^2 which can be described by an index of 5 on the Beaufort wind scale (Met Office, 2017). Figure 4.5 provides data from the VMMS collected for Southern site 1 on a typical O&M journey as defined in section 4.1 of this chapter. The plot shows a stacked plot using data from a CTV (Vessel 1) on an O&M transit day – the 12th of September 2019.

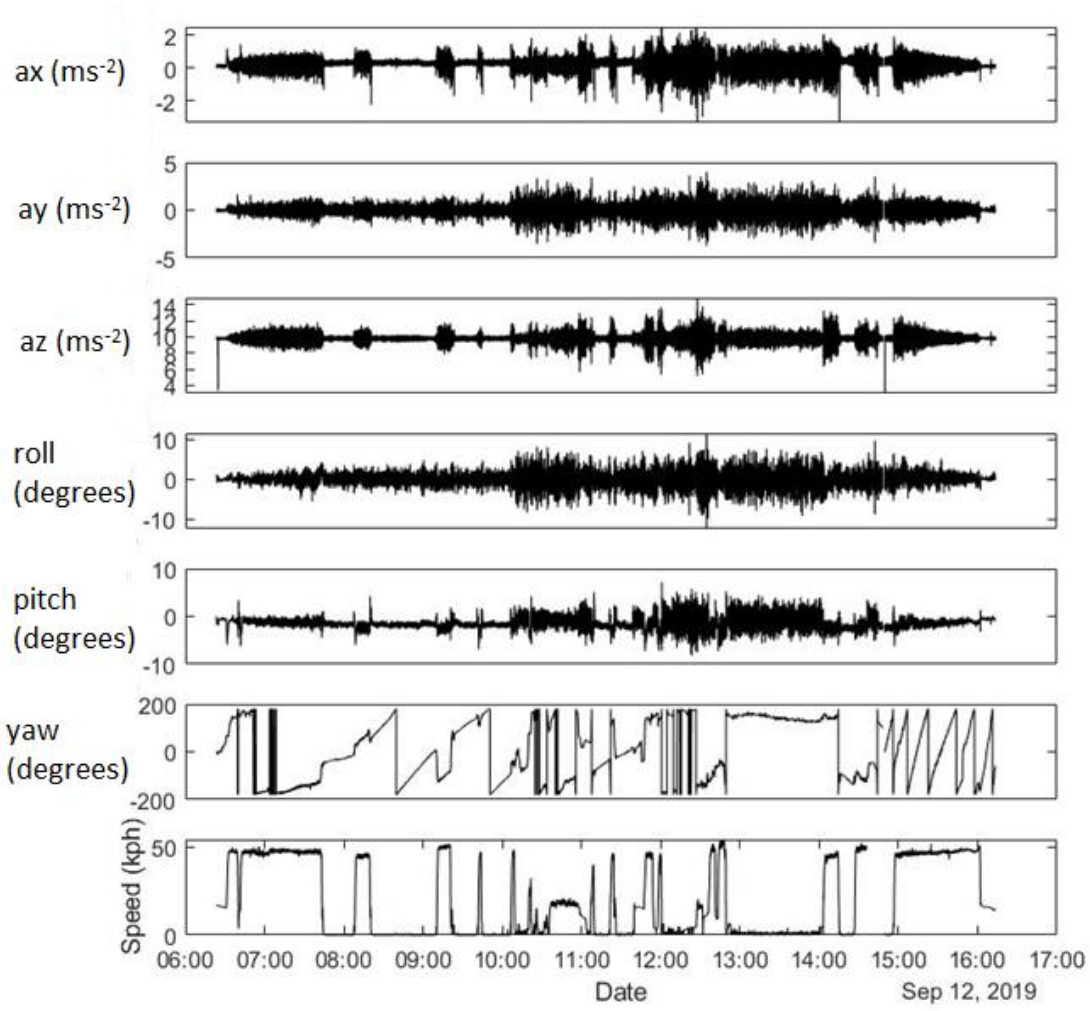

Figure 4. 5 Sample data from a CTV transit day. From top to bottom: i. Vessel x-axis acceleration denoted by ax in m/s^2; ii. Vessel y-axis acceleration denoted by ay in m/s^2; iii. Vessel z-axis acceleration denoted by az in m/s^2; iv. Vessel roll acceleration in degrees; v. Vessel pitch acceleration in degrees; vi. Vessel yaw in degrees; vii. Vessel speed recorded in kph

The stacked plot presents data from a CTV on a maintenance operation over about 9.83 hours (35388 seconds) beginning at 06:23:37 and concluding at 16:13:26 of the same day - 12/09/2019. From top to bottom, the translational accelerations of the vessel ranged from -3.35 m/s^2 to 2.49 m/s^2 for the x-axis acceleration with an average acceleration of 0.23 m/s^2, between -3.75 m/s^2 and 4.00 m/s^2 for the y-axis acceleration with an average acceleration of 0.01 m/s^2, and between 3.01 m/s^2 and 14.84 m/s^2 for the z-axis acceleration with an average acceleration of 9.79 m/s^2. There are distinct periods of greater variations in translational accelerations suggesting changes in vessel behaviour during the transit. Figure 4.5 also presents the vessel's rotational acceleration which ranges from -12 degrees to 12 degrees for

the roll, between -8 degrees and 7 degrees for the pitch, and between -180 degrees and 180 degrees for the yaw. The speed of the vessel, measured in kilometres per hour, ranged from 0 km/h to a maximum of 54.08 km/h and the average speed of the vessel for the duration of the transit was 18.92 km/h. The changes in vessel speed correlate with the changes in the translational acceleration which suggests that the increase in vessel speed during transit leads to an increase in the vessel's translational acceleration and vice versa.

4.2.3 Instantaneous Descriptive Analysis

As described in section 3.6.1 of the third chapter of this thesis, to define the scope of O&M transits, a discretization process was applied to the acceleration data from participating vessels to define and classify the changes in vessel behaviour. Figure 4.6 presents plots of the descriptive analysis process carried out on a participating vessel at southern site 1.

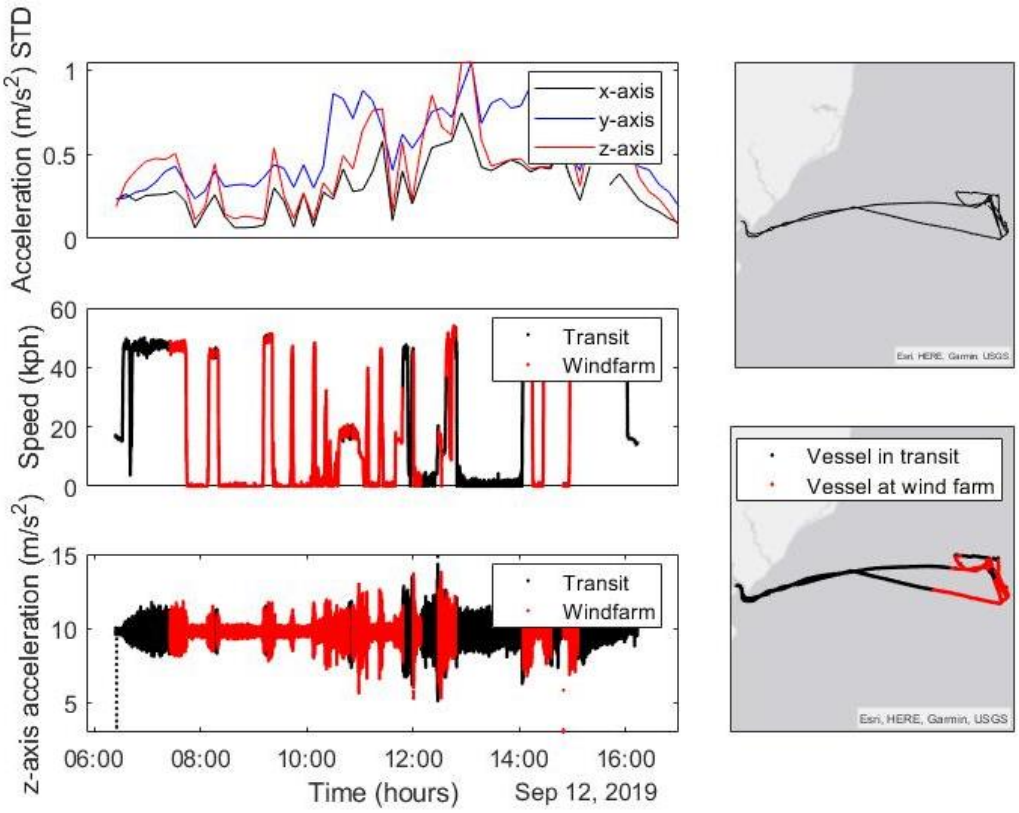

Figure 4. 6 Sample data from a CTV transit day. Left top to bottom: i. Time series plot of the discretized x-axis, y-axis, and z-axis acceleration signals using standard deviation; ii. Time series plot of vessel speed in km/h showing transit classifications between the vessel in transit and the vessel at wind farms; iii. A plot of the z-axis acceleration signal showing transit classifications of the vessel in transit and the vessel at wind farms; Right top to bottom: vi. Vessel transit plot before classification; vii. Vessel transit plot showing classified transit of vessel in transit and vessel at wind farms.

The discretization plot shows the standard deviations of the acceleration between 0.063 m/s^2 and 1.045 m/s^2 which increases during transit to offshore wind farms with peaks that highlight technician transfers (onto and off wind turbine platforms) during the maintenance activity. The individual plots of vessel speed against time and z-axis acceleration with time corroborate the discretization plot and the classification of vessel behaviour between vessels in transit and vessel and wind farm. The resulting categorized plots suggest the practice of pit-stop servicing within maintenance operations – where more than one wind turbine is serviced in one transit by the same vessel.

4.2.4 Estimation of Personnel Comfort and Sickness

Using the process of discretization shown in Figure 4.6 and feature engineering processes for estimating comfort using Composite Weighted Acceleration, and sickness using Motion Sickness Incidence Figure 4.7 presents plots of the welfare variables of sickness and comfort with technician transfer points and *sail and no sail* decisions.

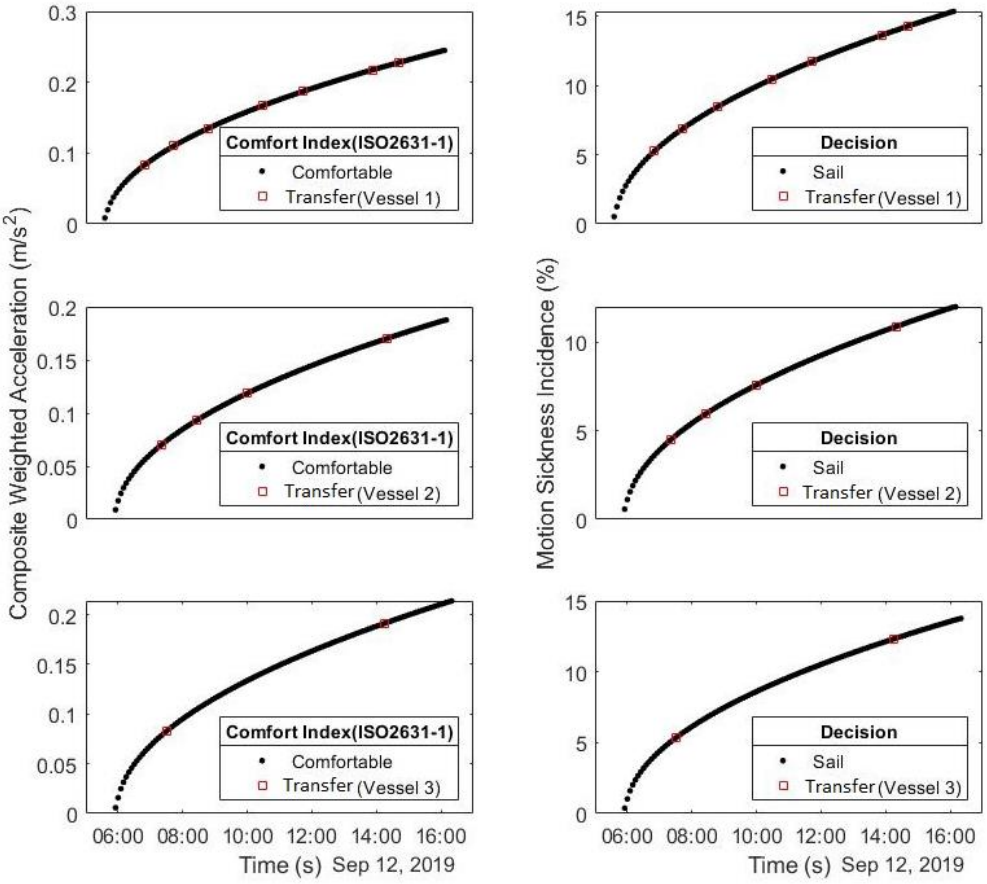

Figure 4. 7 Left top to bottom: i. A time series plot of Composite Weighted Acceleration in m/s^2 showing technician transfer points and estimated human comfort levels as defined by ISO

2631-1 for Vessel 1; ii. A time series plot of Composite Weighted Acceleration in m/s^2 showing technician transfer points and estimated human comfort levels as defined by ISO 2631-1 for Vessel 2; iii. A time series plot of Composite Weighted Acceleration in m/s^2 showing technician transfer points and estimated human comfort levels as defined by ISO 2631-1 for Vessel 3; Right top to bottom: iv. A time series plot of Motion Sickness Incidence in % showing technician transfer points and estimated sail or not-sail decision-based CTV safety thresholds for Vessel 1; v. A time series plot of Motion Sickness Incidence in % showing technician transfer points and estimated sail or not-sail decision-based CTV safety thresholds for Vessel 2; vi. A time series plot of Motion Sickness Incidence in % showing technician transfer points and estimated sail or not-sail decision-based CTV safety thresholds for Vessel 3.

The plots on the left show black dots which indicate values for defined Composite Weighted Acceleration defined from the description given in section 3.6.3 of the third chapter, and categories of colour represent a human reaction to vibrations as defined by ISO 2631-1 shown in Table 4.1 below. However, as Figure 4.7 shows, transit accelerations are below 0.315 m/s^2, and as such are categorised as comfortable represented in black as seen in the figure legends. The plots on the right, indicate the levels of estimated Motion Sickness Incidence (defined in section 3.6.3 of chapter 3) represented in black dots. Colour variations shown in the plot legend show *sail or no sail* decisions based on best sea fairing practices (Phillips et al., 2015) of a 20% Motion Sickness Incidence threshold. However, as levels in the transit plot are below 15%, the transit is categorized as *sail* shown in *black*. The red squares in both plots indicate technician transfer points defined from the discretization process in Figure 4.6. The table below shows the comfort reactions to vibrations defined by ISO 2631-1 used in Figure 4.7.

Less than 0.315 m/s^2	Comfortable
0.315 m/s^2 – 0.633 m/s^2	A little uncomfortable
0.500 m/s^2 – 1.000 m/s^2	Fairly uncomfortable
0.800 m/s^2 – 1.600 m/s^2	Uncomfortable
1.250 m/s^2 – 2.500 m/s^2	Very uncomfortable
Greater than 2.000 m/s^2	Extremely uncomfortable

Table 4. 1 Table showing comfort reactions to vibrations in ms^{-1} (ISO 2631-1, 1997).

Both plots in Figure 4.7 (left and right) seem to follow plots of square root functions as both plots have a minimum y-value of 0, no negative values, and an opening along the x-axis.

4.3 Descriptive Analysis of Northern site 1

This section presents the results of the data collected for northern site 1.

4.3.1 Meteorological Data from Northern site 1

Similar to the data from Southern site 1 in section 4.2.1 above, the meteorological data used for Northern site 1 included wind, wave, and current datasets acquired and licenced from Copernicus Marine Service (CMEMS). However, the meteorological was downloaded for periods between 20/07/2019 and 31/10/2019 and synchronised with the Vessel Motion Monitoring System (VMMS) dataset to correlate with the movements of the vessels as they travel to wind farms using timestamps and vessel GPS locations.

Figure 4.8 below shows that the significant wave height for northern site 1 ranged between 0.29 and 2.03 metres with an average significant wave height of about 0.81 m during the 4-month project period. There were periods of rough weather resulting in higher than 1.5 m significant wave heights in the autumn and winter months. Wave direction ranged between 2 and 317 degrees with an average direction of about 116 degrees. The peak wave period ranged between 2.74 and 14.52 seconds and recorded an average peak wave period of around 6.34 seconds. Recorded current velocities ranged between 0.01 and 0.12 m/s^2 with an average current velocity of 0.05 m/s and distinct periods of higher current velocity in the autumn and winter months. The sea surface height and tidal range during the project period ranged from -1.09 to 1.94 m and 1.60 to 4.04 m, respectively. The wind speeds for the project period ranged between 0.48 and 8.93 m/s^2 with increased activity in the autumn and winter months which recorded wind speeds greater than 9.0 m/s^2 though not within the project's data collection phase. Wind direction ranged between 4 and 349 degrees with an average of 171 degrees.

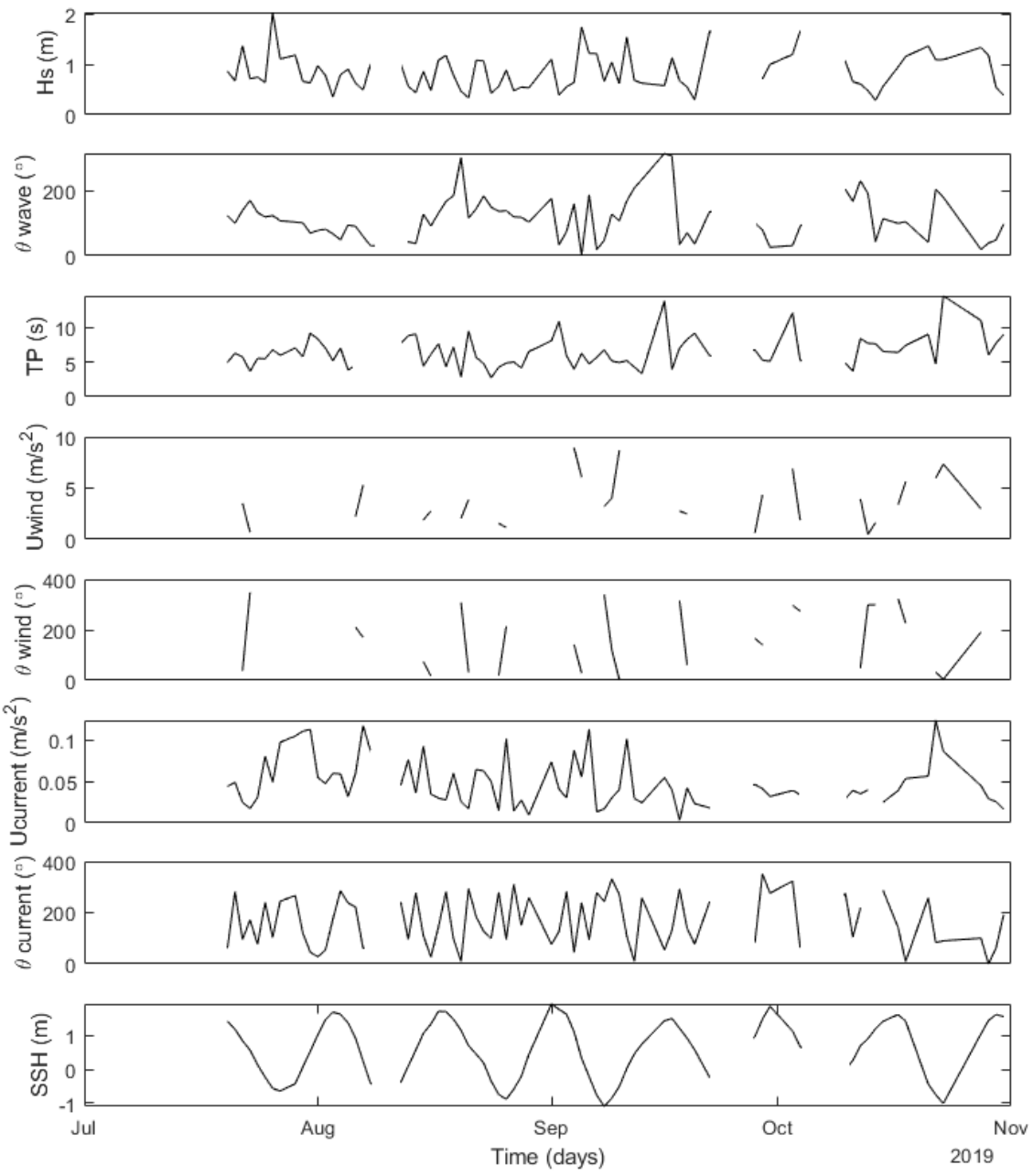

Figure 4. 8 Meteorological data for Northern site 1. From top to bottom: i. Hs, Significant wave height (m); ii. Θwave, Wave direction (°); iii. TP, Peak wave period (s); iv. Uwind, Wind speed (m/s); v. Θwind, Wind direction (°) vi. Ucurrent, Current velocity (m/s); vii. Θcurrent, Current direction (°); viii. SSH, Sea surface height (m);

4.3.2 VMMS Data from Northern site 1

This section presents the results of the Vessel Motion Monitoring System. As with southern site 1 in section 4.2.2, the data collected by VMMS includes GPS location data, vessel speed data, vessel heading, and translational acceleration at 40 Hz. The data was collected over four months, beginning on 20/07/2019 and ending on 31/10/2019. This site recorded 184 O&M

transits, from 3 (three) maintenance vessels with Vessel 4 recording 61 transits, Vessel 5 recording 55 transits and Vessel 6 recording 68 transits.

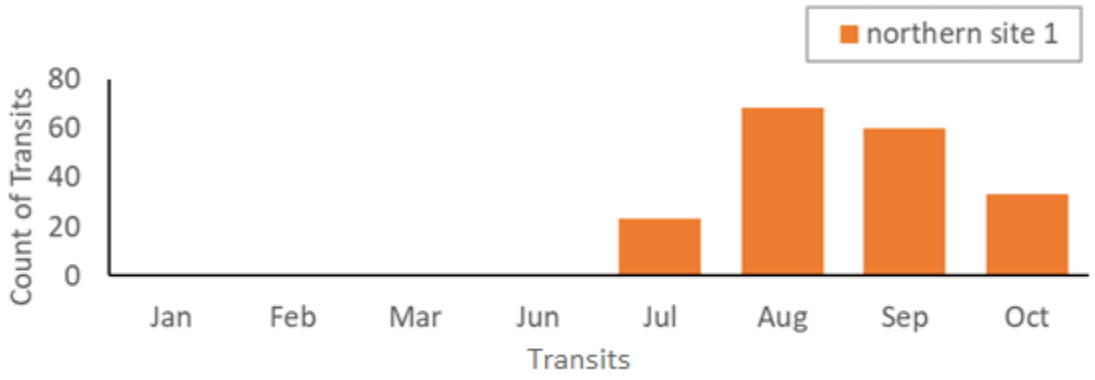

Figure 4. 9 Figure showing the distribution of operation and maintenance (O&M) transit by three CTVs at Northern site 1.

Figure 4.9 shows the presence of increased O&M transits in the summer months, starting in July and ending in October, and an absence of transits in autumn and winter months which corresponds to rougher weather with a higher wave and wind activity in the autumn and winter months for the site.

Figure 4.10 presents the data from the VMMS collected for Southern site 1 on a typical O&M transit as defined in section 4.1 of this chapter.

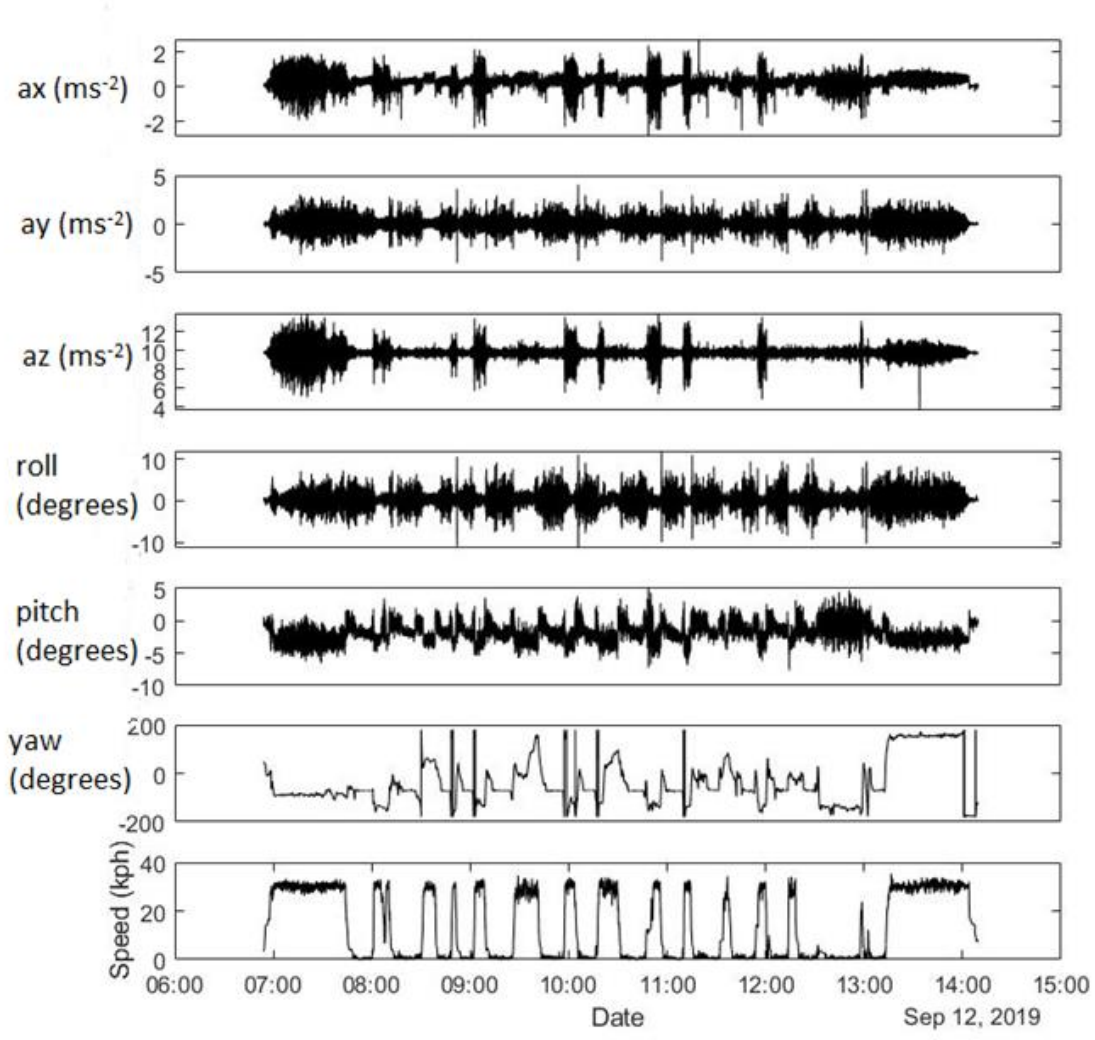

Figure 4. 10 Sample data from a CTV transit day. From top to bottom: i. Vessel x-axis acceleration denoted by ax in m/s^2; ii. Vessel y-axis acceleration denoted by ay in m/s^2; iii. Vessel z-axis acceleration denoted by az in m/s^2; iv. Vessel roll acceleration in degrees; v. Vessel pitch acceleration in degrees; vi. Vessel yaw acceleration in degrees; vii. Vessel speed recorded in kph.

Figure 4.10 The plot shows a stacked plot of the available VMMS data from a CTV (Vessel 4) on an O&M transit on the 12th of September 2019. The plot shows that the transit lasted for about 7.25 hours (26115 seconds) beginning at 06:54:04 and concluding at 14:09:19 of the same day, 12/09/2019. The translational accelerations of the vessel ranged from -2.88 to 2.76 m/s^2 for the x-axis acceleration with an average acceleration of 0.305 m/s^2, between -3.987 and 4.07 m/s^2 for the y-axis acceleration with an average acceleration of 0.04 m/s^2, and between 3.69 and 13.97 m/s^2 for the z-axis acceleration with an average acceleration of 9.77 m/s^2. There are distinct periods of greater variations in translational accelerations suggesting changes in vessel behaviour during the transit. Figure 4.5 also presents the vessel's rotational

acceleration which ranges from -11.40 to 11.99 degrees for the roll, between -8 and 5 degrees for the pitch, and between -180 and 180 degrees for the yaw. The speed of the vessel, measured in kilometres per hour, ranged from zero to a maximum of 35.37 and the average speed of the vessel for the duration of the transit was 13.51 km/h. The changes in vessel speed correlate with the changes in the translational acceleration which suggests that the increase in vessel speed during transit leads to an increase in the vessel's translational acceleration and vice versa.

4.3.3 Instantaneous Descriptive Analysis

As described in section 3.6.1 of the third chapter of this thesis, to define the scope of O&M transits, a discretization process was applied to the acceleration data which was used to define and classify the changes in vessel behaviour. Figure 4.11 presents plots of the descriptive analysis process conducted on a participating vessel at southern site 1.

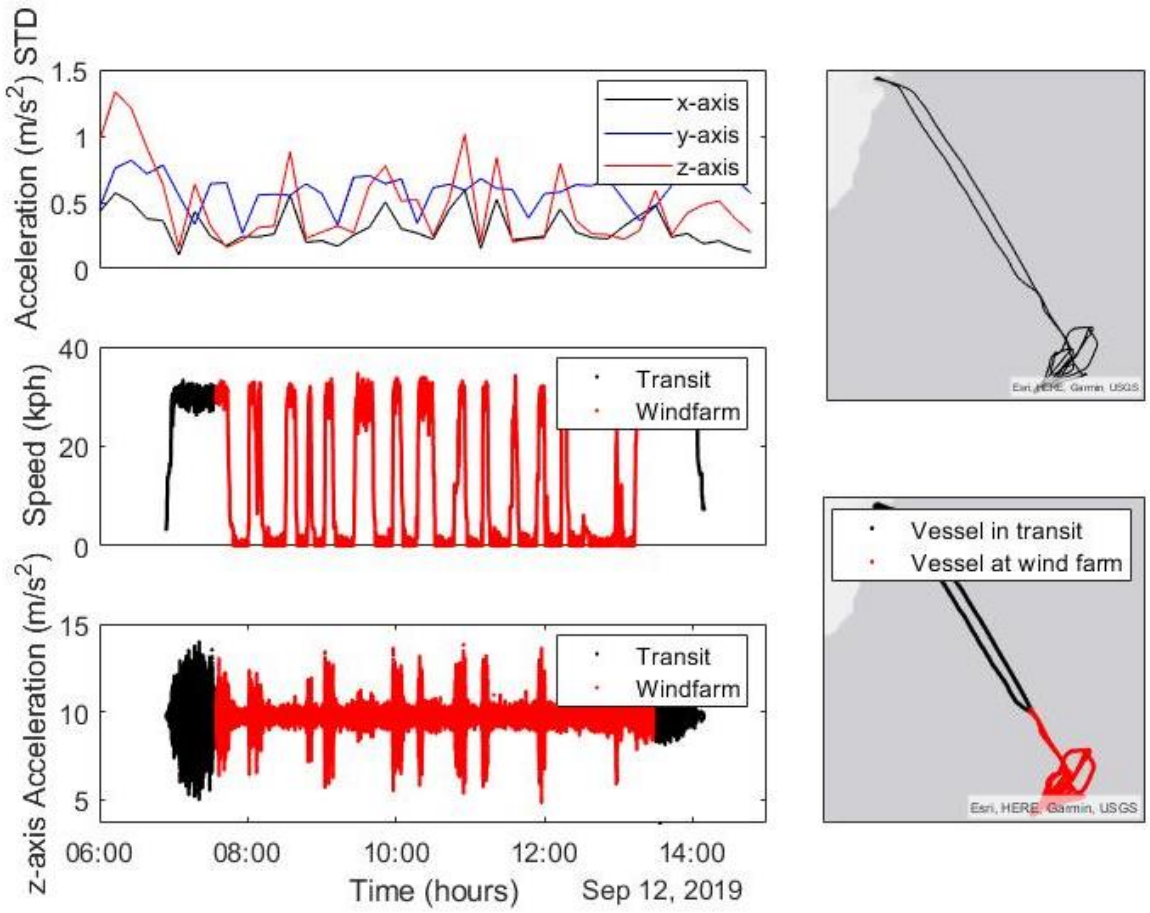

Figure 4. 11 Sample data from a CTV transit day. Left top to bottom: i. Time series plot of the discretized x-axis, y-axis, and z-axis acceleration signals using standard deviation; ii. Time

series plot of vessel speed in km/h showing transit classifications between the vessel in transit and the vessel at wind farms; iii. A plot of the z-axis acceleration signal showing transit classifications of the vessel in transit and the vessel at wind farms; Right top to bottom: vi. Vessel transit plot before classification; vii. Vessel transit plot showing classified transit of vessel in transit and vessel at wind farms.

The discretization plot shows the standard deviations of the acceleration between 1.10 and 1.33 m/s^2 which increases during transit to offshore wind farms with peaks that highlight technician transfers (onto and off wind turbine platforms) during the maintenance activity. The individual plots of vessel speed against time and z-axis acceleration with time corroborate the discretization plot and the classification of vessel behaviour between vessels in transit and vessel and wind farm. The resulting categorized plots suggest the practice of pit-stop servicing within maintenance operations – where more than one wind turbine is serviced in one transit by the same vessel.

4.3.4 Estimation of Personnel Comfort and Sickness

Using the numerical evaluations described in section 3.6 of chapter three, the results of motion sickness evaluation and technician comfort evaluations is presented in Figure 4.12 for three vessels (vessel 4, 5, 6).

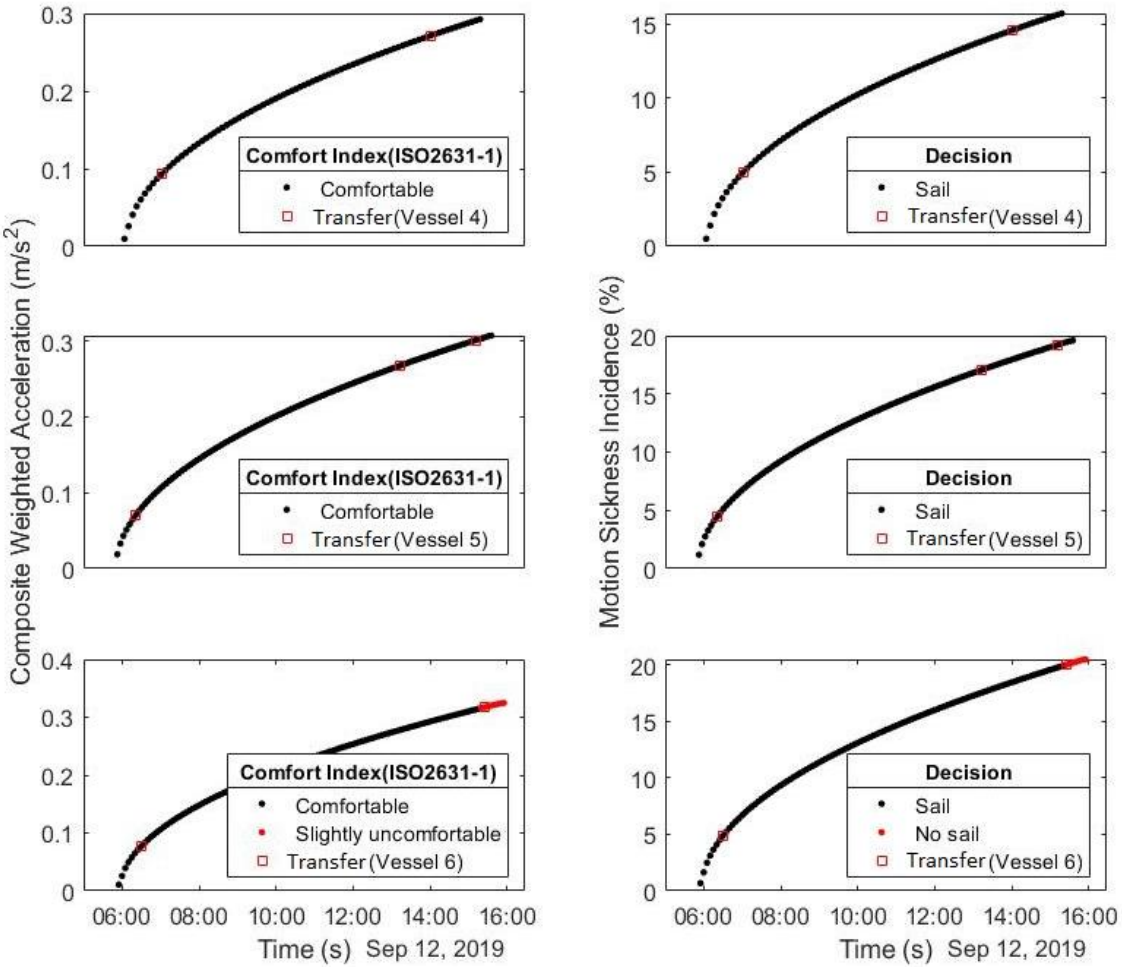

Figure 4. 12 Left top to bottom: i. A time series plot of Composite Weighted Acceleration in m/s^2 showing technician transfer points and estimated human comfort levels as defined by ISO 2631-1 for Vessel 4; ii. A time series plot of Composite Weighted Acceleration in m/s^2 showing technician transfer points and estimated human comfort levels as defined by ISO 2631-1 for Vessel 5; iii. A time series plot of Composite Weighted Acceleration in m/s^2 showing technician transfer points and estimated human comfort levels as defined by ISO 2631-1 for Vessel 6; Right top to bottom: iv. A time series plot of Motion Sickness Incidence in % showing technician transfer points and estimated sail or not-sail decision-based CTV safety thresholds for Vessel 4; v. A time series plot of Motion Sickness Incidence in % showing technician transfer points and estimated sail or not-sail decision-based CTV safety thresholds for Vessel 5; vi. A time series plot of Motion Sickness Incidence in % showing technician transfer points and estimated sail or not-sail decision-based CTV safety thresholds for Vessel 6.

The plots on the left show black and red dots which indicate values for defined Composite Weighted Acceleration, defined from the description given in section 3.7 of chapter three. The black and red colours describe the human comfort reactions to vibrations as defined by ISO 2631-1 shown in Table 4.1 of section 4.2.4 of this chapter. The black coloured dots indicate that the journey is not uncomfortable (below 0.315 m/s^2), and the red dots indicate that the

transit was fairly uncomfortable (between 0.315 m/s^2 and 0.633 m/s^2). The red squares indicate technician transfer points defined from the discretization process in Figure 4.6.

On the right, the black and red dots indicate estimated Motion Sickness Incidence also defined from descriptions given in section 3.7 of chapter three of this thesis. The black dots indicate a *sail* welfare-based decision using 20% thresholds for best sea fairing practices (Phillips et al., 2015), while the red dots indicate a *no sail* welfare-based decision. The red squares also indicate technician transfer points defined from the discretization process in Figure 4.6.

Both plots in Figure 4.12 (left and right) seem to follow plots of square root functions as both plots have a minimum y-value of 0, no negative values, and increasing values along the x-axis. The plots also show that for Vessel 6, at about 15:20, the transits start becoming slightly uncomfortable for technicians onboard the vessel and this categorization seems to seem to coincide with the categorization of *no sail* on the motion sickness plot.

4.4 Descriptive Analysis of Southern site 2

This section presents the results of the data collected for southern site 2.

4.4.1 Meteorological Data from Southern site 2

Meteorological data for southern site 2 included wind, wave, and current datasets acquired and licenced from Copernicus Marine Service (CMEMS) between 03/01/2019 and 28/02/2019. The dataset was synchronised with the Vessel Motion Monitoring System (VMMS) dataset to correlate with the movements of the vessels as they travel to wind farms using timestamps and vessel GPS locations.

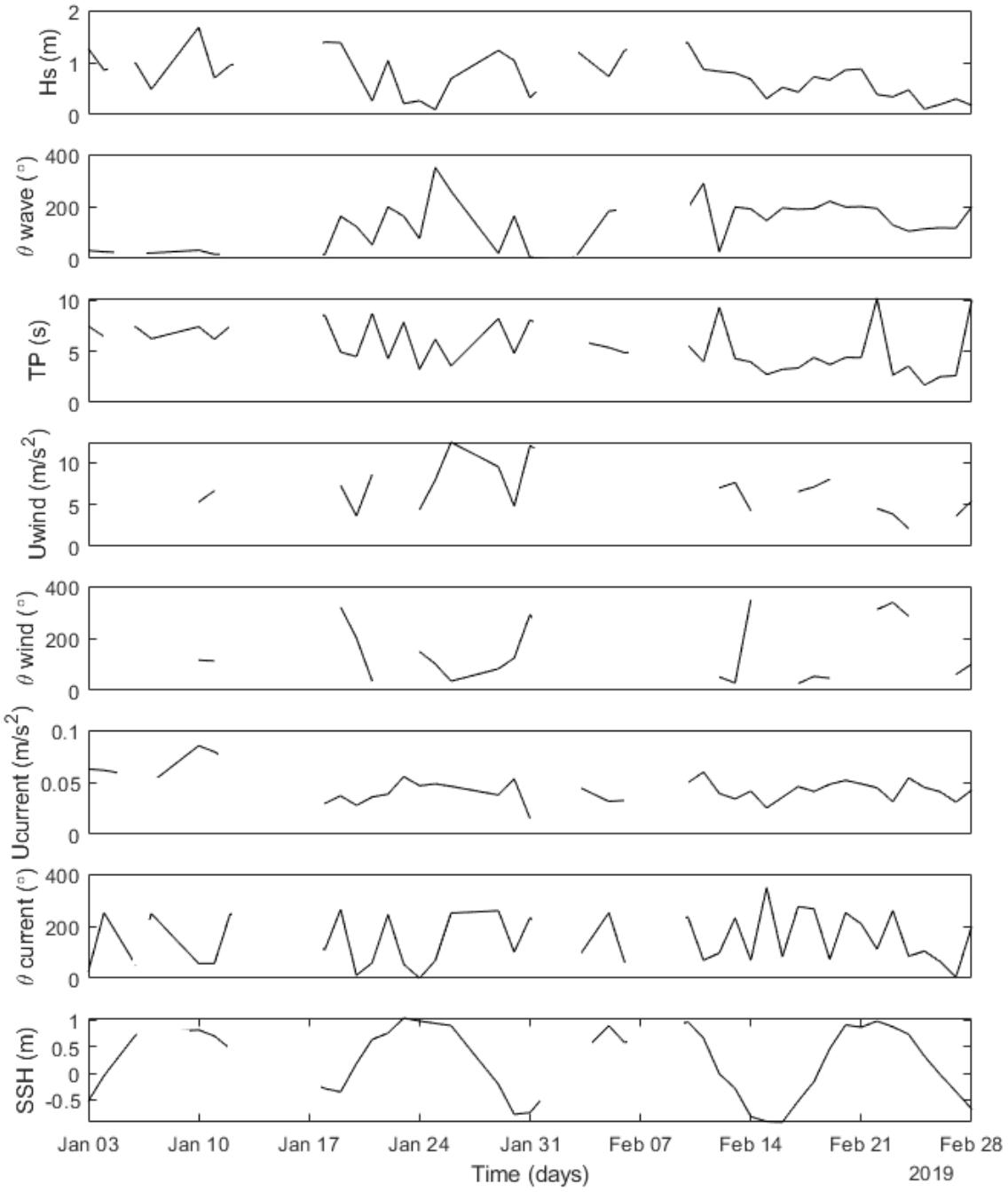

Figure 4. 13 Meteorological data from Copernicus Marine Service (CMEMS) for Southern site 2. From top to bottom: i. Hs, Significant wave height (m); ii. Θwave, Wave direction (°); iii. TP, Peak wave period (s); iv. Uwind, Wind speed (m/s); v. Θwind, Wind direction (°) vi. Ucurrent, Current velocity (m/s); vii. Θcurrent, Current direction (°); viii. SSH, Sea surface height (m);

Figure 4.13 shows that the significant wave height for southern site 2 ranged between 0.09 and 1.68 metres with an average height of about 0.73 m during the 2-month project period. There were periods of rough weather resulting in higher than 1.5 m significant wave heights in the autumn and winter months. Wave direction ranged between 4 and 350 degrees with

an average direction of about 129 degrees. The peak wave period ranged between 1.69 and 10.15 seconds and recorded an average peak wave period of around 5.42 seconds. Recorded current velocities ranged between 0.02 and 0.09 m/s with an average current velocity of 0.05 m/s^2 and distinct periods of higher current velocity in the autumn and winter months. The sea surface height and tidal range during the project period ranged from -0.92 to 1.04 m and 1.69 to 2.77 m, respectively. The wind speeds for the project period ranged between 2.10 and 12.37 m/s^2 with increased activity in the autumn and winter months which recorded wind speeds greater than 9.0 m/s^2 coinciding with increased wave activity in the autumn and winter months. Wind direction ranged between 26 and 348 degrees with an average of 139 degrees.

4.4.2 VMMS Data from Southern site 2

This section presents the results of the Vessel Motion Monitoring System. The data collected using the VMMS includes GPS location data, vessel speed data, vessel heading, translational acceleration data (i.e., accelerations in the x-axis, y-axis, and z-axis) and angular accelerations (i.e., accelerations in roll, pitch, and yaw) at 40 Hz. Over two months, beginning on 03/01/2019 and ending on 28/02/2019, southern site 2 recorded 121 O&M transits, in which transits were recorded from 3 (three) maintenance vessels with Vessel 7 recording 39 transits, Vessel 8 recording 41 transits and Vessel 9 recording 41 transits.

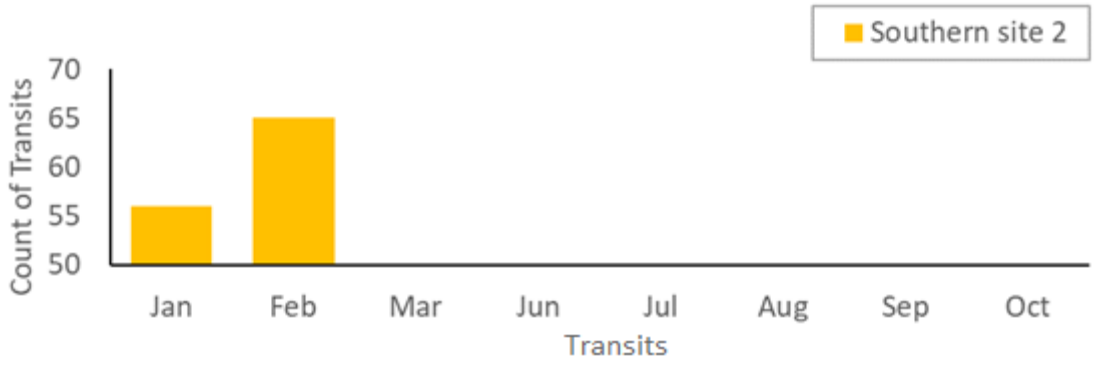

Figure 4. 14 Figure showing the distribution of operation and maintenance (O&M) transit by three CTVs at Southern site 2.

Figure 4.14 shows an increase in O&M transits in January and February and an absence of transits for the rest of the data collection period.

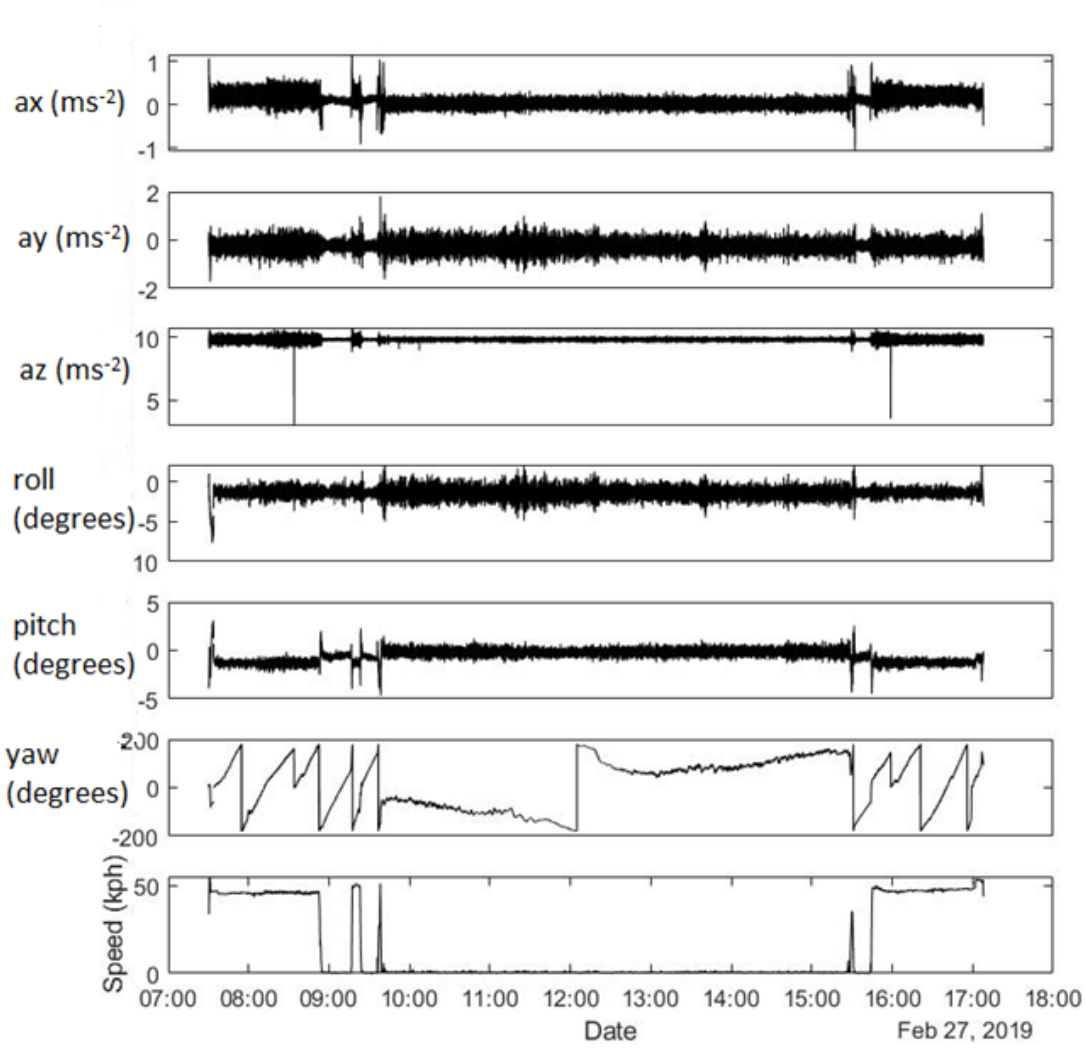

Figure 4. 15 Sample data from a CTV transit day. From top to bottom: i. Vessel x-axis acceleration denoted by ax in m/s^2; ii. Vessel y-axis acceleration denoted by ay in m/s^2; iii. Vessel z-axis acceleration denoted by az in m/s^2; iv. Vessel roll acceleration in degrees; v. Vessel pitch acceleration in degrees; vi. Vessel yaw acceleration in degrees; vii. Vessel speed recorded in kph.

Figure 4.15 shows data from a select vessel (Vessel 7) at Southern site 2. The figure shows about 9.63 hours (34663 seconds) beginning at 07:30:18 and concluding at 17:08:00 on the same day, 27/02/2019. The translational accelerations of the vessel ranged from -1.07 to 1.16 m/s^2 for the x-axis acceleration with an average acceleration of 0.09 m/s^2, between -1.72 and 1.81 m/s^2 for the y-axis acceleration with an average acceleration of -0.23 m/s^2, and between 2.96 and 10.78 m/s^2 for the z-axis acceleration with an average acceleration of 9.82 m/s^2. There are distinct periods of greater variations in translational accelerations suggesting changes in vessel behaviour during the transit. Figure 4.5 also presents the vessel's rotational acceleration which ranges from -8 to 2 degrees for the roll, between -5 and 3 degrees for the

pitch, and between -180 and 180 degrees for the yaw. The speed of the vessel, measured in kilometres per hour, ranged from 0 to a maximum of 54.95 and the average speed of the vessel for the duration of the transit was 14.41 km/h. The changes in vessel speed correlate with the changes in the translational acceleration which suggests that the increase in vessel speed during transit leads to an increase in the vessel's translational acceleration and vice versa.

4.4.3 Instantaneous Descriptive Analysis

As described in Chapter three of this thesis, to define the scope of O&M transits, a discretization process was applied to the acceleration data from participating vessels to define and classify the changes in vessel behaviour. Figure 4.16 presents plots of the descriptive analysis process conducted on a participating vessel at southern site 2.

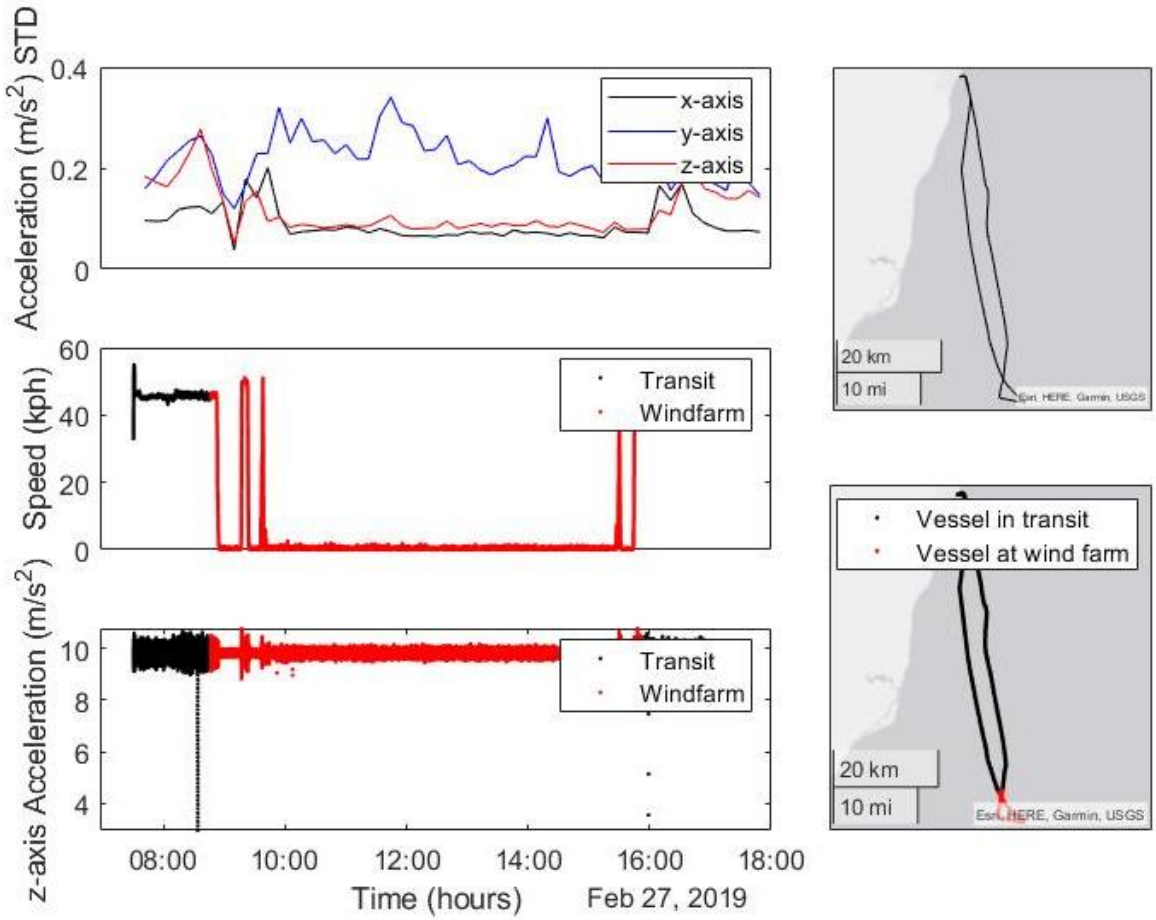

Figure 4. 16 Sample data from a CTV transit day. Left top to bottom: i. Time series plot of the discretized x-axis, y-axis, and z-axis acceleration signals using standard deviation; ii. Time series plot of vessel speed in km/h showing transit classifications between the vessel in transit

and the vessel at wind farms; iii. A plot of the z-axis acceleration signal showing transit classifications of the vessel in transit and the vessel at wind farms; Right top to bottom: vi. Vessel transit plot before classification; vii. Vessel transit plot showing classified transit of vessel in transit and vessel at wind farms.

The discretization plot shows the standard deviations of the acceleration between 0.04 and 0.34 m/s^2 which increases during transit to offshore wind farms with peaks that highlight technician transfers (onto wind turbine platforms) during the maintenance activity. The individual plots of vessel speed against time and z-axis acceleration with time corroborate the discretization plot and the classification of vessel behaviour between vessels in transit and vessel and wind farm. The resulting categorized plots suggest the practice of pit-stop servicing within maintenance operations – where more than one wind turbine is serviced in one transit by the same vessel.

4.4.4 Estimation of Personnel Comfort and Sickness

Using the numerical evaluations described in section 3.6 of chapter three, the results of motion sickness evaluation and technician comfort evaluations is presented in Figure 4.17 for three vessels (vessel 7, 8, 9).

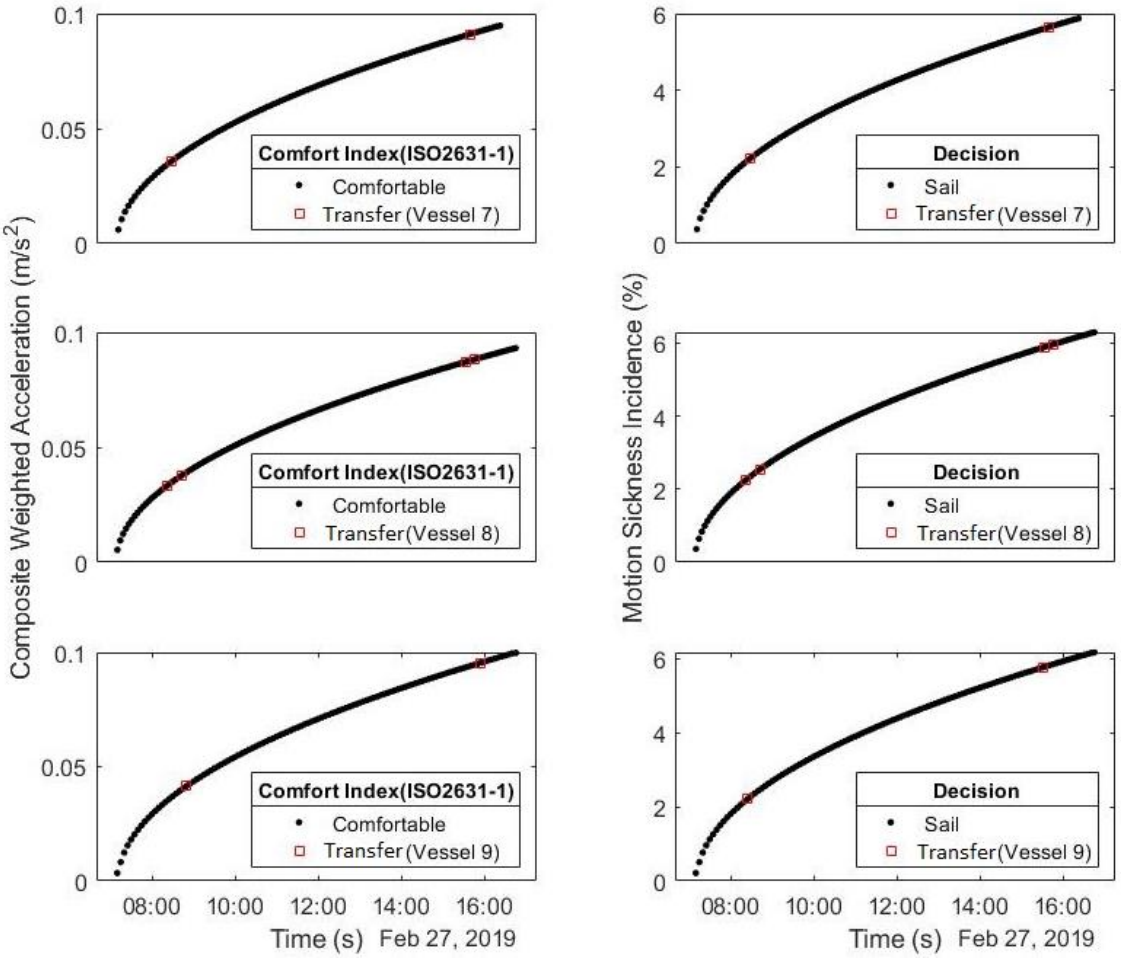

Figure 4. 17 Left top to bottom: i. A time series plot of Composite Weighted Acceleration in m/s^2 showing technician transfer points and estimated human comfort levels as defined by ISO 2631-1 for Vessel 4; ii. A time series plot of Composite Weighted Acceleration in m/s^2 showing technician transfer points and estimated human comfort for Vessel 5; iii. A time series plot of Composite Weighted Acceleration in m/s^2 showing technician transfer points and estimated human comfort levels for Vessel 6; Right top to bottom: iv. A time series plot of Motion Sickness Incidence in % showing technician transfer points and estimated sail or not-sail decision-based CTV safety thresholds for Vessel 4; v. A time series plot of Motion Sickness Incidence in % showing technician transfer points and estimated sail or not-sail decision-based CTV safety thresholds for Vessel 5; vi. A time series plot of Motion Sickness Incidence in % showing technician transfer points and estimated sail or not-sail decision-based CTV safety thresholds for Vessel 6.

The plots on the left show black dots which indicate values for defined Composite Weighted Acceleration, defined from the description given in section 3.7 of chapter three. The black coloured dots also describe the human comfort reactions to vibrations as defined by ISO 2631-1 shown in Table 4.1 of section 4.2.4 of this chapter, with black and red colour categories representing the different comfort levels. The black coloured dots in this plot indicate that

the journey is not uncomfortable (below 0.315 m/s^2), and the red squares indicate technician transfer points defined from the discretization process in Figure 4.6.

On the right, the black dots indicate estimated Motion Sickness Incidence also defined from descriptions given in section 3.7 of chapter three of this thesis. The black coloured dots also indicate a *sail* welfare-based decision using 20% thresholds for best sea fairing practices (Phillips et al., 2015), with black and red colours indicating *sail* and *no sail* welfare-based decisions respectfully. The red squares also indicate technician transfer points defined from the discretization process.

Both plots in Figure 4.17 (left and right) seem to follow plots of square root functions as both plots have a minimum y-value of 0, no negative values, and increasing values along the x-axis.

4.5 Descriptive Analysis of Western site 1

This section presents the results of the data collected for western site 1.

4.5.1 Meteorological Data from Western site 1

Meteorological data including wind speed and direction, significant wave, wind, and current datasets acquired and licenced from Copernicus Marine Service (CMEMS). The meteorological data for Western site 1 were collected from periods between 14/08/2019 and 26/10/2019.

Figure 4.18 below shows that the significant wave height for western site 1 ranged between 0.15 and 1.52 metres with an average height of about 0.64 m during the 3-month project period. There were periods of rough weather resulting in higher than 1.5 m significant wave heights in the autumn and winter months. Wave direction ranged between 4 and 358 degrees with an average direction of about 120 degrees. The peak wave period ranged between 2.04 and 13.63 seconds and recorded an average peak wave period of around 7.05 seconds. Recorded current velocities ranged between 0.01 and 0.11 m/s with an average current velocity of 0.034 m/s and distinct periods of higher current velocity in the autumn and winter months. The sea surface height and tidal range during the project period ranged from -2.98 to 1.70 m and 2.69 to 6.95 m, respectively. The wind speeds for the project period ranged between 1.37 and 9.37 m/s^2 with increased activity in the autumn and winter months which

recorded wind speeds greater than 9.0 m/s^2 coinciding with increased wave activity in the autumn and winter months. Wind direction ranged between 13 and 348 degrees with an average of 183 degrees.

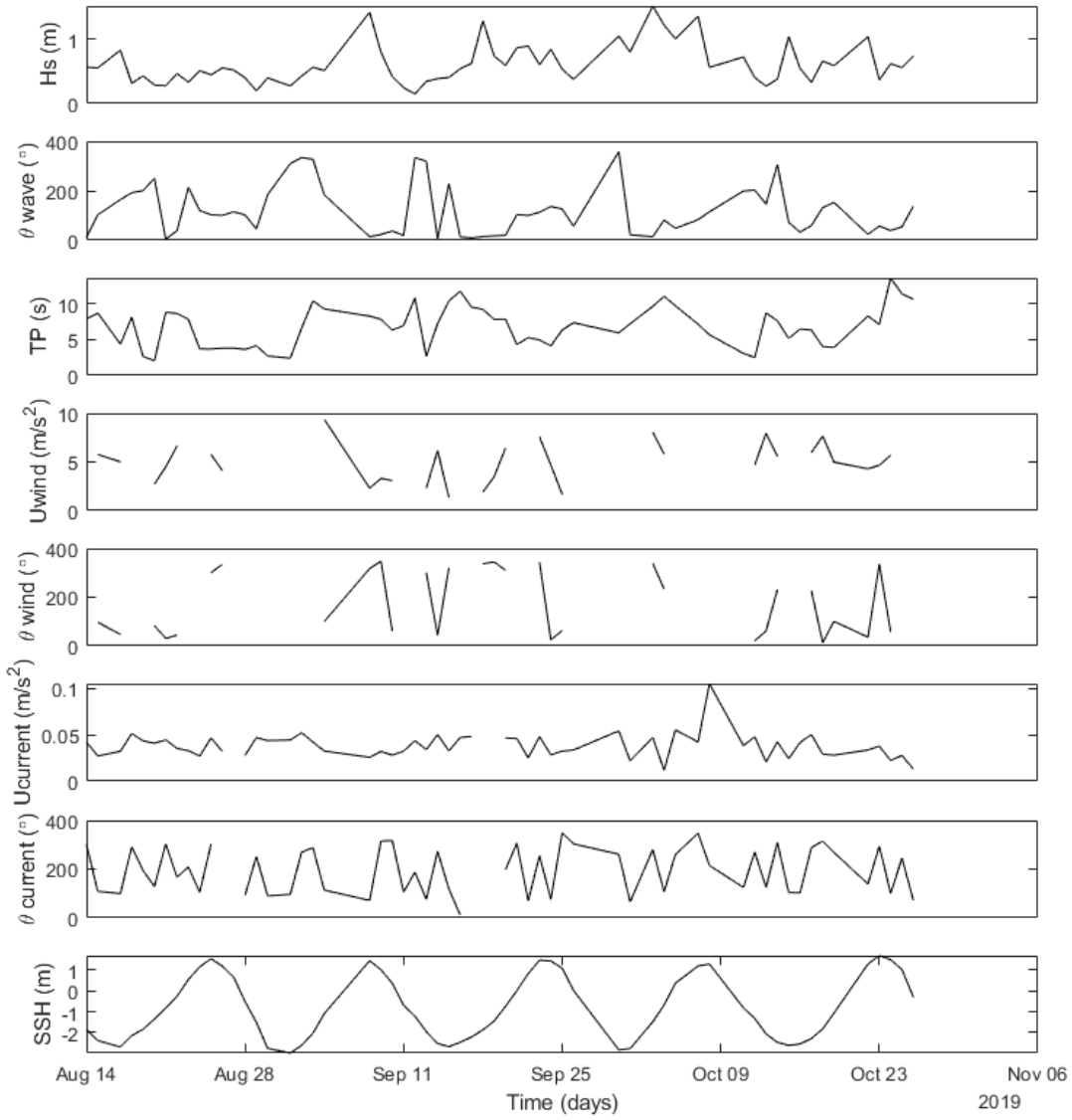

Figure 4. 18 Meteorological data for Western site 1. From top to bottom: i. Hs, Significant wave height (m); ii. Θwave, Wave direction (°); iii. TP, Peak wave period (s); iv. Uwind, Wind speed (m/s); v. Θwind, Wind direction (°) vi. Ucurrent, Current velocity (m/s); vii. Θcurrent, Current direction (°); viii. SSH, Sea surface height (m);

4.5.2 VMMS Data from Western site 1

This section presents the results of the Vessel Motion Monitoring System. The data collected using the VMMS includes GPS location data, vessel speed data, vessel heading, translational acceleration data (i.e., accelerations in the x-axis, y-axis, and z-axis) and angular accelerations

(i.e., accelerations in roll, pitch, and yaw) at 40 Hz. Beginning on 14/08/2019 and concluding on 26/10/2019, Western site 1 recorded 105 O&M transits from 3 (three) maintenance vessels (CTVs) with Vessel 10 recording 15 transits, Vessel 11 recording 39 transits and Vessel 12 recording 51 transits. The figure below (Figure 4.4)presents the total transits to wind farms from the three participating vessels at Western site 1.

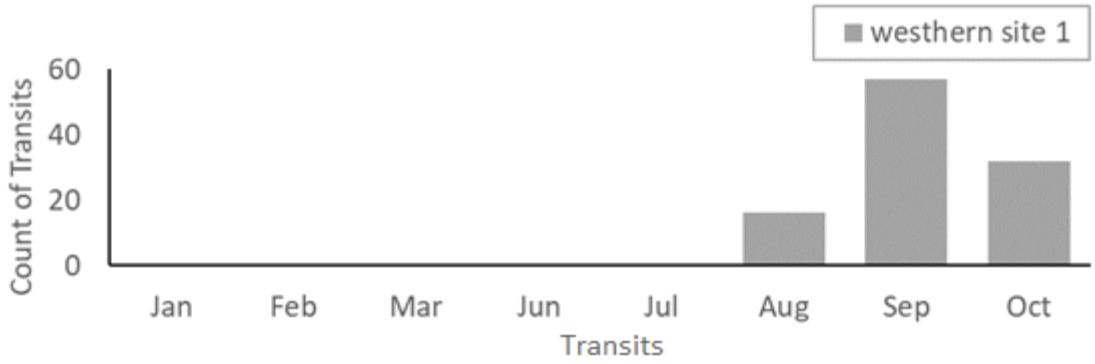

Figure 4. 19 Figure showing the distribution of operation and maintenance (O&M) transits by three CTVs at Western site 1.

Figure 4.19 shows increased O&M transits in the summer months, starting in August, and an absence of transits in the autumn and winter months which loosely corresponds to rougher weather conditions with a higher wave and wind activity.

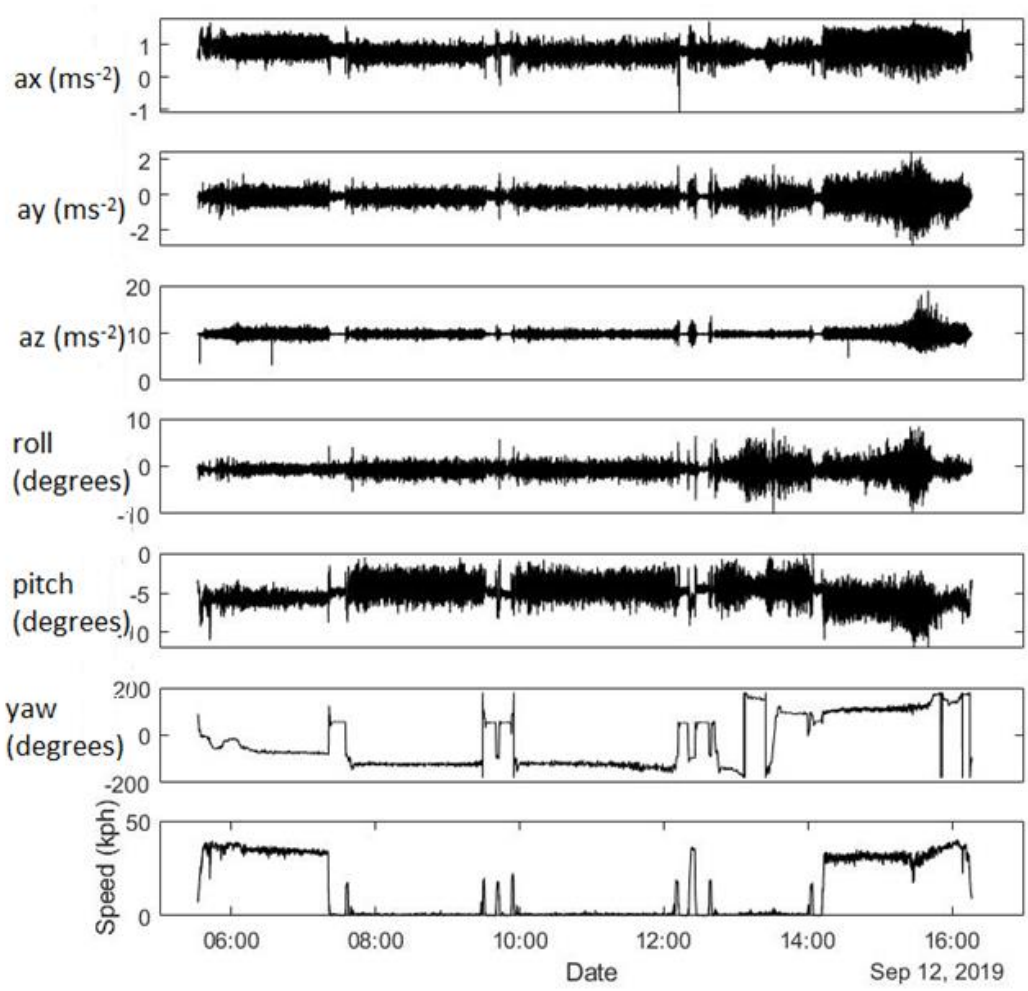

Figure 4. 20 Sample data from a CTV transit day. From top to bottom: i. Vessel x-axis acceleration denoted by ax in m/s^2; ii. Vessel y-axis acceleration denoted by ay in m/s^2; iii. Vessel z-axis acceleration is denoted by az m/s^2; iv. Vessel roll acceleration in degrees; v. Vessel pitch acceleration in degrees; vi. Vessel yaw acceleration in degrees; vii. Vessel speed recorded in kph.

Figure 4.20 shows a stacked plot of the available VMMS data from a CTV (Vessel 10) on an O&M transit on the 12th of September 2019. The plot shows that the transit lasted for about 10.744 hours (38679 seconds) beginning at 05:31:48 and concluding at 16:16:28 on the same day, 12/09/2019. The translational accelerations of the vessel ranged from -1.107 to 1.829 m/s^2 for the x-axis acceleration with an average acceleration of 0.833 m/s^2, between -2.911 and 2.463 m/s^2 for the y-axis acceleration with an average acceleration of -0.116 m/s^2, and between 3.187 and 18.946 m/s^2 for the z-axis acceleration with an average acceleration of 9.788 m/s^2. There are distinct periods of greater variations in translational accelerations suggesting changes in vessel behaviour during the transit. Figure 4.20 also presents the

vessel's rotational acceleration which ranges from -10.045 to 8.380 degrees for the roll, between -11.999 and 0.049 degrees for the pitch, and between -180 and 180 degrees for the yaw. The speed of the vessel, measured in kilometres per hour, ranged from 0 to a maximum of 40.206 and the average speed of the vessel for the duration of the transit was 12.805 km/h. The changes in vessel speed correlate with the changes in the translational acceleration which suggests that the increase in vessel speed during transit leads to an increase in the vessel's translational acceleration and vice versa.

4.5.3 Instantaneous Descriptive Analysis

As described in chapter three of this thesis, to define the scope of O&M transits, a discretization process was applied to the acceleration data from participating vessels to define and classify the changes in vessel behaviour. Figure 4.21 presents plots of the descriptive analysis process conducted on a participating vessel at western site 1.

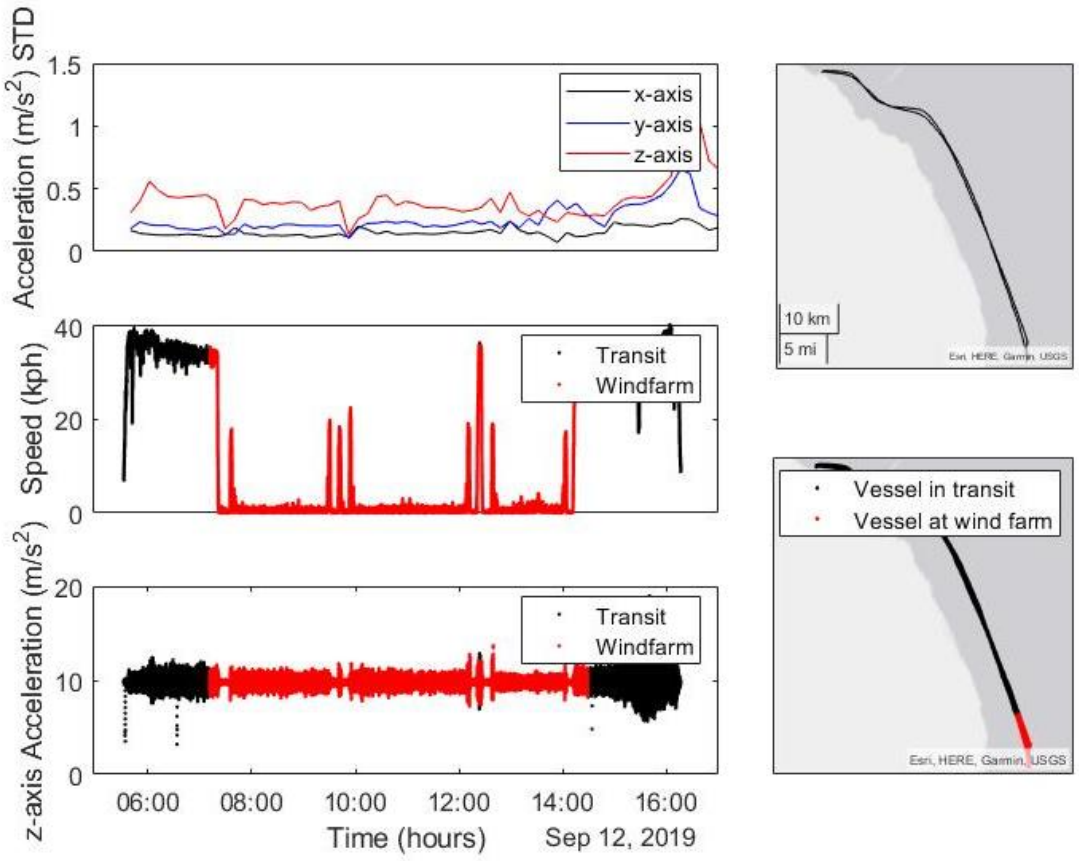

Figure 4. 21 Sample data from a CTV transit day. Left top to bottom: i. Time series plot of the discretized x-axis, y-axis, and z-axis acceleration signals using standard deviation; ii. Time series plot of vessel speed in km/h showing transit classifications between the vessel in transit and the vessel at wind farms; iii. A plot of the z-axis acceleration signal showing transit

classifications of the vessel in transit and the vessel at wind farms; Right top to bottom: vi. Vessel transit plot before classification; vii. Vessel transit plot showing classified transit of vessel in transit and vessel at wind farms.

The discretization plot shows the standard deviations of the acceleration between 0.07 and 1.40 m/s^2 which increases during transit to offshore wind farms with peaks that highlight technician transfers (onto and off wind turbine platforms) during the maintenance activity. The individual plots of vessel speed against time and z-axis acceleration with time corroborate the discretization plot and the classification of vessel behaviour between vessels in transit and vessel and wind farm. The resulting categorized plots suggest the practice of pit-stop servicing within maintenance operations – where more than one wind turbine is serviced in one transit by the same vessel.

4.5.4 Estimation of Personnel Comfort and Sickness

Using the numerical evaluations described in section 3.6 of chapter three, the results of motion sickness evaluation and technician comfort evaluations is presented in Figure 4.22 for three vessels (vessel 10, 11, 12).

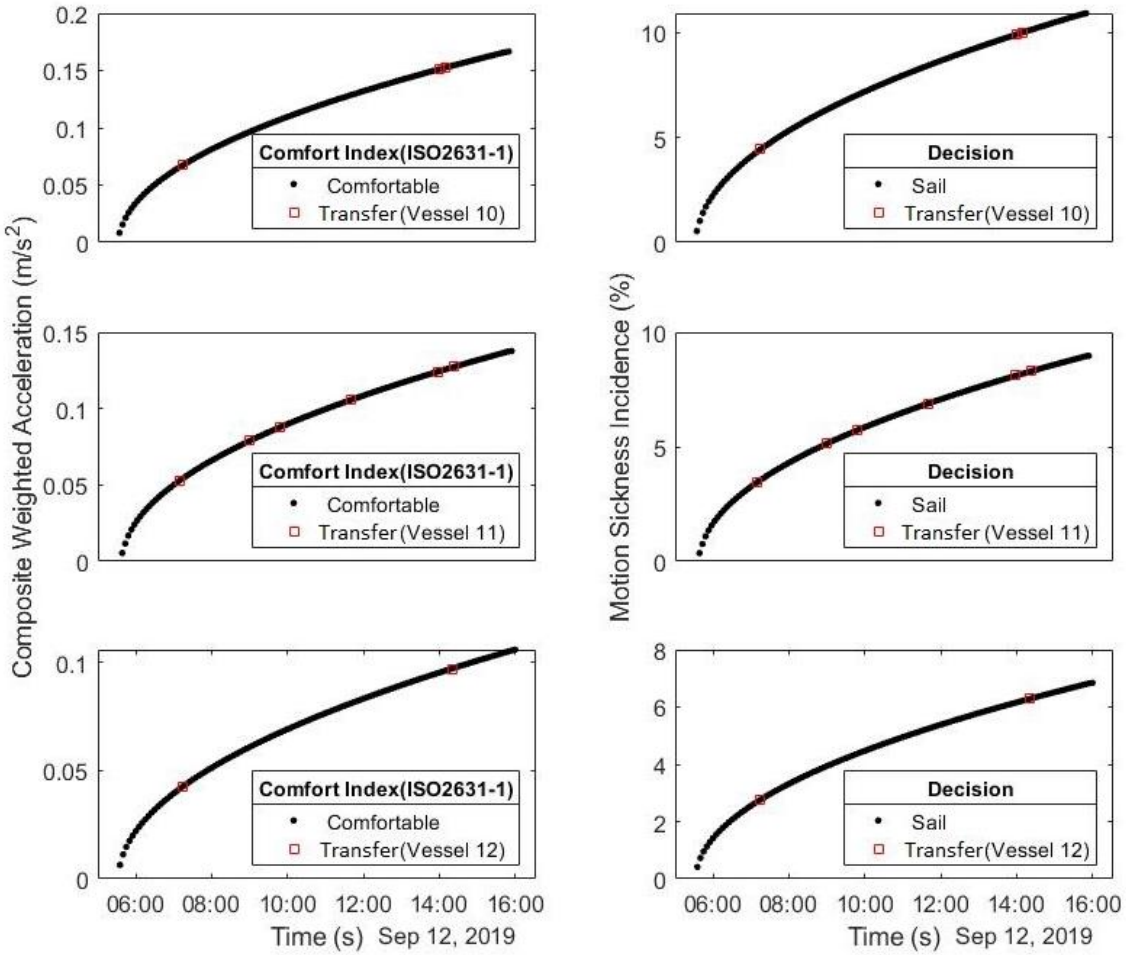

Figure 4. 22 Left top to bottom: i. A time series plot of Composite Weighted Acceleration in m/s² showing technician transfer points and estimated human comfort levels as defined by ISO 2631-1 for Vessel 4; ii. A time series plot of Composite Weighted Acceleration in m/s² showing technician transfer points and estimated human comfort for Vessel 5; iii. A time series plot of Composite Weighted Acceleration in m/s² showing technician transfer points and estimated human comfort levels for Vessel 6; Right top to bottom: iv. A time series plot of Motion Sickness Incidence in % showing technician transfer points and estimated sail or not-sail decision-based CTV safety thresholds for Vessel 4; v. A time series plot of Motion Sickness Incidence in % showing technician transfer points and estimated sail or not-sail decision-based CTV safety thresholds for Vessel 5; vi. A time series plot of Motion Sickness Incidence in % showing technician transfer points and estimated sail or not-sail decision-based CTV safety thresholds for Vessel 6.

The plots on the left show black dots which indicate values for defined Composite Weighted Acceleration, defined from the description given in section 3.7 of chapter three. The black coloured dots also describe the human comfort reactions to vibrations as defined by ISO 2631-1 shown in Table 4.1 of section 4.2.4 of this chapter, with black and red colour categories representing the different comfort levels. The black coloured dots in this plot indicate that

the journey is not uncomfortable (below 0.315 m/s^2). The red squares indicate technician transfer points defined from the discretization process in Figure 4.22.

On the right, the black dots indicate estimated Motion Sickness Incidence also defined from descriptions given in section 3.7 of chapter three of this thesis. The black coloured dots also indicate a *sail* welfare-based decision using 20% thresholds for best sea fairing practices (Phillips et al., 2015), with black and red colours indicating *sail and no sail* welfare-based decisions respectfully. The red squares also indicate technician transfer points defined from the discretization process.

Similar to plots in sections 4.2.4, 4.3.4, and 4.4.4. both plots in Figure 4.22 (left and right) seem to follow plots of square root functions as both plots have a minimum y-value of 0, no negative values, and opening along the x-axis.

Table 4.2 presents a summary of the descriptive analysis performed including mean observations of significant wave height, mean wind speed, mean estimated Composite Weighted Acceleration, mean estimated motion sickness incidence, sea state occurrences in the project sites based on the Beaufort wind force scale (Singleton, 2008), and the observed percentage occurrence of each sea state.

Sea state	Mean significant wave height (m)	Mean wind speed (m/s^2)	Mean Composite Weighted Acceleration (m/s2)	Mean MSI (%)	Percentage of sea state occurrence (%)
1	0.06	5.65	0.23	5.19	2.41
2	0.14	3.44	0.27	5.70	3.25
3	0.42	5.58	0.29	6.15	42.00
4	0.88	6.33	0.39	8.05	52.35%

Table 4. 2 Sea state occurrences in project sites with equivalent values for estimated Composite Weighted Acceleration (aRMS) and motion sickness incidence (MSI).

The data in Table 4.2 shows that the most experienced sea state in the project sites was sea state 4 with a 52.35 per cent occurrence and an equivalent significant wave height of 0.88m. On the other hand, sea states 1 and 2 were the least measured sea states with percentage occurrences of 2.41% and 3.25% respectively. The table also shows the relationships between

sea state, sea state variables, and welfare variables including motion sickness incidence (MSI) and Composite Weighted Acceleration (aRMS). Table 4.2 shows an increase in welfare variables with sea state variables and equivalent sea state numbers.

Section 4.1 to 4.5 presents the results of the descriptive analysis used to describe data from the VMMS, the meteorological data, and created variables needed for the predictive analysis or modelling processes. The next section explores the relevant relationships between the variables and presents and predictive analysis by modelling the comfort of technicians through Composite Weighted Acceleration and the likelihood of seasickness through motion sickness incidence.

4.6 Exploring Relationships and Modelling Technician Welfare

This section presents the results of the exploratory data analysis used in measuring the influence of variables such as the duration of the O&M operation, and significant wave height, on the welfare variables of Composite Weighted Acceleration and Motion Sickness Incidence, as well as predict the welfare variables from other variables.

A pairwise correlation between variables, seen in Figure 4.23 below, indicates relationships between variables in the dataset with some variables being as high as -0.534, however, the pairwise correlation also indicates that some variables are more relevant to one of the welfare variables than they are to the other.

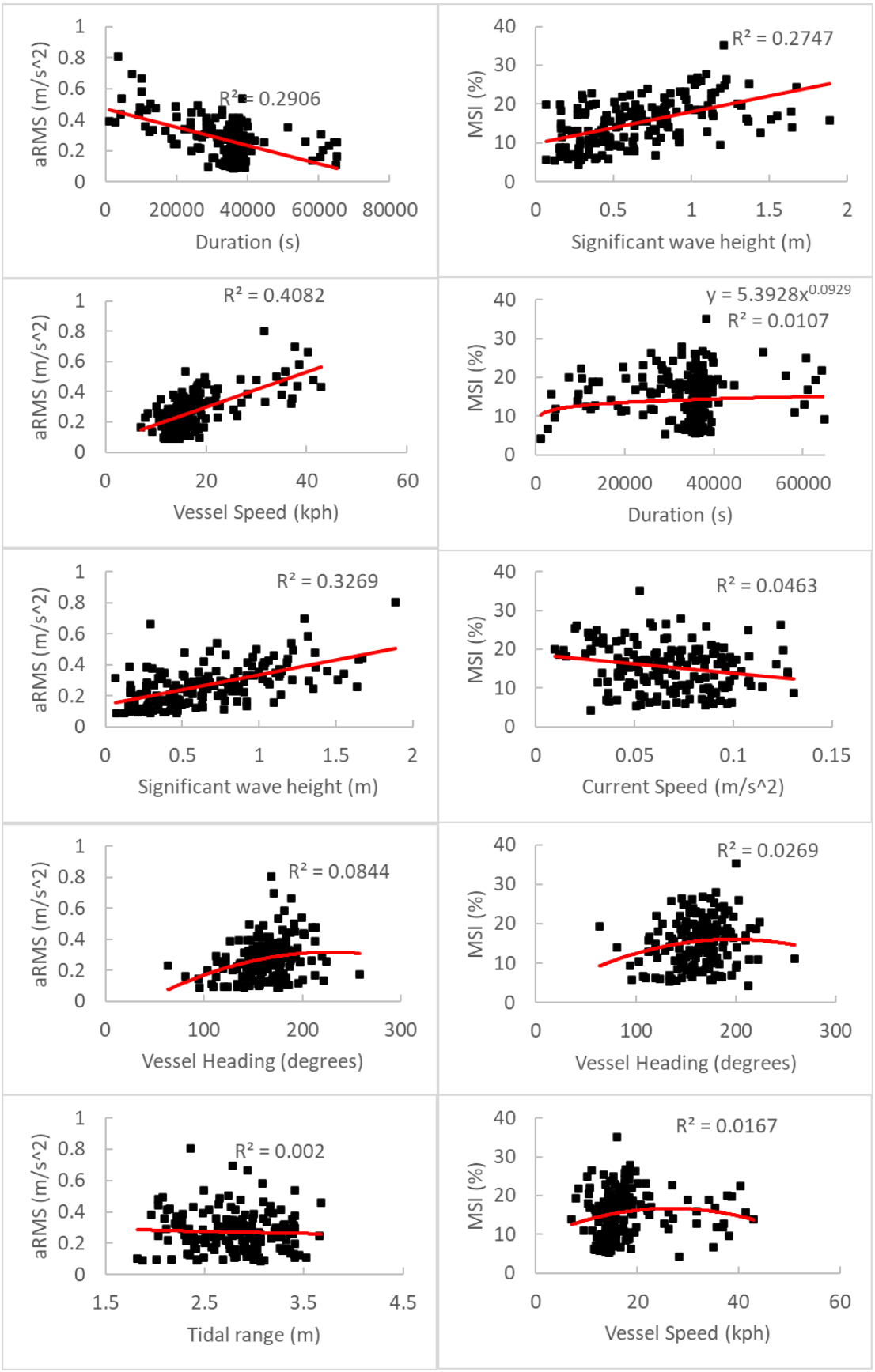

Figure 4. 23 Pairwise correlation showing relevant variable comparisons. Left column, top to bottom: i. Comparison between weighted acceleration and transit duration; ii. Comparison

between weighted acceleration and vessel speed; iii. Comparison between weighted acceleration and significant wave height; iv. Comparison between weighted acceleration and vessel heading; v. Comparison between weighted acceleration and tidal range; Right column, top to bottom: i. Comparison between Motion Sickness Incidence and significant wave height; ii. Comparison between Motion Sickness Incidence and transit duration; iii. Comparison between Motion Sickness Incidence and current speed; ii. Comparison between Motion Sickness Incidence and vessel heading; ii. Comparison between Motion Sickness Incidence and vessel speed.

Figure 4.23 shows the pairwise correlation of six variables, instead of eleven, and the welfare variables. The pairwise correlation also indicated that for relevant variables, there is a moderate linear relationship with the welfare variables with the presence of identifiable outliers which during the diagnostic analysis were identified as relevant to the study. It was, therefore, determined that a principal component analysis (PCA) would reduce the dimensionality of the large dataset for eventual modelling which would also prevent overfitting and underfitting. As the pairwise correlation highlighted, the PCA was performed on each welfare variable to identify variables relevant to each principal component.

Figure 4.24 below presents the PCA processes performed on the combined VMMS and meteorological dataset for the composite weighted analysis variable.

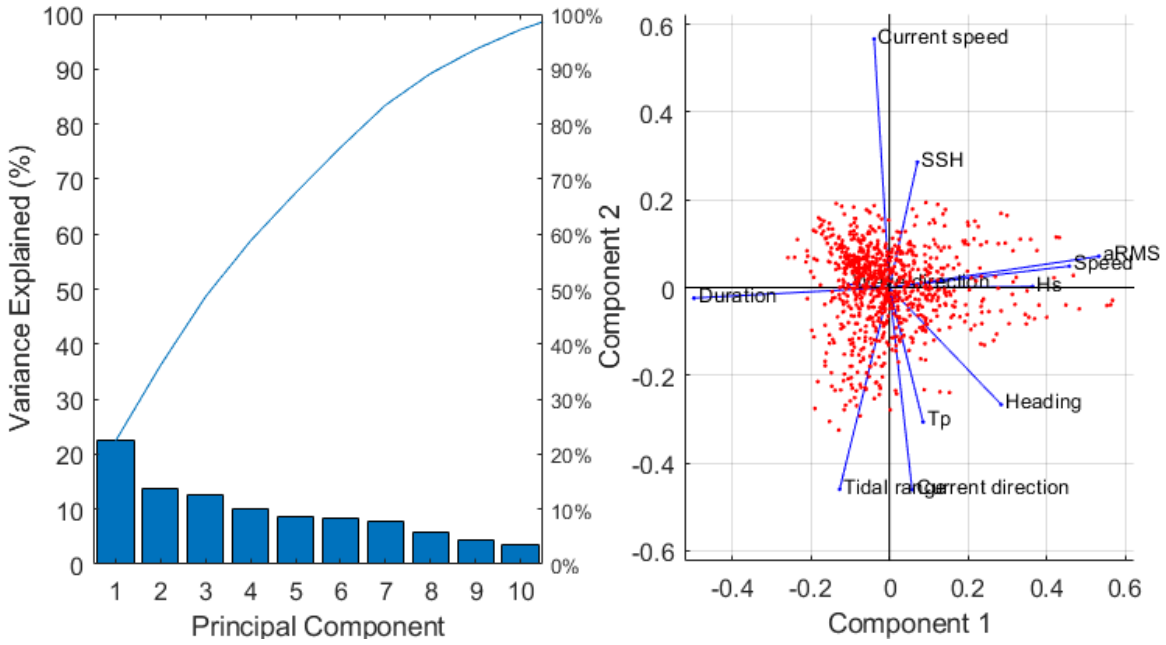

Figure 4. 24 Figure showing Principal Component Analysis results performed on VMMS and meteorological dataset for the composited weighted acceleration variable

This scree plot (left plot) only shows the first ten (instead of the total eleven) components that explain 95% of the total variance. The only clear break in the amount of variance accounted for by each component is between the first and second components. However, the first component by itself explains a little less than 25% of the variance, which highlights the need for more components. The figure also shows that the first six principal components explain roughly three-quarters of the total variability in the standardized ratings, suggesting an adequate dataset for exploration.

The second plot on the left of Figure 4.24, shows an orthonormal principal component coefficient plot for each variable and the principal scores for each observation. Figure 4.24 shows that all eleven variables are represented in this bi-plot by a vector, and the direction and length of the vector indicate how each variable contributes to the two principal components in the plot. The first principal component, on the horizontal axis, has positive coefficients for seven variables, including sea surface height, vessel speed, significant wave height, vessel heading, current direction, wave period, and wave direction, seen on the right half of the plot. The first component also has three negative variables including current speed, vessel duration, and tidal range, as seen on the left. The largest coefficient in the first principal component is the current speed coefficient followed by the duration of the vessel transit. The second principal component, on the vertical axis, has five positive coefficients and five negative variables including current speed, sea surface height, significant wave height, wave direction, and vessel speed for positive variables and vessel duration, tidal range, wave period, vessel heading and current direction for negative variables, seen on the top and bottom sides respectively. This indicates that the second component distinguishes between vessels that have high values for the first set of variables and low for the second, and vessels that have the opposite. The largest coefficient in the second principal component is the current speed coefficient. The PCA, therefore, shows that the relevant variables needed to model Composite Weighted Acceleration, and protect against over and underfitting are current speed, the vessel transit duration, the speed of the vessel, tidal range, current direction, and significant wave height.

Figure 4.25 below shows the PCA processes performed on the combined VMMS and meteorological dataset for the motion sickness variable.

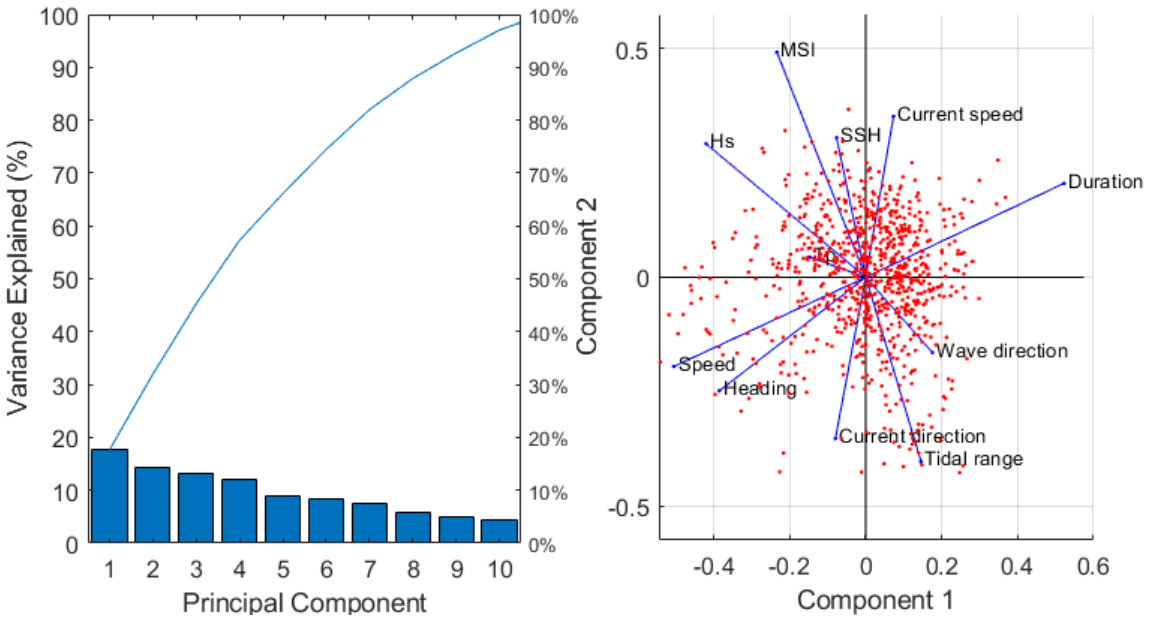

Figure 4. 25 Figure showing Principal Component Analysis results performed on VMMS and meteorological datasets for the Motion Sickness Incidence variable

The PCA analysis indicated that there exists a pairwise correlation between variables in the dataset with the highest correlation at 0.485. The left scree plot in Figure 4.25 only presents the first ten (instead of the total eleven) components that explain 95% of the total variance. The plot indicates a clear break in the amount of variance between the first and second components and between the fourth and fifth components. However, the first component by itself explains about 18% of the variance, which indicates a need for more components. The plot indicates that the first six principal components explain roughly three-quarters of the total variability in the standardized ratings, suggesting an adequate dataset for exploration.

The plot on the left of Figure 4.25, shows an orthonormal principal component coefficient plot for each variable and the principal scores for each observation. All eleven variables are represented in this bi-plot by a vector, and the direction and length of the vector indicate how each variable contributes to the principal component – Motion Sickness Incidence (MSI). The first principal component, on the horizontal axis, has 4-positive variables, seen on the right half of the plot, and 5-negative variables, seen on the left including current speed, wave direction, tidal range, and vessel duration for the positive variables, and sea surface height, significant wave height, vessel speed, vessel heading, and current direction for negative variables. The largest coefficient in the first principal component is the duration of the vessel transit. The second principal component, on the vertical axis, has 4-positive and 5-negative

coefficients seen on the top and bottom sides, respectively. The positive variables include vessel duration, vessel sea surface height, significant wave height, and current speed, while the negative variables include vessel speed, vessel heading, current direction, tidal range, and wave direction. The largest coefficient in the second principal component is the speed of the vessel. The PCA further shows that variables such as wave direction are more relevant to MSI than they are to Composite Weighted Acceleration and shows that in modelling Motion Sickness Incidence, the relevant variables needed are vessel transit duration, vessel heading, vessel speed, significant wave height, tidal range, current speed, and current direction.

The newly dimensioned dataset was then used in the modelling process described in section 3.7 of chapter 3 of this thesis. To validate the model used, this thesis applied a standard hold-out machine learning approach (Stetco et al., 2019). This approach held out sets of data by splitting the data set into a 637 training set (75% of the dataset) and a 212 testing set (25% of the dataset). Using the training dataset, k-fold cross-validation (k = 10) is performed in the MATLAB workspace to build a more generalized model by partitioning the data within the training data before training the model. A few measures were used to show the validity of the regression model behaviour. These measures, described in section 3.7 of chapter 3 of this thesis, based on the model prediction, included Mean Absolute Error (MAE), Mean Squared Error (MSE), Root Mean Squared Error (RMSE), and the Coefficient of Determination (R^2). These metrics were selected as they are best used in expressing regression-based models (Stetco et al., 2019).

4.6.1 Modelling Composite Weighted Acceleration

Figure 4.26 presents the results of the regression model used to assess the trained model comfort model using predictions of Composite Weighted Acceleration.

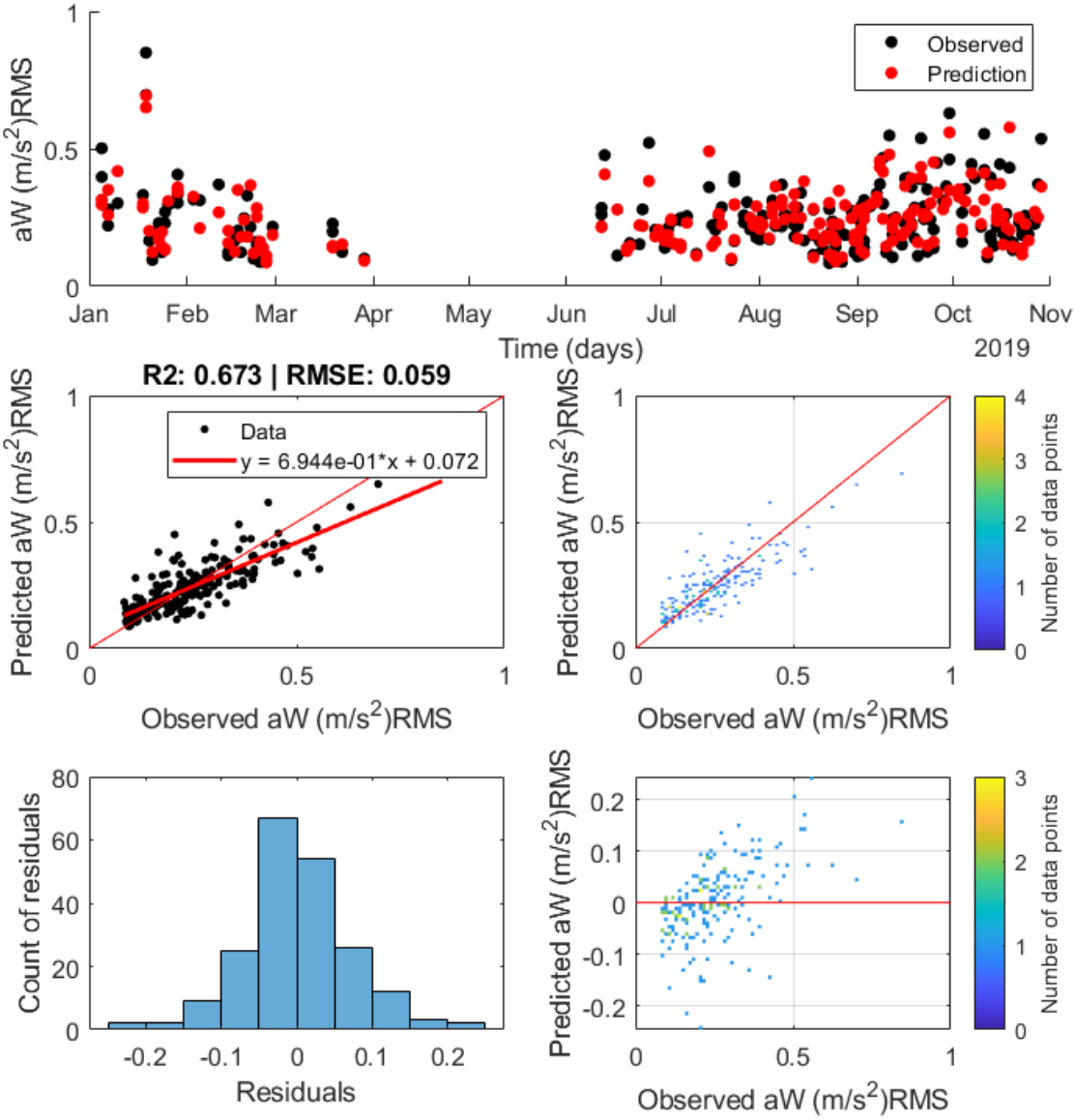

Figure 4. 26 Modelled Composite Weighted RMS Acceleration (m/s²) denoted by aW (m/s²) RMS. From top row: i. Response plot of observed Composite Weighted Acceleration and predicted Composite Weighted Acceleration with time; the second row left to right: ii. Predicted against the observed plot of Composite Weighted Acceleration, iii. Predicted against the observed plot of Composite Weighted Acceleration with the number of data points; the third row left to right: iv. Histogram of residuals, v. Residual plot with the number of data points.

Figure 4.26 shows a moderate linear correlation between the predicted and observed values of Composite Weighted Acceleration. The response plot shows a similar pattern between predicted and observed values with slight differences of about 0.06 m/s^2 between values indicating that the predicted values of Composite Weighted Acceleration could be off by 0.06 m/s^2. There are more dots below the perfect prediction line (thin red line) at the right of the

predicted against the observed plot which shows that the predicted values tend to be lower than the observed values for less common predicted values of Composite Weighted Acceleration values (between 0.5 and 1 m/s^2). The prediction against the observed plot with the number of data points shows that the densest area of the plot, shown in the yellow dots, is above the diagonal line which means that the model overestimates the most common values of Composite Weighted Acceleration (between 0.1 and 0.3 m/s^2). The histogram of residuals shows that most points are centred around zero, but the range of the x-axis shows that some of the residuals are large, with some predictions off by 0.25 m/s^2. This is a large value considering the MAE is 0.055 m/s^2 shown in Table 4.3 below. The model also has a p-value less than 0.01 which rejects the project null hypothesis of no statistical relationship between predicted Composite Weighted Acceleration and estimated composited weighted acceleration. The residual plot with the number of data points shows that the smallest Composite Weighted Acceleration is overestimated, as the yellow areas are below zero, and the spread of residuals changes over the response value, meaning that the variance of residuals is not uniform. This suggests that the model will be more accurate for some values than it is with others and the error is not consistent across responses. This means that in predicting technician comfort levels, this model will overestimate technician comfort levels deemed as comfortable and a little uncomfortable according to ISO 2631-1, (1997) and underestimate dangerously uncomfortable levels up to 1 m/s2 considered uncomfortable by ISO 2631-1, (1997) see Table 4.1 in section 4.2.3 of this chapter.

The table below provides the results for both the training data set and the testing dataset for the regression model of best fit.

	RMSE	R^2	MSE	MAE	Speed	time	Model
Train	0.073	0.63	0.005	0.055	25000	12.111	Rational quadratic Gaussian process regression
Test	0.059	0.67	0.004	0.043	8800	3.046	

Table 4. 3 Table of model results

4.6.2 Modelling Motion Sickness Incidence

This section presents the observed and predicted values of Motion Sickness Incidence using the testing dataset.

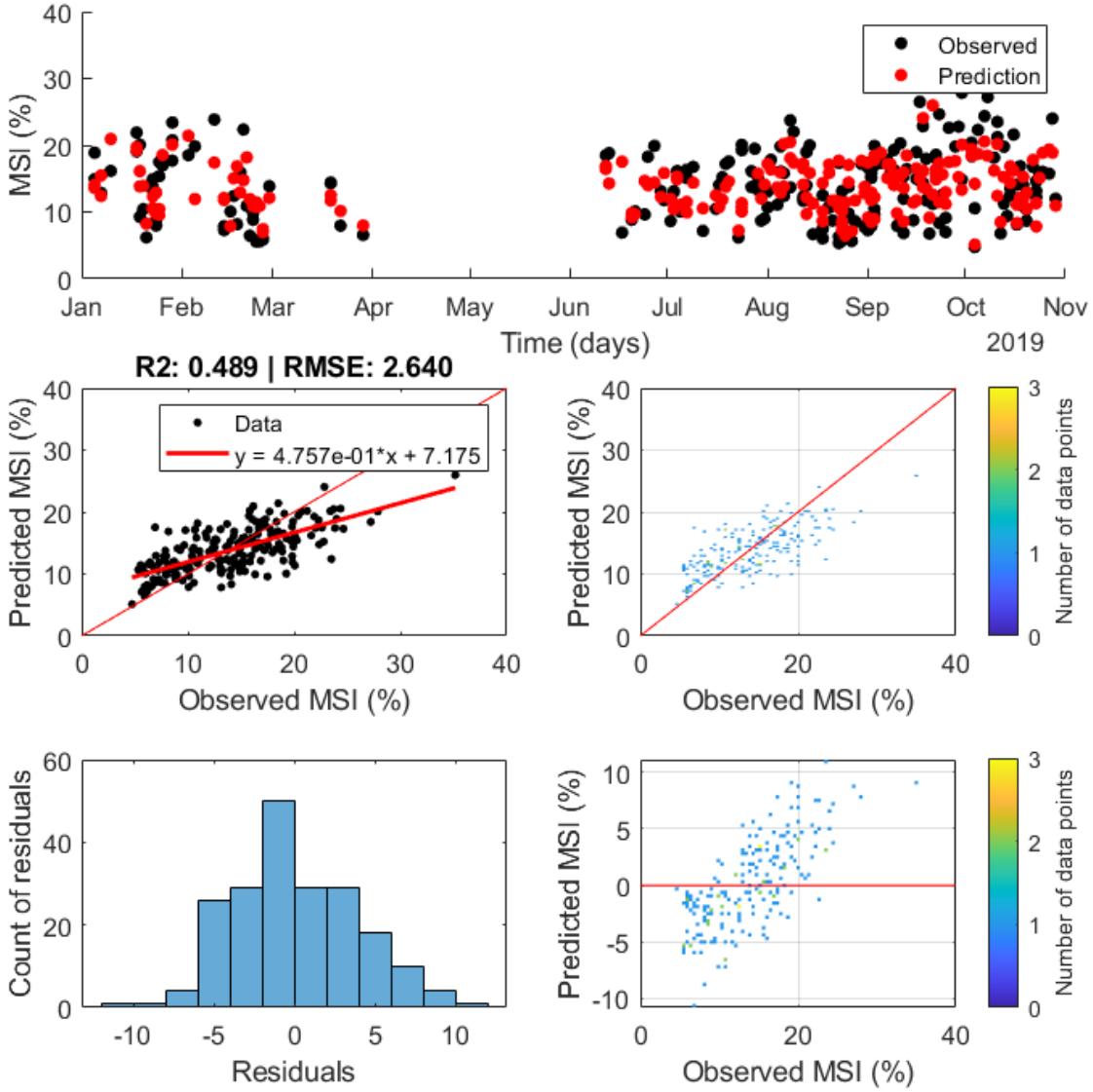

Figure 4. 27 Comparison between observed (true) and predicted Motion Sickness Incidence (%). From top row: i. Response plot of observed Motion Sickness Incidence (%) and predicted Motion Sickness Incidence with time; the second row left to right: ii. Predicted against the observed plot Motion Sickness Incidence (%), iii. Predicted against the observed plot of Motion Sickness Incidence (%) with the number of data points; the third row left to right: iv. Histogram of residuals, v. Residual plot with the number of data points

Similar to the comfort model, Figure 4.27 shows a moderate linear correlation between the predicted and observed values of Composite Weighted Acceleration. The response plot shows a similar pattern between predicted and observed values with slight differences of about 2% between some values indicating that the predicted values of Motion Sickness Incidence could be off by 2%. The predicted against the observed plot shows more dots below the perfect prediction line (thin red line) at the right which shows that the predicted values tend to be lower than the observed values for less common predicted values of Motion Sickness

Incidence values (between 22% and 36%). The prediction against the observed plot with the number of data points shows that the densest area of the plot, shown in the yellow dots, is above the diagonal line which means that the model overestimates the most common values of Motion Sickness Incidence (between 5% and 12%). The histogram of residuals shows that most points are centred around zero, but the range of the x-axis also shows that some of the residuals are also large, with some predictions off by 12%. The model also has a p-value of 6.068e-31, a value less than 0.05 which rejects the project null hypothesis of no statistical relationship between predicted Motion Sickness Incidence and estimated Motion Sickness Incidence. The residual plot with the number of data points shows that the densest areas of the plot (yellow dots) are below zero, which means that the smaller values of Motion Sickness Incidence are overestimated, and the plot has a spread of residuals which means that the error is predictions are not equal but vary. This suggests that the model will overestimate Motion Sickness Incidence below 12% (regarded as optimal levels) and underestimate values greater than 22% (dangerous levels).

The table below provides the results for both the training data set and the testing dataset for the regression model of best fit.

	RMSE	R^2	MSE	MAE	Speed	time	Model
Train	4.018	0.460	16.146	3.158	34000	16.559	Rational quadratic Gaussian process regression
Test	2.640	0.489	6.970	1.780	8800	12.111	

Table 4. 4 Table of model results

4.6.3 Modelling the welfare of technicians

This section presents the results of the welfare model produced using predictions of Composite Weighted Acceleration and Motion Sickness Incidence.

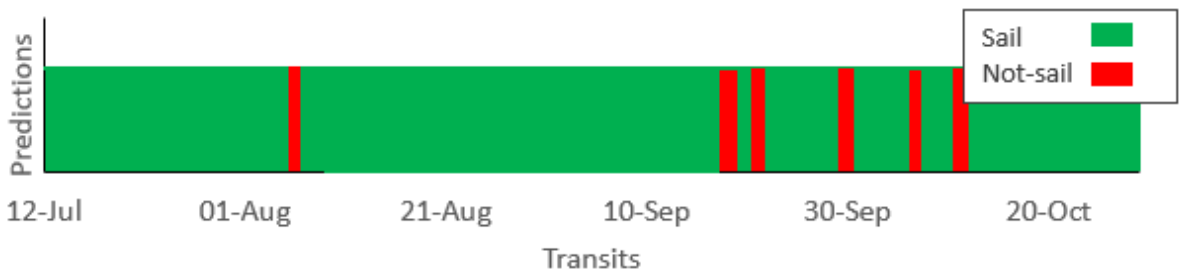

Figure 4. 28 Welfare model showing predicted sailing decisions.

Figure 4.28 presents a visualisation of the results of the welfare model with predictions of *sail and not-sail* decisions made from operational limits applied to input variables. The plot shows four-month-long model predictions including 7 *not-sail* decisions from 139 predictions.

4.7 Summary

This chapter presented, described, and explained the results generated from modelling the welfare of technicians during transits to offshore wind farms using predictions of Composite Weighted Acceleration and predictions of Motion Sickness Incidence. To meet the thesis aims and objectives, this research used data from vessel motion monitoring systems (VMMS) deployed on twelve (12) crew transfer vessels operating across four wind farms (4) by four wind farm operators in the North Sea. The VMMS recorded vessel acceleration data in the six-axis of freedom as well as GPS data, vessel speed data, timestamp data, and vessel heading data. The data collection used in this project began in January of 2019 and ended in October of the same year, covering eight months, and resulting in eight hundred and fifty (850) defined operation and maintenance transit days after data processing and cleaning. To describe sea state, this research used hindcast metocean data which was synchronised to crew transfer vessels' transit routes between port and wind farms using the GPS coordinates and timestamps from the VMMS. The data used to describe the sea state included significant wave height, wave period, wave direction, current direction, current speed, sea surface height, wind speed, and wind direction.

An instantaneous descriptive analysis process highlighted the presence of multiple transfer points during O&M transits which suggests the practice of service trains, as such, a daily dose analysis was considered in accounting for multiple transfers in O&M. A dimensionality reduction analysis was performed to identify variables in the dataset most relevant to predicting Composite Weighted Acceleration and Motion Sickness Incidence which represented the comfort and health of technicians, respectively. The dimensionality reduction process involved a pairwise correlation and a principal component analysis which

identified the vessel transit duration, averaged vessel speed, averaged vessel heading, significant wave height, wave direction, wave period, current speed, current direction, and tidal height variables as relevant to 70% of the variation in predicting Composite Weighted Acceleration and Motion Sickness Incidence.

Machine learning applications in the MATLAB workspace were used to determine a model of best fit for predicting Composite Weighted Acceleration and Motion Sickness Incidence using vessel transit duration, averaged vessel speed, averaged vessel heading, significant wave height, wave direction, wave period, current speed, current direction, and tidal height, as independent variables. Results show a rational quadratic gaussian process regression model able to predict Composite Weighted Acceleration with an R^2 value of 0.67, and a rational quadratic gaussian process regression model able to predict Motion Sickness Incidence with an R^2 value of 0.49. Operational limits were applied to model outputs of Composite weighted Acceleration and Motion Sickness Incidence to form a dual-criterion input model that predicts sailing decisions in a welfare model.

5 Analysis

5.1 Introduction

This chapter analyses the results of the data from the vessel motion monitoring systems (VMMS) deployed on participating vessels and data from operational ocean models used to achieve the thesis aim of modelling the welfare of technicians on crew transfer vessels during transits to offshore wind farms. For technicians the main concern is their comfort, health, and safety during transit (Phillips et al., 2015), as such, this thesis applies measurable aspects of these concerns from available data, which is described in the thesis scope.

5.1.1 Scope

In exploring human response to vessel motions for the technician welfare analysis, this research uses proxy variables derived from whole-body accelerations to describe the comfort and health of technicians and as such the welfare of technicians in transit. The proxy variables are used due to relationships to whole-body accelerations which are supported by findings in the literature explored. The factors used to describe technician welfare in this thesis were also selected based on available research data and the standards for mechanical vibration evaluation (ISO 2631-1, 1997). This thesis differs from the scope of the SPOWTT project, where vessel measurements were acquired, as this project delivers a framework for assessing the well-being of technicians in transit while the SPOWTT project intended to understand the effect sailing on Crew Transfer Vessel (CTVs) can have on the mental and physical wellbeing of technicians on board (Earle et al., 2021). The image in Figure 5.1 presents a clear boundary between the scope of the SPOWTT project and this thesis.

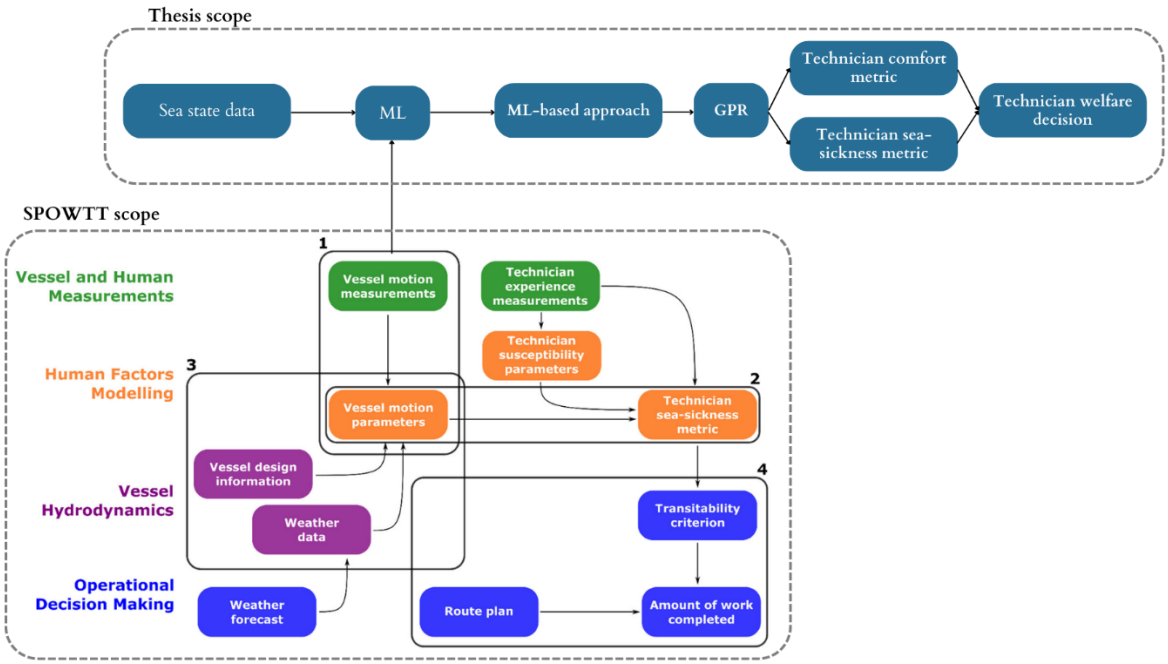

Figure 5. 1 Image showing the boundary between the SPOWTT project and the scope of this thesis. Image adapted from Earle et al., (2021).

Within the scope of this study, this research assumes that during transits to offshore wind farms, technicians are in a seated position and in this position, the transmission of acceleration is through the seats of crew transfer vessels (CTVs). This means the path of acceleration transmission begins from the action of the surface of the sea to the crew transfer vessels, from the crew transfer vessels to the seats and footrests on the vessels, and finally, through to the crew members and technicians on the vessels. Therefore, the accelerations experienced by the technicians are whole-body accelerations. To describe comfort, the measuring metric used in this research is composite root-mean-square (RMS) acceleration which refers to the cumulative multi-axis RMS of whole-body acceleration with time expressed in equation 2.14 of chapter two from the recommendations of the ISO 2631-1 to describe the human response to vessel accelerations from frequency weightings – objective one. On the other hand, to explore the health of technicians, this thesis investigates the impact of vessel accelerations on the likelihood of inducing seasickness using Motion Sickness Incidence (MSI) – objective two. This research used weighted root-mean-square (RMS) of the vector sum of tri-axial translational accelerations and the RMS vertical accelerations in assessing the comfort and Motion Sickness Incidence of technicians. This is done following the guidelines from the ISO 2631-1 presented in equation 2.14 and equation 2.15 of the

second chapter, however, the thesis methodology explores the application of the six-axis of acceleration in the analysis process. To achieve both objectives, this research explores the relevant relationships that affect weighted accelerations and Motion Sickness Incidence during transits in order to define input variables for both models. This is done by synchronising metocean data with the data from the vessel motion monitoring systems in order to describe the sea state across crew transfer vessel transit routes, thereby creating a complete dataset of operational and oceanographic characteristics. Therefore, to reach the aim of the thesis, Machine Learning Tools were used to fit a regression model from the complete dataset which was then used to predict comfort and health-based responses of Composite Weighted RMS Acceleration and Motion Sickness Incidence, respectively, as dual-criterion variables for technician welfare during maintenance transits – objective 3. The research algorithm used to achieve the thesis aim is presented in Figure 5.2 below. This algorithm is expanded from the thesis methodology presented in Figure 1.1 of this thesis and shows the detailed phases undertaken to create the welfare model.

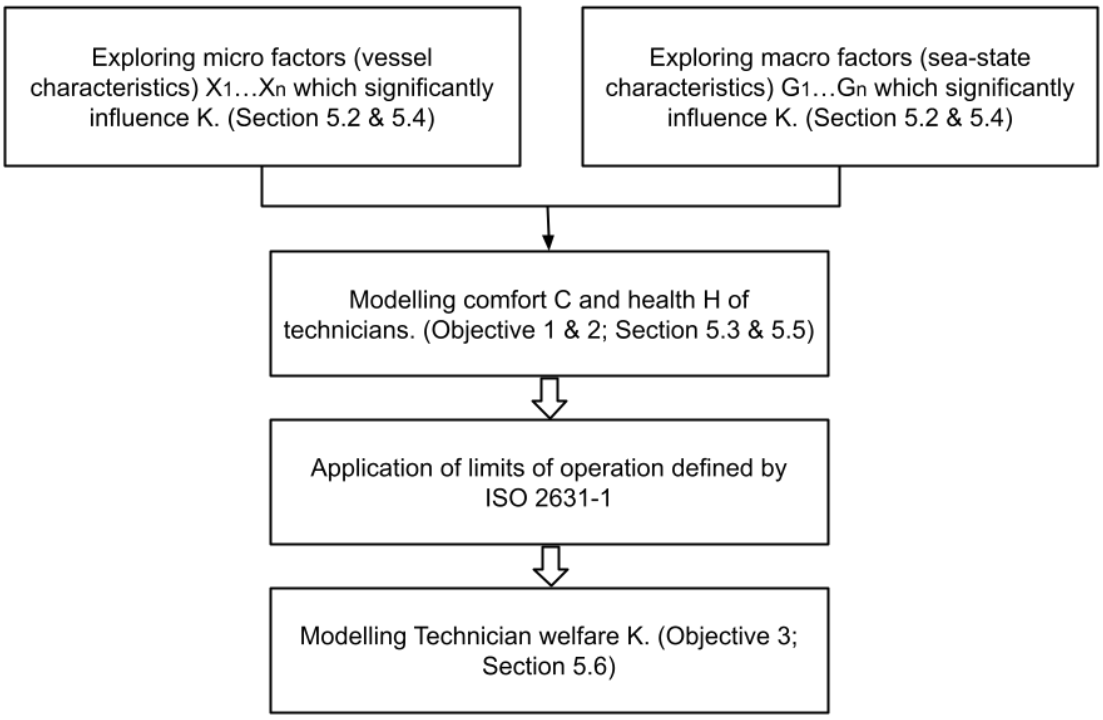

Figure 5. 2 Revised methodology to achieve the thesis aim expanded from Figure 1.1 where: X_1… X_n is the vessel characteristics, G_1… G_n is sea-state characteristics, C and H are the comfort-based and health-based models, and K is the welfare model.

Figure 5.2 illustrates the process of achieving the thesis aim described above over five phases. The first phase explores the significant micro factors (X_1… X_n) and macro factors (G_1… G_n) in the available dataset that influence the prediction of Composite Weighted RMS Acceleration for the comfort and Motion Sickness Incidence for the health of technicians. From the exploratory analysis, the comfort-based model (C) and health-based (H) models are developed using the explored input micro and macro variables. Limits of operation defined by ISO 2631-1 are applied to the outputs of the comfort-based model and health-based model which are used as input variables for the welfare model (K). The welfare model determines *sail or not sail* decisions (Y) based on the inputs with defined limits. The welfare model K can be expressed as:

$$Y = K(X_1, \dots, X_n, G_1, \dots, G_n) \qquad 5.1$$

Where: Y, is the estimated design variable for *sail or not sail* decisions; X_1… X_n, are micro factor input design variables including transit duration, vessel speed, and vessel heading; G_1… G_n, are macro factor input design variables including significant wave height, current speed, current direction, and tidal height.

The term micro factor in this thesis refers to the operational vessel parameters associated with whole-body accelerations from crew transfer vessels identified during analysis processes to include the magnitude of accelerations, the duration of exposure, the speed of the crew transfer vessel, and the heading of the vessel. On the other hand, macro factors refer to environmental parameters associated with whole-body accelerations which were identified during the thesis analysis described in chapter three of this thesis to include sea-state parameters. Physiological factors such as fatigue, diet, and sleep are not included within the scope of this study due to the defined thesis objectives and the availability of data within this study. Additionally, for the assessment of motion sickness, susceptibility factors such as age, environment, and psychology were not included in the models created due to data availability and as described in section 2.6.2.1 of this thesis, these factors increase the susceptibility to motion sickness rather than cause motion sickness (Kluijven, 2016). As such the models created are based on discomfort and motion sickness caused by whole-body accelerations alone which are transferred through crew transfer vessels from the sea state.

This chapter is structured into sections. This section (section 5.1) provides a brief introduction to the chapter and an overview of subsequent sections within this chapter. Along with relevant literature relating to the subject matter, section 5.2 discusses the exploration of variables for modelling Composite Weighted Acceleration as a metric for the comfort of technicians during transits to offshore wind farms. Section 5.3 analyses and discusses the model created for the comfort of technicians on crew transfer vessels during transits and explores potential applications of the model in offshore wind operation and maintenance. Along with relevant literature relating to the subject matter, section 5.4 discusses the exploration of variables for modelling Motion Sickness Incidence as a metric for the health of technicians during transits to offshore wind farms. Section 5.5 analyses and discusses the model created for the health of technicians on crew transfer vessels during transits and explores potential applications of the model in offshore wind operation and maintenance. Section 5.6 analyses and discusses the welfare model created for day-to-day *sail or no-sail* decision-making and its potential application to operation and maintenance.

	Objective 1	**Objective 2**	**Objective 3**
Criterion	Comfort	Health	Welfare
Thesis section	Section 5.3	Section 5.5	Section 5.6

Table 5. 1 Structure of thesis objectives

The next section explores relevant relationships in predicting Composite Weighted Acceleration.

5.2 Exploring relationships in assessing the comfort of technicians using Composite Weighted Acceleration.

This section explores the impact of micro and macro factors on the whole-body accelerations felt by technicians on crew transfer vessels in order to explore relationships in predicting Composite Weighted Acceleration which is used as a proxy for the comfort of technicians during transits to offshore wind farms for maintenance operations. Generally, most researchers apply response amplitude operators (RAO) along with wave energy spectra to produce response spectra (Jenkins et al., 2021), or numerical models combined with seat

models to describe sea-state (Griffin, 1990; Olausson & Garme, 2013). This allows researchers to model sea states along with defined vessel parameters such as vessel heading and vessel profiles when predicting acceleration exposure in humans (Olausson, 2015). This is due to the time-consuming nature of experimental measurements which would require measuring sea state, and accelerations on vessels. This research applies metocean products to describe sea state from oceanographic models including the WAVEWATCH-III model (H.W. Lewis et al., 2019) and NEMO model (Tonani et al., 2019). This allowed sea state variables no typically used when exploring human response to vibration to be explored.

5.2.1 Exploring notable relationships in assessing the comfort of technicians

The exploratory analysis phase of this project explores multiple variables to assess the discomfort of technicians using their relationship to the acceleration measured on participating vessels. The analysis was performed on a synchronised dataset that included micro variables of Composite Weighted RMS Acceleration, vessel transit duration, averaged vessel speed, and averaged vessel heading, and included macro variables of significant wave height, wave direction, wave period, current speed, current direction, tidal height, sea surface height, wind speed, and wind direction. The exploratory analysis involved dimension reduction processes using pairwise correlations and principal component analysis to avoid overfitting the model and determine the variables most relevant to the prediction of Composite Weighted Acceleration. Figure 4.23 presents the results of exploring major relationships and Figure 4.24 shows the result of the principal component analysis where the variables identified included vessel transit duration, averaged vessel speed, averaged vessel heading, significant wave height, current speed, current direction, and tidal height, after the dimension reduction process.

The most correlated relationships with Composite Weighted Acceleration identified were the relationships with vessel transit duration, vessel speed, and significant wave height. There was a moderate negative correlation between the duration of transit and Composite Weighted Acceleration for daily transits up to about 18 hours seen in the first plot of Figure 5.2. This confirms the guidelines of the ISO 2631-1 and supports the findings in the explored publications in section 2.6.1 such as Clevenson et al., (1978), Griffin & Whitham, (1998), and

Kjellberg & Wikström, (1985a). The plot also follows a similar path to the study by Maeda and Morioka, (1998) seen in Figure 2.19 of this thesis and further corroborations can be found in a few other studies (Kjellberg & Wikström, 1985b). Therefore, the analysis confirms the duration dependency of weighted accelerations suggesting that low vibration levels are acceptable over longer periods. The plot in Figure 5.2, however, presents this relationship in daily doses by using daily transit duration. On a smaller scale, the relationship between duration and weighted acceleration was presented in the left plots of Figure 4.7, Figure 4.12, Figure 4.17, and Figure 4.22, where weighted acceleration was compared with duration in hours ranging between two and eight hours. The plots show an increase in Composite Weighted Acceleration with time between two and six hours for most transits which also corroborates the findings of some explored literature in section 2.6.1 such as Griffin & Whitham, (1980) and Miwa et al., (1973). Additionally, the findings by Kjellberg & Wikström, (1985a) are also corroborated in Figures 4.7, 4.12, 4.17, and 4.22, as the increase in weighted acceleration seems to be less rapid as duration increases leading to a possible plateau. As such, the findings from this research suggest that for daily dose values, weighted acceleration decreases with longer transit durations while weighted acceleration increases with shorter transit durations.

As the literature explored in section 2.6.1 has shown that transits become progressively more uncomfortable as the magnitude of acceleration increases (Mansfield et al., 2000), the relevance of this relationship in operation and maintenance planning is that in scheduling maintenance operations the daily dose weighted accelerations give an estimate for the average daily acceleration experienced by technicians which can inform decision-making if the comfort of technicians is taken into account. Figures 4.7, 4.12, 4.17, and 4.22, also show that initial technician transfer between two and six hours could prove to be uncomfortable as Composite Weighted Acceleration increases with time especially since the data from the vessel motion monitoring systems confirm the practice of service trains – where more than one wind turbine is maintained by the same crew transfer vessel (CTV) in a wind farm (Solano, 2021) – also shown in Figures 4. 4.7, 4.12, 4.17, and 4.22. Additionally, the literature review also suggests that the current trend in the offshore wind industry is the development of wind turbines further offshore which also suggests longer durations (Newman, 2015).

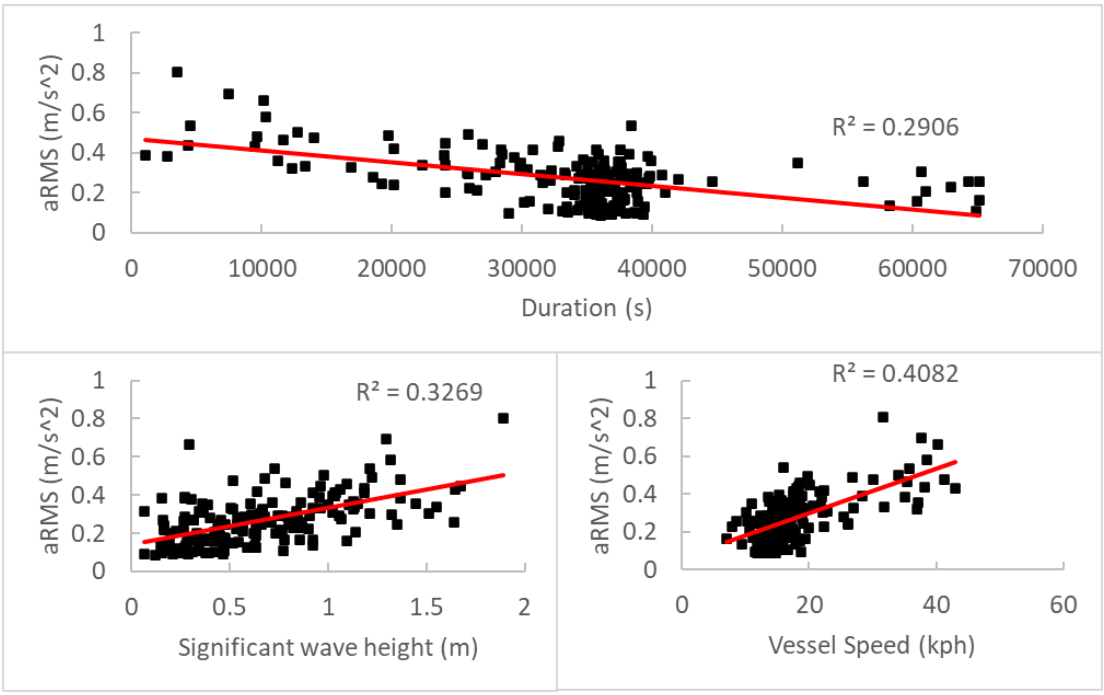

Figure 5. 3 Comparison between daily Composite Weighted RMS Acceleration (aRMS) and the most correlated relationships. Top plot: i. Comparison between daily Composite Weighted Acceleration and duration; Bottom plot: ii. Comparison between daily Composite Weighted Acceleration and significant wave height; iii. Comparison between daily Composite Weighted Acceleration and vessel speed.

Whilst the regression determined the relationship between weighted acceleration and duration, the lack of a high R^2 value and clear spread of results meant that other variables could exist for more accurately predicting Composite Weighted Acceleration such as vessel speed, and significant wave height.

The plot in Figure 5.3 also shows the comparison between composite weight acceleration and vessel speed (bottom right). The plot shows a positive linear relationship between weighted acceleration and average vessel speed which suggests that there is an increase in weighted acceleration with vessel speed. It is rare to find time-series collaborations between speed and weighted acceleration when predicting exposure to accelerations in available research. This is because this relationship is usually defined in vessel parameters where operating parameters are explored on defined speeds ranging from high to low (Olausson, 2015). These studies have similar findings where defined speeds in the design parameters had an increasing effect on the magnitude of acceleration including Derakhshanjazari et al., (2018), Hostens & Ramon, (2003) and Eger et al., (2011). Similarly, Figure 5.2 also presents the comparison between composite weight acceleration and significant wave height (bottom left). The

comparison shows a moderate linear relationship where Composite Weighted Acceleration increases with significant wave height between 0.1 m and 2.0 m. Generally, in predicting exposure to accelerations, the sea-state is modelled using numerical models and such as vessel speed, predictions are made for defined sea-states (wave spectra) (Olausson, 2015; Stevens & Parsons, 2002). As such, comparisons between significant wave height and Composite Weighted Acceleration are also rare in the available literature and are usually included in studies relating to vessel design.

The other variables explored in this thesis are shown in Figure 5.4 which shows the comparison between Composite Weighted Acceleration and four identified variables including vessel heading, current speed, current direction, and tidal range. Unlike the previously identified variables, there is little correlation between these variables and weighted acceleration, and there is not an easily identifiable trend in the comparisons. The comparison with vessel heading seems to cluster around the average vessel headings with observable outliers where weighted acceleration peaks between 150˚ and 200˚. Similar clusters are found in the comparison with the current direction where two clusters are seen with identifiable outliers where weighted acceleration peaks between 50˚ and 90˚, and between 220˚ and 280˚. The comparison with the tidal range shows a cluster between 1.8 m and 3.0 m, and there is no observable trend in the relationship between weighted acceleration and current speed. Despite these much weaker relationships, the principal component analysis showed that these variables, along with the first three variables presented, were relevant to 70% of the variation of Composite Weighted Acceleration.

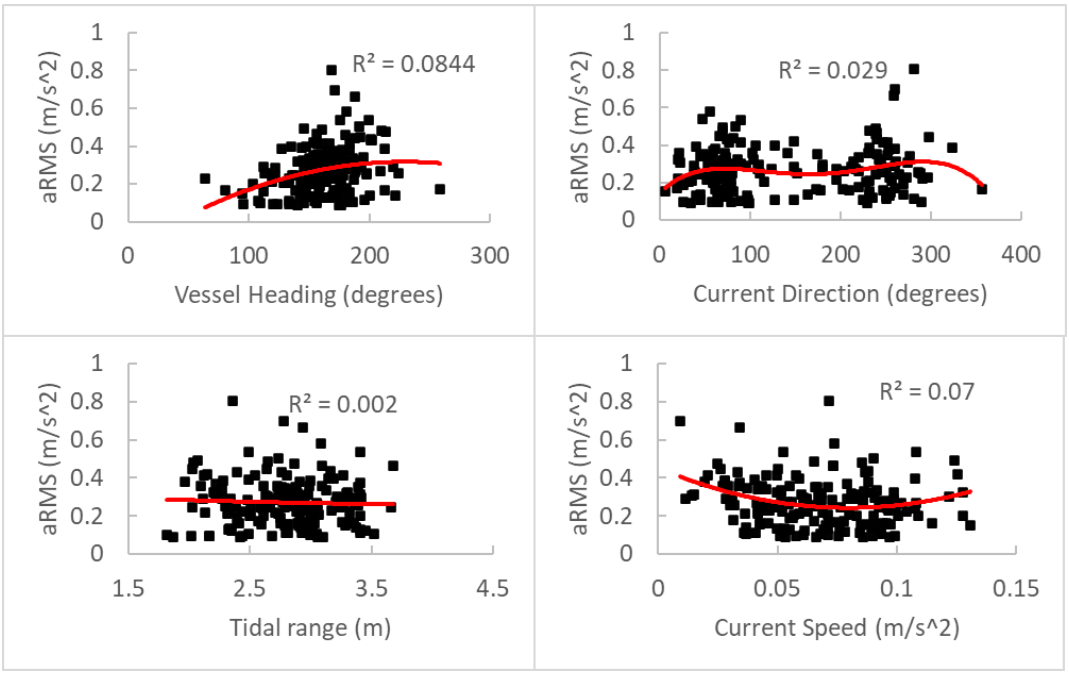

Figure 5. 4 Comparison between daily Composite Weighted RMS Acceleration (aRMS) and variable identified during dimension reduction. Top left to right: i. Comparison between daily Composite Weighted Acceleration and vessel heading; ii. Comparison between daily Composite Weighted Acceleration and current direction; Bottom left to right: iii. Comparison between daily Composite Weighted Acceleration and tidal range; iv. Comparison between daily Composite Weighted Acceleration and current speed.

As with vessel speed, the relationship between weighted acceleration and vessel heading or other sea-state characteristics is presented and is usually seen in included vessel design parameters and operating parameters (Olausson, 2015). Additionally, the literature explored in this thesis shows that mathematical models exist for planning boat motions in sea-states including (Akers, (1999), Keuning, (1994), and Zarnick, (1978), however, this is not usually explored concerning human performance.

5.2.2 Summary

This section showed the relevant variables explored during the dimension reduction process in order to model the discomfort of technicians during transits to offshore wind farms. Principal component analysis processes were used to identify variables most relevant to the prediction of Composite Weighted Acceleration. The process revealed that vessel transit duration, averaged vessel speed, averaged vessel heading, significant wave height, wave direction, wave period, current speed, current direction, and tidal height, are relevant to 70% of the variation in predicting Composite Weighted Acceleration. Significant relationships were

found between vessel transit duration, vessel speed, and significant wave height, however, there was no observable trend seen in the comparisons between Composite Weighted Acceleration and vessel heading, current speed, current direction, and tidal range, even though the principal component analysis shows in addition to vessel transit duration, vessel speed, and significant wave height, these variables account for 70% of the variation for predicting weighted acceleration. The following section discusses and analyses the modelling of comfort in technicians using the variables explored in this section.

5.3 Analysis and Discussion of Objective One

5.3.1 Modelling the comfort of technicians during transits on crew transfer vessels using whole-body acceleration.

While reviewing decision support models for maintenance operations in offshore wind farms, Seyr & Muskulus, (2019) stated that existing models aiding the decision-making in operation and maintenance (O&M) can be improved by applying more advanced mathematical methods, including uncertainties in input variables, and most importantly, regarding more influential factors, and collecting, analysing, and using more accurate data. This section analyses and discusses the comfort model created and its use as a risk-based decision-making tool in the *sail or not-sail* decision-making process of maintenance planning. Specifically, this model estimates the discomfort of technicians using whole-body accelerations in the absence of other discomfort-causing aspects of crew habitability on marine vessels from standard sea-faring guidelines such as noise, temperature, and lighting (McSweeney et al., 2008). Therefore, this research developed a model that can be used to estimate the level of discomfort in a comfort-based model (C) that predicts Composite Weighted Acceleration (Y) based on explored input variables:

$$Y = C(X_1, \dots, X_n, G_1, \dots, G_n) \qquad 5.2$$

Where Y, is the estimated design variable for Composite Weighted Acceleration; $X_1 \dots X_n$, are micro factor input design variables including transit duration, vessel speed, and vessel heading; $G_1 \dots G_n$, are macro factor input design variables including significant wave height, current speed, current direction, and tidal height.

The model was created following a machine learning training process that identified a rational quadratic gaussian process regression model presented in Figure 4.26 of chapter four as the model of best fit. The model of best fit was selected from metrics that assessed the model's performance including the coefficient of determination (R^2), root-mean-square error (RMSE), and mean average error (MAE) which identified the best fit from multiple models including linear regression models, regression trees, support vector machines, Gaussian process regression models, ensembles of trees, and neural networks. Gaussian process regression methods have been reported as an efficient tool in estimating predictions (Baiz et al., 2020), especially for non-linear relationships requiring fewer data samples (Richardson et al., 2017). Gaussian process regression has also been used in different fields such as medicine (Swain et al., 2016) and energy (Richardson et al., 2017). Therefore, the gaussian process regression model proved to be suitable for predicting technician welfare. However, at the time of writing, the use of Gaussian process regression models in comfort or seasickness assessments and predictions has not been reported.

The testing set of the model was assessed achieving an R^2 of 0.67, an RMSE of about 0.06 m/s^2, and a p-value of less than 0.01 which shows that the null hypothesis of there being no statistically significant relationship can be rejected. As such, the model's quality expressed in terms of an R^2 value expressed that predicted Composite Weighted Acceleration is influenced by the selected independent variables that make up over 70% of its variation. This shows that for this model, 67% of the variation of estimated Composite Weighted Acceleration, can be explained by the independent variables, and as such, only 33% reside in the residual. This gives a measure of improvements that need to be done in improving the model which is relevant since there could be some unexplored, uncontrollable, and undeterminable or unknown factors that could influence the measured acceleration on the participating CTVs. The RMSE and MSE not only explored the errors present in the model but also provides measures to compare future models against. As such where future work, discussed in chapter six, is applied to this study such as an increased dataset, the subsequent model results can be compared. The model results, however, show that more than half of the variance in predicting Composite Weighted Acceleration was explained and as such, the model presents an acceptable level of performance. This is visible in the response plot in Figure 4.26 of predicted against observed values which were used to show the effectiveness of the model and showed

a correlated track. Subsequent plots in Figure 4.26 also highlight where the model overestimates and underestimates values. It should be noted that some prediction errors can be explained by a few reasons such as the accuracy of the *in-situ* measuring devices, the efficiency of frequency weightings and Composite Weighted Acceleration estimations.

5.3.2 Discussion of Objective One

As a decision-support tool, the comfort-based model in section 5.3.1 provides predictions on Composite Weighted Acceleration in m/s^2 rather than a prediction for vessel acceleration magnitudes, this provides an estimation of the daily dose accelerations felt by technicians during transits. The model does not, however, predict human comfort but uses the magnitude of modelled Composite Weighted Acceleration as an indicator for discomfort based on studies that show significant correlations between discomfort and acceleration magnitudes (Mansfield et al., 2000). As such, Composite Weighted Acceleration is used as a proxy indicator for comfort when ISO 2631-1 levels of likely reactions to magnitudes of accelerations are applied. This presents a measurable short-term indicator for comfort, however, it should be noted that this indicator is not tested against real-life measured levels of discomfort in technicians during transits. As such the model's results are not validated. Additionally, while the relationship between weighted acceleration and the discomfort of passengers has been explored in literature, consideration has to be made for the way discomfort is assessed, the nature of questionnaires used to assess discomfort, and the type of vessels or simulations used and the impact of this on the ranges of discomfort experienced.

This research has also contributed to knowledge in previous literature by exploring a framework for using experimental measurements in the prediction of motion exposure. The literature explored in section 2.6.1 of this thesis showed that studies on predicting acceleration exposure typically calculate the RMS of vessel acceleration using a response amplitude operator (RAO) along with wave energy spectra to produce response spectra (Jenkins et al., 2021)(Jenkins et al., 2021)(Jenkins et al., 2021), or numerical models combined with seat models to describe sea-state (Griffin, 1990; Olausson & Garme, 2013). This research adds to this by using available experimental vessel motion measurements from participating vessels in this research, synchronised with oceanographic data to describe the sea state in predicting acceleration exposure. In addition to this, studies into predicting acceleration

exposure do not usually use the non-homogeneous random variables of sea-state and vessel parameters such as different speeds and heading but define operational conditions for a set of sea-states, and vessel parameters. As such the merging of sea-state data and measured acceleration data and applying machine learning processes in assessing human reactions allows for a more variable comparison not typically seen in available literature such as the comparisons between Composite Weighted Acceleration and vessel speed, vessel heading, significant wave height, current speed, current direction, and tidal height.

In practical application, the model will potentially be used for pending maintenance activities on Crew Transfer Vessels where a *sail or not sail* decision needs to be made for a transfer plan. The potential phases for this decision-making include:

1. Comfort level assessment is required for pending maintenance activities before a transfer plan is created or as part of the transfer plan.
2. Input operational values including duration to a turbine, average speed, vessel heading, significant wave height, current speed, current direction, and tidal height, into the model as input variables.
3. The model predicts values for Composite Weighted Acceleration.
4. The assessment is reviewed.

The next section explores relevant relationships in predicting Motion Sickness Incidence.

5.4 Exploring relationships in assessing the health of technicians using Motion Sickness Incidence.

Literature on the operation and maintenance of offshore wind farms show that for the technicians' onboard crew transfer vessels (CTVs), the main concern is their comfort, safety, and their ability to do work (Phillips et al., 2015). Literature in section 2.6.2 of this thesis identifies motion sickness as a major limiting factor when considering the short-term impacts of accelerations on human health maintenance (Coyte et al., 2016; Mette et al., 2018; Scheu et al., 2018), stating that motion sickness can cause vomiting, hyper-salivation, fatigue, lethargy sweating, pallor, and human performance (Dobie, 2019; Lackner, 2014; Smyth et al., 2019; Zhang et al., 2016). Therefore, predicting exposure to motion sickness is fundamental

to both ensuring the comfort and safety of passengers, and fundamental to ensuring the efficient completion of tasks. This research assesses motion sickness in technicians using Motion Sickness Incidence (MSI) which is a well-known method for assessing motion sickness and is also presented in ISO 2631-1 seen in equation 2.18. This measure estimates the probability of accelerations inducing vomiting as a percentage value.

This section discusses the relevant relationships explored in the exploratory analysis phase of this research to predict motion sickness in technicians during transit to offshore wind farms using Motion Sickness Incidence as a measuring metric.

5.4.1 Exploring relationships in assessing the health of technicians using Motion Sickness Incidence

Similar to the exploratory analysis in section 5.3.1, multiple variables to assess the health of technicians were explored using their relationship to Motion Sickness Incidence. The analysis was performed on a synchronised dataset that vessel transit duration, averaged vessel speed, averaged vessel heading, significant wave height, wave direction, wave period, current speed, current direction, tidal height, sea surface height, wind speed, and wind direction. Following dimension reduction processes using pairwise correlations and principal component analysis, a dataset of variables was identified to be of most significance in predicting Motion Sickness Incidence. Figure 4.23 presents the results of exploring major relationships and Figure 4.25 shows the result of the principal component analysis where the variables identified included vessel transit duration, averaged vessel speed, averaged vessel heading, significant wave height, current speed, current direction, and tidal height.

The most correlated relationship with estimated Motion Sickness Incidence was the relationship with significant wave height where a moderate linear correlation between Motion Sickness Incidence and significant wave height between 0 m and 2.0 m is shown in Figure 5.6. Expressions for this relationship are rare but section 2.6.2 explores literature where sea-state is used in predicting Motion Sickness Incidence such as Piscopo & Scamardella, (2015) where there was an increase in Motion Sickness Incidence with increases in significant wave height which correlates with the findings from this study. It should be noted that these studies usually predict MSI concerning the design phase of ships, thereby testing MSI for different operating criteria and design characteristics (Cepowski, 2009, 2012;

Piscopo & Scamardella, 2015; Rumawas et al., 2018). The lack of a high R^2 value and clear spread of results also meant that other variables could exist for more accurately predicting Motion Sickness Incidence.

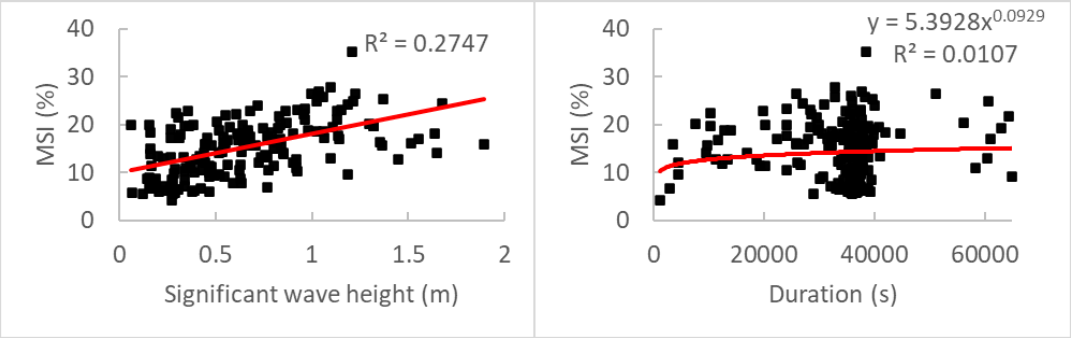

Figure 5. 5 Left to right: i. Comparison between daily estimated Motion Sickness Incidence and significant wave height; ii. Comparison between daily estimated Motion Sickness Incidence and vessel transit duration

Figure 5.5 also presents the plot of comparison between daily estimated Motion Sickness Incidence and duration (right plot). The plot shows a square root relationship between Motion Sickness Incidence and duration where MSI increases with duration and seems to plateau at about two hours with increasing duration. A correlated expression can be found with Stevens & Parsons, (2002), however, their review covers a duration of up to three days and there seems to be a decline in Motion Sickness Incidence after ten hours in this review. It is also important to note that the review by Stevens & Parsons, (2002), was performed on naval vessels and not high-speed crew transfer vessels.

Figure 5.6 shows the comparisons between Motion Sickness Incidence and vessel speed, vessel heading, current speed, current direction, and tidal range. The regression analysis between variables did not reveal any observable trends or correlation between Motion Sickness Incidence and these variables, however, the principal component analysis in Figure 4.25 shows that these variables along with the significant wave height and vessel transit duration make up 70% of the variation in predicting Motion Sickness Incidence.

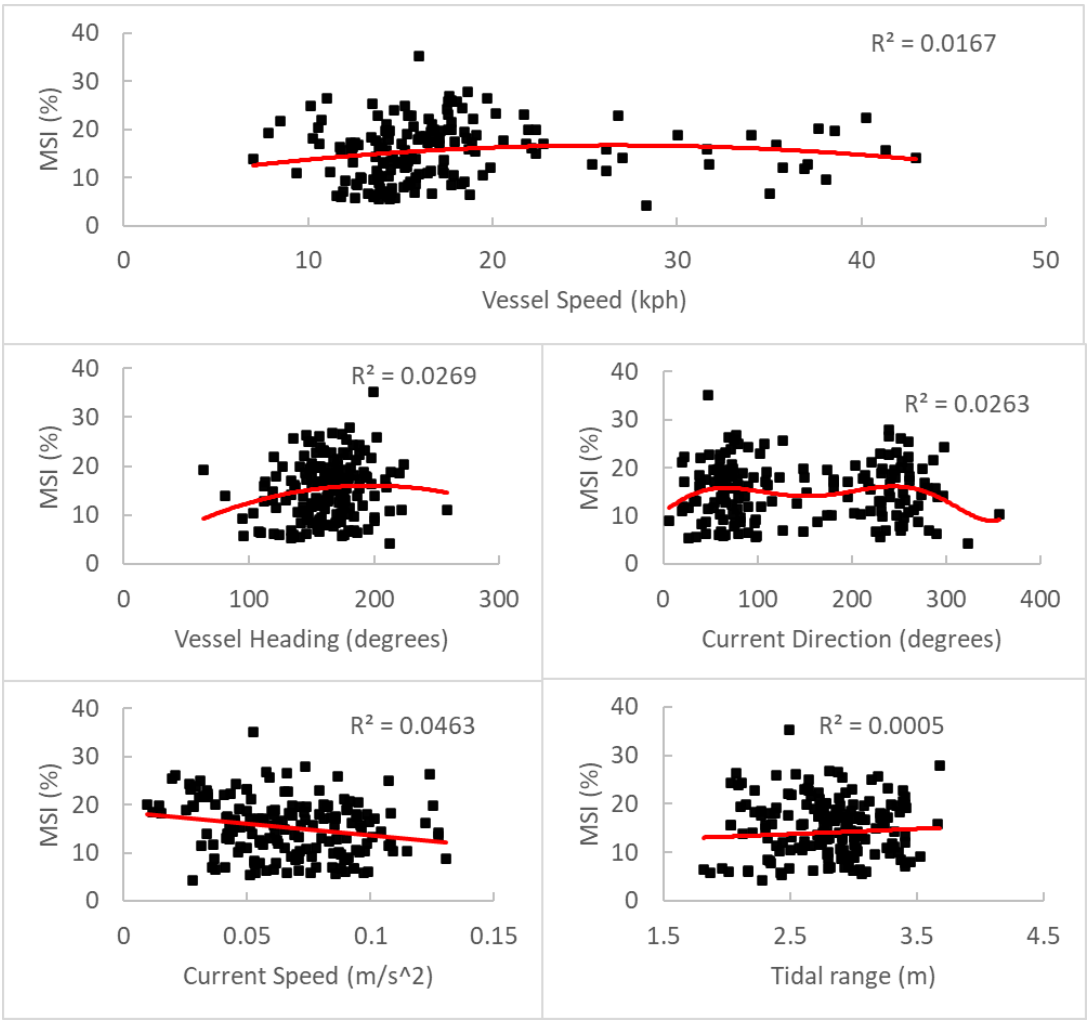

Figure 5. 6 Pairwise correlation showing the relationship between input variables and daily estimated Motion Sickness Incidence MSI. Top plot: i. Comparison between MSI and vessel speed; Second row from left to right: ii. Comparison between MSI and vessel heading; iii. Comparison between MSI and current direction; third row from left to right: iv. Comparison between MSI and current speed; v. Comparison between MSI and tidal range.

The comparison between daily estimated Motion Sickness Incidence and vessel heading appears to form a cluster that peaks between 150˚ and 180˚ which follows the same trajectory as Piscopo & Scamardella, (2015) explored in section 2.6.2 though rather than Motion Sickness Incidence, this study uses overall Motion Sickness Incidence – defined as the mean Motion Sickness Incidence over the main deck area of a vessel, for a specific angle, and a specific sea state. Similarly, the comparison with current direction appears to form clusters that peak between 50˚ and 90˚ and between 220˚ and 280˚, the comparison with tidal range forms a cluster between 2.5 m and 3.5 m, and the comparison with current speed showed no observable trends. In predicting motion sickness, numerical modelling has generally been used to describe sea-state parameters as such these comparisons are also rare in the available

literature. Where sea-state variables are included is usually in studies that set out operating limits for ships using the principal particulars of vessels such as the length of the hull, beam, and draft, vessel speed, and sea-state conditions such as wave height and wave period (Cepowski, 2009, 2012; Cheung & Nakashima, 2006; Piscopo & Scamardella, 2015; Polymeropoulos et al., 2020; Rumawas et al., 2018; Youn & Park, 2020). This research takes a different approach by applying experimental acceleration data collected on participating vessels merged with sea-state data and as such could explore the non-homogeneous random variables of sea-state and vessel parameters.

5.4.2 Summary

This section showed the relevant variables explored during the dimension reduction process to model Motion Sickness Incidence in technicians during transits to offshore wind farms. Principal component analysis processes were used to identify variables most relevant to the prediction of Motion Sickness Incidence including vessel transit duration, averaged vessel speed, averaged vessel heading, significant wave height, wave direction, wave period, current speed, current direction, and tidal height. A significant relationship was found between motion MSI and significant wave height, and the comparison with vessel transit duration was found to corroborate findings in the literature. The comparisons with vessel speed, vessel heading, current speed, current direction, and tidal range, however, did not reveal observable trends, though the principal component analysis revealed the variables to account for 70% of the variation for predicting Motion Sickness Incidence along with significant wave height and vessel transit duration. The following section discusses and analyses the modelling of the health of technicians from the incidence of motion sickness in technicians using the variables explored in this section.

5.5 Analysis and Discussion of Objective Two

5.5.1 Modelling the health of technicians during transits on crew transfer vessels using Motion Sickness Incidence.

This section analyses and discusses the health-based model created to estimate Motion Sickness Incidence (MSI) which can be used to describe the probability of seasickness in

technicians as a percentage value using the mathematical model developed by Reason & Brand, (1975). This presents a risk-based decision-making tool that provides *sail or not-sail* decisions based on predictions of Motion Sickness Incidence. Therefore, this research developed a health-based model (H) that estimates Motion Sickness Incidence (Y) based on explored input variables described in section 5.4:

$$Y = H(X_1, \dots, X_n, G_1, \dots, G_n) \qquad 5.3$$

Where: Y, is the estimated design variable for Motion Sickness Incidence (MSI); $X_1 \dots X_n$, are micro factor input design variables including transit duration, vessel speed, and vessel heading; $G_1 \dots G_n$, are macro factor input design variables including significant wave height, current speed, current direction, and tidal height.

The input variables explored in section 5.4.1 were used within MATLAB's machine learning processes described in chapter three of this thesis to identify the model of best fit. The resultant rational quadratic gaussian process regression model is presented in Figure 4.27 and shows the test for a relationship between the explored independent variables and estimated Motion Sickness Incidence. The performance of the model was shown in Table 4.4 of chapter four with a Mean Average Error (MAE) of about 1.8%, and a Root-Mean-Square Error (RMSE) of about 4%. The goodness of fit was tested using the R^2 coefficient of determination at 0.49, showing that 49% of the variation of estimated Motion Sickness Incidence, can be explained by the independent variables, and the statistical significance was tested using the p-value less than 0.01 which rejects the null hypothesis of there being no statistically significant relationship. The efficiency of the model was shown in Figure 4.27 where the predicted values of Motion Sickness Incidence follow a similar trajectory to the estimated values of Motion Sickness Incidence, however, there is a slight difference in prediction. The predicted against observed plots (the second row left and right plots) in Figure 4.27, confirms this observation showing data points that fall below the perfect prediction line between above 15%, and data points that fall above the perfect prediction line between 5% and 12%. This suggests that the model slightly overestimates values of estimated Motion Sickness Incidence between 5% and 12% and underestimates values of estimated Motion Sickness Incidence above 15%. As the plot on the right of the second row in Figure 4.27 also shows a higher frequency of data points below 12%, this suggests that the values overestimated are the most common predictions for

Motion Sickness Incidence while the values the model underestimated are the more common predictions of Motion Sickness Incidence.

The testing set of this model achieved an R^2 of 0.49, an RMSE of about 4%, and a p-value less than 0.01 which shows that the null hypothesis of there being no statistically significant relationship can be rejected. The model's performance expressed in terms of an R^2 value showed that more than half of the variance, up to 51% resided in the residual as such, the variables explored do not make up most of the variation in predicting MSI. This shows that a significant amount of work needs to be done to improve the models' prediction as such, the model does not present an acceptable level of performance.

5.5.2 Discussion of objective two

Motion Sickness Incidence was chosen as a measurable short-term indicator of the health of technicians. It should be noted that this model predicts Motion Sickness Incidence which by definition is the incidence of vomiting (a symptom of motion sickness) and does not account for other symptoms of motion sickness or other susceptibility factors associated with motion sickness including sweating, changes in temperature, and headaches (Earle et al., 2021). As such, Motion Sickness Incidence is not an indicator of motion sickness but an indicator of vomiting caused by motion sickness. This, therefore, means that technicians could be exposed to the many other explored symptoms of motion sickness which can affect their well-being and ability to work. Additionally, relevant motion sickness susceptibility factors are not included such as cabin temperature and a lack of visual reference, which could have a significant impact in inducing motion sickness (Kluijven, 2016). Bos et al., (2022) state that the effect of a lack of visual reference was not included in ISO 2631-1 because, at the time, observations from experimental participants without organs of balance appeared to be almost insensitive to motion sickness while blind participants suffer the effects of motions sickness. However, current studies identified the impact of vision on motion sickness, especially in relation to virtual and car sickness (Schmidt et al., 2020; Stanney et al., 2020). As such, MSI may not be a sufficient indicator of the welfare of technicians in transit. As such, it has become clear that relevant factors are missing from motion sickness estimations (Bos et al., 2022). Therefore, there is a need to expand the dimensions of ISO 2631-1 to include more ranges of symptoms and as such, expand the dimensions of this thesis though this inclusion

would require knowledge of vessel architecture in relation to seating to account for visual impacts, as well as other measured parameters not included such as temperature. Consideration also has to be made for the genetic component which contributes to motion sickness susceptibilities such as gender and age (Hromatka et al., 2015). As such, MSI in its current form, may not be a sufficient indicator of the welfare of technicians in transit. However, similar to the comfort-based model, this research contributes to existing knowledge in exploring relationships with variables not typically presented in research predicting the incidence of motion sickness including vessel speed, vessel heading, significant wave height, current speed, current direction, and tidal height. This is because generally, numerical models are used to describe sea-state and in predicting motion sickness, defined sea-state parameters and operational conditions are used. As such, this research presents a framework for using near-real-time metocean data to predict Motion Sickness Incidence in technicians during transit.

Like the comfort-based model, predicting Motion Sickness Incidence for practical application will potentially be used for pending maintenance activities where a *sail or not sail* decision needs to be made for a transfer plan. The potential phases for a health-based assessment include:

1. A sea-sickness assessment is required for pending maintenance activities before a transfer plan is created or as part of the transfer plan.
2. Input operational values including duration to a turbine, average speed, vessel heading, significant wave height, current speed, current direction, and tidal height, into the model as input variables.
3. The model predicts values for Motion Sickness Incidence.
4. The assessment is reviewed.

The next section analyses and discusses the welfare model used in predicting *sail and not sail* decisions to aid maintenance planning in offshore wind farms.

5.6 Analysis and Discussion of Objective Three

Section 5.3 and 5.5 discusses the comfort-based and health-based models developed to predict Composite Weighted Acceleration and Motion Sickness Incidence for technicians in transit to offshore wind farms during maintenance. Both models used variables in sections 5.2 and 5.4 as input variables relevant to the prediction of the comfort-based and health-based models respectively. Operational limits defined in sections 2.61 and 2.6.2 were applied to both model outputs in order to describe optimum operational conditions for technicians based on the daily dose discomfort level of the transit and the daily dose predicted Motion Sickness Incidence. Therefore, this section discusses a technician welfare model that accounts for the comfort of technicians, using predicted values of Composite Weighted Acceleration, and the health of technicians from motion sickness, using the predicted values of Motion Sickness Incidence, in creating *sail or not sail* decisions for maintenance scheduling.

5.6.1 Developing a criterion-based decision-making model for maintenance scheduling based on technician welfare.

In applying limiting criteria for the comfort-based model, this research uses the recommendation by ISO 2631-1 expressed in sections 2.6.1 and 2.6.2 of this thesis. The operating limits used to describe technician discomfort are based on the identified relationship between discomfort and the magnitude of acceleration where studies have shown that increases in the magnitude of acceleration result in increases in the degree of discomfort in passengers (Mansfield et al., 2000). This relationship has been made in various experimental studies where subjects were asked to rate stimuli based on vessel motions which led to the development of semantic rating scales based on the magnitude of acceleration (Huston et al., 2000; Nielsen, 1987; Shoenberger, 1982; Wikström et al., 1991). A similar rating scale is presented in the recommendations of the ISO 2361-1 used in this research and presented in Table 2.2 which shows estimations for human response to accelerations. Table 2.2 shows a range of magnitudes of acceleration between 0 ms^{-2} to 2 ms^{-2} which have defined human reactions ranging from not uncomfortable to extremely uncomfortable. It should, however, be noted that the limits presented, act as approximate indications of likely reactions to the stated levels of acceleration magnitudes during transits and further depend on other factors such as the activities performed or expected to be

performed by passengers as well as the duration of the transit. These scales are also specific to the environment used, for instance, concerning the discomfort of people in residential or industrial buildings, a different scale found in the ISO 2631-2 should be used (ISO 2631-1, 1997). In applying the scales described, this research defines *sail* decisions on values of predicted composited weighted accelerations less than 0.315 ms^{-1}, and *not sail* decisions on values greater than or equal to 0.315 ms^{-1} in a simple logic model for scales described as comfortable and uncomfortable respectively.

Similarly, the health-based model applies operational conditions based on limits of acceptable working conditions and the duration of exposure which suggests a threshold of 20% Motion Sickness Incidence (Stevens and Parsons, 2002; Phillips et al., 2015; Saha et al., 2020). As such, this research defines *sail* decisions on values of predicted Motion Sickness Incidence less than 20%, and *not sail* decisions on values greater than or equal to 20%in a simple logic model. Figure 5.6 below presents the results of the welfare model developed.

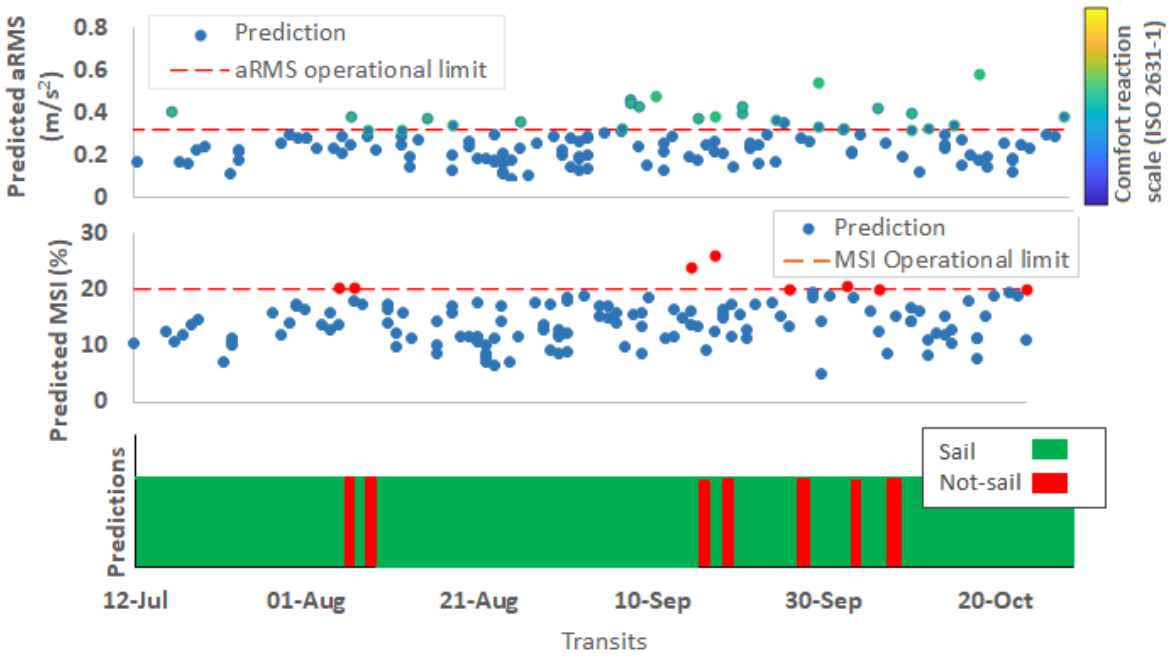

Figure 5. 7 Plot of the developed technician welfare model showing sail and not sail decisions for O&M transits over three months.

Figure 5.7 shows a plot of the predictions from the welfare model between the 9th of July and the 29th of October 2019. The plot shows *sail* and *not-sail* predictions (top plot) based on

model output prediction from the comfort-based model (second row), and the predictions from the health-based model (bottom row). In 163 predictions, the model shows 129 *sail* predictions (shown in green) and 34 *not-sail* predictions including 11 *not-sail* decisions where transits were predicted to be both uncomfortable and where the incidence of motion sickness was predicted to be above 20% of the population. Additionally, the model also shows 23 *not-sail* predictions where transits were predicted to be uncomfortable, but Motion Sickness Incidence was predicted to be below 20% (such as between 8/9/2019 and 26/9/2019) but none, where Motion Sickness Incidence was predicted above 20% and the transit, was predicted comfortable. This suggests that in some cases, transits could be predicted as uncomfortable but not able to cause seasickness to a large population of technicians during transits.

The model presented shows that the welfare of technicians can be modelled and accounted for in *sail or not sail* decision-making based on both the health and comfort of technicians. The potential application of this model can avoid potential waiting times in cases where access is possible but exposure to motion is unacceptable (Scheu et al., 2018). Additionally, this model can allow for the successful completion of a range of tasks that could be affected by whole-body accelerations ranging from less complex tasks such as reading, writing, and eating (Mansfield, 2005), to complex tasks including manual tasks and other task associated with handgrip, vertical-jump, and push. Furthermore, distractions, annoyance, elevated blood pressure and stress-related symptoms that are associated with whole-body accelerations (Marjanen & Mansfield, 2011) can be avoided.

5.6.1.1 Comparison between welfare model output and limits of operation.

To further analyse the model's performance, this research compared the estimated values of Composite Weighted Acceleration and Motion Sickness Incidence with predicted values in all the project sites to the standard sea-faring operational limits for Motion Sickness Incidence to determine how the model's predictions would compare to possible sailing decisions by wind farm operators.

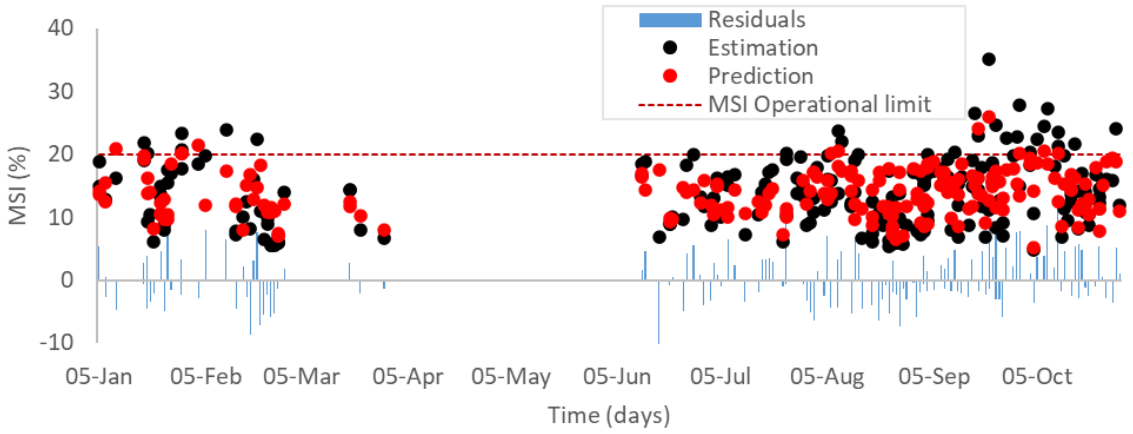

Figure 5. 8 A plot of predicted and estimated Motion Sickness Incidence for all sites, denoted by MSI, with the Motion Sickness Incidence operational limit.

Figure 5.8 shows the estimated and model-predicted Motion Sickness Incidence (MSI) with the standard motion sickness operational limit of 20% of Motion Sickness Incidence. The residual from the predicted and estimated values showed that of 212 predictions, 23 were false predictions, and of the 23 false predictions, there were 7 false *not sail* predictions and 16 false *sail* predictions. This means that in practice, there were 7 transits where the model predicted a not *sail* decision instead of a *sail* decision and 23 transits where the model predicted a *sail* decision for a *not sail* decision, based on Motion Sickness Incidence limits. Therefore, based on applied limits the model would have a 12.2% error rate in practical application.

The implementation of comfort assessments is rarely seen in the literature concerning the operations and maintenance of offshore wind farms, however, the Health and Safety Executive presents acceleration exposure limitations for the reduction of back pain in workers which can be used as a guide. The regulations found in the 'The Control of Vibration at Work Regulations, 2005,' suggests that employers introduce a technical and or organisational measure to decrease acceleration exposure for acceleration exposures up to 0.5 m/s^2 during a workday (usually estimated to be 8 hours). However, as suggested in section 5.1, lower back pain is a long-term effect of acceleration exposure, and this thesis provides a framework for short-term predictions and only considers the short-term effects of acceleration such as the effect on the comfort of technicians. Figure 5.8 shows predicted and estimated values of Composite Weighted Acceleration with exposure limits.

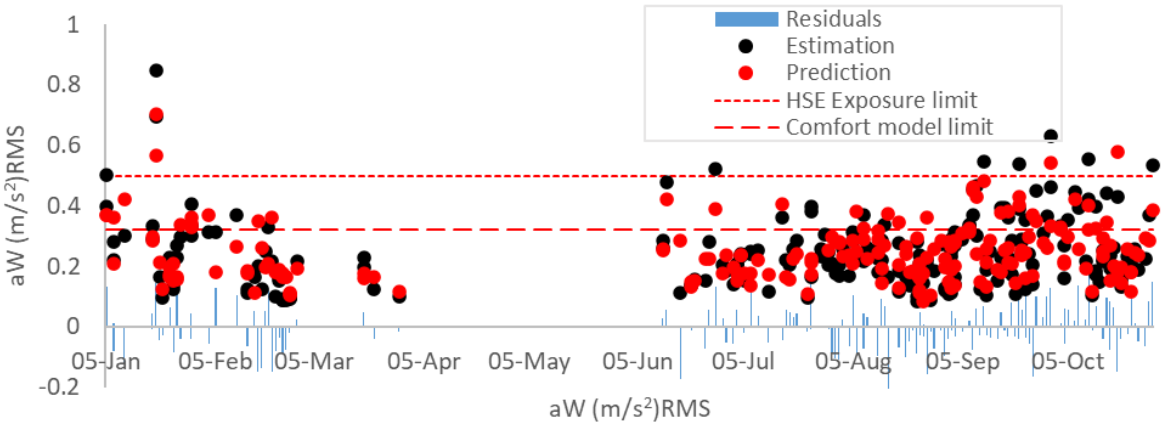

Figure 5. 9 A plot of predicted and estimated composited weighted RMS acceleration, denoted by aW (m/s2) RMS, with the Health and Safety Executive HSE defined exposure limit and the comfort model limit.

As current literature and information from industry experts suggest that comfort assessments are rarely used in operations and maintenance planning, it is difficult to determine sailing decisions that could be made by offshore wind farm operators. However, where the comfort model limit is applied at 0.315 m/s^2 for increasing levels of discomfort, the plot in Figure 5.9 shows that for 212 predictions, 19 were false predictions, and of the 19 false predictions, there were 9 false *not sail* predictions and 10 false *sail* predictions. This means that in practice, there were 7 transits where the model predicted a *not sail* decision instead of a *sail* decision and 23 transits where the model predicted a *sail* decision for a *not sail* decision, based on the set comfort-based limits. Therefore, based on applied limits the model would have a 9.8% error rate in practical application.

To further test the models against operations and maintenance strategies, the research compares the standard limit of operation for crew transfer vessels (1.5m of significant wave height), as outlined in section 2.6.2, with model predictions for Motion Sickness Incidence and Composite Weighted Acceleration to identify if established limits were sufficient in accounting for the welfare of technicians in transit. Figure 5.9 shows that when considering the likelihood of seasickness occurring in technicians, the welfare model predicted *not-sail* decisions for transits below 1.5m, and similarly, when considering the comfort of technicians, the welfare model predicted *not-sail* decisions for significant wave heights below 1.5m.

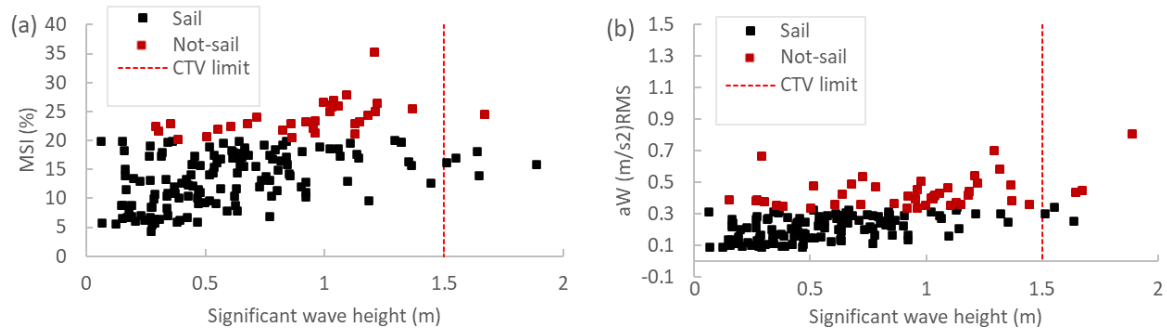

Figure 5. 9 (a) A plot of Motion Sickness Incidence (MSI) against significant wave height with crew transfer vessel operational limits denoted by CTV limit; (b) A plot of Composite Weighted Acceleration aW(m/s^2) RMS against significant wave height with crew transfer vessel operational limits denoted by CTV limit.

This suggests that the traditional crew transfer vessel limits of operation were insufficient in accounting for the welfare of technicians for the dataset explored and based upon estimations of Motion Sickness Incidence and Composite Weighted Acceleration. This corroborates suggestions made by Scheu et al., (2018) for the inclusion of human motion criteria in operation and maintenance planning when studying human exposure to acceleration during maintenance on floating offshore wind turbines. Scheu et al., (2018) further expressed the importance of the inconsistency between standard success criteria and human motion criteria stating that human motion criteria should be treated the same way as weather windows as there could be situations where a wind turbine could be accessible but exposure to motion is unacceptable. As such this research proposes the potential application of the welfare model in typical maintenance planning for decision-making. The image in Figure 5.10 outlines the potential process for obtaining a technician welfare assessment using the welfare model.

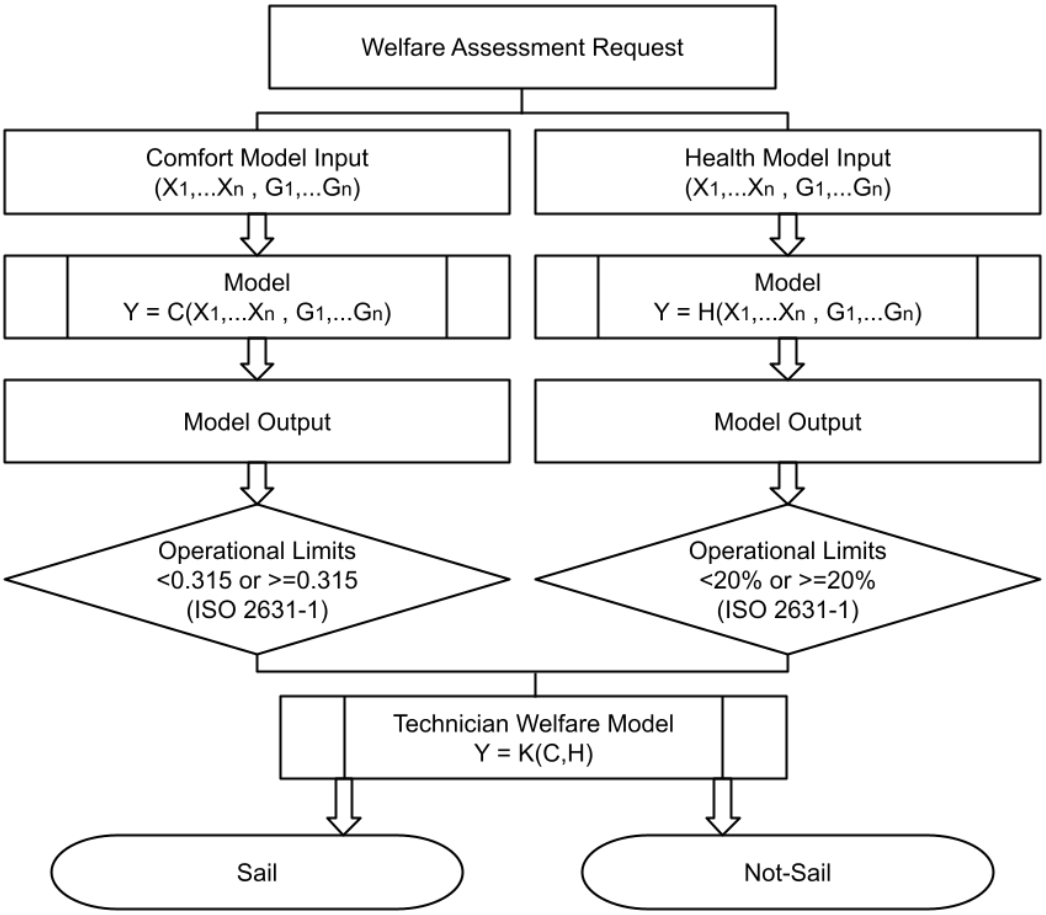

Figure 5. 10 Process for obtaining a welfare assessment

The phases described in Figure 5.7 above include a request for a welfare assessment for a pending maintenance activity before a transfer plan is created or as part of the transfer plan; Input variables are applied to the comfort and health-based models which provide outputs for Composite Weighted Acceleration and Motion Sickness Incidence respectively. Operational limits are applied following ISO 2631-1 guideline; Model outputs are used in the welfare model to determine *sail or not-sail* decisions and the welfare model output is reviewed.

5.6.2 Limitations and Recommendations

This section discusses the limitations encountered during this research and provides areas where improvements can be made.

The results of both the comfort-based model and health-based model show the lack of a high R^2 value which suggests other variables or factors could exist for more accurately predicting Composite Weighted Acceleration and Motion Sickness Incidence in technicians. This could

be related to vessel parameters not included in the dataset used for the thesis analysis. As such, more iterations are needed that include a bigger dataset, as well as more variables to improve model predictions but at the same time avoid overfitting.

While sufficient in meeting the thesis objectives the predictions of Motion Sickness Incidence for describing seasickness in technicians, and Composite Weighted Acceleration for describing discomfort, are estimations of likely response to whole-body accelerations. The results of this thesis could benefit from validations with real-life measurements of seasickness and discomfort in technicians during transits. There have been efforts to apply physiological correlates which can be considered, especially for motion sickness, such as changes in heart rate, temperature, respiration rate, the occurrence of yawning, and gastrointestinal activity (Bos et al., 2022). A measure of both physiological changes and questionnaire-based symptomatic ratings would measure the relationship between the proxy variables against actual measurements and expressions of discomfort and seasickness made by technicians. This process would inform future exploration of input parameters and greatly improve the thesis model as it eliminates the subjective nature of the operational limits used to define safe operations for technicians. In addition to this, the operational limits suggested by guidelines can also be tested against the welfare of technicians and their ability to do work. However, it should be stated that the operational limits used have been tested in various experimental studies though most of these studies explored these limits for vessels of varying sizes, some of which are different from the crew transfer vessels used in operation and maintenance activities.

The welfare model also functions as a generalised representation of the well-being of technicians in transits and while accounting for the likelihood of seasickness and discomfort, the model does not present weighted RMS of acceleration limits to the type of work being performed such as the limits introduced by Nielsen, (1987) which applies limits to the type of work performed ranging from light manual work to intellectual work for vertical and lateral root-mean-square accelerations. While the limits can be applied to the comfort model which predicts weighted RMS of acceleration, it should be noted that the limits provided by Nielsen, (1987) were for naval vessels on naval missions and as such the limits may need to be re-evaluated when considering the motions of high-speed vessels at sea. Moreover, the highest prediction of RMS acceleration for the dataset explored in this research was below 0.9 ms^{-2},

a value less than the lowest limiting motion criteria for different kinds of work by Nielsen, (1987) and as such, the impact of this limiting criteria on this dataset was not explored. Additionally, the welfare model predicts *sail and not-sail* decisions for crew transfer vessels and as such cannot be used in predicting technician welfare in other vessels used in operation and maintenance activities such as service operating vessels (SOVs) which are much larger in comparison to crew transfer vessels, and helicopters which are not restricted by sea-state which along with vessel parameters, make up the model's input variables.

5.6.3 Summary

This section analysed and discussed the technician welfare model used in predicting *sail and not-sail* decisions for technicians during transits to offshore wind farms for maintenance operations. Operational limits described in sections 2.6.1 and 2.6.2 were applied to model outputs from the comfort-based model discussed in section 5.3, and the health-based model discussed in section 5.5. The operational limits described predictions for composited weighted accelerations less than 0.315 ms^{-1}, as comfortable for technicians during transit and predictions greater than or equal to 0.315 ms^{-1} as progressively uncomfortable. Similarly, predictions for Motion Sickness Incidence less than 20% are defined as safe for transit while predictions for Motion Sickness Incidence greater than or equal to 20% as unsafe for transit. The results of the technician welfare model show that the welfare of technicians can be modelled able to account for both the health and comfort of technicians using Composite Weighted Acceleration and Motion Sickness Incidence to make *sail or not sail* decisions. In predicting the welfare of technicians, the results of the model show that in some cases, transits could be predicted as uncomfortable but not able to cause seasickness to a large number of the population of technicians. In comparing model outputs for *sail and not-sail* decisions with standard crew transfer limits of operation, the results of the welfare model showed that standard crew transfer vessel limits of operation were insufficient in accounting for the welfare of technicians for the dataset explored and based upon estimations of Motion Sickness Incidence and Composite Weighted Acceleration.

5.7 Conclusion

This chapter analysed and discussed the results of the data from the vessel motion monitoring systems (VMMS) deployed on participating vessels and meteorological data to achieve the thesis aim of modelling the welfare of technicians on crew transfer vessels during transits to offshore wind farms. To model the welfare of technicians, this research defined the welfare of technicians as the comfort and health of technicians during transits and modelled the comfort and health of technicians using Composite Weighted Acceleration and Motion Sickness Incidence. This research employed a novel method for describing sea-state when predicting human exposure acceleration by using metocean data synchronised with vessel GPS locators to describe sea-state. To predict the comfort of technicians, an exploratory analysis process was used to identify the most relevant variables to predict Composite Weighted Acceleration including vessel transit duration, averaged vessel speed, averaged vessel heading, significant wave height, wave direction, wave period, current speed, current direction, and tidal height, which were relevant to 70% of the variation in predicting Composite Weighted Acceleration. This research adds to existing research by exploring the relationships between Composite Weighted Acceleration and the identified variables. Significant relationships were found between vessel transit duration, vessel speed, and significant wave height, however, there was no observable trend seen in the comparisons between Composite Weighted Acceleration and vessel heading, current speed, current direction, and tidal range. The identified variables were used as independent variables in the comfort-based model which predicted composited weighted acceleration in ms^{-1} with a coefficient of determination R^2 of 0.67. Similarly, to predict the health of technicians during transit, an exploratory analysis process was used to identify the most relevant variables to predict Motion Sickness Incidence including vessel transit duration, averaged vessel speed, averaged vessel heading, significant wave height, wave direction, wave period, current speed, current direction, and tidal height, which were relevant to 70% of the variation in predicting Composite Weighted Acceleration. This research added to existing research by exploring the relationships between Motion Sickness Incidence and explored variables. Significant relationships were found between Motion Sickness Incidence and significant wave height, and the comparison with vessel transit duration was found to corroborate findings in the literature. However, the comparisons with vessel speed, vessel heading, current speed,

current direction, and tidal range, did not reveal observable trends. The identified variables were used as independent variables in the health-based model which predicted Motion Sickness Incidence as a percentage with a coefficient of determination R^2 of 0.49. By applying relevant limits of operations to the outputs of the comfort-based model and the health-based model, a simple logic model was used to define *sail or not-sail* decisions for decision-making in offshore wind maintenance scheduling. The results of the model showed that in some cases, transits could be predicted as uncomfortable but not able to cause seasickness to a large number of the population of technicians. The results of the technician welfare model show that the welfare of technicians can be modelled able to account for both the health and comfort of technicians using Composite Weighted Acceleration and Motion Sickness Incidence to make *sail or not sail* decisions. In comparing model outputs for *sail and not-sail* decisions with standard crew transfer limits of operation, the results of the welfare model showed that standard crew transfer vessel limits of operation were insufficient in accounting for the welfare of technicians for the dataset explored and based upon estimations of Motion Sickness Incidence and Composite Weighted Acceleration.

6 Conclusion

This thesis has made significant contributions to the knowledge of maintenance planning in offshore wind farms. Generally, the planning of maintenance activities in offshore wind farms has involved accounting for weather and sea state, and the availability of maintenance resources to determine whether a wind turbine is accessible. More recently, decision-support tools have been developed to aid this decision-making process by modelling daily maintenance planning based on the key factors mentioned. However, the literature review showed that available models do not account for the welfare of technicians and their ability to do work after transits to offshore wind turbines for maintenance. Where technicians are accounted for in literature, this account is usually in relation to the number of technicians available, the length of shifts, the number of technicians per service order or the number of service orders per technician, the type of technician available, and the availability technician for work orders. This exposes some uncertainties in maintenance scheduling and a gap in the literature as research has shown that vibrations caused by vessels in transit to offshore wind farms affect the comfort and health of the technicians on board in a number of symptoms including discomfort, seasickness, and inability to do work. Additionally, the available guidance on the discomfort caused by vibrations in the offshore wind industry is limited, but there is some guidance (though also limited) on the occurrence of seasickness-related issues which states that individuals feeling the effects of seasickness are to stay onboard the vessel until the effects subside. This exposed further uncertainties such as increased waiting times, especially in cases where wind turbines are assessable but exposure to vibrations is unacceptable. Therefore, there was a need to account for the comfort and health of technicians during transits in maintenance scheduling. The aim of this research was to apply technician welfare criteria in the same way operational limits are applied in *sail or no sail* decisions to ensure the comfort, health and safety of technicians and ensure their ability to do work on arrival at offshore wind turbines.

To explore human exposure to vibration, this research used data from vessel motion monitoring systems (VMMS) deployed on twelve (12) crew transfer vessels operating across four wind farms (4) by four wind farm operators in the North Sea to measure acceleration data. The dataset was synchronised with sea-state data including significant wave height,

wave period, wave direction, current direction, current speed, sea surface height, wind speed, and wind direction.

To model the welfare of technicians, this research defined the welfare of technicians as the comfort and health of technicians during transits to offshore wind farms. Therefore, for objectives one and two, this study modelled the comfort of technicians using Composite Weighted Acceleration as a proxy indicator and modelled Motion Sickness Incidence as a proxy indicator for the health of technicians describing the likelihood of vomiting due to motions experienced on Crew Transfer Vessels. These indicator variables were chosen as measurable short-term indicators of the comfort and health of technicians. However, the models created did predict human comfort or health but used the magnitude of modelled Composite Weighted Acceleration and percentage values of Motion Sickness Incidence to describe levels of discomfort and the likelihood of vomiting from vessel motions based on the guidance of international standards and previous studies.

The Composite Weighted Acceleration and Motion Sickness Incidence variables were feature engineered and added to the thesis dataset using the expressions described in ISO 2631-1 and an exploratory analysis process was used to identify the most relevant variables to predict both indicator variables. The identified variables included vessel transit duration, averaged vessel speed, averaged vessel heading, significant wave height, wave direction, wave period, current speed, current direction, and tidal height, which were relevant to 70% of the variation in predicting proxy variables. The use of a merged sea-state and measured vessel motion data allowed relationships to be explored that are not usually explored in research which added to existing literature. The comparison between vessel transit duration and Composite Weighted Acceleration confirmed that there is a decrease in daily weighted acceleration with increased duration, the comparison between the vessel speed and Composite Weighted Acceleration suggested that an increase in vessel speed resulted in an increase in daily weighted acceleration, and the comparison between significant wave height and Composite Weighted Acceleration showed that there was an increase in daily weighted acceleration with increases in significant wave height. The comparison between vessel transit duration and Motion Sickness Incidence confirmed relationships found in available literature where there was an increase in Motion Sickness Incidence with vessel transit duration which plateaued. The relationship between Motion Sickness Incidence and significant wave height suggested that

there was an increase in Motion Sickness Incidence with increases in significant wave height. The identified variables were used as independent variables

in a machine learning process that trained a training dataset against multiple models, identifying a Gaussian Process Regression (GPR) model as the model of best fit for both variables. The goodness of fit was tested for both models using the R^2 coefficient of determination which had results of 0.67 for the model predicting weighted acceleration and 0.49 for the model predicting MSI. This showed that for objective one, 67% of the variation of estimated Composite Weighted Acceleration, can be explained by the explored independent variables, and as such, only 33% reside in the residual. This gives a measure of improvements that need to be done in improving the model which is relevant since there could be some unexplored, uncontrollable, and undeterminable or unknown factors that could influence the measured acceleration on the participating CTVs. For objective two, The model created revealed that more than half of the variation (51%) in predicting Motion sickness Incidence could not be explained by the variables explored in the research. Therefore, this thesis showed that significant work is needed to improve the model's performance. Additionally, the mean average error (MAE) and Root-Mean-Square error (RMSE) were used to explore the errors present in the models as well as provide measures to compare future models against. Typically, R^2 values higher than 0.5 are seen as acceptable goodness of fit, depending on the data and field, however, this thesis uses this measure to evaluate the effectiveness of the explored input variables in predicting the proxy variables, as such, where the residual variance is greater than the variance of the data, as with the model predicting MSI, more work is needed to explore variables more relevant to predicting the proxy variable. Therefore, for the intended purpose of this thesis, the model predicting weighted acceleration showed satisfactory performance while the model predicting MSI showed that more work was needed to improve performance.

For the third objective, the welfare model was developed by applying relevant limits of operations to the outputs of the comfort-based model and the health-based model, as defined by ISO 2631-1 for limits of human operation. For the output of the comfort-based model, predictions of Composite Weighted Acceleration above 0.315 ms^{-1} were categorised as uncomfortable based on the ISO 2631-1 estimation for human comfort response to vibrations. For the output of the health-based model, a threshold equal to or above 20% for

the predictions of motion sickness was applied to show unfavourable sailing conditions where there was a probability to induce seasickness in 20% of technicians on crew transfer vessels. Using the limits of operation applied to the outputs of the comfort and health-based model, a simple logic model was used to define *sail or not-sail* decisions for decision-making in offshore wind maintenance scheduling. The results of the model showed that in some cases, transits could be predicted as uncomfortable but not able to cause seasickness to a large number of the population of technicians (Motion Sickness Incidence below 20%). The results of the technician welfare model showed that the welfare of technicians can be modelled able to account for both the health and comfort of technicians using Composite Weighted Acceleration and Motion Sickness Incidence to make *sail or not sail* decisions.

Major contributions from this project were achieved by merging measured vessel motion data with ocean model data. This is because research into the human response to vessel motion is expensive and time-consuming, as such, numerical models are usually used to define vessel parameters in the available literature (Olausson, 2015). Through these models, operational conditions have usually been defined for specific sea states and vessel parameters which has not allowed significant relationships to be explored fully in literature. This research on the other hand benefited from the wide spatial and temporal variations made available by metocean products (acquired from Copernicus Marine Service CMEMS) which when synchronised with data from the vessel motion monitoring system, using GPS coordinates and timestamps to describe crew transfer vessel's transit routes between port and wind farms, allowed for statistical analysis to be made that identified significant relationships with weighted acceleration and Motion Sickness Incidence that is rarely explored in literature. Major relationships were found with vessel parameters such as vessel duration and vessel speed, and sea-state parameters like significant wave height. While some of the relevant variables explored have been used either as vessel parameters and/or sea-state parameters for models exploring human response to vibrations at sea, analysis showing the relevance of these variables in predicting weighted acceleration and Motion Sickness Incidence is not typically seen in literature. Additionally, relationships with variables such as tidal height, current speed, and current direction which were found to have some importance to the variation when predicting weighted acceleration and Motion Sickness Incidence, but not enough observable significance when comparisons were made, has not been explored in

literature. The major contributions to operation and maintenance practice by this research were expressed in accounting for the overall well-being of technicians in maintenance planning by accounting for the likelihood of seasickness and the comfort of technicians which has not previously been explored. This is particularly important as available literature shows that vibrations caused by sea-state cannot only cause discomfort and seasickness but can also affect the ability to perform functions in technicians ranging from less complex functions such as writing and eating to complex tasks involving manual handling, cognitive tasks, and physical capacities such as handgrip, and vertical-jump and push. Additionally, other vibration-caused impairments can be avoided including a reduction of human reaction time, impairment of balance, and mental and physical fatigue. In addition to the effects of vibration on technicians, when modelling *sail or not sail* decisions, major findings from the welfare model showed that typical crew transfer vessel operational limits of 1.5m of significant wave height are not enough to account for the well-being of technicians during transits. This is because the welfare model showed that some transits below 1.5m of significant wave height can still be uncomfortable for technicians and may likely cause seasickness in 20% or above of the population of technicians in transit. These findings are also applicable in lighter vessels like daughter crafts which while not used in model predictions are also limited by significant wave height operational limits and are typically about 12m in length which can expose passengers to significant vessel motions (Snyder, 2020; Reid, 2021). Therefore, the findings from this research further inform maintenance planning, especially when applied before or when a maintenance work order has been issued as proposed in this thesis. The findings from this thesis also highlight the relevance of near-real-time and forecast data as a helpful and less expensive tool for maintenance planning which can fill gaps in the temporal and spatial variations of the marine environment. This was further expressed in this thesis where validations were made against *in-situ* measurements.

This research can also provide a framework for regulatory compliance as the model limits fall below the limits provided in the code of practice for reducing the risks from whole-body vibration on ships by the Maritime and Coastguard Agency (Maritime and Coastguard Agency - Great Britain, 2009), and The Control of Vibration at Work Regulations 2005 (The Control of Vibration at Work Regulations, 2005). Additionally, wind farm operators are able to apply a well-being criterion in decision-making in order to mitigate risks following the guidelines

under the Health and Safety at Work etc Act 1974 (Health and Safety at Work Etc Act, 1974). As such, this thesis does not affect established regulations but presents a method for compliance by making sailing decisions that eliminate the risk of not meeting regulatory compliance.

6.1 Limitations and future work

Despite meeting the thesis aims and objectives, there were key limitations that need to be highlighted, some of which can be addressed in future work. The vessel motion monitoring system (VMMS) data used in this thesis was secondary data which amongst other measurements, measured acceleration data from participating crew transfer vessels. The VMMS data were made available to this research from the SPOWTT project which was aimed at improving the safety and productivity of offshore turbine technicians, and as such was acquired for a different purpose than the thesis aims and objectives. For this reason, some assumptions had to be made within the course of this research regarding the calibration of the accelerometers on the Vessel Motion Monitoring System (VMMS), and the placement of the VMMS on the participating vessels which can create errors in validation due to the physical constraints of the device, and the location of the device in relation to the personnel on board.

A drawback of this study is that it does not include a model validation against measured discomfort and seasickness, which can be acquired from subjective questionnaires (Golding, 1998). This would measure the relationship between the proxy variables against expressions of discomfort and seasickness made by technicians through designed surveys. This process would inform future exploration of input parameters and greatly improve the thesis model as it eliminates the subjective nature of the operational limits used to define safe operations for technicians. In addition to this, the operational limits suggested by guidelines can also be tested against the welfare of technicians and their ability to do work in relation to Vessels specific to the maintenance of offshore wind farms. However, it should be stated that the operational limits used have been tested in various experimental studies though most of

these studies explored these limits for vessels of varying sizes, some of which are different from the crew transfer vessels used in operation and maintenance activities. Future work will need to be undertaken to test the created models against technician data to explore model accuracy and variations. In addition to this, the scope of this research can also be further expanded using data collected specifically for this research to include other ambient environmental aspects of vessel habitability including the effect of noise and temperature on technicians. This would involve the exploration of the effect of noise on cognitive performance (Jafari et al., 2019), and the effect of thermal comfort on technicians (Khan et al., 2021) to apply limits of operability for risk-based decision-making that can further inform the ability to do work in technicians.

Further improvements can be made to the comfort, health, and welfare models by the iterative addition of relevant variables that improve the model predictions, and the definition of the welfare variables used such as Motion Sickness Incidence (MSI). While MSI is a measurable metric for seasickness, the literature review showed that other symptoms of motion sickness including fatigue, cognitive symptoms, and temperature-based symptoms are not included in this metric. Additionally, MSI as developed by Reason and Brand, (1975), has typically been used for larger vessels such as naval vessels which have significantly different shapes, weights, and functions to CTVs. Therefore, a novel seasickness metric that includes more symptoms and developed from crew transfer vessel characteristics would be beneficial in maintenance planning. In addition to this, it should be noted that this model predicts the incidence of vomiting (a symptom of motion sickness) and does not account for other susceptibility factors that can induce motion sickness such as a lack of visual reference to the motion being experienced especially in ships and temperature in vessels (Bos et al., 2022). As such, Motion Sickness Incidence is not an indicator of motion sickness but an indicator of vomiting caused by motion sickness and may not be a sufficient indicator of the welfare of technicians in transit. This, therefore, means that technicians could be exposed to the many other explored symptoms of motion sickness which can affect their well-being and work.

It will also be beneficial to improve the modelling process for vessel sizes with more variability as the welfare model predicts *sail and not-sail* decisions for crew transfer vessels and as such cannot be used in predicting technician welfare in other vessels used in operation and

maintenance activities such as service operating vessels (SOVs) which are much larger in comparison to crew transfer vessels. The welfare model also functions as a generalised representation of the well-being of technicians in transits and while accounting for the likelihood of seasickness and discomfort, the model does not present limits to the type of work being performed light manual work, heavy manual work, and intellectual work. Existing literature shows that limiting exposure criteria for different kinds of work can be applied (Payne, 1976), however, further work needs to be done to relate this to specific vessels used in offshore wind maintenance activities.

To improve the machine learning process, improvements can be made by increasing the data used in making predictions. Though this research demonstrated promising results, the success of created models is largely due to the size of the dataset. While the dataset used in this project can be rare and complicated to generate, a system of cooperation between industry and academia can allow the collection of vessel information during transits to be acquired especially since the resulting research can be beneficial to industry partners. The comfort, health, and welfare models can further be improved by increasing spatial and temporal variability. The current model includes data from some sites including Southern site 2 and Western site 1 which contain data that only cover part of the year in autumn and winter. This shows that meteorological conditions for those sites do not cover the variability of conditions and as such can affect model predictions for predictions within the uncovered months. Future work would need to be done to improve spatial variability such as modelling the welfare of technicians in the Irish Sea for different seasons.

6.2 Researcher Development

This section presents a reflection, in the first person, on my personal experience and development as a researcher during this research project.

This research required an interdisciplinary understanding of human exposure to vibration and the operation and maintenance of offshore wind, and for this reason, in-depth research into relevant and related literature was carried out as well as interviews with industry

professionals on related topics. This improved my ability as a researcher to explore existing literature, conduct interviews with specialists, draw out conclusions, and identify relevant gaps in both research and within the industry that needed to be addressed. The exploration of literature and information allowed me to address initial biases I had concerning the relevance of technician welfare in the offshore wind industry at the start of this project which informed my analysis and writing process following. In addition to this, my views on how comfort and seasickness were addressed and assessed have also adapted to the current knowledge available and its applicability to health and safety standards. To achieve the set aims and objectives of this thesis, it was necessary to learn new skills and develop already learned skills including skills in data analysis and exploration, feature engineering, machine learning, teaching, and dissemination, as well as personal skills such as communication, presentation, and writing skills. In addition, I applied the use of software tools within the course of this research project including MATLAB for data exploration, analysis, data visualisations, and machine learning, BRAT for exploring satellite data, ArcGIS for exploring spatial data and data from the vessel motion monitoring system, and Microsoft Excel for small-scale data analysis and visualisations. I was able to explore and develop skills in using different methods of research in order to gain a thorough perspective of the subject area, especially for a research area relevant to the industry. This allowed me to gain useful domain knowledge in the field that was necessary when analysing data collected and when defining the scope of the research and analysis. The nature of this research project required continuous adaptation to achieve the thesis aims based on the type and availability of data and the relevance of results in practice. I learnt that while relationships within datasets could be discovered, their relevance to industry practice should be taken into account.

Overall, the research project allowed me to gain analytical skills, and research skills and enabled me to learn new and relevant software for research purposes. I was also able to develop interpersonal and transferable skills such as skills in communication, presenting, and writing.

References

Akers, R. 1999. Dynamic Analysis of Planning Hulls in the Vertical Plane *In*: *Meeting of the New England Section of The Society of Naval Architects and Marine Engineers* [Online]. The Society of Naval Architects and Marine Engineers, pp.2–19. [Accessed 6 July 2022]. Available from: https://www.academia.edu/4972207/Dynamic_Analysis_of_Planing_Hulls_in_the_Vertical_Plane?auto=download.

Alkan, A.D. 2011. Comfort on board evaluations for high speed vessels *In*: *9th High Speed Marine Vehicles*. Naples: HSMV, pp.1–4.

Andrews, J. and Jelley, N. 2007. *Energy Science: Principles, technologies, and impacts*. New York: Oxford University Press.

Arora, N.K. and Mishra, I. 2021. COP26: more challenges than achievements. *Environmental Sustainability 2021 4:4*. **4**(4), pp.585–588.

Asgarpour, M. and van de Pieterman, R. 2014. *O&M Cost Reduction of Offshore Wind Farms - A Novel Case Study* [Online]. Available from: https://www.ecn.nl/publications/PdfFetch.aspx?nr=ECN-E--14-028.

Baiz, A.A., Ahmadi, H., Shariatmadari, F. and Karimi Torshizi, M.A. 2020. A Gaussian process regression model to predict energy contents of corn for poultry. *Poultry Science*. **99**(11), pp.5838–5843.

Bao-Ji, Z. and Song-Nan, M. 2019. Research on Motion Response and Sickness Incidence of the Fishing Boat in Heading and Quartering Seas. *Journal of Fisheries Sciences*. **13**(2), pp.26–33.

Besnard, F., Fischer, K. and Tjernberg, L.B. 2013. A model for the optimization of the maintenance support organization for offshore wind farms. *IEEE Transactions on Sustainable Energy*. **4**(2), pp.443–450.

Bos, J.E., Diels, C., Souman, J.L., Rahmatalla, S. and Boileau, P.-É. 2022. Beyond Seasickness: A Motivated Call for a New Motion Sickness Standard across Motion Environments. *Vibration 2022, Vol. 5, Pages 755-769*. **5**(4), pp.755–769.

Bos, Jelte.E. 2004. How Motions Make People Sick Such That They Perform Less: A Model Based Approach *In*: *Symposium on Habitability of Compact and Transport Sehicles: Noise Vibration and Motion*. Prague, Czech Republic, pp.1–11.

Browell, J., Dinwoodie, I. and McMillan, D. 2017. Forecasting for day-ahead offshore maintenance scheduling under uncertainty *In*: *Risk, Reliability and Safety: Innovating Theory and Practice - Proceedings of the 26th European Safety and Reliability Conference, ESREL 2016*. CRC Press/Balkema, p.182.

BS EN 13306 2010. *Maintenance — Maintenance terminology*. BSI Standards Publication.

Buljan, A. 2021. North Star Renewables to Contract UK Shipyard for Hybrid Daughter Craft. *OffshoreWIND.biz*. [Online]. [Accessed 18 December 2022]. Available from: https://www.offshorewind.biz/2021/07/20/north-star-renewables-to-contract-uk-shipyard-for-hybrid-daughter-craft/.

Bussel Van, G.J.W. and Schöntag, C. 1997. *Operation and Maintenance Aspects of Large Offshore Windfarms* [Online]. Delft. Available from: http://www.ct.tudelft.nl/windenergy/ivwhome.htm.

BVG Associates 2019. *Guide to an offshore wind farm* [Online]. Swindon, UK. [Accessed 4 September 2020]. Available from: www.thecrownestate.co.uk.

Calvert, John.J. 2005. *Motion sickness, crew performance, and reduced manning in high-speed vessel operations*.

Cardinale, M. and Pope, M.H. 2003. The effects of whole body vibration on humans: dangerous or advantageous? *Acta physiologica Hungarica*. **90**(3), pp.195–206.

Carroll, J., McDonald, A., Dinwoodie, I., McMillan, D., Revie, M. and Lazakis, I. 2017. Availability, operation and maintenance costs of offshore wind turbines with different drive train configurations. *Wind Energy*. **20**, pp.361–378.

Cepowski, T. 2009. On the modeling of car passenger ferryship design parameters with respect to selected sea-keeping qualities and additional resistance in waves. *Polish Maritime Research*. **16**(3), pp.3–10.

Cepowski, T. 2012. The prediction of the Motion Sickness Incidence index at the initial design stage. *Zeszyty Naukowe Akademia Morska w Szczecinie*. **31**(103), pp.45–48.

Chandrashekar, G. and Sahin, F. 2014. A survey on feature selection methods. *Computers & Electrical Engineering*. **40**(1), pp.16–28.

Cheung, B. and Nakashima, A. 2006. *A review on the effects of frequency of oscillation on motion sickness* [Online]. Toronto, Canada. [Accessed 12 January 2022]. Available from: https://apps.dtic.mil/sti/pdfs/ADA472991.pdf.

Cho, K.-H., Wang, H. v, Shen, J., Valle-Levinson, A. and Teng, Y.-C. 2012. A modeling study on the response of Chesapeake Bay to hurricane events of Floyd and Isabel. *Ocean Modelling*. **49–50**, pp.22–46.

Clevenson, S., Dempsey, T. and Leatherwood, J. 1978. *Effect of vibration duration on human discomfort* [Online]. [Accessed 6 June 2022]. Available from: https://www.semanticscholar.org/paper/Effect-of-vibration-duration-on-human-discomfort-Clevenson-Dempsey/e1c95d59ed3434cfb124fe3046987d9f6dda2af5.

CMEMS 2020. E.U. Copernicus Marine Service Information. *https://resources.marine.copernicus.eu/?*.

Coyte, J.L., Stirling, D., Du, H. and Ros, M. 2016. Seated Whole-Body Vibration Analysis, Technologies, and Modeling: A Survey. *IEEE Transactions on Systems, Man, and Cybernetics: Systems*. **46**(6), pp.725–739.

Crown Estate, T. 2021. *The Crown Estate Offshore Wind Report 2021*. London.

Dalgic, Y., Lazakis, I., Dinwoodie, I., McMillan, D. and Revie, M. 2015. Advanced logistics planning for offshore wind farm operation and maintenance activities. *Ocean Engineering*. **101**, pp.211–226.

Dalgic, Y., Lazakis, I. and Turan, O. 2015. Investigation of Optimum Crew Transfer Vessel Fleet for Offshore Wind Farm Maintenance Operations. *Wind Engineering*. **39**(1), pp.31–52.

Dallinga, R.P., Pinkster, D.J. and Bos, J.E. 2002. Human factors in the operational performance of ferries *In*: *Proceedings RINRINA Symposium: Human Factors in ship design and operation II*. London: Royal institute of Naval architects (RINA), pp.89–97.

Davidson, M.A., O'hare, T.J. and George, K.J. 2008. Tidal modulation of incident wave heights: Fact or Fiction? *Journal of Coastal Research*. **24**(2B), pp.151–159.

Dawid, R., Mcmillan, D. and Revie, M. 2016. Development of an O&M tool for short term decision-making applied to offshore wind farms *In*: *Wind Europe Summit 2016* [Online]. Hamburg, Germany: Wind Europe, pp.1–5. [Accessed 24 December 2021]. Available from: https://strathprints.strath.ac.uk/58072/1/Dawid_etal_WES2016_Development_of_an_O_M_tool_for_short_term_decision_making.pdf.

Derakhshanjazari, M., Monazzam, M.R., Hosseini, S.M. and Poursoleiman, M.S. 2018. One-way ANOVA model to study whole-body vibration attributes among taxi drivers – An emphasis on the role of speed: *Journal of Low Frequency Noise, Vibration and Active Control*. **37**(1), pp.156–164.

Díaz, H. and Guedes Soares, C. 2020. Review of the current status, technology and future trends of offshore wind farms. *Ocean Engineering*. **209**, pp.107–381.

Ding, F. and Tian, Z. 2012. Opportunistic maintenance for wind farms considering multi-level imperfect maintenance thresholds. *Renewable Energy*. **45**, pp.175–182.

Dinwoodie, I., McMillan, D., Revie, M., Lazakis, I. and Dalgic, Y. 2013. Development of a combined operational and strategic decision support model for offshore wind *In*: *Energy Procedia*. Elsevier Ltd, pp.157–166.

Dobie, T.G. 2019. *Motion Sickness: A Motion Adaptation Syndrome* (N. I. Xiros, ed.). New Orleans: Springer.

Donohew, B.E. and Griffin, M.J. 2004. Motion sickness: Effect of the frequency of lateral oscillation. *Aviation Space and Environmental Medicine*. **75**(8), pp.649–656.

Douard, F., Domecq, C. and Lair, W. 2012. A probabilistic approach to introduce risk measurement indicators to an offshore wind project evaluation - Improvement to an existing tool ECUME. *Energy Procedia*. **24**, pp.255–262.

Dubovik, O., Schuster, G.L., Xu, F., Hu, Y., Bösch, H., Landgraf, J. and Li, Z. 2021. Grand Challenges in Satellite Remote Sensing. *Frontiers in Remote Sensing*. **2**, p.1.

Durakovic, A. 2020. HTM Helicopters Orders Airbus Choppers for Offshore Wind Operations. *Offshorewind.biz*. [Online], pp.1–1. [Accessed 19 November 2020]. Available from: https://www.offshorewind.biz/2020/09/21/htm-helicopters-orders-airbus-choppers-for-offshore-wind-operations/.

Earle, F., Huddlestone, J., Williams, T., Stock-Williams, C., van der Mijle-Meijer, H., de Vries, L., van Heemst, H., Hoogerwerf, E., Koomen, L., de Ridder, E.J., Serraris, J.J., Struijk, G., Stormonth-Darling, A., Cline, J., Jenkins, M., dos Santos, J.G., Coates, I., Corrie, A. and Moore, G. 2021. SPOWTT: Improving the safety and productivity of offshore wind technician transit. *Wind Energy*. **25**(1), pp.34–51.

Eger, T., Contratto, M. and Dickey, J. 2011. Influence of Driving Speed, Terrain, Seat Performance and Ride Control on Predicted Health Risk Based on ISO 263I-I and EU Directive 2002/44/EC: *Journal of Low Frequency Noise, Vibration and Active Control*. **30**(4), pp.291–312.

Ehrlich, R. 2013. *Renewable Energy: A First Course*. New York: CRC Press.

Endrerud, O.E. v., Liyanage, J.P. and Keseric, N. 2015. Marine logistics decision support for operation and maintenance of offshore wind parks with a multi method simulation model *In*: *Winter Simulation Conference*. Savannah, USA: IEEE, pp.1712–1722.

Endrerud, O.E.V. and Liyanage, J.P. 2015. Decision support for operations and maintenance of offshore wind parks. *Lecture Notes in Mechanical Engineering*. **19**, pp.1125–1139.

Ensign, W., Hodgdonl, J.A., Prusaczyk, W.. K., Ahlers, S. and Shapiro, D. 2000. *A Survey of Self-Reported Injuries Among Special Boat Operators* [Online]. San Diego, California,. [Accessed 28 July 2022]. Available from: http://www.dtic.mil/docs/citations/ADA421234.

Feng, Y., Tavner, P.J. and Long, H. 2010. Early experiences with UK round 1 offshore wind farms *In*: *Proceedings of the Institution of Civil Engineers - Energy*. ICE, pp.167–181.

Fu, L.-L., Lee, T., Liu, W.T. and Kwok, R. 2019. 50 Years of Satellite Remote Sensing of the Ocean. *Meteorological Monographs*. **59**(1), 5.1-5.46.

G+ 2020. *Good practice guidelines G+ Offshore wind farm transfer* [Online]. London. [Accessed 11 January 2022]. Available from: https://publishing.energyinst.org.

Garme, K., Rosén, A., Stenius, I. and Kuttenkeuler, J. 2014. Rough water performance of lightweight high-speed craft *In*: *Proceedings of the Institution of Mechanical Engineers Part M: Journal of Engineering for the Maritime Environment*. SAGE Publications Ltd, pp.293–301.

Gilbert, C., Browell, J. and McMillan, D. 2021. Probabilistic access forecasting for improved offshore operations. *International Journal of Forecasting*. **37**(1), pp.134–150.

Gintautas, T. and Sørensen, J. 2017. Improved Methodology of Weather Window Prediction for Offshore Operations Based on Probabilities of Operation Failure. *Journal of Marine Science and Engineering*. **5**(2), pp.1–20.

Griffin, M.J. 1990. *Handbook of Human Vibration* 1st ed. London: ACADEMIC PRESS LIMITED.

Griffin, M.J. and Whitham, E.M. 1980. Discomfort produced by impulsive whole-body vibration. *Journal of the Acoustical Society of America*. **68**(5), pp.1277–1284.

Griffin, M.J. and Whitham, E.M. 1998. Time dependency of whole-body vibration discomfort. *The Journal of the Acoustical Society of America*. **68**(5), p.1523.

Hagen, B., Simonsen, I., Hofmann, M. and Muskulus, M. 2013. A multivariate Markov Weather Model for O&M Simulation of Offshore Wind Parks. *Energy Procedia*. **35**, pp.137–147.

Halvorsen-Weare, E.E., Gundegjerde, C., Halvorsen, I.B., Hvattum, L.M. and Nonås, L.M. 2013. Vessel fleet analysis for maintenance operations at offshore wind farms *In*: J. O. G. Tande, T. Kvamsdal and M. Muskulus, eds. *DeepWind'2013 – Selected papers from 10th Deep Sea Offshore Wind R&D Conference*. Trondheim, Norway: Energy Procedia, pp.167–176.

Hardisty, J. 1990. *Beaches: Form and Process* 1st ed. London: Springer.

Hassan, G.G., Phillips, J., Fitch-Roy, O., Reynolds, P. and Gardner, P. 2013. *A guide to UK offshore wind operations and maintenance* [Online]. London. [Accessed 19 November 2020]. Available from: https://www.researchgate.net/publication/327721479_A_guide_to_UK_offshore_wind_operations_and_maintenance.

Hevia-Koch, P. and Klinge Jacobsen, H. 2019. Comparing offshore and onshore wind development considering acceptance costs. *Energy Policy*. **125**, pp.9–19.

Hofmann, M. and Sperstad, I.B. 2013. NOWIcob-A tool for reducing the maintenance costs of offshore wind farms *In*: J. O. G. Tande, T. Kvamsdal and M. Muskulus, eds. *DeepWind'2013 – Selected papers from 10th Deep Sea Offshore Wind R&D Conference*. Trondheim, Norway: Energy Procedia, pp.177–186.

Holthuijsen, L.H. 2007. *Waves in Oceanic and Coastal Waters*. New York: Cambridge University Press.

Hostens, I. and Ramon, H. 2003. Descriptive analysis of combine cabin vibrations and their effect on the human body. *Journal of Sound and Vibration*. **266**(3), pp.453–464.

Hromatka, B.S., Tung, J.Y., Kiefer, A.K., Do, C.B., Hinds, D.A. and Eriksson, N. 2015. Genetic variants associated with motion sickness point to roles for inner ear development, neurological processes and glucose homeostasis. *Human Molecular Genetics*. **24**(9), pp.2700–2708.

Huston, D.R., Zhao, X. and Johnson, C.C. 2000. Whole-body shock and vibration: frequency and amplitude dependence of comfort. *Journal of Sound and Vibration*. **230**(4), pp.964–970.

IEA 2020. Data & Statistics . *International Energy Agency*. [Online], pp.1–1. [Accessed 5 December 2021]. Available from: https://www.iea.org/data-and-statistics/data-browser?country=WORLD&fuel=Energy%20transition%20indicators&indicator=ETISharesInPowerGen.

IEA 2021. Renewable Energy Market Update: Outlook for 2021 and 2022. *International Energy Agency*. [Online], pp.1–29. [Accessed 16 December 2022]. Available from: https://www.iea.org/reports/renewable-energy-market-update-2021.

IEA and Bojek, P. 2022. Wind Electricity . *IEA*. [Online]. [Accessed 27 October 2022]. Available from: https://www.iea.org/reports/wind-electricity.

IPCC 2020. Global Warming of 1.5 °C. *Intergovernmental Panel on Climate Change*. [Online], pp.1–1. [Accessed 9 July 2020]. Available from: https://www.ipcc.ch/sr15/.

IPCC 2021. *Summary for Policymakers. In: Climate Change 2021: The Physical Science Basis. Contribution of Working Group I to the Sixth Assessment Report of the Intergovernmental Panel on Climate Change* [Online] (V. Masson-Delmotte, P. Zhai, Y. Chen, L. Goldfarb, M. I. Gomis, J. B. R. Matthews, S. Berger, M. Huang, O. Yelekçi, R. Yu, B. Zhou, E. Lonnoy, T. K. Maycock, T. Waterfield, K. Leitzell, & N. Caud, eds.). [Accessed 11 January 2022]. Available from: www.ipcc.ch.

Irawan, C.A., Ouelhadj, D., Jones, D., Stålhane, M. and Sperstad, I.B. 2017. Optimisation of maintenance routing and scheduling for offshore wind farms. *European Journal of Operational Research*. **256**(1), pp.76–89.

IRENA 2019. Wind energy. *IRENA*. [Online]. [Accessed 9 July 2020]. Available from: https://www.irena.org/wind.

IRENA 2021. Wind energy. *irena.org*. [Online]. [Accessed 5 December 2021]. Available from: https://www.irena.org/wind.

Irvine, T. 2006. Vibration Response Spectrum . *MATLAB Central File Exchange*.

ISO 2631-1 1997. *Mechanical vibration and shock -Evaluation of human exposure to whole-body vibration*.

Jafari, M.J., Khosrowabadi, R., Khodakarim, S. and Mohammadian, F. 2019. The Effect of Noise Exposure on Cognitive Performance and Brain Activity Patterns. *Open Access Macedonian Journal of Medical Sciences*. **7**(17), p.2931.

Jenkins, B., Prothero, A., Collu, M., Carroll, J., McMillan, D. and McDonald, A. 2021. Limiting Wave Conditions for the Safe Maintenance of Floating Wind Turbines *In*: *Journal of Physics: Conference Series* [Online]. IOP Publishing, p.012023. [Accessed 14 July 2022]. Available from: https://iopscience.iop.org/article/10.1088/1742-6596/2018/1/012023.

Joseph, J.A. and Griffin, M.J. 2008. Motion sickness: Effect of the magnitude of roll and pitch oscillation. *Aviation Space and Environmental Medicine*. **79**(4), pp.390–396.

Kaidis, C., Uzunoglu, B. and Amoiralis, F. 2015. Wind turbine reliability estimation for different assemblies and failure severity categories. *IET Renewable Power Generation*. **9**(8), pp.892–899.

Keuning, J.A. 1994. *Nonlinear Behaviour of Fast Monohulls in Head Waves (1994) | www.narcis.nl*.[Online] Delft: Delft University of Technology. [Accessed 6 July 2022]. Available from: https://www.narcis.nl/publication/RecordID/oai%3Atudelft.nl%3Auuid%3Aa2d52ad2-29b7-498e-b030-9306052ca1f5.

Khalid, H., Turan, O., Bos, J.E. and Incecik, A. 2011. Application of the subjective verticalhorizontal-conflict physiological motion sickness model to the field trials of contemporary vessels. *Ocean Engineering*. **38**(1), pp.22–33.

Khan, A.M., Finlay, J.M., Clarke, P., Sol, K., Melendez, R., Judd, S. and Gronlund, C.J. 2021. Association between temperature exposure and cognition: a cross-sectional analysis of 20,687 aging adults in the United States. *BMC Public Health*. **21**(1), pp.1–12.

Kjellberg, A. and Wikström, B.O. 1985. Subjective reactions to whole-body vibration of short duration. *Journal of Sound and Vibration*. **99**(3), pp.415–424.

Kjellberg, Anders and Wikström, B.O. 1985. Whole-body vibration: Exposure time and acute effects-a review. *Ergonomics*. **28**(3), pp.535–544.

Kluijven, V.P. 2016. *MOTION SICKNESS AT SEA*. Rotterdam.

Koohestani, A., Nahavandi, D., Asadi, H., Kebria, P.M., Khosravi, A., Alizadehsani, R. and Nahavandi, S. 2019. A Knowledge Discovery in Motion Sickness: A Comprehensive Literature Review. *IEEE Access*. **7**, pp.85755–85770.

Kumari, B. and Swarnkar, T. 2011. Filter versus Wrapper Feature Subset Selection in Large Dimensionality Micro array: A Review. *International Journal of Computer Science and Information Technologies*. **2**(3), pp.1048–1053.

Lackner, J.R. 2014. Motion sickness: More than nausea and vomiting. *Experimental Brain Research*. **232**(8), pp.2493–2510.

Lal, T.N., Chapelle, O., Western, J. and Elisseeff, A. 2006. Embedded methods *In*: *Feature Extraction. Studies in Fuzziness and Soft Computing* [Online]. Springer Verlag, pp.137–165. [Accessed 29 December 2022]. Available from: https://link.springer.com/chapter/10.1007/978-3-540-35488-8_6.

Lange, M. 2005. On the Uncertainty of Wind Power Predictions—Analysis of the Forecast Accuracy and Statistical Distribution of Errors. *Journal of Solar Energy Engineering*. **127**(2).

Laura, C.S. and Vicente, D.C. 2014. Life-cycle cost analysis of floating offshore wind farms. *Renewable Energy*. **66**, pp.41–48.

legislation.gov.uk 1974. *Health and Safety at Work etc Act*. London: UK Statutory Instruments.

legislation.gov.uk 1999. *Management of Health and Safety at Work Regulations*. London: UK Statutory Instruments.

legislation.gov.uk 2005. *The Control of Vibration at Work Regulations 2005*. London: UK Statutory Instruments.

Leung, A.W.S., Chan, C.C.H., Ng, J.J.M. and Wong, P.C.C. 2006. Factors contributing to officers' fatigue in high-speed maritime craft operations. *Applied ergonomics*. **37**(5), pp.565–576.

Lewis, H.W., Manuel Castillo Sanchez, J., Siddorn, J., King, R.R., Tonani, M., Saulter, A., Sykes, P., Pequignet, A.C., Weedon, G.P., Palmer, T., Staneva, J. and Bricheno, L. 2019. Can wave coupling improve operational regional ocean forecasts for the north-west European Shelf? *Ocean Science*. **15**(3), pp.669–690.

Lewis, M.J., Palmer, T., Hashemi, R., Robins, P., Saulter, A., Brown, J., Lewis, H. and Neill, S. 2019. Wave-tide interaction modulates nearshore wave height. *Ocean Dynamics*. **69**(3), pp.367–384.

Li, X., Ouelhadj, D., Song, X., Jones, D., Wall, G., Howell, K.E., Igwe, P., Martin, S., Song, D. and Pertin, E. 2016. A Decision Support System for Strategic Maintenance Planning in Offshore Wind Farms. *Renewable Energy*. **99**, pp.784–799.

Longuet-Higgins, M.S. and Stewart, R. w. 1964. Radiation stresses in water waves; a physical discussion, with applications. *Deep-Sea Research and Oceanographic Abstracts*. **11**(4), pp.529–562.

Maeda, S. and Morioka, M. 1998. MEASUREMENT OF WHOLE-BODY VIBRATION EXPOSURE FROM GARBAGE TRUCKS. *Journal of Sound and Vibration*. **215**(4), pp.959–964.

Malek, M.A., Maruf, A.A. and Hossain, M.M. 2009. Sea Sickness in Naval Personnel. *Pakistan Journal of Biological Sciences*. **12**(18), pp.1237–1245.

Malenovský, Z., Rott, H., Cihlar, J., Schaepman, M.E., García-Santos, G., Fernandes, R. and Berger, M. 2012. Sentinels for science: Potential of Sentinel-1, -2, and -3 missions for scientific observations of ocean, cryosphere, and land. *Remote Sensing of Environment*. **120**, pp.91–101.

Mansfield, N.J. 2005. *Human Response to Vibration*. New York: CRC Press.

Mansfield, N.J., Holmlund, P. and Lundström, R. 2000. COMPARISON OF SUBJECTIVE RESPONSES TO VIBRATION AND SHOCK WITH STANDARD ANALYSIS METHODS AND ABSORBED POWER. *Journal of Sound and Vibration*. **230**(3), pp.477–491.

Maritime and Coastguard Agency - Great Britain 2009. Code of practice for controlling risks due to whole-body vibration on ships. *TSO (The Stationery Office)*., p.73.

Marjanen, Y. and Mansfield, N.J. 2011. Application of ISO 2631-1 (1997) for evaluating discomfort from whole-body vibration: Verification using field and laboratory studies *In*: *40th International Congress and Exposition on Noise Control Engineering 2011, INTER-NOISE 2011*., pp.3475–3480.

Masood, E. and Tollefson, J. 2021. 'COP26 hasn't solved the problem': scientists react to UN climate deal. *Nature*. **599**(7885), pp.355–356.

Matsangas, P., McCauley, M.E. and Becker, W. 2014. The effect of mild motion sickness and sopite syndrome on multitasking cognitive performance. *Human Factors*. **56**(6), pp.1124–1135.

McPhee, B., Foster, G.D. and Long, A. 2009. *Bad Vibrations : A Handbook on Whole-Body Vibration Exposure in Mining* [Online] 2nd ed. Sydney: Coal Services Health & Safety Trust. [Accessed 10 July 2022]. Available from: https://www.bookdepository.com/Bad-Vibrations-Barbara-McPhee/9780957906228#.

McSweeney, Kevin.P., McCafferty, Denise.B. and Baker, Clifford.C. (American B. of S. 2008. Crew Habitability on Workboats: Comprehensive Guidance *In*: *Offshore Supply Journal Conference*. London, UK: American Bureau of Shipping, p.8.

Medina-Lopez, E., McMillan, D., Lazic, J., Hart, E., Zen, S., Angeloudis, A., Bannon, E., Browell, J., Dorling, S., Dorrell, R.M., Forster, R., Old, C., Payne, G.S., Porter, G., Rabaneda, A.S., Sellar, B., Tapoglou, E., Trifonova, N., Woodhouse, I.H. and Zampollo, A. 2021. Satellite data for the offshore renewable energy sector: Synergies and innovation opportunities. *Remote Sensing of Environment*. **264**, pp.112–588.

Met Office 2017. Beaufort wind force scale - Met Office. *metoffice.gov.uk*. [Online]. [Accessed 18 March 2022]. Available from: https://www.metoffice.gov.uk/weather/guides/coast-and-sea/beaufort-scale.

Mette, J., Velasco Garrido, M., Harth, V., Preisser, A.M. and Mache, S. 2018. Healthy offshore workforce? A qualitative study on offshore wind employees' occupational strain, health, and coping. *BMC Public Health*. **18**(1).

Michiel, A.J. uit het B., Veldman, J., Fazi, S. and Greijdanus, R. 2019. Evaluating resource sharing for offshore wind farm maintenance: The case of jack-up vessels. *Renewable and Sustainable Energy Reviews*. **109**, pp.619–632.

Miedema, R. 2012. *Offshore Wind Energy Operations and Maintenance Analysis*.[Online] Available from: http://sciencecentre.amccentre.nl/studies/Thesis_Robert_Miedema.pdf.

Miles, J.W. 1957. On the generation of surface waves by shear flows. *Journal of Fluid Mechanics*. **3**(2), pp.185–204.

Miwa, T., Yonekawa, Y. and Kojima-Sudo A. 1973. Measurement and evaluation of environmental vibrations. Part 3: Vibration exposure criterion. *Industrial Health*. **11**, pp.185–196.

Morton, G., Cipriani, A. and Mceachern, D. 1947. Mechanism of motion sickness. *Archives of Neurology And Psychiatry*. **57**(1), pp.58–70.

Musial, W. and Ram, B. 2010. *Large-Scale Offshore Wind Power in the United States: Assessment of Opportunities and Barriers* [Online]. Colorado, USA. [Accessed 4 September 2020]. Available from: https://www.nrel.gov/docs/fy10osti/40745.pdf.

Myers, S.D., Dobbins, T.D., King, S., Hall, B., Holmes, S.R., Gunston, T. and Dyson, R. 2012. Effectiveness of suspension seats in maintaining performance following military high-speed boat transits. *Human Factors*. **54**(2), pp.264–276.

Myhr, A., Bjerkseter, C., Ågotnes, A. and Nygaard, T.A. 2014. Levelised cost of energy for offshore floating wind turbines in a lifecycle perspective. *Renewable Energy*. **66**, pp.714–728.

Natasha Fogaça and Francisco Antônio Coelho Junior 2016. Is "Happy Worker" More Productive. *Management Studies*. **4**(4), pp.149–160.

Newell, G.S. and Mansfield, N.J. 2008. Evaluation of reaction time performance and subjective workload during whole-body vibration exposure while seated in upright and twisted postures with and without armrests. *International Journal of Industrial Ergonomics*. **38**(5–6), pp.499–508.

Newman, M. 2015. *Operations and maintenance in offshore wind: key issues for 2015/16* [Online]. Glosgow. [Accessed 4 September 2020]. Available from: https://pdfs.semanticscholar.org/93ac/c7c22b705811c153679ee49d8f256ae21f77.pdf.

NHS 2020. Antihistamines - NHS. *NHS*. [Online]. [Accessed 4 January 2022]. Available from: https://www.nhs.uk/conditions/antihistamines/.

Nielsen, I.R. 1987. *Assessment of ship performance in a seaway : the Nordic co-operative project: 'Seakeeping Performance of ships'* [Online]. Copenhage: Nordforsk. [Accessed 3 June 2022]. Available from: http://resolver.tudelft.nl/uuid:86b3ba36-3939-4ea7-8636-a8cea122055d.

Nielsen, J.J. and Sørensen, J.D. 2011. On risk-based operation and maintenance of offshore wind turbine components. *Reliability Engineering & System Safety*. **96**(1), pp.218–229.

Offshore Energy 2016. BMO Offshore Presents CTV Engine Monitoring - Offshore Energy. *Offshore-energy.biz*. [Online]. [Accessed 3 November 2022]. Available from: https://www.offshore-energy.biz/bmo-offshore-presents-ctv-engine-monitoring/.

O'Hanlon, J.F. and McCauley, M.E. 1974. Motion sickness incidence as a function of the frequency and acceleration of vertical sinusoidal motion. *Aerospace Med.* **45**(4), pp.366–369.

Olabarrieta, M., Warner, J.C. and Kumar, N. 2011. Wave-current interaction in Willapa Bay. *Journal of Geophysical Research: Oceans*. **166**(C12), pp.1–27.

Olausson, K. 2015. *On Evaluation and Modelling of Human Exposure to Vibration and Shock on Planing High-Speed Craft*. Thesis, Stockholm, Sweden: KTH Royal Institute of Technology.

Olausson, K. and Garme, K. 2013. Simulation-based assessment of HSC crew exposure to vibration and shock *In*: *12th International Conference on Fast Sea Transportation (FAST2013)* [Online]. Delft, The Netherlands: FAST Organizing Committee. [Accessed 27 July 2022]. Available from: https://www.researchgate.net/publication/289763938_Simulation-based_assessment_of_HSC_crew_exposure_to_vibration_and_shock.

ORE Catapult 2022. Wind farm costs – Guide to an offshore wind farm. *guidetoanoffshorewindfarm.com*. [Online]. [Accessed 27 October 2022]. Available from: https://guidetoanoffshorewindfarm.com/wind-farm-costs.

Orsted 2019. 7 top facts about the Service Operations Vessel Edda Mistral. *Orsted.co.uk*. [Online]. [Accessed 19 November 2020]. Available from: https://orsted.co.uk/media/newsroom/news/2019/06/7-top-facts-about-the-service-operations-vessel-edda-mistral.

Pahlke, T. 2007. *Software & Decision Support Systems for Offshore Wind Energy Exploitation in the North Sea Region* [Online]. Oldenburg,. [Accessed 24 December 2021]. Available from: http://pcoe.nl/@api/deki/files/1900/=12wp1_executivesummary_sdss-studie_2007-1119.

Payne, P. 1976. On quantizing ride comfort and allowable accelerations *In*: *AIAA/SNAME, Advanced Marine Vehicles Conference* [Online]. Annapolis, Maryland: American Institute of Aeronautics and Astronautics (AIAA). [Accessed 16 August 2022]. Available from: https://arc.aiaa.org/doi/10.2514/6.1976-873.

Phillips, S., Shin, I. and Armstrong, C. 2015. Crew Transfer Vessel Performance Evaluation *In*: S. Phillips, I. Shin and C. Armstrong, eds. *Design and Operation of Wind Farm Support Vessels: RINA International Conference* [Online]. London: Royal Institution of Naval Architects, pp.1–5. [Accessed 23 November 2020]. Available from: https://app.knovel.com/web/toc.v/cid:kpDOWFSVR5/viewerType:toc/.

Piscopo, V. and Scamardella, A. 2015. The overall motion sickness incidence applied to catamarans. *International Journal of Naval Architecture and Ocean Engineering*. **7**(4), pp.655–669.

Pisula, P.J., Lewis, C.H. and Bridger, R.S. 2012. Vessel motion thresholds for maintaining physical and cognitive performance: A study of naval personnel at sea. *Ergonomics*. **55**(6), pp.636–649.

Polymeropoulos, V.M., Czeisler, M., Gibson, M.M., Anderson, A.A., Miglo, J., Wang, J., Xiao, C., Polymeropoulos, C.M., Birznieks, G. and Polymeropoulos, M.H. 2020. Tradipitant in the Treatment of Motion Sickness: A Randomized, Double-Blind, Placebo-Controlled Study. *Frontiers in Neurology*. **11**, p.563373.

Rademakers, L.W.M.M., Braam, H. and Obdam, T.S. 2008. Estimating costs of operation & maintenance for offshore wind farms *In*: *European Wind Energy Conference*. Energy.

Rasmussen, C.E. 2004. Gaussian Processes in machine learning *In*: *Lecture Notes in Computer Science (including subseries Lecture Notes in Artificial Intelligence and Lecture Notes in Bioinformatics)* [Online]. Springer Verlag, pp.63–71. [Accessed 10 January 2023]. Available from: https://link.springer.com/chapter/10.1007/978-3-540-28650-9_4.

Ravindranath, B. 2016. *Modelling short term decision support tool for O and M of Offshore wind farms*. Lisbon.

Reason, James.T. and Brand, Joan.J. 1975. *Motion sickness* 1st ed. London: Academic Press Inc.

Reid, M. 2021. A new era in hybrid SOVs and world-leading daughter craft. *NOF*. [Online]. [Accessed 18 December 2022]. Available from: https://www.nof.co.uk/news/2021/november/a-new-era-in-hybrid-sovs-and-world-leading-daughter-craft/.

RenewableUK 2015. *Vessel Safety Guide Guidance for Offshore Renewable Energy Developers* [Online]. London. [Accessed 9 January 2022]. Available from: www.RenewableUK.com.

RenewableUK 2022. Wind Energy - RenewableUK. *RenewableUK*. [Online]. [Accessed 9 November 2020]. Available from: https://www.renewableuk.com/page/WindEnergy.

Richardson, R.R., Osborne, M.A. and Howey, D.A. 2017. Gaussian process regression for forecasting battery state of health. *Journal of Power Sources*. **357**, pp.209–219.

Ris, R.C. 1997. *Spectral modelling of wind waves in coastal areas*. Delft, Netherlands: Delft University Press.

Roberts, S., Osborne, M., Ebden, M., Reece, S., Gibson, N. and Aigrain, S. 2013. Gaussian processes for time-series modelling. *Philosophical Transactions of the Royal Society A: Mathematical, Physical and Engineering Sciences*. **371**(1984), p.20110550.

Röckmann, C., Lagerveld, S. and Stavenuiter, J. 2017. Operation and maintenance costs of offshore wind farms and potential multi-use platforms in the Dutch North Sea *In*: B. Buck and R. Langan, eds. *Aquaculture Perspective of Multi-Use Sites in the Open Ocean: The Aquaculture perspective of multi-use sites in the open ocean: Untapped Potential for Marine Resources in the Anthropocene*. Springer, pp.97–113.

Rubio, S., Weichenthal, L. and Andrews, J. 2011. Motion sickness: comparison of metoclopramide and diphenhydramine to placebo. *Prehospital and disaster medicine*. **26**(4), pp.305–309.

Rumawas, V., Asbjørnslett, B.E. and Klöckner, C.A. 2018. Human Factors Evaluation in Ship Design and Operation: An Case Study in Norwegian Sea *In*: *Maritime Safety International Conference (MASTIC 2018)*. Bali, Indonesia: CSP, pp.66–78.

Rusu, L., Bernardino, M. and Guedes Soares, C. 2011. Modelling the influence of currents on wave propagation at the entrance of the Tagus estuary. *Ocean Engineering*. **38**(10), pp.1174–1183.

Saha, G.K., Mahdi, M.A. and Kona, A. 2020. A study on motion sickness incidence at several positions of a ship in irregular waves *In*: *International Shipping Conference (ISCO 2020)* [Online]. Kolkata, India: International Shipping Conference, pp.1–10. [Accessed 21 July 2022]. Available from: https://www.researchgate.net/publication/354198937_A_STUDY_ON_MOTION_SICKNESS_INCIDENCE_AT_SEVERAL_POSITIONS_OF_A_SHIP_IN_IRREGULAR_WAVES.

Salas-Vallina, A., Pozo-Hidalgo, M. and Gil-Monte, P.R. 2020. Are Happy Workers More Productive? The Mediating Role of Service-Skill Use. *Frontiers in psychology*. **11**, p.456.

Salem, M.E.M. 2016. *Design of a pitch angle control system for a horizontal axis small wind turbine.*

Scheu, M., Matha, D., Hofmann, M. and Muskulus, M. 2012. Maintenance strategies for large offshore wind farms. *Energy Procedia*. **24**, pp.281–288.

Scheu, M., Matha, D., Schwarzkopf, M.A. and Kolios, A. 2018. Human exposure to motion during maintenance on floating offshore wind turbines. *Ocean Engineering*. **165**, pp.293–306.

Schmidt, E.A., Kuiper, O.X., Wolter, S., Diels, C. and Bos, J.E. 2020. An international survey on the incidence and modulating factors of carsickness. *Transportation Research Part F: Traffic Psychology and Behaviour*. **71**, pp.76–87.

Schulz, E., Speekenbrink, M. and Krause, A. 2018. A tutorial on Gaussian process regression: Modelling, exploring, and exploiting functions. *Journal of Mathematical Psychology*. **85**, pp.1–16.

Seemann, J., Horstmann, J., Lueder, L., Baschek, B. and Senet, C. 2015. Accuracy of wave direction estimation from directional wave rider buoy time series *In*: *2015 IEEE/OES 11th Current, Waves and Turbulence Measurement, CWTM 2015*.

Seyr, H. and Muskulus, M. 2019. Decision Support Models for Operations and Maintenance for Offshore Wind Farms: A Review. *Applied Sciences*. **9**(2), p.278.

Shafiee, M., Brennan, F. and Espinosa, I.A. 2016. A parametric whole life cost model for offshore wind farms. *The International Journal of Life Cycle Assessment*. **21**(7), pp.961–975.

Shaw, C.C. 1954. On the Dynamics of Motion Sickness in a Seaway. *The Scientific Monthly*. **78**(2), pp.110–116.

Shoenberger, R. W. 1982. Discomfort judgements of translational and angular whole-body vibrations. *Aviation, Space, and Environmental Medicine*. **53**(5), pp.454–457.

Shoenberger, R.W 1982. Discomfort judgements of translational and angular whole-body vibrations. *Aviation, space, and environmental medicine*. **53**(4), pp.454–457.

Singleton, F. 2008. The Beaufort scale of winds – its relevance, and its use by sailors. *Weather*. **63**(2), pp.37–41.

Smyth, J., Birrell, S., Mouzakitis, A. and Jennings, P. 2019. Motion Sickness and Human Performance – Exploring the Impact of Driving Simulator User Trials *In*: *International Conference on Applied Human Factors and Ergonomics: Advances in Human Aspects of Transportation* . Springer Verlag, pp.445–457.

Snyder, J. 2020. Daughter craft and rescue boats find new applications offshore. *Riviera*. [Online]. [Accessed 18 December 2022]. Available from: https://www.rivieramm.com/news-content-hub/news-content-hub/daughter-craft-and-rescue-boats-find-new-applications-offshore-59354.

Soares-Ramos, E.P.P., de Oliveira-Assis, L., Sarrias-Mena, R. and Fernández-Ramírez, L.M. 2020. Current status and future trends of offshore wind power in Europe. *Energy*. **202**, pp.117–787.

Solano, A. 2021. Pooling resources: a streamlined service in offshore wind. *Siemens Gamesa Renewable Energy*. [Online]. [Accessed 6 June 2022]. Available from: https://www.siemensgamesa.com/en-int/explore/journal/2021/07/service-train-pit-stop-offshore.

Sørensen, J.D. 2009. Framework for risk-based planning of operation and maintenance for offshore wind turbines. *Wind Energy*. **12**(5), pp.493–506.

Soukissian, T.H. and Papadopoulos, A. 2015. Effects of different wind data sources in offshore wind power assessment. *Renewable Energy*. **77**, pp.101–114.

Sperstad, I.B., Halvorsen-Weare, E.E., Hofmann, M., Nonås, L.M., Stålhane, M. and Wu, M. 2014. A comparison of single- and multi-parameter wave criteria for accessing wind turbines in strategic maintenance and logistics models for offshore wind farms. *Energy Procedia*. **53**, pp.221–230.

Spinks, A. and Wasiak, J. 2011. Scopolamine (hyoscine) for preventing and treating motion sickness. *The Cochrane database of systematic reviews*. **2011**(6), pp.1465–1858.

Stålhane, M., Christiansen, M., Kirkeby, O. and Mikkelsen, A.J. 2017. Optimizing Jack-up vessel strategies for maintaining offshore wind farms. *Energy Procedia*. **137**, pp.291–298.

Stanney, K., Lawson, B.D., Rokers, B., Dennison, M., Fidopiastis, C., Stoffregen, T., Weech, S. and Fulvio, J.M. 2020. Identifying Causes of and Solutions for Cybersickness in Immersive Technology: Reformulation of a Research and Development Agenda. *https://doi.org/10.1080/10447318.2020.1828535*. **36**(19), pp.1783–1803.

Stavenuiter, W. 2009. *The missing link in the offshore wind industry: Offshore wind support ship*.

Stetco, A., Dinmohammadi, F., Zhao, X., Robu, V., Flynn, D., Barnes, M., Keane, J. and Nenadic, G. 2019. Machine learning methods for wind turbine condition monitoring: A review. *Renewable Energy*. **133**, pp.620–635.

Stevens, S.C. and Parsons, M.G. 2002. Effects of Motion at Sea on Crew Performance: A Survey. *Marine Technology and SNAME News*. **39**(01), pp.29–47.

Stock-Williams, C. and Swamy, S.K. 2019. Automated daily maintenance planning for offshore wind farms. *Renewable Energy*. **133**, pp.1393–1403.

Stoffregen, T.A. and Smart, L.J. 1998. Postural instability precedes motion sickness. *Brain Research Bulletin*. **47**(5), pp.437–448.

Swain, P.S., Stevenson, K., Leary, A., Montano-Gutierrez, L.F., Clark, I.B.N., Vogel, J. and Pilizota, T. 2016. Inferring time derivatives including cell growth rates using Gaussian processes. *Nature Communications 2016 7:1*. **7**(1), pp.1–8.

Tan, H.Z., Wei, L.V., Jin, L.W., Liu, Z.C. and Feng, J.S. 2016. Modeling and solution of offshore wind farm maintenance scheduling *In*: *2nd International Conference on Sustainable Energy and Environmental Engineering* [Online]., pp.1–15. [Accessed 24 December 2021]. Available from: https://www.dpi-proceedings.com/index.php/dteees/article/view/6527.

Toffoli, A. and Bitner-Gregersen, E.M. 2017. Types of Ocean Surface Waves, Wave Classification *In*: *Encyclopedia of Maritime and Offshore Engineering* [Online]. Chichester, UK: John Wiley & Sons, Ltd, pp.1–8. [Accessed 29 November 2020]. Available from: http://doi.wiley.com/10.1002/9781118476406.emoe077.

Tonani, M., Sykes, P., King, R.R., McConnell, N., Péquignet, A.C., O'Dea, E., Graham, J.A., Polton, J. and Siddorn, J. 2019. The impact of a new high-resolution ocean model on the Met Office North-West European Shelf forecasting system. *Ocean Science*. **15**(4), pp.1133–1158.

Tonner, P.D., Darnell, C.L., Engelhardt, B.E. and Schmid, A.K. 2017. Detecting differential growth of microbial populations with Gaussian process regression. *Genome Research*. **27**(2), pp.320–333.

Tracht, K., Westerholt, J. and Schuh, P. 2013. Spare parts planning for offshore wind turbines subject to restrictive maintenance conditions *In*: Pedro. F. Cunha, ed. *Forty Sixth CIRP Conference on Manufacturing Systems 2013*. Elsevier B.V., pp.563–568.

Uchiyama, Y., McWilliams, J.C. and Shchepetkin, A.F. 2010. Wave-current interaction in an oceanic circulation model with a vortex-force formalism: Application to the surf zone. *Ocean Modelling*. **34**(1–2), pp.16–35.

UK 2005. *The Control of Vibration at Work Regulations 2005* [Online]. The Stationery Office Limited . [Accessed 11 September 2022]. Available from: https://www.legislation.gov.uk/uksi/2005/1093/regulation/4/made.

USBR 2001. Remote Sensing Techniques *In*: USBR, ed. *Engineering Geology Field Manual*. Washington DC: USBR, pp.1–50.

Wang, W. and Syntetos, A.A. 2011. Spare parts demand: Linking forecasting to equipment maintenance. *Transportation Research Part E: Logistics and Transportation Review*. **47**(6), pp.1194–1209.

Warner, J.C., Sherwood, C.R., Signell, R.P., Harris, C.K. and Arango, H.G. 2008. Development of a three-dimensional, regional, coupled wave, current, and sediment-transport model. *Computers and Geosciences*. **34**(10), pp.1284–1306.

Wertheim, A.H., Bos, J.E. and Bles, W. 1998. Contributions of roll and pitch to sea sickness. *Brain Research Bulletin*. **47**(5), pp.517–524.

West Essex Medicines 2022. Anticholinergic side-effects and prescribing guidance. *Medicines Management Team at West Essex CCG*. [Online], pp.1–3. [Accessed 4 January 2022]. Available from: https://www.nice.org.uk/guidance/cg161.

Wikström, B.O., Kjellberg, A. and Dallner, M. 1991. Whole-body vibration: A comparison of different methods for the evaluation of mechanical shocks. *International Journal of Industrial Ergonomics*. **7**(1), pp.41–52.

Wolf, J. and Prandle, D. 1999. Some observations of wave-current interaction. *Coastal Engineering*. **37**(3–4), pp.471–485.

Xia, J. and Zou, G. 2023. Operation and maintenance optimization of offshore wind farms based on digital twin: A review. *Ocean Engineering*. **268**, pp.113–322.

Xsens 2017. BMO Offshore - Vessel Black Box. *xsens.com*. [Online]. [Accessed 3 November 2022]. Available from: https://www.xsens.com/cases/bmo-offshore-vessel-black-box.

Youn, D.H. and Park, C.H. 2020. A study on the Motion Sickness Incidence According to the Position in the Ship. *International Journal of Engineering and Technology*. **12**(1), pp.18–21.

Young, I.R. 1999. *Wind Generated Ocean Waves*. Oxford: ELSEVIER.

Yu, Y. -Y 1952. Breaking of waves by an opposing current. *Eos, Transactions American Geophysical Union*. **33**(1), pp.39–41.

Zarnick, E.E. 1978. *A Nonlinear Mathematical Model of Motions of a Planning Boat in Regular Waves* [Online]. Maryland. [Accessed 6 July 2022]. Available from: https://apps.dtic.mil/sti/citations/ADA052039.

Zhang, L.L., Wang, J.Q., Qi, R.R., Pan, L.L., Li, M. and Cai, Y.L. 2016. Motion Sickness: Current Knowledge and Recent Advance. *CNS Neuroscience & Therapeutics*. **22**(1), pp.15–24.

Zheng, Y., Wei, J., Zhu, K. and Dong, B. 2020. Reliability analysis assessment of the wind turbines system under multi-dimensions: *Composites and Advanced Materials*. **29**, pp.1–9.

Appendix A

A.1 Exploring the potential of near-real-time data for decision-making in the operation and maintenance of offshore wind farms.

As previously highlighted in the literature review (section 2.3), the day-to-day maintenance and the decisions involving the planning and scheduling of maintenance are influenced and affected by the validity of short-term forecasts with specific relevance to the sea state (Medina-Lopez et al., 2021). Most studies predicting human exposure to accelerations use numerical models to describe sea-state, this is because there are a handful of on-site met-ocean sensors that provide detailed high-resolution site data. This is most likely due to the expense and impracticality of using *in-situ* measurements to cover wide areas. These include measurements from wave buoys equipped with accelerometers from which time-series data can be collected, tide gauges, and met masts amongst other instruments. Amidst other limitations such as the presence of currents and steep waves, and maintenance needs such as the removal of marine growth (Medina-Lopez et al., 2021), these *in-situ* devices, and are limited to measurements in the areas they are moored and the local measurements from these devices are usually assumed to be representative for the entire area being monitored and used by wind farm managers to direct operations. As such, complete spatial coverage has not yet been accomplished (Medina-Lopez et al., 2021). The numerical models exist to mitigate the problems associated with *in-situ* devices including Simulating Waves Nearshore (SWAN), Wave Watch-III, WAM WAM, and Meteo France Wave Model (MFWAM), that take non-linear energy transfer between frequencies into account (Medina-Lopez et al., 2021). Other models exist that have been used with specific reference to human exposure to acceleration in existing publications such as the JONSWAP model which uses significant wave height, modal period, and spectral shape have been used to define sea conditions (Phillips et al., 2015). Similarly, the WAMIT software used by Scheu et al., (2018) in exploring human exposure to motion during maintenance, can calculate first-order wave force and motion transfer functions, second-order wave drift forces, hydrostatic stiffness, and radiation forces for wetted areas around floating bodies in the water. These models, in relation to this thesis

aim, have been used specifically to define parameters that describe the wave interactions of floating bodies in the water, but do not usually use the non-homogeneous random variables of sea-state and vessel parameters such as different speeds and heading but define operational conditions for a set of sea-states, and vessel parameters (Olausson, 2015). Additionally, some of these models require expert calibration and validation against in-situ measurements as it is not always possible to overlap *in-situ* measurements and modelled data (Medina-Lopez et al., 2021). In recent years, however, satellite data has proven to be a helpful tool in ocean monitoring and short-term forecasting. According to Hasager et al., (2013), satellite-based data can fill gaps in the temporal and spatial variations of the marine environment especially as the offshore environment is less known. In the operation and maintenance of offshore wind farms, this is particularly relevant as unlike data available from *in-situ* measurements, satellite data can provide data over a wide spatial coverage using different sensors and can also overcome some of the problems of physical forecast models (Medina-Lopez et al., 2021). In addition, coupling systems exist that merge satellite observation data with numerical forecasting models to improve the accuracy of data. Bruciaferri et al., (2021a) state that this ocean-wave coupling can improve the accuracy of the predicted surface dynamics by about 4% and about 8% in the open ocean and on the shelf respectively.

This research explores the potential of near-real-time metocean and satellite data from Copernicus Marine Service with measured acceleration data to predict acceleration exposure in technicians. This study used hindcast metocean products in research, however, near-real-time satellite observations as well as short-term forecast models exist to explore the potential application of near-real-time products in exposure assessments. As described in chapter three of this thesis, the data from the WAVEWATCH III wave model (Tolman, 2014) can provide daily analyses and 10 days forecasts for the global ocean sea surface waves. Similarly, other model input parameters such as current, and tidal data are produced using the NEMO (Nucleus for European Modelling of the Ocean) forecasting model, which provides a 6-day forecast. On the other hand, satellite data was acquired from altimeter and synthetic-aperture radar (SAR) measurements from the Copernicus Marine Service.

To ensure an accurate representation of the sea state, this research applies a comparison ocean model and satellite measurements with available buoys for wave measurements.

A.1.1 Comparison between metocean and satellite data with directional wave rider buoy data

Chapter three of this thesis describes the processes taken to synchronise sea state data for locations within the thesis project sites to *in-situ* measurements collected by the vessel motion monitoring system (VMMS) using GPS data within datasets. The resulting dataset shows the routes taken by vessels merged with their associated meteorological data along the transit routes in Figures 4.7, 4.12, 4.17, and 4.22. The meteorological data used in this thesis included wave data, current data, tidal data, and wind data. In order to validate the synchronisation process, metocean and satellite datasets were compared with *in-situ* measurements from directional wave rider buoys. Werdell & McClain, (2019) describe a straightforward approach to this validation which involves the comparison of simultaneously collected data. For this study, the comparison was made using data from directional wave riders acquired from Cefas and funded by Environment Agency, licensed under the Cefas WaveNet Non-Commercial Licence v1.0. The wave measurements were recorded in thirty-minute (30-minute) samples and the significant wave height data measurement was selected for comparison using hindcast data and the GPS location of the directional wave riders. The comparison assessed standard metric errors including the root mean square error (RMSE), the correlation coefficient (R), the coefficient of determination (R^2), and the probability value (p-value). The results for the comparison are presented below in Table 5.4.

Category	**R^2**	**RMSE**	**p-value**	**Parameter**
Metocean and buoy data	0.89	0.20	<0.05	Significant wave height
Metocean and buoy data	0.84	0.25	<0.05	Significant wave height
Metocean and buoy data	0.986	0.15	<0.05	Significant wave height
Satellite and buoy data	0.71	0.50	<0.05	Significant wave height
Satellite and met station data	0.54	1.74	<0.05	Wind speed
Satellite and met station data	0.90	0.18	<0.05	Wind speed

Table 5. 2 Comparison between metocean and satellite data products with in-situ data

Overall, the result of the comparisons shows good agreement between metocean and *in-situ* data and between satellite data and the data from the *in-situ* devices which corroborates findings by Boudière et al., (2013) who stated that wave data produced by wave models compared well between satellite altimeters and buoy measurement. Another satellite data validation was performed by Werdell & McClain, (2019) who also found a good relationship between the datasets as well as the slight differences between satellite measurements and *in-situ* measurements which are present in the findings by Boudière et al., (2013), however, Werdell & McClain, (2019) explained the differences to be due to a few reasons including erroneous estimations, missing data from satellite trajectory, inaccurate and missing *in-situ* values, and errors due to empirical regressions. In application, however, this exploration showed that metocean products were more suited to welfare predictions in offshore wind farms. Though this research shows that the time-consuming nature of experimental human reaction to vessel acceleration research can be mitigated with satellite data, this research also highlights the practical limitations of satellite data in forecasting which is relevant for welfare predictions. This is because satellite products are able to provide hindcast datasets and in some cases, near-real-time datasets, however, short-term forecast data is needed for maintenance planning operations which can be achieved from numerical ocean models able to provide near-real-time and forecast outputs. As such, the models created in this research used metocean data in model predictions. The models created can be deployed as a web application or integrated into existing operation and maintenance models which can both improve decision-making and risk management in operation and maintenance and in some cases, reduce costs associated with delayed and rescheduled maintenance brought about by seasickness in technicians (Stock-Williams & Swamy, 2019).

A.1.2 Discussion and conclusion

This section illustrated the potential for the use of ocean models and satellite data in decision-making for the operation and maintenance of offshore wind farms using a practical application. Ocean model and satellite data were used to provide spatial coverage for areas within project sites. In order to validate both sea state datasets, a comparison was made with an available *in-situ* device in the project area. A comparison was made between *in-situ* data and ocean model and satellite which showed a good agreement between the datasets suggesting that ocean-modelled, and satellite-measured data can add significant value to

offshore wind energy as well as other offshore renewable energy industries. Medina-Lopez et al., (2021) make similar statements while exploring the opportunities of satellite data in the renewable energy sector. They state that there is a need for the provision of more data with improved spatial resolutions which could improve the offshore renewable sector in the context of operational and environmental conditions, and more specifically to this thesis's aims, improve decision-making in the sector. The decision-making process of operation and maintenance in offshore wind is heavily influenced by environmental conditions which can define the type of vessel used for a maintenance operation or even whether or not a maintenance operation can be performed safely. As such this research demonstrated that near-real-time data and in some cases short-term forecast data can used in combination with machine learning methods can be used for risk-based decision-making in the operation of offshore wind farms (described in sections 5.3 and 5.4 of this chapter) to estimate the comfort and health of technicians on crew transfer vessels during transits for maintenance operations. Where project sites included large areas around wind farms, transit routes, and areas around exit ports, modelled ocean data and satellite data were vital in providing high-resolution spatial coverage for areas not initially covered by *in-situ* data. However, the exploration of practical applications showed that numerically modelled data was better suited to maintenance planning due to the limitation of satellite data to provide forecast data. As this research showed, a major limitation to the use of satellite data was that the current satellite products available are only able to provide hindcast and near-real-time data (usually one to three hours behind), and in practice, a welfare model will benefit from real-time data in describing sea-state. Further limitations to the use of satellite data in the operation and maintenance of offshore wind farms could be a lack of knowledge in integrating satellite data with standard operation and maintenance techniques (Medina-Lopez et al., 2021). However, as this thesis, shows a combination of domain knowledge and the extra level of information provided by satellite data is possible and can supplement *in-situ* data for purposes such as model validation in areas out of *in-situ* coverage. Other limitations to the use of satellite data include errors caused by cloud cover (Werdell & McClain, 2019), though some SAR satellites can acquire images under cloudy conditions (Notti et al., 2018), and latency and the time of the satellite pass for real-time data (Notti et al., 2018), which could be an important factor in day-to-day maintenance decision-making. Nevertheless, forecast products exist that can complement near-real-time data for short-term forecasts, however, these forecast models

are based on some of the numerical forecast models already used in available research. Where raw real-time data can be made available for use, measures will need to be taken to process this data before model predictions can be made. The potential for metocean data in planning operations can, however, be extended to other areas of operations in offshore wind energy.

Further work will include the addition of more datasets to inform and improve the created models, and the integration of the created models into existing models for real-life applications. Additionally, the created models can be improved by modelling the welfare of technicians using vessels of more variable sizes such as service operating vessels (SOVs), and modelling welfare in variable sea-states other than the North Sea for greater spatial variation. Further application and recommendations from these findings include having a wider network of satellite data provision services for free and open-access data for the implementation of more use cases not only for the operation and maintenance of offshore wind farms but also for other offshore renewable energy sectors including tidal and wave energy.

Appendix B

B.1 Data

Table B.1 presents more information on the satellite and ocean model data used in achieving the thesis aim and objectives.

Parameter	Information	
Current speed; current direction; sea surface height	Source	Copernicus Marine Service
	Product	NORTHWESTSHELF_ANALYSIS_FORECAST_PHY_004_013
	Details	Numerical model; 0.014˚ x 0.03˚ spatial resolution; hourly instantaneous, daily mean, and 15-minute instantaneous temporal resolution; NetCDF-4 file format; Description: E.U. Copernicus Marine Service, n.d. Atlantic - European Northwest

		Shelf - Ocean Physics Analysis and Forecast, [Product] marine.copernicus.eu, https://doi.org/10.48670/moi-00054; Public data
Current speed; current direction; sea surface height	Source	Copernicus Marine Service
	Product	SEALEVEL_GLO_PHY_L4_MY_008_047
	Details	Satellite observation; 0.25˚ x 0.25˚ spatial resolution; 3 hourly instantaneous temporal resolution; NetCDF-4 file format; Description: Copernicus Marine Service, n.d. Global Ocean Gridded L4 Sea Surface Heights and Derived Variables Reprocessed (1993-Ongoing), [Product] marine.copernicus.eu, https://doi.org/10.48670/moi-00148; Public data
Significant wave height; wave period; wave direction	Source	Copernicus Marine Service
	Product	NWSHELF_REANALYSIS_WAV_004_015
	Details	Numerical model; 0.017˚ x 0.017˚ spatial resolution; 3 hourly instantaneous temporal resolution; NetCDF-4 file format; Description: Copernicus Marine Service, n.d. Atlantic- European Northwest Shelf- Wave Physics Reanalysis, [Product] marine.copernicus.eu, https://doi.org/10.48670/moi-00060; Public data
Significant wave height; wave period; wave direction	Source	Copernicus Marine Service
	Product	WAVE_GLO_WAV_L3_SPC_NRT_OBSERVATIONS_014_002
	Details	Satellite-observation; 0.017˚ x 0.017˚ spatial resolution; 3 hourly instantaneous temporal resolution; NetCDF-4 file format; Description: Copernicus Marine Service, n.d. Global Ocean L3 Spectral Parameters from NRT Satellite Measurements, [Product] marine.copernicus.eu, https://doi.org/10.48670/moi-00175; Public data

Wind speed; wind direction	Source	Copernicus Marine Service
	Product	WIND_GLO_WIND_L4_REP_OBSERVATIONS_012_006
	Details	Satellite-observation; 0.25° × 0.25° spatial resolution; 6 hourly mean temporal resolution; NetCDF-4 file format; Description: Copernicus Marine Service, n.d. Global Ocean Wind L4 Reprocessed 6 hourly Observations, [Product] marine.copernicus.eu, https://doi.org/10.48670/moi-00185; Public data
Significant wave height	Source	CEFAS
	Product	West Gabbard 2 WaveNet Site
	Details	*In-situ* observation; Location: 51°57'.18N 002°06'.54E in 41m water depth are currently recorded using a Directional Waverider MkIII; Data provided by Channel Coastal Observatory on behalf of the Environment Agency and the Anglian Coastal Monitoring Programme; Public data
Significant wave height	Source	CEFAS
	Product	Felixstowe waverider
	Details	*In-situ* observation; Location: 51°56'.29N 001°23'.63E in 8m water depth are currently recorded using a Directional Waverider; Data provided by Channel Coastal Observatory on behalf of the Environment Agency and the Anglian Coastal Monitoring Programme; Public data
Significant wave height	Source	CEFAS
	Product	North well waverider
	Details	*In-situ* observation; Location: 53°03'.45N 000°28'.48E in 31m water depth are currently recorded using a Directional Waverider; Data provided by Channel Coastal Observatory on behalf of the Environment Agency and the Anglian Coastal Monitoring Programme; Public data
Wind speed	Source	Channel Coastal Observatory

	Product	Felixstowe
	Details	*In-situ* observation; Meteorological station; Location: 51°56'.13N 001°19'.10E; Instrument: Gill windsonic anemometer; Elevation 15.92m; Data courtesy of the Anglian Regional Coastal Monitoring Programme; Public data
Wind speed	Source	Channel Coastal Observatory
	Product	Chapel point
	Details	*In-situ* observation; Meteorological station; Location: 53°13'.85N 000°20'.18E; Instrument: Gill windsonic anemometer; Elevation 15.92m; Data courtesy of the Anglian Regional Coastal Monitoring Programme; Public data

Table 3. 5 Summary of metocean product information

Appendix C

The script presented in this section outlines the code used to streamline the analysis process for feature engineering, data analysis, and predictive modelling.

C.1 Feature engineering welfare variables. Code adapted from Irvine, (2006)

Using a MSI estimation tool, the values of duration in first column and acceleration in the second is created.

```
%Input
%create matrix of duration and signal


matrix = [full_trip.duration, full_trip.("accZ")];
matrix = fillmissing(matrix,"nearest");


%Input
%Ammended tool below
THM = matrix;
%
t=THM(:,1);
f=THM(:,2);
%
tmx=max(t);
tmi=min(t);
n = length(f);
dt=(tmx-tmi)/(n-1);
```

```
sr=1./dt;
%
dtmin=min(diff(t));
dtmax=max(diff(t));
%
ncontinue=1;
if(((dtmax-dtmin)/dt)>0.01)
    disp(' ')
    disp(' Warning:  time step is not constant.  Continue calculation? 1=yes
2=no ')
    ncontinue=input(' ');
end
%Input
%Set start and end time
st=0;
%
te=endtime_rtn;
%
j=1;
jfirst=1;
jlast=max(size(THM));
for i=1:max(size(THM))
    if(THM(i,1)<st)
        jfirst=i;
    end
    if(THM(i,1)>te)
        jlast=i;
        break;
    end
end
%
tim=double(THM(jfirst:jlast,1));
amp=double(THM(jfirst:jlast,2));
%
%
[fwl,fw,fwu,wk,wd,wf,wc,AW_rms,wj,wb,www,iweight]=weight_trial();
%
aw=zeros(length(amp),1);
%
iband=3;  % bandpass filtering
iphase=1; % refiltering for phase correction
%
progressbar;
for i=1:44
%
    progressbar(i/44);
%
    fh=fwl(i);  % highpass filter frequency
    fl=fwu(i);  % lowpass filter frequency
%
    if(fl<sr/2.1)
        [y,mu,sd,rms(i)]=...
                Butterworth_filter_function_alt(amp,dt,iband,fl,fh,iphase);
```

```
%
        aw=aw+y*www(i);
    end
%
end
%
pause(0.5);
progressbar(1);
%
n=length(aw);
%
AW=std(aw);
MTW=AW;
%
VDV=0;
for i=1:n
    VDV=VDV+aw(i)^4;
end
VDV=(VDV*dt)^0.25;
%
out1=sprintf('\n Composite Weighted Level  AW = %8.4g (m/sec^2)RMS ',AW);
disp(out1);
%
out1=sprintf('\n Maximum Transient Vibration MTW = %8.4g (m/sec^2)RMS ',MTW);
disp(out1);
%
out1=sprintf('\n Fourth Power Vibration Dose VDV = %8.4g (m/sec^(1.75))
\n',VDV);
disp(out1);
%
out1=sprintf('\n                          MTW/AW = %8.4g\n',MTW/AW);
disp(out1);
End
```

C.2 Model training and validation

```
function [trainedModel, validationRMSE] =
trainRegressionModel(trainingData)
% [trainedModel, validationRMSE] = trainRegressionModel(trainingData)
% Returns a trained regression model and its RMSE.
%  Input:
%      trainingData: A table containing the same predictor and response
%       columns as those imported into the app.
%
%  Output:
%      trainedModel: A struct containing the trained regression model. The
%       struct contains various fields with information about the trained
%       model.
%
%      trainedModel.predictFcn: A function to make predictions on new data.
%
%      validationRMSE: A double containing the RMSE. In the app, the
%       History list displays the RMSE for each model.
%
```

```
% Use the code to train the model with new data. To retrain your model,
% call the function from the command line with your original data or new
% data as the input argument trainingData.
%
% For example, to retrain a regression model trained with the original data
% set T, enter:
%   [trainedModel, validationRMSE] = trainRegressionModel(T)
%
% To make predictions with the returned 'trainedModel' on new data T2, use
%   yfit = trainedModel.predictFcn(T2)
%
% T2 must be a table containing at least the same predictor columns as used
% during training. For details, enter:
%   trainedModel.HowToPredict

% Auto-generated by MATLAB on 11-May-2022 12:34:40


% Extract predictors and response
% This code processes the data into the right shape for training the
% model.
inputTable = trainingData;
predictorNames = {'duration', 'heading', 'speed', 'cur_speed', 'cur_dir',
'tidalrange', 'Hs'};
predictors = inputTable(:, predictorNames);
response = inputTable.Arms;
isCategoricalPredictor = [false, false, false, false, false, false, false];

% Train a regression model
% This code specifies all the model options and trains the model.
regressionGP = fitrgp(...
    predictors, ...
    response, ...
    'BasisFunction', 'constant', ...
    'KernelFunction', 'rationalquadratic', ...
    'Standardize', true);

% Create the result struct with predict function
predictorExtractionFcn = @(t) t(:, predictorNames);
gpPredictFcn = @(x) predict(regressionGP, x);
trainedModel.predictFcn = @(x) gpPredictFcn(predictorExtractionFcn(x));

% Add additional fields to the result struct
trainedModel.RequiredVariables = {'Hs', 'cur_dir', 'cur_speed', 'duration',
'heading', 'speed', 'tidalrange'};
trainedModel.RegressionGP = regressionGP;
trainedModel.About = 'This struct is a trained model exported from
Regression Learner R2020a.';
trainedModel.HowToPredict = sprintf('To make predictions on a new table, T,
use: \n  yfit = c.predictFcn(T) \nreplacing ''c'' with the name of the
variable that is this struct, e.g. ''trainedModel''. \n \nThe table, T,
must contain the variables returned by: \n  c.RequiredVariables \nVariable
formats (e.g. matrix/vector, datatype) must match the original training
data. \nAdditional variables are ignored. \n \nFor more information, see <a
href="matlab:helpview(fullfile(docroot, ''stats'', ''stats.map''),
''appregression_exportmodeltoworkspace'')">How to predict using an exported
model</a>.');

% Extract predictors and response
% This code processes the data into the right shape for training the
```

```
% model.
inputTable = trainingData;
predictorNames = {'duration', 'heading', 'speed', 'cur_speed', 'cur_dir',
'tidalrange', 'Hs'};
predictors = inputTable(:, predictorNames);
response = inputTable.Arms;
isCategoricalPredictor = [false, false, false, false, false, false, false];

% Perform cross-validation
partitionedModel = crossval(trainedModel.RegressionGP, 'KFold', 5);

% Compute validation predictions
validationPredictions = kfoldPredict(partitionedModel);

% Compute validation RMSE
validationRMSE = sqrt(kfoldLoss(partitionedModel, 'LossFun', 'mse'));
```

Appendix D

Project Engagement

Engagement for this project included engagement with industry specialists comprising of informal interviews including the Offshore Renewable Energy Catapult, The Carbon Trust, and The Centre of Competence EHS Offshore Siemens Gamesa.

Publications

A Machine Learning Approach to Comfort Assessment for Offshore Wind Farm Technicians. Ocean Engineering (Submitted).

A data-driven Assessment of the Welfare of Technicians During Transits to Offshore Wind Farms. (Under review).

Conferences

Human Factors in the Operation and Maintenance of Offshore Wind Turbines," ICYMARE International Conference for Young Marine Researchers. September 2021 (presentation).

Human Factors in the Operation and Maintenance of Offshore Wind Turbines," University of Hull Postgraduate Research Conference. February 2021 (presentation).